Synthesis and optical properties of heteroaromatic small molecules and oligomers for light-emitting devices

Hughes, Gregory

SYNTHESIS AND OPTICAL PROPERTIES OF HETEROAROMATIC SMALL MOLECULES AND OLIGOMERS FOR LIGHT-EMITTING DEVICES

GREGORY HUGHES, B.SC.

USTINOV COLLEGE

DEPARTMENT OF CHEMISTRY

UNIVERSITY OF DURHAM

A Thesis submitted for the degree of Doctor of Philosophy

at the University of Durham

June 2004

STATEMENT OF COPYRIGHT

DECLARATION

The work described in this thesis was carried out in the Department of Chemistry at the University of Durham, between October 2000 and September 2003. All the work was carried out by the author unless otherwise stated, and has not previously been submitted for a degree at this or any other university.

TABLE OF CONTENTS

ABSTRACT

Synthesis and Optical Properties of Heteroaromatic Oligomers for Light-Emitting Devices

Gregory Hughes, University of Durham, 2004

New π-electron deficient heteroaromatic oligomers **175** and **225** have been synthesised by Suzuki cross-coupling methodology and incorporated into OLEDs. Using **175** as the emissive layer in the device configuration ITO/PEDOT/**175**/Ca/Al: blue-green light λ_{max} 500 nm, most likely emanating primarily from excimer states is emitted at a high turn-on voltage. Blue electroluminescence, λ_{max} 444 nm, (onset 6.5V) is observed for the device structure ITO/PEDOT/**225**/Ca/ with no long-wavelength emission from π-aggregates or exciton states.

New 2,5-diphenyl-1,3,4-oxadiazoles and 2-phenyl-5-(2-thienyl)-1,3,4-oxadiazoles heteroaryl-functionalised derivatives have been prepared under standard Sonogashira cross-coupling conditions. UV-Vis absorption and photoluminescence spectra establish that the substitution of a phenyl ring in the 2,5-diphenyl-1,3,4-oxadiazole derivative **232d** λ_{max} (PL) 380 nm, by a thienyl ring **239d** λ_{max} (PL) 415 nm, leads to a red shift in the lowest energy band. The absorption and emission spectra of **240** λ_{max} (PL) 480 nm, is further red-shifted compared to **239f** λ_{max} (PL) 425 nm, which is consistent with the extended π-conjugation of the central bis(ethynylthiophene) unit of **240**.

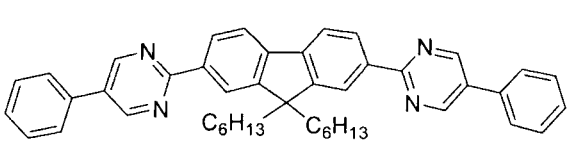

175

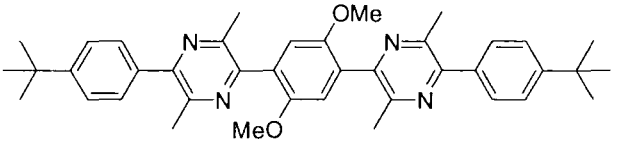

225

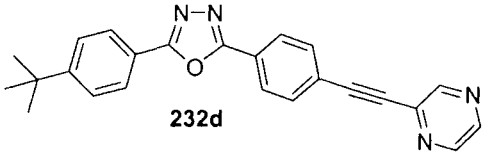

232d

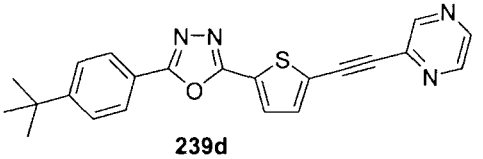

239d

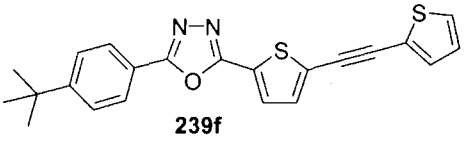

239f

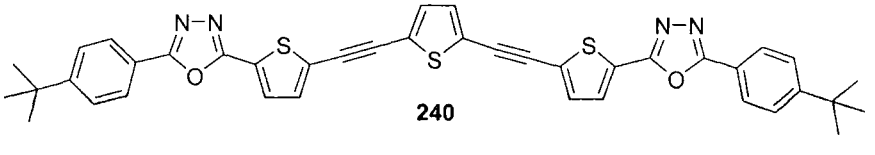

240

ACKNOWLEDGEMENTS

I would like to express my grateful thanks to several people whose assistance and support have been invaluable during my Ph.D, and as a result eased the preparation of this work.

My supervisor Professor Martin R Bryce for accepting me into his research group, and his direction over the past years. Dr Changsheng Wang is particularly deserving of my gratitude. His patient listening, instructional skill, exemplar methods of operation and unfailing good humour have proved inspirational. Special thanks to Dr David Kreher and Dr Igor Perepichka for their practical assistance and IT support: and Dr T Sato and Ben Lyons for fabrication of OLEDs.

All members of the Bryce group past and present. Specifically, Christian for a warm welcome, continued friendship and hospitality in Copenhagen. Steve for his wisecracks, engaging banter, witty repartee and acting as my chauffeur in Colorado. Paul, for the many nights out in Durham and Monkey Hanging Land (Hartlepool). Similarly, Steve Burdon and Ian Smith, who although not members of the Bryce group itself, deserve honorary membership.

Members of the academic, administrative and technical staff at the University of Durham for providing appropriate instruction and support on a regular basis. In particular Dr Alan Kenwright and Catherine Hefferman for their unstinting advice and assistance regarding NMR matters. Dr Andrei Batsanov for solving X-ray crystal structures. Lenny Laughlan in chromatography, for his committed management of the Chemistry five-a-side team plus many interesting debates on Newcastle United and the error of their ways. Elizabeth, Jimmy and Tony for providing supplies as required. Also the tea ladies, especially Val, Miriam and Sandra for allowing me to operate a "slate".

On a personal note my friends at home, Paul, Mark, Matthew, Rachael and Luke for their support and encouragement during research and writing up periods.

Finally, the deepest debt of gratitude must lie with my parents; my father who died during the final year of this study, and my mother who continues to be "there" when ever needed.

The intellect of man is forced to choose
Perfection, of the life, or of the work

The Choice
W. B. Yeats

ABBREVIATIONS

Alq_3	-	tris-(8-hydroxyquinoline)aluminium **2**
CV	-	Cyclic voltammetry
DCM	-	Dichloromethane
ECHB	-	Electron-conducting / hole-blocking
EI	-	Electron Impact
EL	-	Electroluminescence
EQE	-	External quantum efficiency
ES	-	Electrospray
HOMO	-	Highest occupied molecular orbital
ITO	-	Indium tin oxide
LUMO	-	Lowest unoccupied molecular orbital
MEH-PPV	-	poly[2-(2'-ethylhexyloxy)-5-methoxy-1,4-phenylenevinylene] **11**
mp	-	Melting point
NEt_3	-	Triethylamine
NMR	-	Nuclear magnetic resonance
OLEDs	-	Organic light-emitting devices
PBD	-	5-(4-biphenyl)-2-(4-*tert*-butylphenyl)-1,3,4-oxadiazole **25**
PEDOT	-	poly(ethylenedioxy-thiophene)
PET	-	poly(ethyleneterphthalate)
PL	-	Photoluminescence
PLQY	-	Photoluminescence quantum yield
PPV	-	poly(*p*-phenylenevinylene) **8**
PPY	-	poly(pyridine-2,5-diyl) **67**
PPym	-	poly(pyrimidine-2,5-diyl) **86**
PVK	-	poly(vinylcarbazole) **32**
TIPD	-	2,2′,2″-(1,3,5-benzenetriyl)*tris*(1-phenyl)-1H-benzimidazole **33**
Tg	-	Glass transition temperature
THF	-	Tetrahydrofuran
TLC	-	Thin layer chromatography
UV	-	Ultraviolet
Vis	-	Visible

1 MATERIALS FOR ORGANIC LIGHT-EMITTING DEVICES

Since the serendipitous discovery of polymer organic light-emitting devices (OLEDs) in 1989 by Ph.D. student Jeremy Burroughes, in Richard Friend's laboratory at Cambridge University OLEDs have attracted considerable interest and are now viewed as an important competitor with liquid crystal displays (LCDs) for a wide variety of display applications. Current research focuses on the use of small molecule and polymer materials to make organic electroluminescent (EL) displays with both passive and active matrix technologies.[1]

1.1 ORGANIC ELECTROLUMINESCENCE

Organic electroluminescence (EL), or the generation of light by the electrical excitation of an organic molecule, was first reported in 1963 by applying *ca.* 400 V across single crystals of anthracene immersed in an electrochemical cell.[2] The cell contained an electrolytic solution of negatively charged anthracene ions, prepared from a solution of anthracene and sodium in THF next to the cathode and a solution of positively charged anthracene ions, prepared from a solution of anthracene and aluminium trichloride in nitromethane, next to the anode. The two liquid electrolytic solutions responsible for charge transport were physically separated from each other by the solid anthracene crystal. EL was witnessed in the part of the anthracene crystal next to the hole-injecting anode, which suggests an imbalance of charge-carrier injection and transport.[3] In 1982 Vincett *et al.* reported the next development in organic EL using organic thin films. Approximately 0.6 μm vacuum-deposited anthracene films were prepared and when subjected to lower drive voltages, *e.g.* 30 V exhibited strong blue EL.[4] However, the quantum efficiencies (defined as photons emitted/electrons injected) and the lifetimès of these devices were considerably lower than those based on inorganic systems which continued to be the focus of attention. It was the seminal work of Tang and VanSlyke with bilayers of low molecular weight organic molecules, reported in 1987, which initiated worldwide interest in the development of organic light-emitting devices (OLEDs).[5] The device structure was conceptually simple, comprising evaporated thin layers of organic compounds, which were chosen for their ability to act as fluorophores and to transport charge carriers, sandwiched between two electrodes one of which was transparent. The device was fabricated by vacuum deposition, which ensured that both layers were smooth and continuous. In addition, the two-layer sstructure minimises the probability of overlapping pinholes wihtin

the thin-film. Green EL was observed with devices comprising the bis(triarylamine) **1** as the hole-transporting layer and tris(8-hydroxyquinoline)aluminium (Alq_3) **2** as the emitter and electron-transporting layer in the configuration ITO/**1**/**2**/Mg:Ag. A brightness of > 1000 cd m^{-2} at an operating voltage of < 10 V was achieved. Devices with photon/electron quantum efficiencies of 1% could now be realised. This discovery significantly enhanced the prospects for producing large area, inexpensive, flat panel displays that could rival cathode ray tubes (CRT).[6]

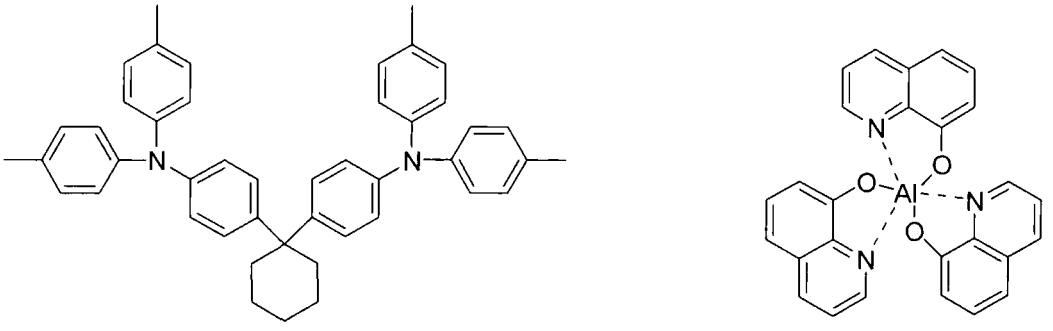

1 **2**

Scheme 1: Molecular structures of diamine 1 and Alq_3 2 used by Tang and VanSlyke in the first two-layer sublimed molecular film device.[5]

The next fundamental breakthrough was reported by Friend *et al.* in 1990, who demonstrated that the highly fluorescent conjugated polymer poly(*p*- phenylenevinylene) (PPV) **8** could serve as the active material emitting yellow-green light in a single-layer OLED of configuration ITO/PPV/Al.[7] The introduction of substituents into the PPV skeleton provides derivatives which are soluble in organic solvents and induces a lower glass transition temperature (*Tg*) compared to that of PPV. This removes the necessity of carrying out chemistry and thermal processing of the substrate.[3] In 1991 Braun and Heeger reported a red-orange emitting OLED based on poly[2-methoxy-5-(2-ethylhexyloxy)-*p*-phenylenevinylene] (MEH-PPV) **11** in the configuration ITO/MEH-PPV/Ca with an external quantum efficiency of 1%.[8] These discoveries have led to intense worldwide interest in new materials for incorporation into OLEDs for practical applications, notably full-colour flat-panel displays. The world market for display devices using OLEDs is expected to grow to > $2500m by 2007.[9] The study of organic electroluminescence is a multi-disciplinary field, which crosses the traditional boundaries of synthetic chemistry, applied and theoretical physics, materials science and device engineering.

There are three principle categories of organic EL material: small molecules, oligomers and light-emitting polymers. Each classification should exhibit a high *Tg* in order to form a stable amorphous glassy state thereby inhibiting crystallisation during the lifetime of the device. Small molecules and oligomers must be capable of being deposited as a pure, uniform, thin solid film by vapour deposition under high vacuum. They are of considerable interest to organic material scientists due to their monodisperse character, flexibility of synthesis and good processability as thin solid films. An additional advantage is the improved properties observed due to the propensity of certain classes of these organic materials to self-organise in a supramolecular structure on the desired substrate surface. A distinct disadvantage of small molecules and to lesser extent oligomers is the tendancy to form defects and traps at crystal grain boundaries over time.[3] Polymers are made up of a large number of building blocks linked in a repetitive fashion (macromolecular structure), oligomers constitute their lower homologs, since they will contain only one or a few of these units.[10] Small molecules and oligomers have to be deposited by sublimation or vapour depositon under high vacuum. This is an expensive process consequently not ideally suited for mass production of display technologies. In contrast, uniform thin films of conjugated light-emitting polymers can be deposited from dilute organic solutions by spin-coating. A further advantage is the reproducibility of polymer production. Without the incorporation of solubising substituents into the polymer framework the alternating configuration of single and double bonds results in a rigid, linear, and planar molecular confirmation. This results in very high melting points and severely limited solubility in organic solvents.

For this research project we chose substituted small molecules and oligomers because they are ideally suited to small-scale laboratory synthesis by Suzuki coupling reactions. Our primary objective was the preparation of glassy materials allowing formation of amorphous solid thin films in the fabrication of efficient OLEDs.

1.2 SYNTHESIS OF POLY(*P*-PHENYLENEVINYLENE) AND ITS DERIVATIVES

PPV **8** is a bright yellow, fluorescent polymer. Its emission maxima at λ 551 nm (2.25 eV) and 520 nm (2.4 eV) are in the yellow-green region of the visible spectrum.[11] PPV is a robust, intractable, insoluble polymer when produced directly from its monomer starting material. However, the physical and processability limitations of PPV have been overcome

by the introduction of a solution processible sulfonium precursor route devised by Wessling and Zimmerman.[12,13]

Treatment of 1,4-bis(dichloromethyl)benzene **3** with tetrahydrothiophene affords the bis–sulfonium salt **4**. Polymerisation of a methanolic solution of monomer **4** is induced by the addition of slightly less than 1 mol equivalent of aqueous sodium hydroxide at 0-5 °C. It has been suggested that the *p*-quinodimethane intermediate **5** undergoes radical polymerisation, although anionic progagation cannot be completely excluded. The almost completely colourless solution of the precursor polymer **6** is dialyzed against distilled water to remove impurities with low molecular weight. Treatment with refluxing methanol gives the neutral polymer **7** which by gel-permeation chromatography shows a number average molar mass M_n of >100,000 $gmol^{-1}$. The precursor polymer **6** is converted into PPV **8** by thermal evaporation. Under these conditions by-products of the elimination (tetrahydrothiophene and hydrogen chloride) escape easily.[11]

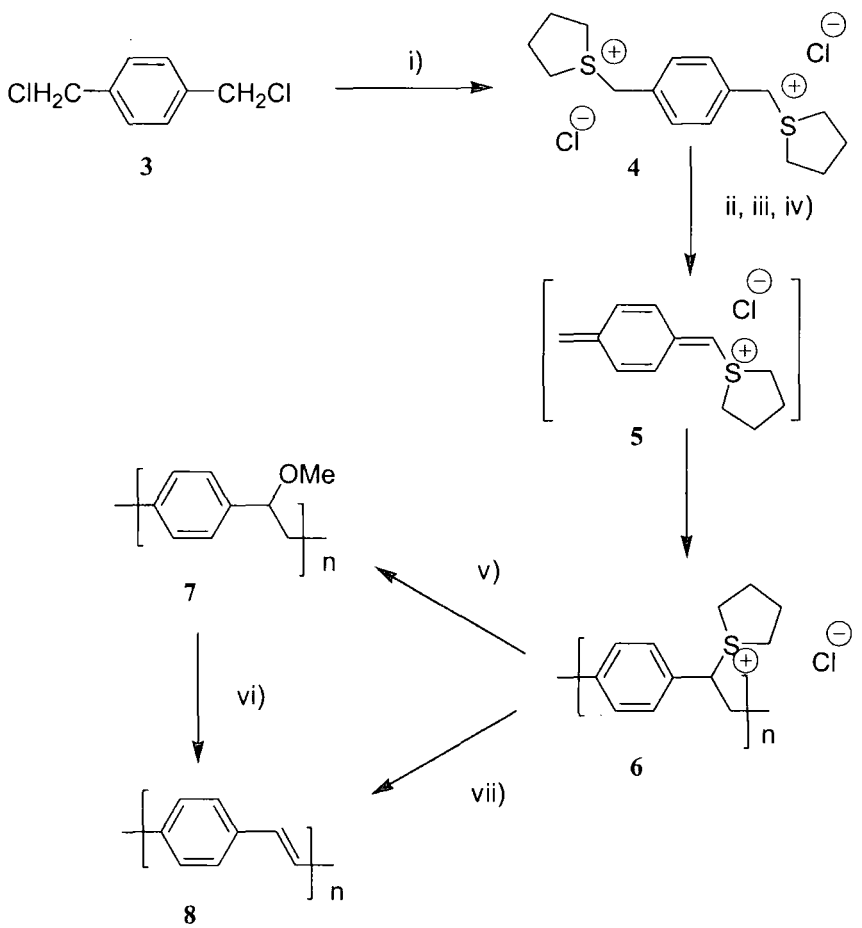

Scheme 2: Synthesis of PPV 8: i) tetrahydrothiophene, MeOH, 65 °C; ii) NaOH, MeOH/H_2O or Bu_4NOH, MeOH, 0°C; iii) neutralisation (HCl); iv) dialysis (water); v) MeOH, 50 °C; vi) 220 °C, HCl (g)/Ar, 22 h; vii) 180-300 °C, vacuum, 12 h.

Alternative methods for the preparation of PPV suitable for OLEDs involve chemical vapour deposition (CVD)[14] and a ring-opening metathesis polymerisation (ROMP).[15,16] The materials produced by these routes may differ from PPV prepared by the Wessling route in molar mass, molar mass distribution, film quality and resulting device efficiency.[11]

Solution processible analogues of PPV allow direct deposition as components in OLEDs. This eliminates the need for thermal elimination treatment of the soluble precursor polymer **6**, which is one of the disadvantages of the Wessling sulfonium precursor route. However, solution processible polymers tend to have lower glass transition temperatures (*Tg*). Dialkoxy-substituted derivatives of PPV such as poly[2-(2'-ethylhexyloxy)-5-methoxy-1,4-phenylenevinylene] MEH-PPV **11** are readily soluble in solvents such as chloroform, THF and xylene. The alkoxy side chains have a beneficial effect on the polymer's fluorescence and EL quantum yields as demonstrated by a red shifted emission maximum of 590 nm (2.1 eV) (i.e red-orange) for MEH-PPV compared to 551 nm (2.25 eV) and 520 nm (2.4 eV) for PPV.

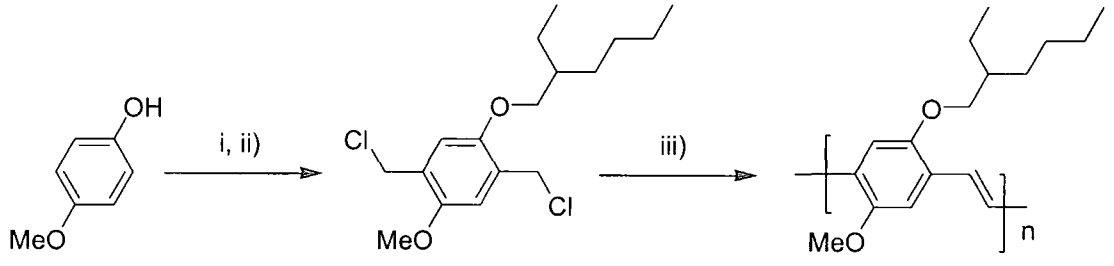

9 **10** **11**

Scheme 3: Synthesis of MEH PPV 11: i) 3-(bromomethyl)heptane, KOH, EtOH, reflux, 16 h; ii) HCHO, concd, HCl, dioxane, 20 °C, 18 h, reflux, 4 h; iii) KOtBu, THF, 20 °C, 24 h.

The importance of PPV as a material for OLEDs is reflected in the number of analogous compounds that have been synthesized and fabricated into devices since its discovery. Examples include cyano-dialkoxyPPV **12**,[17,18] dimethyloctylsilyl-PPV **13**,[19] and 2-phenylated and 2,3-diphenylated PPVs **14** with solubilizing side chains.[20]

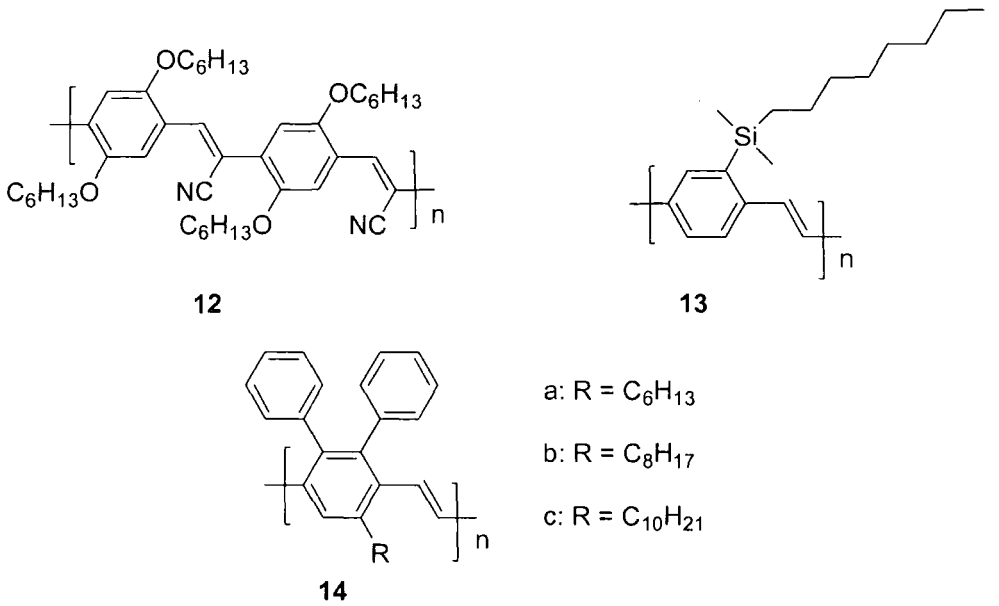

Scheme 4: Examples of soluble, dialkoxy-substituted PPV derivataives.

This group of polymers showed very good photoluminescence (PL) efficencies up to 65% in the solid state with blue shifted emission, PL λ_{max} 490 nm, for a fully conjugated PPV system. PPV and its derivatives still command substantial research showing huge promise as materials for commercial display technologies. It is, however, difficult to achieve blue light with this class of conjugated polymer and, in addition, there are fears regarding the susceptibility of the vinyl linkages to oxidative degradation.

1.3 Simple Organic Electroluminescent Devices Based on PPV

The device pioneered by Tang and VanSlyke[5] in 1987 comprising an aromatic diamine and Alq_3 sandwiched between two electrodes provided the foundation for EL devices using PPV as the emissive layer. Organic EL devices are made up of a sandwich like structure. PPV as the light-emitting polymer is spin-coated onto an indium-tin oxide (ITO) glass or polymer substrate that is semitransparent, then a low work function metal cathode such as Al, Ca or Mg is positioned directly onto the polymer surface. Such a device structure is denoted as ITO/polymer/metal. Poly(ethyleneterphthalate) (PET) is often used as the polymer substrate.

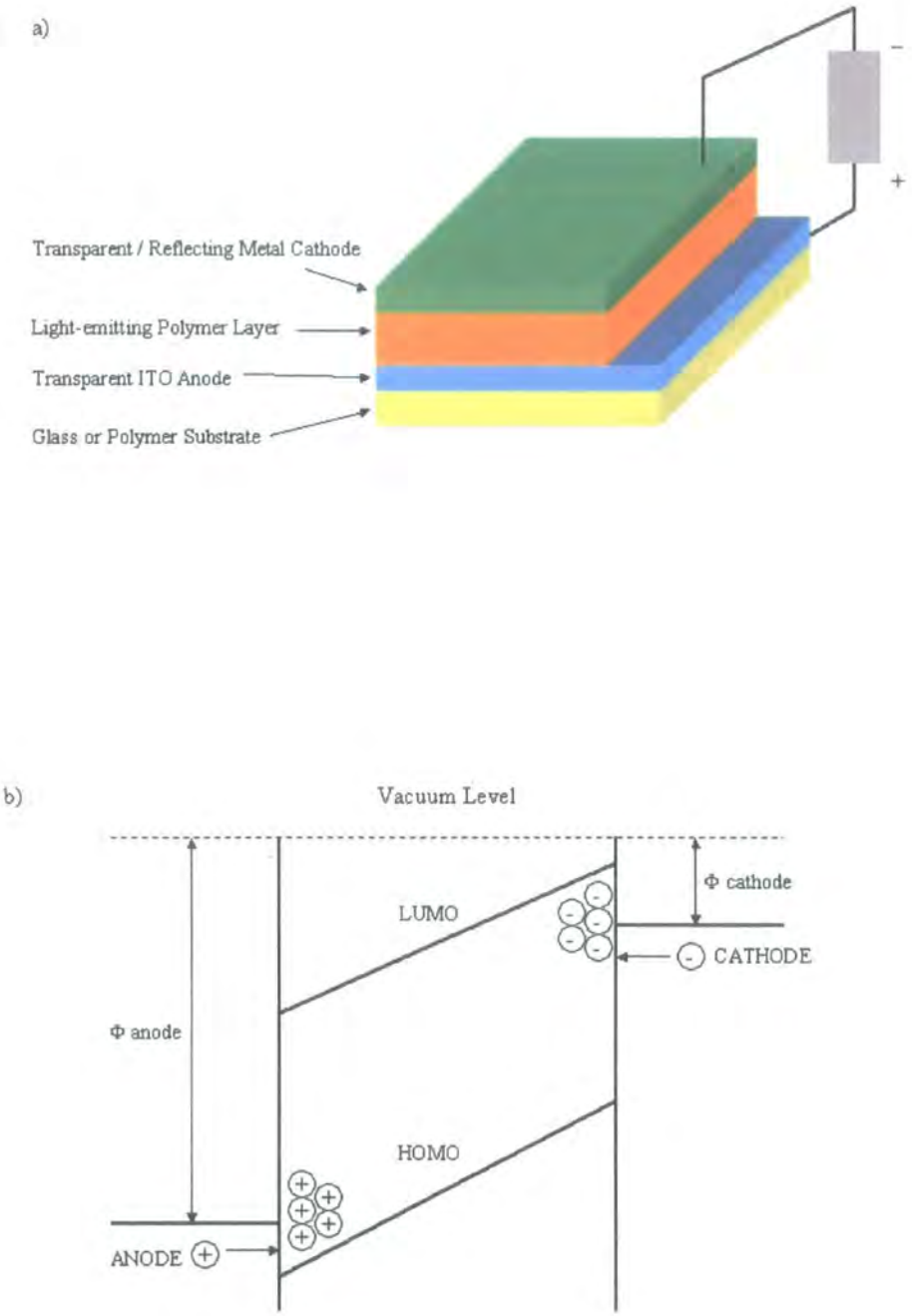

Figure 1: a) Schematic drawing of a single-layer electroluminescent device. b) Schematic energy level diagram of a generalised monolayer OLED (Redrawn from reference 3).

Light emission is a consequence of radiative decay of excitons generated by the combination of electrons and holes. Organic EL devices operate by the injection of electrons and holes

from positive and negative electrodes, respectively. The mechanism for light emission can be summarised as follows: electrons are injected into the LUMO forming radical anions and holes are injected into the HOMO forming radical cations of the EL polymer material. Charge migration along the polymer chain occurs under the influence of an applied electric field. When a radical anion and radical cation combine on a single conjugated polymer segment, singlet and triplet states are formed of which the singlet states can emit light.[11] The external quantum efficiency (EQE), η_{ext}, of monolayer OLEDs, *i.e.* the number of photons actually seen by the observer, is related to the number of photons emitted per electrons injected. In the case of PPV this value is low 0.05%.[7] The observed EQE, η_{ext}, is much lower than the internal efficiency, η_{int}, as given by the following relationship.[3]

$$\eta_{ext} = \eta_{int} / 2n^2$$

Equation 1: External quantum efficiency (EQE), η_{ext}, where n is the refractive index of the organic material.

1.3.1 Additional Charge Transport Layers

Since most common organic semiconductors are predominately hole transporting (p-dopable), electrons and holes usually combine in the vicinity of the cathode. As a consequence, the lifetimes and efficiencies of the corresponding diodes are limited.[21] The inclusion of an additional organic layer between the emissive material and the cathode metal can promote the passage of electrons through the EL material and, at the same time, inhibit the passage of holes. Such a layer is called an electron-conducting/hole-blocking (ECHB) layer. The ECHB material enhances the flow of electrons but resists oxidation. Electrons and holes accumulate near the PPV/ECHB interface. Charge recombination and photon generation occurs within the PPV segment and away from the cathode.[11] The overall effect of such charge transport layers is to reduce the operating voltage, increase the quantum efficiency and the device stability. One of the earliest examples of an ECHB material is Alq_3 **2**.

Electron-transport materials need to have a high electron affinity, *i.e.* be electron deficient. The most widely applied electron-transport materials are π-electron-deficient heterocyclcics carrying imine nitrogens in the aromatic ring. The polarisation of the $C^{\delta+}$-$N^{\delta-}$ bond due to the electron-withdrawing nitrogen atom lowers the energy of the LUMO and HOMO levels. This increases the electron affinity and promotes electron injection from the cathode.[3]

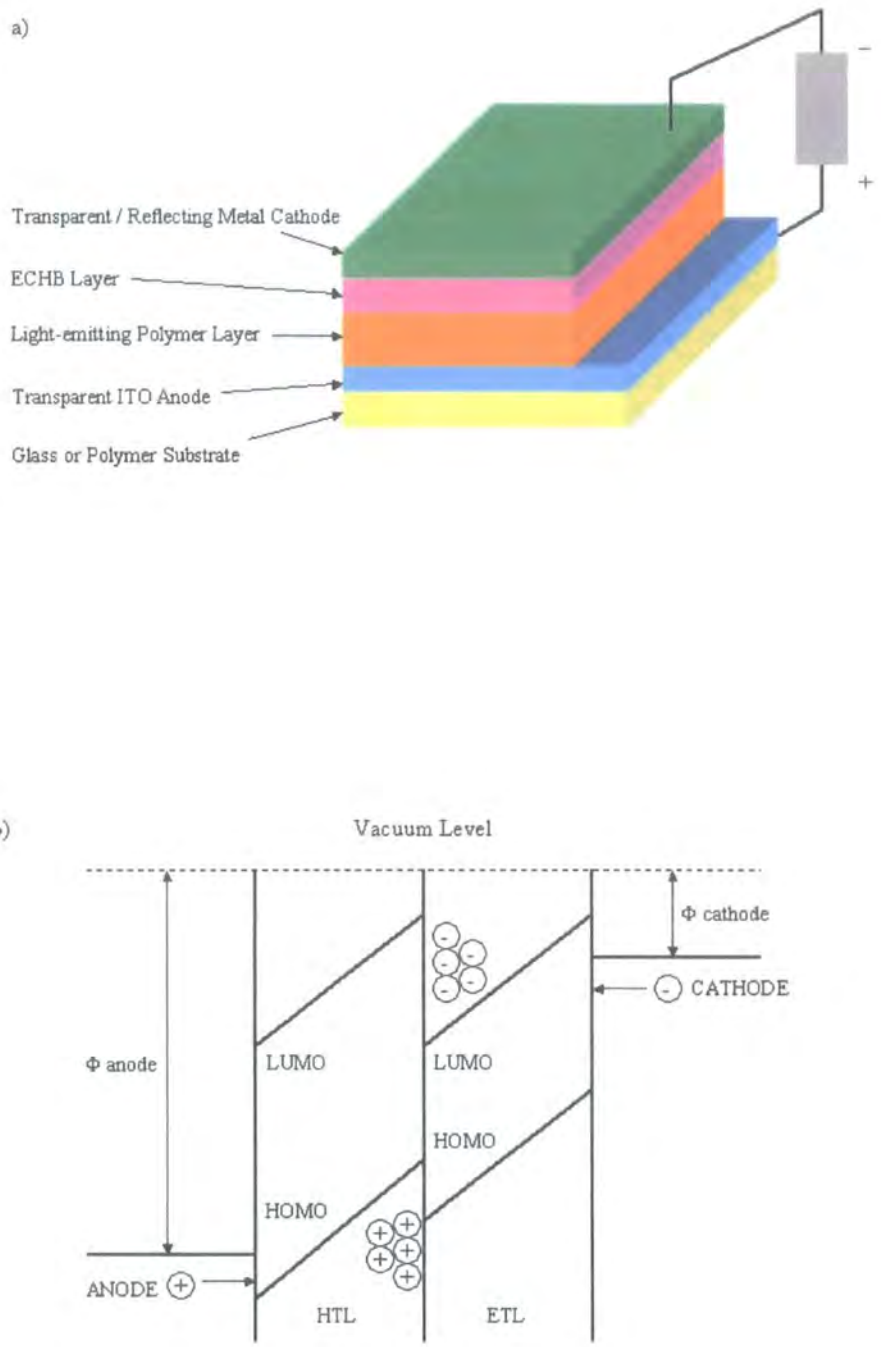

Figure 2: a) Schematic drawing of a bilayer OLED with an extra ECHB layer adjacent to the metal cathode. b) Schematic energy level diagram of a generalised bilayer OLED. Illustrating the accumulation of charge carriers at the interface of the hole-transport and electron-transport layers (Redrawn from reference 3).

π-Electron-deficient heterocycles have been widely used as ECHB layers, such as 1,3,4-oxadiazoles, 1,3-oxazoles, 1,2,4-triazoles, pyridines, pyrimidines, pyrazines, 1,3,4-triazines, quinolines, quinoxalines and pyrazoloquinoline derivatives. The remainder of this chapter will review the application of these classes of low-molecular-weight and polymeric materials as ECHB layers as well as emissive materials in EL devices.

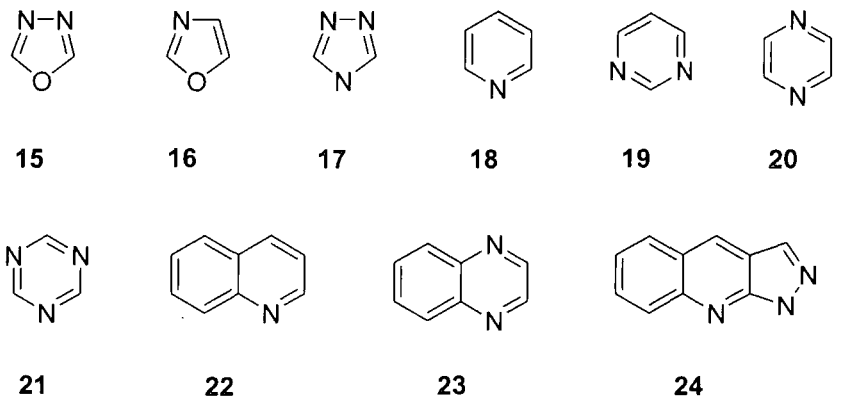

Scheme 5: Molecular structures of π-electron deficient heterocyclics with imine nitrogen atoms which have been incorporated into low molecular weight compounds and polymeric materials for use as ECHB materials.

1.4 1,3,4-OXADIAZOLES

2,5-Diaryl-substituted 1,3,4-oxadiazoles have received considerable attention as electron transporting materials in EL devices due to their electron-deficient nature and thermal stability. The majority of investigations have used 5-(4-biphenyl)-2-(4-*tert*-butylphenyl)-1,3,4-oxadiazole (PBD) **25** as the electron transporting material in sublimed thin films or spin-coated polymer blends.[11]

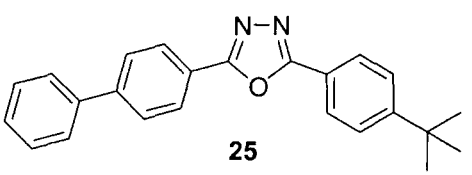

Scheme 6: Molecular structures of 5-(4-biphenyl)-2-(4-*tert*-butylphenyl)-1,3,4-oxadiazole (PBD) 25.

There are two common methods for the synthesis of 2,5-diaryl-1,3,4-oxadiazoles **26**. The first involves a ring closure dehydration reaction of bishydrazides **27** using reagents such as $POCl_3$.[22] The second, which is considered a more efficient method, is the reaction of tetrazoles **28** with acid chlorides **29**.[23]

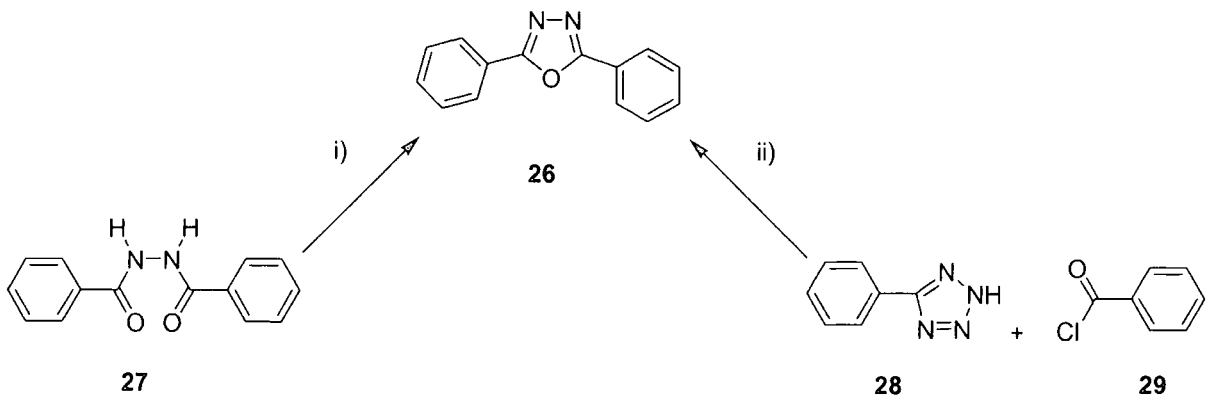

Scheme 7: Synthesis of 2,5-diaryl-1,3,4-oxadiazoles 26: i) $POCl_3$; ii) Pyridine, Δ.

1.4.1 Low Molecular Weight Oxadiazoles

Brown *et al*[24] demonstrated that PBD was a suitable ECHB material by blending the material in a film-forming poly(methylmethacrylate) on top of a PPV layer. An 8-10 fold increase in the EL efficiency was achieved compared with a simple EL PPV device. Zhang *et al* dispersed PBD into an active semiconducting polymer: dramatic increases in quantum efficiencies were reported by doping the soluble green emitter poly(2-cholestanoxy-5-thexyldimethysilyl-1,4-phenylenevinylene) (CS-PPV) **30**.[25]

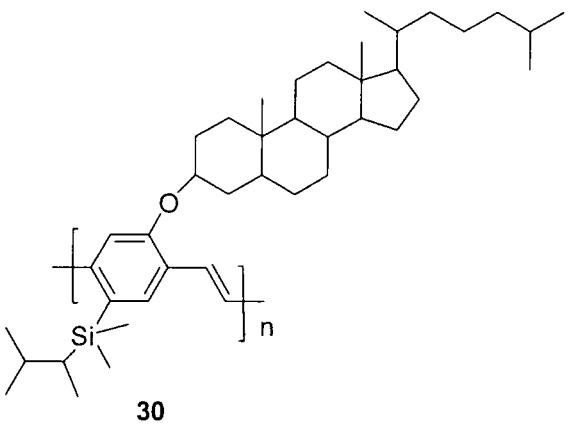

Scheme 8: Molecular structure of poly(2-cholestanoxy-5-thexyldimethysilyl-1,4-phenylenevinylene) (CS-PPV) 30.

Vaeth and Tang[26] reported the fabrication of polymer LEDs based on the emission from the phosphorescent molecule tris(2-phenylpyridine)iridium [$Ir(ppy)_3$] **31** doped into a poly(vinylcarbazole) (PVK) **32** host. To completely confine the emission zone to the $Ir(ppy)_3$:PVK layer a trilayered device was assembled. By replacing 10% of the PVK with PBD **25** and including the electron transporting materials 2,2′,2″-(1,3,5-benzenetriyl)*tris*(1-phenyl)-1H-benzimidazole (TPBI) **33** and Alq_3 **2** an exceptionally high external quantum

efficiency of 8.5% was observed. The device configuration was as follows ITO/$Ir(ppy)_3$:$PVK_{0.9}PBD_{0.1}$/TPBI/Alq_3/$Mg_{0.9}Ag_{0.1}$. However, further increases in PBD percentage levels into the polymer layer were found to reduce device performance.

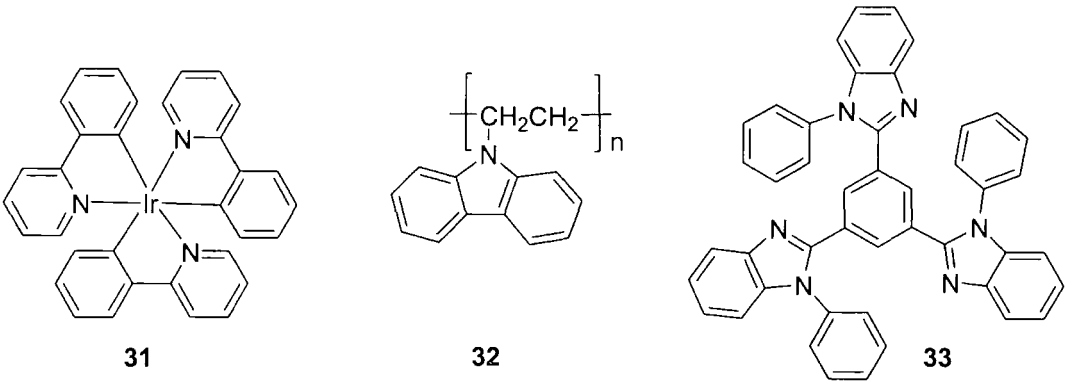

31 32 33

Scheme 9: Molecular structures of tris(2-phenylpyridine) iridium ($Ir(ppy)_3$) 31, poly(vinyl carbazole) (PVK) 32 and 2,2′,2″-(1,3,5-benzenetriyl)*tris*(1-phenyl)-1H-benzimidazole (TPBI) 33.[26]

Bipolar materials with electron accepting and donating capabilities provide a real alternative to bilayer devices involving the use of ECHB layers. Chien *et al*[27] reported 9,9′-spirobifluorene-bridged bipolar systems containing 1,3,4-oxadiazole-conjugated oligoaryl and triarylamine moieties. In this bipolar molecule **34** the 1,3,4-oxadiazole-conjugated oligoaryl system acts as the electron acceptor, while the triarylamine moiety acts as the donor counterpart. Guan *et al*[28] fabricated a highly stable, high performance blue electroluminescent device. Electron transporting 1,3,4-oxadiazole and hole transporting carbazole moieties were combined to create 2-(4-biphenylyl)-5-(4-carbazole-9-yl)phenyl-1,3,4-oxadiazole **35**. A three layered device with a configuration of ITO/TPD/CzOxa/Alq_3/$Mg_{0.9}Ag_{0.1}$/Ag exhibited blue emission at λ_{max} 470 nm with a maximum luminance of 26200 cd m^{-2} at a drive voltage of 15 V and a maximum luminous efficiency of 2.25 lm W^{-1}.

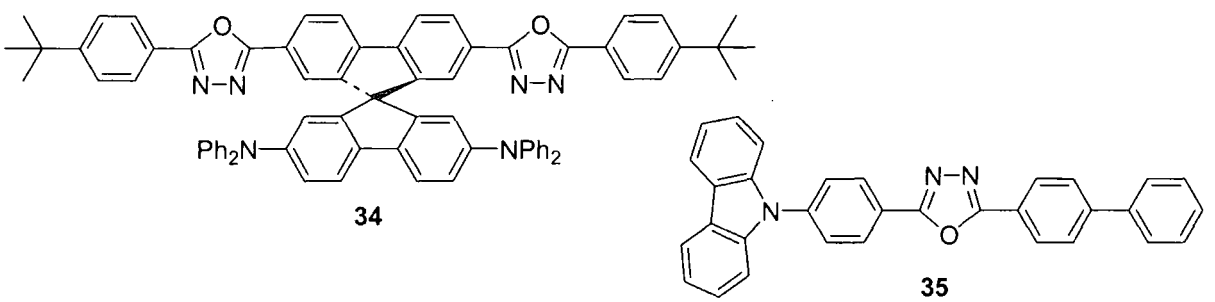

34 35

Scheme 10: Molecular structures of 9,9′-spirobifluorene-bridge[27] 34 and 2-(4-biphenylyl)-5-(4-carbazole-9-yl)phenyl-1,3,4-oxadiazole[28] 35 bipolar materials.

Within our group C. Wang has synthesised a series of 1,3,4-oxadiazole-pyridine and 1,3,4-oxadiazole-pyrimidine hybrids. In addition, vinylene and phenylene analogues were also prepared and their ECHB properties investigated.[29,30]

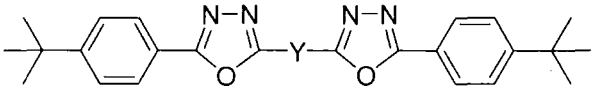

36 a-h

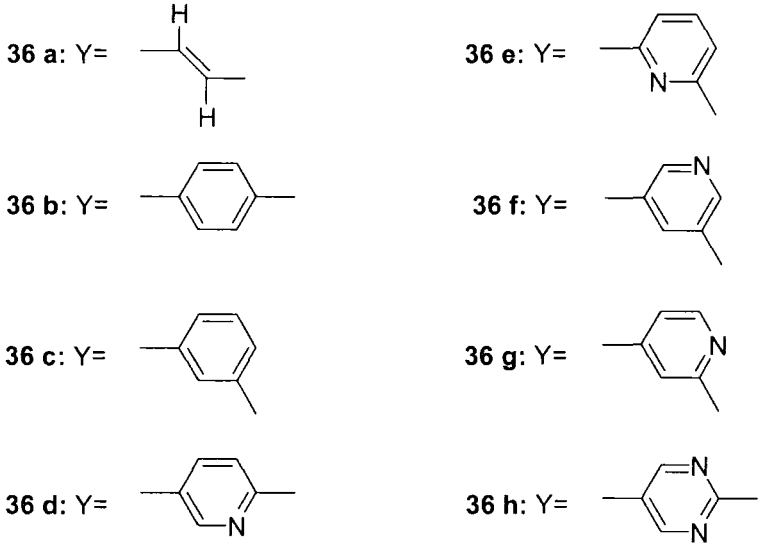

Scheme 11: Series of 1,3,4-oxadiazole hybrids synthesised by Wang *et al.*[29,30]

Initial studies focused on the fabrication and comparison of four types of devices: a single-layer LED using MEH-PPV **11** as the emissive material, ITO as the anode, and aluminium as the cathode; and the three bilayer LEDs with the structure ITO/MEH-PPV/PD**X**DP/Al where PD**X**DP layer was **36a**, **36b**, or **36d**. The three bilayer structures yielded almost identical current versus electric field data, suggesting similar electrical transport processes in the three devices. The turn-on electric field for EL was lower for the bilayer structures than for the single layer counterpart. The lowest value was observed for the LED with **36d**. External quantum efficiencies (EQE) were as follows: for the MEH-PPV device 0.0059%, for the bilayer device using **36a** 0.011%, for the **36b** containing structure 0.042%, and 0.24% for the LED incorporating **36d**. The EQE of the MEH-PPV single layer device was approximately doubled by using **36a**, increased by 6 times with **36b**, and increased by about 30 times with **36d**. EL emission for the bilayer devices was characteristic of MEH-PPV emission and independent of the PDXDP electron transport layer, indicating that all light originates from the MEH-PPV layer.

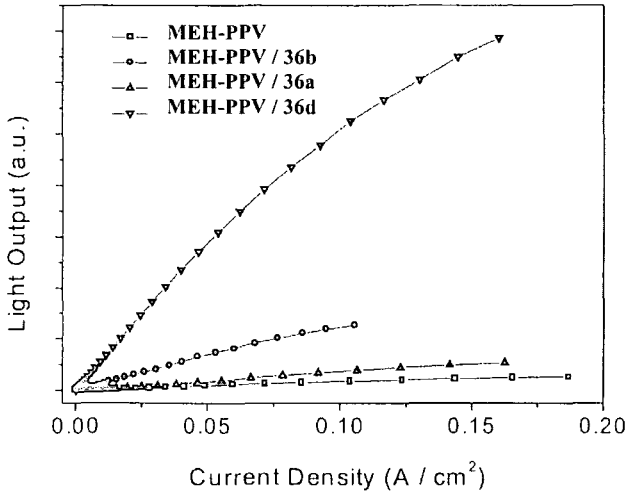

Figure 3: Light output versus current density for the single-layer and bilayer LED devices of 1,3,4-oxadiazole hybrids prepared by Wang and co-workers.[29]

The improved electron transporting performance of **36d** over the two analogues **36a** and **36b** was due to increased electron deficiency arising from the more electronegative nitrogen atom in the pyridine moiety, and secondly that electron mobility is higher in crystalline **36d** than the other two materials.[29] The X-ray crystal structure of **36d** was obtained.

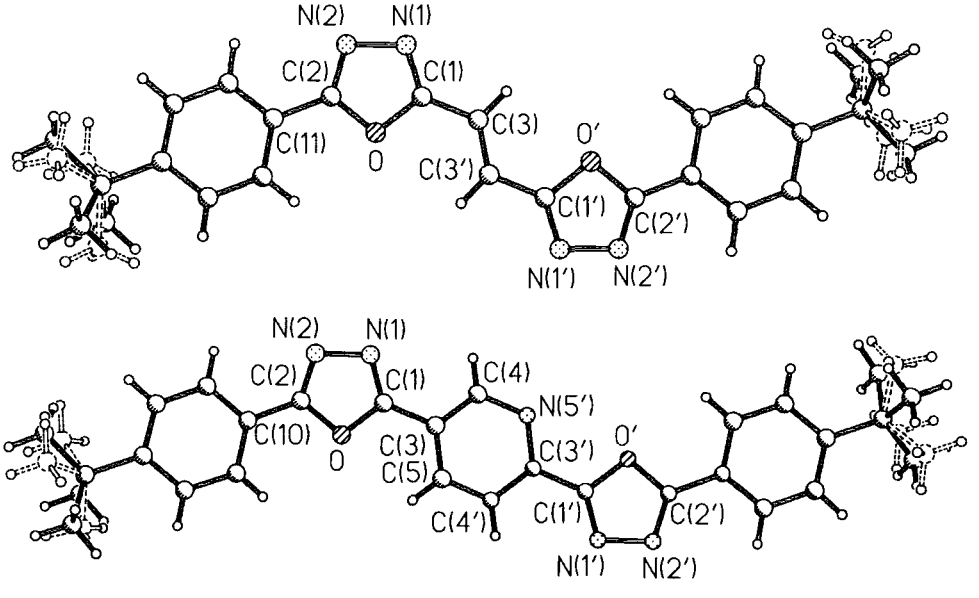

Figure 4: X-ray molecular structures of 36a (top) and 36d (bottom), showing the disorder of the *tert*-butyl groups. Primed atoms are generated by inversion centres. The pyridine N atom in 36d is disordered between positions 4, 4′, 5, and 5′.[29]

Continuing investigations in our laboratories demonstrated that OXD-7[31] **36c** and its *para* isomer **36b**, had different electron-injecting abilities in bilayer LEDs using MEH-PPV as the emissive material.[32] In view of this observation and the success of **36d**, geometrical isomers

36e-g were synthesised. The success of **36d** was attributed to its increased electron deficiency compared to its vinylene and phenylene counterparts. Therefore **36h** was prepared as an analogue of **36d** with an additional nitrogen atom introduced into the central conjoining ring.

Devices were constructed using ITO as the anode, rubrene doped (20% by weight) MEH-PPV [MEH(Ru)] as the emissive material and Al as the cathode. A single layer rubrene doped MEH-PPV device was used as a reference. Bilayer devices were of the general configuration ITO/MEH(Ru)/compound **36**/Al. In every case the inclusion of a 1,3,4-oxadiazole containing material as an ECHB layer increased electron injection. This was clearly reflected in the EQEs, which showed increases of 5 to 20 times greater than that of the rubrene doped reference. The EQE for reference ITO/MEH(Ru)/Al device was 0.07%. For **36d** and **36e** an EQE of 0.14% was achieved for both respective devices. The more electron deficient **36h** achieved a lower figure of 0.12% which is comparable with that of 0.11% for **36b**.

Further increases in EQEs for this series of materials have been achieved by optimising both the MEH(Ru) and ECHB layers. An EQE of 0.7% was achieved by ITO/MEH(Ru)(90 nm)/**36d** (55 nm)/Al structure.

Figure 5: A photograph of a bilayer LED ITO/MEH(Ru)(90 nm)/36d (55 nm)/Al working at a current density of *ca.* 100 mAcm^{-2} under forward bias, without encapsulation. The peak external quantum efficiency of the LED was *ca.* 0.7% and the brightness was *ca.* 4,000 cd m^{-2}.[30]

As with previous observations, EL of the bilayer LEDs had almost identical emission profiles as the single layer device, indicating that charge-combination and light emission took place exclusively in the MEH(Ru) layer.[30]

Although such low molecular weight 1,3,4-oxadiazole materials can be easily prepared and purified, their amorphous films can suffer from a lack of stability since crystallisation occurs with time or increased device operation temperature. 1,3,4-Oxadiazole polymers **(Section 1.4.2)** can be prepared conveniently but effective purification can be difficult. In contrast, dendrimers are highly-branched well-defined compounds and, like polymers, they have the advantage of forming stable amorphous glasses.[33]

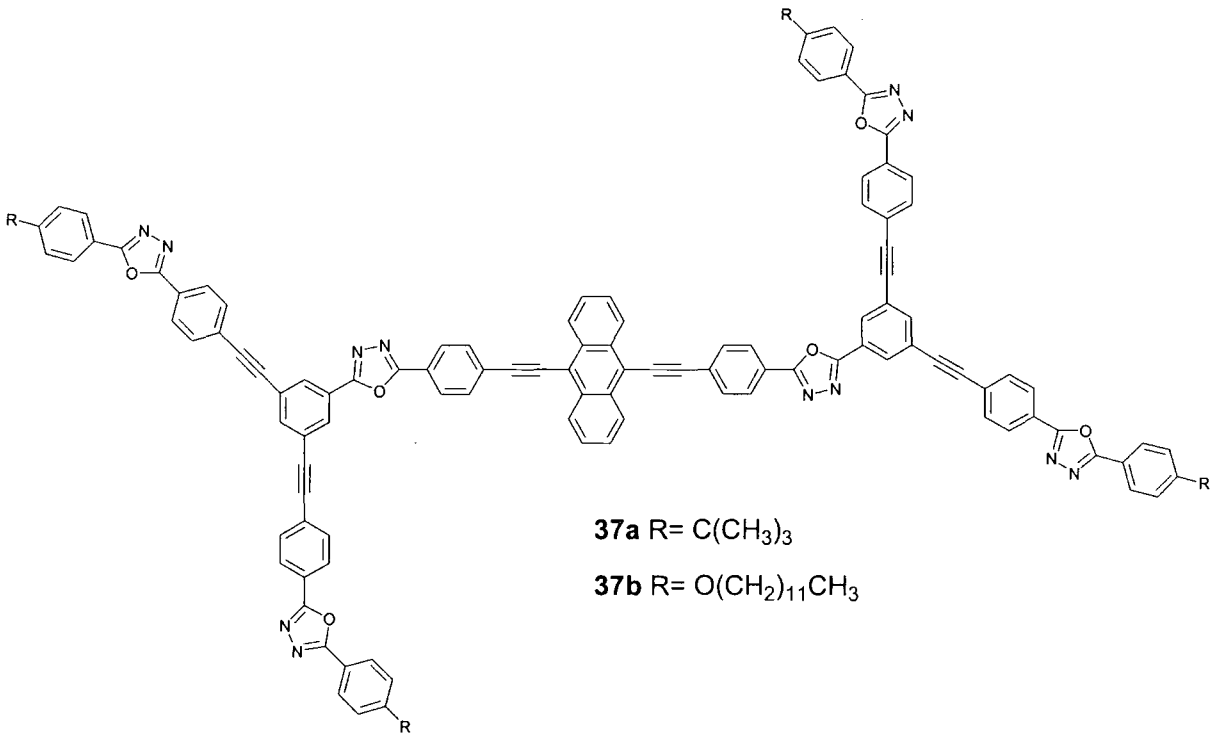

37a R= $C(CH_3)_3$

37b R= $O(CH_2)_{11}CH_3$

Scheme 12: Molecular structures of four-armed conjugated dendrimers containing 1,3,4-oxadiazole moieties.[34]

Cha and co workers[34] successfully synthesised two, four-armed conjugated dendritic structures with a 9,10-bis(phenylethynyl)anthracene core and 1,3,4-oxadiazole rings incorporating peripheral alkyl tail groups. It was found that **37b** has a high glass transition temperature (*Tg*: 211 °C) and exhibits good solubility in organic solvents, which resulted in good quality thin films by spin coating. In contrast, its *tert*-butyl counterpart **37a** has poor solubility which gave inferior quality thin films. An EL device structure of ITO/PEDOT-PSS/**37b**/Li:Al emitted only red light with an EQE of 0.02%. The (phenylethynyl)anthracene core is the only red light emitting chromophore in the structure which indicated that the outer diphenyloxadiazole moieties act only as electron transporters.

The thermal and EL properties of tetraphenylmethane-based compounds has remained largely unexplored. Tetraphenylmethane is a useful structural unit for forming glassy films that can

be readily incorporated into light-emitting or charge-transporting materials by varying the peripheral substituents. Yeh *et al*[35] produced a series of compounds with this core structural unit, e.g. the amorphous bipolar blue fluorescent **38**, which has a high *Tg* of 150 °C.

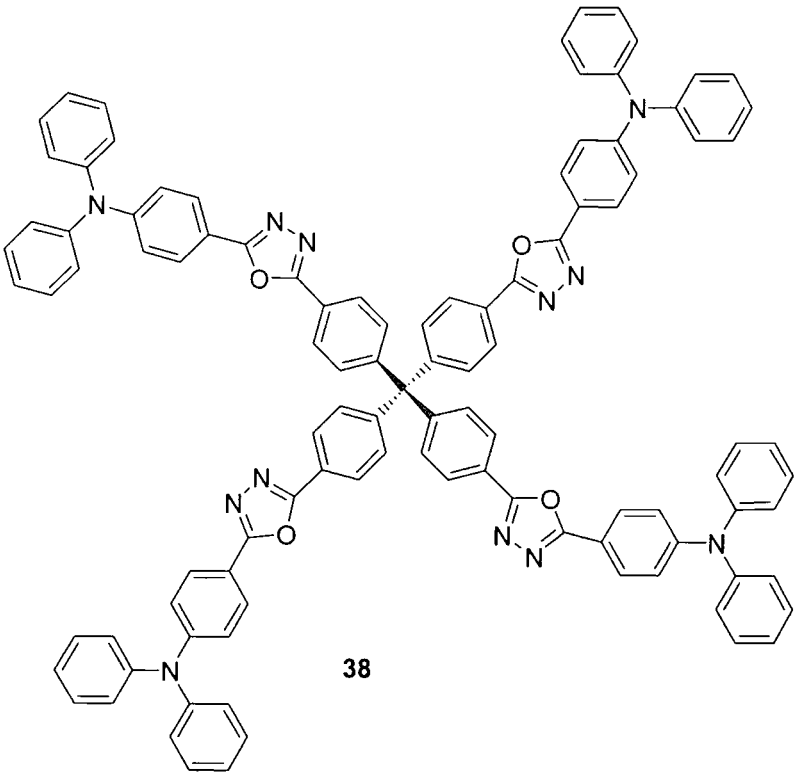

38

Scheme 13: Amorphous bipolar blue fluorescent 38.[35]

A single layer device of the structure ITO/**38**/Ca/Ag showed blue luminescence at low applied voltage that turned to bluish-white at elevated applied voltages. The device had a photometric efficiency of ~0.7 cd A at a current density of ~10 mA cm^{-2}. The device brightness reached a maximum of 1690 cd cm^{-2} under a driving voltage of ~14 V. Since **38** functions as an electron transporting material, doping an emissive layer host material may provide a more efficient device. Doping of PVK with **38** in a 3:1 weight ratio for the device configuration ITO/**38**:PVK/Ca/Ag resulted in an enhanced photometric efficiency of 0.8 cd/A with a current density of less than 8 mA cm^{-2}. This demonstrated that the 4-fold symmetrical tetraphenylmethane is an effective skeleton for improving thermal properties, which are high melting temperature and stable glass phase.

Liang *et al*[36] reported the successful synthesis of the blue emitting hydroxyphenyloxadiazole lithium complex **39**. To investigate its EL properties, OLEDs based on **39** as the emitting and electron injection/transport layers were constructed. **39** as the emitting layer displayed blue EL emission centred at λ_{max} 468 nm for the configuration ITO/TPD/**39**/Al with a maximum

luminance of 2900 cd m^{-2}. A current efficiency of 3.9 cd A^{-1}, and power efficiency of 1.1 lm W^{-1} was obtained. TPD was chosen for its hole-transporting qualities. The efficiency of an ITO/NPB/Alq_3/Al device increased considerably when **39** was inserted between Alq_3 and aluminium. The performance of **39** as an interface material is directly related to optimum thickness of the lithium complex. The device specification was as follows, ITO/NPB(40 nm)/Alq_3(60 nm)/ **39** (*x* nm)/Al where *x* = 2 nm gave the best performance with a maximum luminance of 18389 cd m^{-2} at a turn-on voltage of 3.0 V. Furthermore, this device exhibited high current and power efficiencies with values of 5.21 cd A^{-1} and 2.4 lm W^{-1}, respectively. The impressive EL efficiency may be attributed to i) the oxadiazole segment in **39** has excellent electron-transporting ability and ii) the lithium salt is favourable for electron injection.

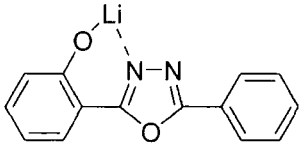

39

Scheme 14: Hydroxyphenyloxadiazole lithium complex 39.[36]

1.4.2 Polymeric Oxadiazoles

The synthesis of π-conjugated polyoxadiazoles has been achieved by direct analogy with their low-molecular-weight counterparts, that is by ring closure of polyhydrazides with reagents such as $POCl_3$ and polyphosphoric acid or, alternatively, reaction of bis(tetrazole)s with bis(acid chloride)s. In addition, poly(oxadiazole ether)s can be prepared by activated nucleophilic substitution polycondensation of oxadiazole difluorides with aromatic diols. The electron deficient oxadiazole ring is incorporated directly into the main chain of the polyaryl ether or by attaching it as a pendant group to the polymeric aryl backbone.

Zheng and co-workers[37] reported a series of alternating copolymers containing 1,3,4-oxadiazole groups in the conjugated chain, together with flexible spacer units, with the objective of raising electron-transport ability. The effects of chromophore substituents on the optical properties of the copolymers were investigated.

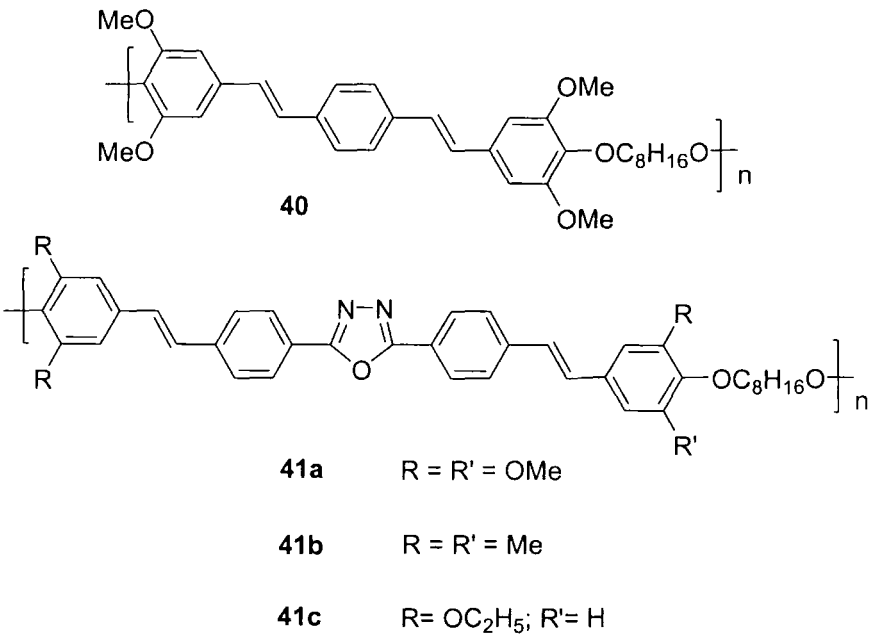

41a R = R' = OMe

41b R = R' = Me

41c R= OC_2H_5; R'= H

Scheme 15: Segmented reference and 1,3,4-oxadiazole copolymers as prepared by Zheng et al.[37]

Blue-green light was observed for the copolymers as single-layer devices relative to that of the reference copolymer **40**. The general device configuration was ITO/copolymer **40a-c**/Ca/Al; EL maxima for devices based on **41a**, **41b**, **41c** and the reference **40** were λ_{max} 494, 509, 480 and 477 nm, respectively. EL for **41a** and **41b** were comparable with their corresponding PL λ_{max} 475 and 458 nm, which indicated that EL and PL originate from the same excited state. However, EL for **41c** was significantly red-shifted compared with its PL λ_{max} 455 nm. The copolymers not only were used as blue-green EL materials, but also were effective as ECHB layers in polymer LEDs. For the double-layer OLED ITO/PPV/**41c**/Ca/Al no emission was observed from **41c** indicating that the PPV serves as the emissive layer and **41c** as the electron transport layer. The brightness and efficiency of its single-layer counterpart ITO/PPV/ Ca/Al was improved by more than a factor of 10^3 with the introduction of **41c**. The double-layer device had a brightness of 2400 cd m^{-2} at 6.8 V with an EQE of 0.094%. This work demonstrates that the oxadiazole moiety in **41c** moves the recombination zone away from the cathode interface and increases the probability of hole/electron recombination in the PPV emitting layer.

Bipolar polymeric materials have attracted great interest as researchers attempt to harness both hole and electron transporting properties. Zhang *et al*[38] published the synthesis of two bipolar transporting luminescent polymers containing hole-deficient triphenylamine and electron-deficient 1,3,4-oxadiazole units in the main chain.

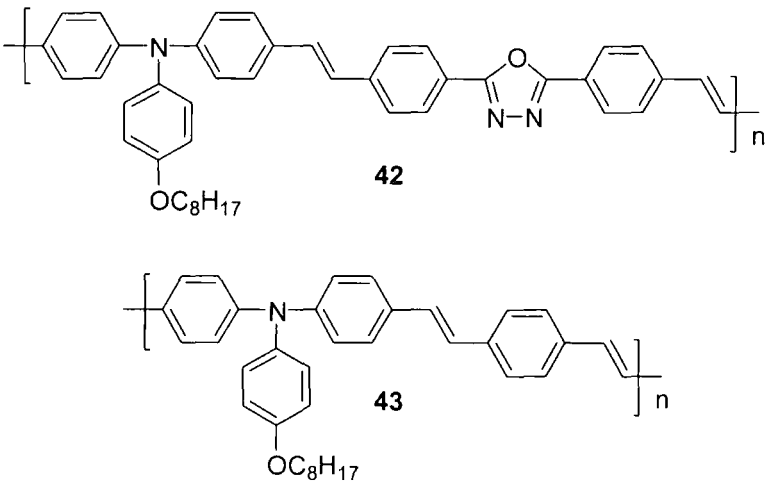

42

43

Scheme 16: Bipolar luminescent polymers prepared by Zhang *et al.*[38]

UV-vis absorption spectra of thin films of the two polymers showed that the main absorption peak is red-shifted from λ_{max} 470 to 495 nm due to the inclusion of the electron-deficient oxadiazole ring. A similar red-shift was also observed in the PL spectra, from λ_{max} 545 to 555 nm. The introduction of the oxadiazole unit increases the conjugated length of the polymer, which results in the red shift. Devices of the configuration ITO/PEDOT/polymer **42** or **43**/CsF/Al gave blue EL. The polymer with oxadiazole units **42** has a maximum brightness of 3600 cd m^{-2} and a maximum EL efficiency of 0.65 cd A^{-1} equal to an EQE of 0.3%. In contrast, the performance of polymer **43** has a significantly reduced maximum brightness of 248 cd m^{-2} and lower EL efficiency of 0.042 cd A^{-1}. Devices constructed using **42** were 15 times brighter and 15 times more efficient than the corresponding polymer without oxadiazole moieties.

Another example of a bipolar polymeric material is **44** prepared by Meng *et al.*[39] **44** emits greenish-blue light at 475 nm. A preliminary device of the configuration ITO/**44**/Al was constructed and emitted blue light (observable in a dark room) at 8 V with a current density of 1.14 cd m^{-2}. Initial findings suggest that **44** could be a potential novel active material as it has a similar LUMO but higher HOMO energy level when compared to MEH-PPV **11**. This implies that it has more balanced charge injection, which ultimately enhances EL EQEs.

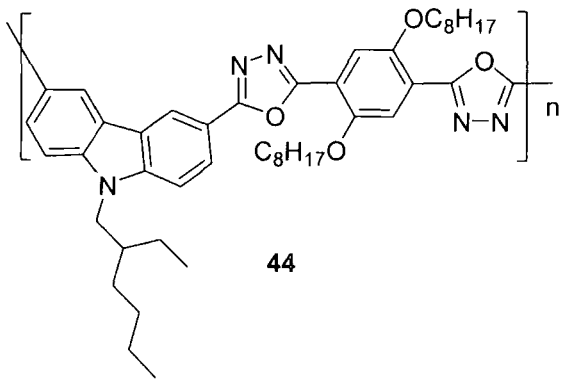

44

Scheme 17: Polymeric structure of PCOPO 44.[39]

p-OXD **45** was used a ECHB material in PPV based devices and its electron–transporting capabilities evaluated against triazine (*p*-TRZ) and quinoxaline (*p*-QUX) counterparts. [40]

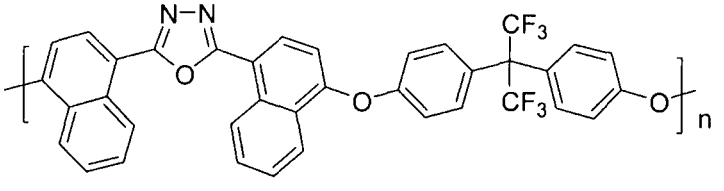

45

Scheme 18: Structure of *p*-OXD 45 synthesised from the corresponding difluoroheterocyclic monomers with hexafluorobisphenol via a nucleophilic displacement reaction of fluorine atoms by intermediate phenolate anion.[40]

Polymer **45** forms stable glasses with a *Tg* of 220 °C measured by DSC; it also has high thermal stability with a decomposition temperature of 415 °C. Optical data showed no absorption in the visible region of the spectrum [λ_{max} (abs) 347 nm] and a fluorescence λ_{max} (emission) 433 nm. Polymer **45** is readily soluble in common organic solvents and possesses excellent film forming properties.

A bilayer device of configuration ITO/PPV/**45**/Al demonstrated that **45** possesses hole-blocking capabilities showing increased operational performance in comparison to the reference single layer device. A maximum brightness of 55 cd m^{-2} at a current density of 155 mA cm^{-2} was recorded at a onset voltage of 7.0 V, compared to the reference which gave a maximum brightness of 2 cd m^{-2} at a current density of 436 mA cm^{-2}, although a lower onset voltage of 6.0 V was achieved.

Peng *et al*[41] reported polymers containing both electron-accepting oxadiazole and hole-accepting alkoxy-phenylenevinylene segments, as an alternative to bilayer/multilayer devices. Fabrication of multilayer devices is difficult, and stability can be a problem.

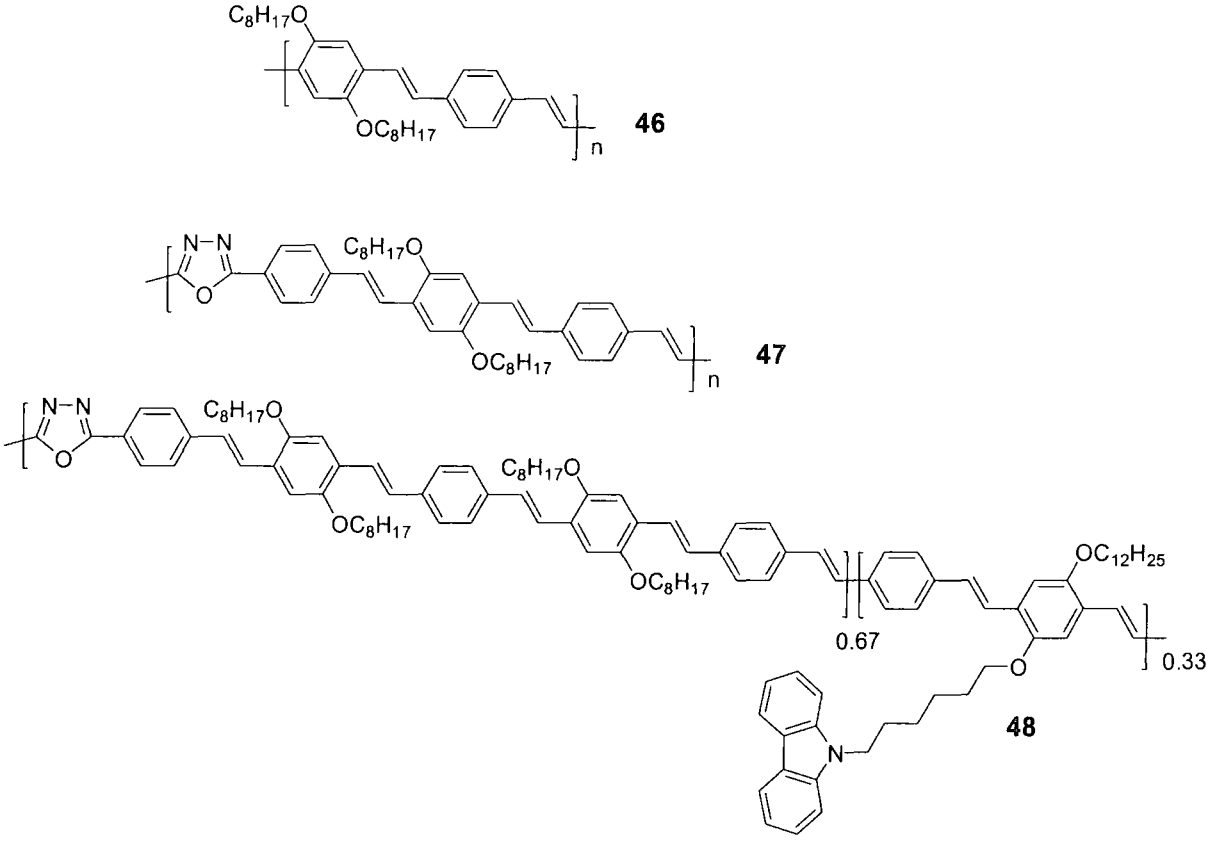

Scheme 19: Structures of polymers 46, 47 and 48.

UV-Vis absorption spectra of **47** and **48** in THF solution are very similar to **46**, although the structures are very different with λ_{max} ca. 450 nm, showing no observable effect of the oxadiazole ring. Compounds **47** and **48** have similar PL in THF solution with emission peaks at 505 nm and a shoulder around 540 nm, similar to that of **46**. As solid films **47** and **48** have significantly different PL, **48** has emissions red-shifted by 50 nm due to aggregation. **47**, however, showed a smaller red shift of 35 nm.

As single-layer devices using ITO and Al as the contacts, **47** and **48** showed good light-emitting device characteristics with enhanced brightness compared to **46**. These results support the hypothesis that the oxadiazole units in the main chain improve electron acceptor ability and electron mobility in the device structure. The carbazole substituent in **48** had little effect, suggesting that the polymer backbone itself has sufficient hole-transporting ability.

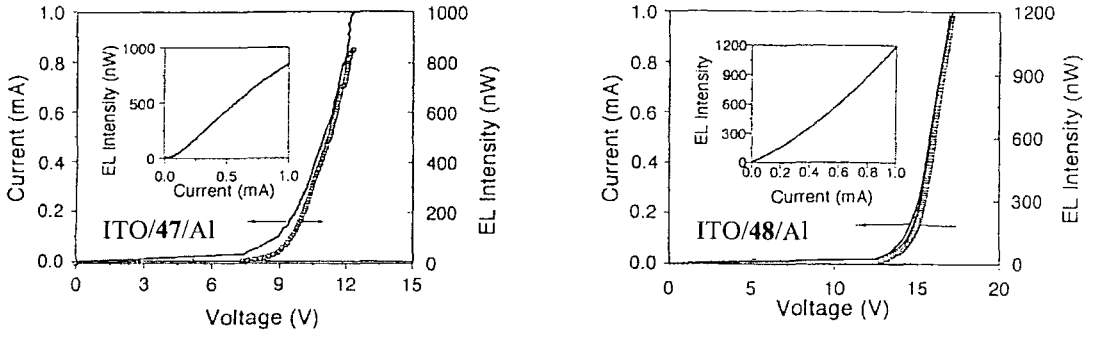

Figure 6: Current-light-voltage characteristics for single layer devices of polymers 47 and 48. The insets show light vs current for the two respective devices.[41]

PBD **25** has been extensively used as a small-molecule electron-transport material due to its known capabilities of dramatically improving the EQE in OLEDs. In our group Wang *et al*[42] prepared the alkoxyPBD **49** derivative and its dipyridyl analogue **50** using Suzuki coupling methodology. These were the first polymeric materials containing PBD as the repeating unit. The alkoxy substituents impart good solubility in organic solvents.

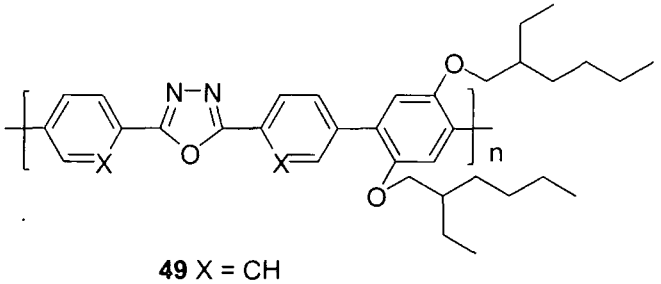

49 X = CH

50 X = N

Scheme 20: Polymeric alkoxyPBD 49 and its dipyridyl analogue 50 prepared by Wang *et al.*[42]

Thermal gravimetric analysis established that polymers **49** and **50** are highly stable up to 370 °C and 334 °C, respectively. The two polymers are also amorphous with *Tg* values of 196 °C for **49** and 113 °C for **50**. PL spectra of films spun from chloroform solution showed strong blue PL with λ_{max} 444 nm. Polymer **50** has a PL quantum yield (PLQY) of 27% measured as a thin film using an integrated sphere. The dipyridyl analogue displayed blue PL with λ_{max} 475 nm, which is significantly red-shifted compared to the emission of **49**. Attempts to measure the PLQY for **50** were hampered by film degradation; however, the authors estimate the value to be 6% with a large percentage error. A possible explanation for this degeneration of the film could be cleavage of the polymer chain, leading to instability of the sample and low PLQY. Device studies were not pursued further with **50** since questions had been raised

over the material's stability. Polymer **49** was investigated as an electron-transporting polymer in bilayer LEDs with MEH-PPV as the emissive layer onto which **49** was spun. For the device ITO/PEDOT/MEH-PPV/**49**/Al an EQE of 0.26% and brightness of 800 cd m^{-2} was readily achieved. For comparison a similar device without **49** was fabricated i.e., with MEH-PPV as the only semiconducting polymer layer. An EQE of 0.01% and brightness of 15 cd m^{-2} was realised. Orange emission was seen from both single and bilayer devices the spectra of which were identical to the EL from MEH-PPV.

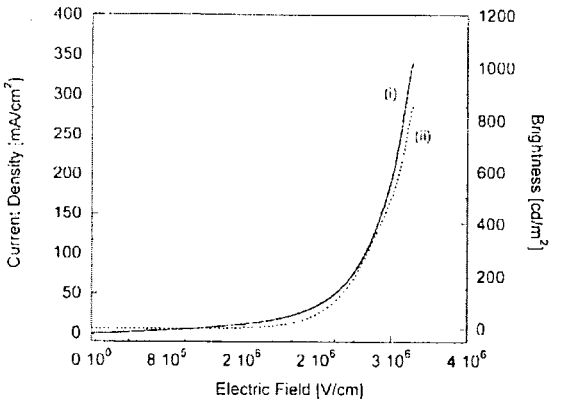

Figure 7: Current density-field (i) and light-output-field (ii) of an ITO/PEDOT/MEH-PPV/49/Al device.[42]

Two PPV-based polymers with pendant oxadiazole units were reported by Chen *et al*,[43] with the intention of imitating PDB and utilising the EL abilities of both PPV and PDB. The copolymer **51** was completely soluble in organic solvents, which was in contrast to the insolubility of homopolymer **52**.

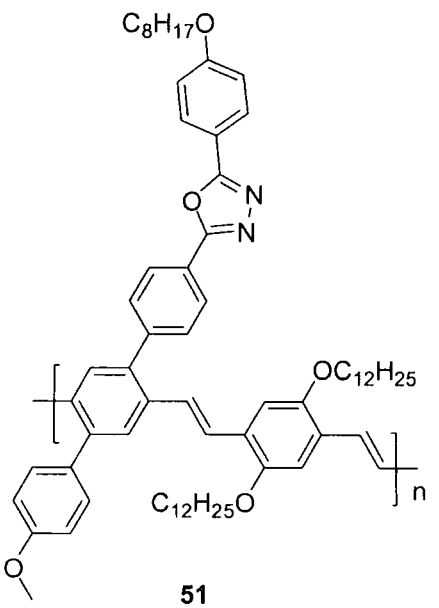

51

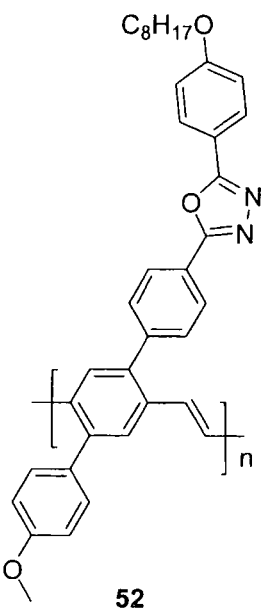

52

Scheme 21:Structures of oxadiazole containing PPV polymers prepared by Chen *et al*.[43]

Copolymer **51** is highly stable with an onset for degradation at 386 °C. A high *Tg* of 205 °C was also reported which is rarely the case for a PPV derivative such as MEH-PPV. When excited at 426 nm, PL spectra of copolymer **51** showed λ_{max} 560 nm, which corresponds to orange-yellow light.

Several other groups have reported attaching PDB as a pendant unit directly to the PPV backbone. Lee *et al*[44] reported two new PPV derivatives bearing PDB **53** and **54**. The only structural difference between the two polymers is the presence of an additional 2-ethylhexyloxy side chain in **54**.

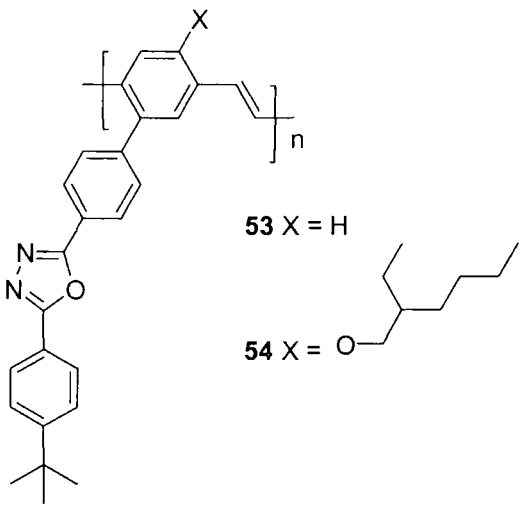

Scheme 22: Structures of PPV derivatives bearing PDB pendants prepared by Lee *et al*.[44]

Excitation at 420 nm gave PL λ_{max} of 530 nm and 534 nm for polymers **53** and **54**, respectively, which are comparable with 540 nm for PPV. EQEs for devices of **53** and **54** were, respectively, 16 and 56 times the value of their PPV analogue. In particular, the device of configuration ITO/PEDOT/**54**/Al:Li has a maximum brightness of 1090 cd m^{-2} with a EQE of 0.045%. Device investigations demonstrate that the incorporation of the 2-ethylhexyloxy substituent of **54** improves EL efficiency in comparison to **53**, which does not bear that substituent. This is supported by earlier findings of Wudl *et al* that the presence of long or bulky substituents enhances the device efficiency by reducing the possibility of the formation of polaron pairs.[45] In addition, the bulk substitution with aromatic rings and electron-withdrawing oxadiazole containing side chains on the phenylene ring also has the potential advantage of dispersing the electron density on the vinylene segment so as to minimise oxidation.[43] Further increases in EQE for PPV related polymers have been achieved by incorporating additional oxadiazole units into both the main chain and pendant side chains.[46]

1.5 1,3-OXAZOLES

1,3-Oxazoles are less electron deficient than 1,3,4-oxadiazoles. Consequently there are far fewer examples of 1,3-oxazole OLED materials than their 1,3,4-oxadiazole counterparts. 2,5-Diaryl-1,3-oxazoles **56** are prepared by the cyclocondensation of the amides **55**. In practice this dehydration can be carried out using a broad range of acids or acid anhydrides such as phosphoric acid, $POCl_3$, phosgene and thionyl chloride.[47]

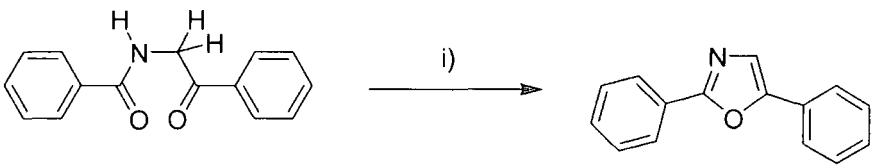

55 **56**

Scheme 23: Synthesis of 2,5-diaryl-1,3-oxazole 56: i) Phosphoric acid, $POCl_3$, phosgene or thionyl chloride.[47]

1.5.1 Low Molecular Weight Oxazoles

Jordan *et al*[48] reported the fabrication and characterisation of a white-light emitting OLED which has a maximum brightness of 4700 cd m^{-2} and a luminescent efficiency of 0.5 lm W^{-1}. A thin layer of the blue emitting material **57** was inserted between, hole-transporting TAD **59** and electron-transporting Alq_3 **2** layers in the device configuration ITO/TAD/**57**/Alq_3/Al which produced white light emission. Compounds **57** and **58** were prepared as detailed in the literature reference[49].

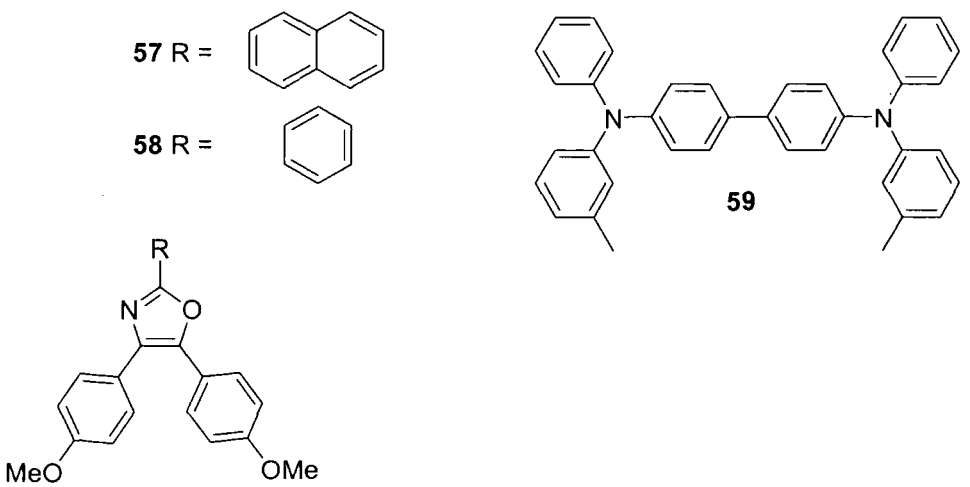

Scheme 24: Structures of compounds 57, 58 and TAD 59.[48]

Compound **57** has a broad luminescence spectrum spanning the range 400-650 nm with a significant fraction of emission occurring at wavelengths where Alq_3 emits poorly. The

corresponding single layer device (without **57**) emitted green light λ_{max} 540 nm. More light was observed by increasing the thickness of the **57** layer. Charge recombination must occur in this vicinity, therefore, **57** may be considered primarily as an electron transport material. Substitution of **57** with **58**, which does not emit light but possesses similar transport properties, produces EL emission typical of a TAD/Alq_3 device. This indicates that **57** is responsible for the blue spectral components of the white emission, and not TAD. The proportion of red and green wavelengths was tailored by incorporating low percentages of the reddish dye DCM 1 into the Alq_3 at the **57** interface.

1.6 1,2,4-TRIAZOLES

1,2,4-Triazoles are π-electron deficient thermostable heterocyclic materials similar to 1,3,4-oxadiazoles. Synthesis of 3,5-diaryl-1,2,4-triazoles **62** involves a ring closure dehydration reaction of bis(hydrazides) **60** with aryl amines **61** in the presence of strong acids or alternatively by reaction of 5-aryltetrazole **63** with imine chloride **64** in pyridine.[11]

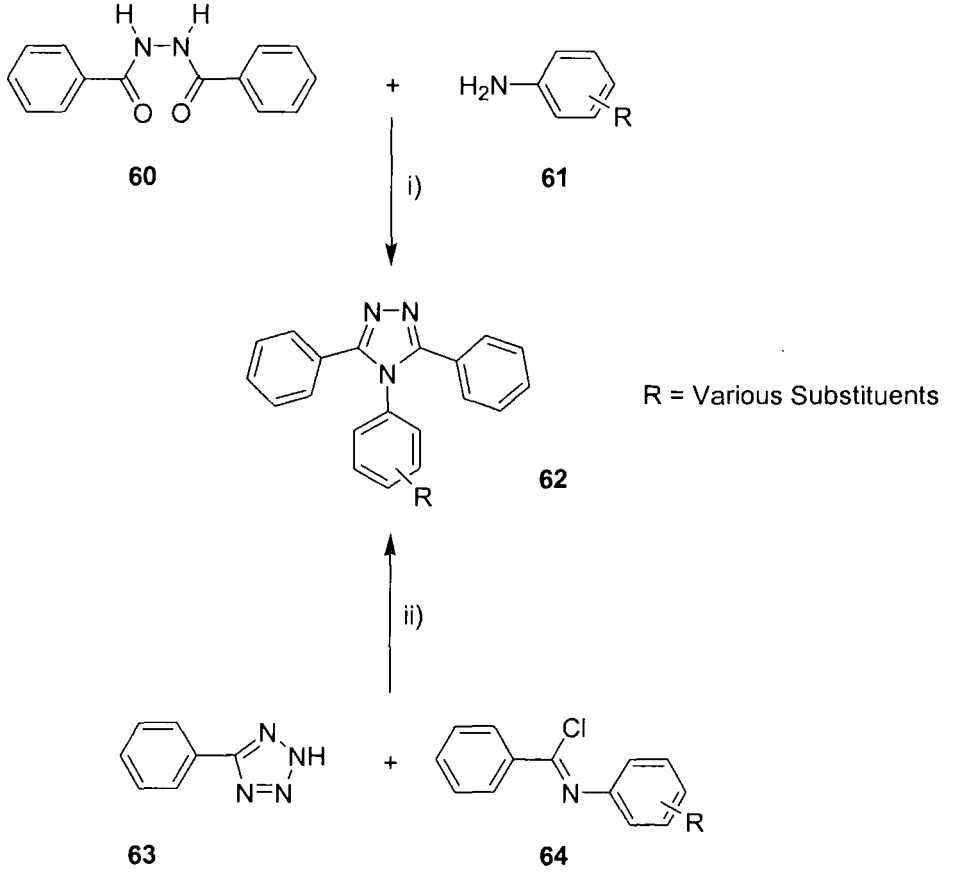

Scheme 25: Synthesis of 3,5-diaryl-1,2,4-triazoles 62: i) Polyphosphoric acid (PPA); ii) Pyridine, Δ.

1.6.1 Low Molecular Weight Triazoles

The literature contains fewer examples of low molecular weight triazole compounds compared to their oxadiazole counterparts. The most commonly used is TAZ **65**, which has been shown to be a superior hole-blocking material compared to PBD **25**. Furthermore, the electron mobility in **65** is lower than that of Alq_3.[50]

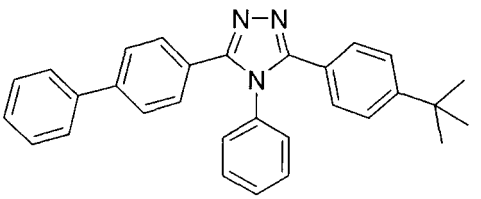

65

Scheme 26: Structure of low molecular weight triazole TAZ 65.

Kido *et al*[51] demonstrated that **65** can be efficiently applied as a hole-blocking layer in a triple layer device ITO/PVK/**65**/Alq_3/Mg:Ag; blue light with a λ_{max} of 410 nm was emitted. In this device PVK functions as the emitting material and Alq_3 acts as an electron transport layer. In the absence of **65** EL is red-shifted λ_{max} of 530 nm with light emission originating from Alq_3. White light was also realised for the same device configuration by doping PVK with fluorescent dyes.[52] Jiang and co-workers[53] showed that white light could also be produced from the following device ITO/CuPc/NPB/**65**:rubrene/Alq_3/Mg:Ag, in which **65** is used as a hole-blocking layer doped with 1.5% rubrene. Compound **65** has also been used as a ECHB layer for devices in which PVK has been blended individually with two d^{10} metal ion complexes gold (I) and copper (I) compounds.[54]

1.6.2 Polymeric Triazoles

Burn *et al*[55] reported a blue-emitting triazole-based conjugated polymer **66** which when used as an ECHB component achieved significant improvement in device performance.

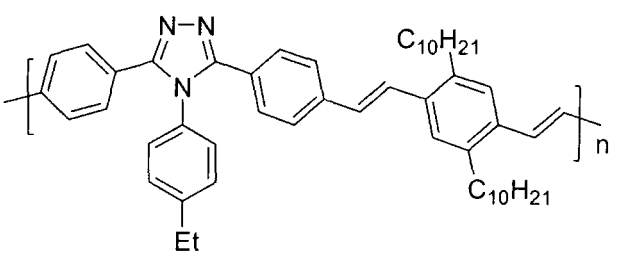

66

Scheme 27: Structure of triazole-based conjugated polymer 66.[55]

UV-Vis absorption of **66** as a thin film showed a strong π-π^* transition at λ_{max} 3.30 eV (375 nm). The absorption in solution is at 3.31 eV (376 nm), corresponding to a shift of only 0.01 eV (1.14 nm) with respect to the solid film. Solid-state PL emission at λ_{max} 2.55 eV (486 nm), PL in solution was blue-shifted by 0.11 eV (19.3 nm) with respect to that of the solid state at λ_{max} 2.66 eV (466 nm). The larger observed blue-shift in the emission, in comparison with the absorption was explained by efficient exciton migration and excimer formation in the thin film. A PLQY of 33% was calculated for **66**.

Polymer **66** was studied in both single- and double-layer devices; blue light was emitted and EL reached a maximum at 2.5 eV (496 nm). A peak luminescence of 50 cd/m^2 was recorded at a driving voltage of 18 V at a current density of 100 mA/cm^2 for the single layer device ITO/**66**/Al which corresponds to an EQE of 0.02%. A second, single-layer device achieved a reduced EQE of 0.015% when aluminium was substituted for a gold cathode. Since single-layer device investigations indicated that electrons are the majority charge carriers in **66**, bilayer devices incorporating PPV as the hole-transporting emissive layer were fabricated using ITO and aluminium as the respective contacts. Light emission originated from the PPV layer and a device EQE reached 0.08% at a luminescence of 250 cd m^{-2} for a driving voltage of 14 V and a current density of 100 mA cm^{-2}. Polymer **66** has also been used in conjunction with MEH-PPV as the hole-transporting emissive layer with a internal quantum efficiency of 0.65%.[56]

1.7 PYRIDINES

Compared to benzene, pyridine is π-electron-deficient, consequently, the derived polymers have increased electron affinity, improved electron-transporting properties, and the symmetry of poly(phenylene) systems is broken.

1.7.1 Poly(pyridine-2,5-diyl) (PPY)

Poly(pyridine-2,5-diyl) (PPY) **67** has a number of attractive features: it has excellent resistance to photochemical and electrochemical oxidation; it has a PLQY of up to 37%; and is solution processible from formic acid giving solvent orthogonality with most commonly

used materials so enabling the simple fabrication of OLEDs. However, the efficiency of **67** single layer OLEDs with ITO and aluminium contacts is very low with an EQE of 0.001%.[57]

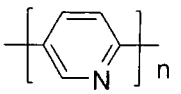

67

Scheme 28: Structure of PPY 67 prepared by dehalogenation polycondsensation of 2,5-dibromopyridine.[57]

Polymer **67** EL emission is broad and featureless peaking at λ_{max} 590 nm and with poor device performance it is considered unsuitable as an emissive material in single layer devices. However, **67** has proved to be an excellent electron-transporting layer in PPV devices. Hwang *et al*[58] reported the incorporation of a **67** layer provides improvement in the conversion efficiency of current density to brightness by a factor of 17, whereas Dailey and co-workers[59] stated that the inclusion of **67** as an additional electron-transport layer in PPV based devices gave an EQE of 0.25% when using aluminium contacts, 10 times greater than similar devices without the electron-transporting layer.

In addition to PPV based devices, Halim *et al*[57] have also demonstrated the use of **67** in conjunction with dendrimers containing a distyrylbenzene core and stilbene dendrons. Green light λ_{max} 570 nm was observed which is characteristic of **67**. This indicated that charge recombination and light emission occurs within the **67** layer. In this study the effect of the dendrimer is to act as a hole-transporting layer, and assist in the injection of holes into **67**. An EQE of 0.01% at maximum brightness was achieved for this green emitting OLED which is ten times greater than the EQE for a single layer **67** device.

1.7.2 Polymeric Pyridines

Ng *et al*[60] synthesised a series of soluble blue-emissive alternating copolymers comprising π-deficient pyridine and π-rich dialkoxy-functionalised phenyl rings. All polymers exhibited an onset of degradation at >300 °C indicating high thermal stability which is essential for fabricating OLED devices.

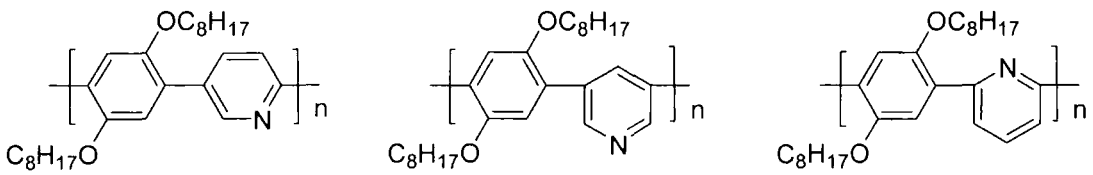

68 **69** **70**

Scheme 29: Structure of donar/acceptor polymers synthesised using Suzuki-coupling reaction by Ng *et al.*[60]

Polymer **68** has a PL λ_{max} 434 nm in chloroform solution, and 440 nm in the solid state. For **69** and **70** the λ_{max} were blue-shifted to 397 and 404 nm in solution and 422 and 414 nm in thin films, respectively. Single layer devices were fabricated using ITO as the anode and magnesium-indium alloy as the cathode and blue light was emitted. Emission peaks for **68**, **69**, and **70** were 444, 432 and 428 nm, respectively. Similarly as for PL, polymers with *meta*-linkages showed blue-shifted peak emission in comparison to **68**, due to a reduction in the π-conjugation lengths arising from the *meta* linkages. EL and PL spectra were similar indicating that charge recombination was the same in both cases.

In our laboratory Wang *et al*[61] reported the synthesis and luminescence properties of new pyridine-containing conjugated polymers, two of which were successfully used as electron-transport layers in OLEDs.

71 R= C_6H_{13} X= Br

72 R= C_6H_{13} X= Ph

73 R= C_6H_{13} X= Br

74 R= C_6H_{13} X= Ph

75 R= H X= Br

Scheme 30: Structures of pyridine-containing polymers prepared by Wang *et al.*[61] Synthesis involved Suzuki coupling reactions of 2,5-dibromo-4-hexylpyridine and 2,5-dibromopyridine with 1,4-benzenediboronic acid and 2,5-dimethoxy-1,4-benzenediboronic acid.

Polymer **71** shows an absorption at λ_{max} 322 nm for a thin film, which is similar to that of poly(6-hexyl-2,5-pyridylene) (PHexPY) at 327 nm and poly(para-phenylene) (PPP) at 330 nm, but significantly blue-shifted from the first absorption band of PPY at 382 nm. Polymer **71** is a blue luminescent material with a solid state peak emission at 447 nm, which is blue-shifted with respect to the maximum emission of PPP, PHexPY and PPY. Absorption and PL

spectra of the phenyl-terminated polymers **72** and **74** were essentially very similar to their dibrominated precursors **71** and **73**. Measurements of the PLQY of films of **71** and **72** afforded respective efficiencies of 15 ± 2 % and 13 ± 2 %, suggesting that non-radiative quenching of the excited polymers by terminal bromines was not a significant consideration for these two polymers. However, for films of **73** and **74**, the corresponding PLQY values were 5 ± 1 % and 17 ± 2 %, respectively.

The effect of the methoxy groups was identified by comparison of the spectra of polymers **71** and **73**. In the absorption spectra, the first absorption band at 332 nm was red-shifted to 348 nm for the film with the appearance of an additional band at 285 nm. PL emission was blue-shifted from 447 nm to 438 nm for thin films.

A comparison of the spectra of **73** and **75** revealed the considerable influence of the hexyl side chain on the photophysical properties of these two polymers. In both the absorption and emission profiles, a blue-shift was brought about by the presence of the hexyl group. This is particularly evident in the PL spectra where the shift is 103 nm to give λ_{max} 531 nm. Two possible explanations account for the difference in the spectra of **73** and **75**. Firstly the steric repulsion introduced by the hexyl group serves to substantially increase the inter-ring torsion within the polymer chain, thus reducing conjugation leading to a blueshift in the spectra. Alternatively, differences in the degree of intermolecular interaction could lead to the formation of excimers or aggregates, which would account for the substantial red-shift in the absorption and PL spectra of **75**.

Polymers **71** and **73** were used as electron-transport materials in MEH-PPV based devices with the general architecture ITO/MEH-PPV/polymer **71** or **73**/Al. Whereas the EQE for the single-layer device was 0.0026%, the bilayer device incorporating polymer **73** had an efficiency of 0.03%, an order of magnitude larger. Orange light was emitted which shows that light emission originates entirely from the MEH-PPV layer. Bilayer devices containing polymer **71** had a higher EQE of 0.06%, but only very low current densities and consequently brightness of only a few cd m^{-2} could be obtained. The increases in EQE can be understood to arise from a better balance of electron and hole injection in the bilayer structure.

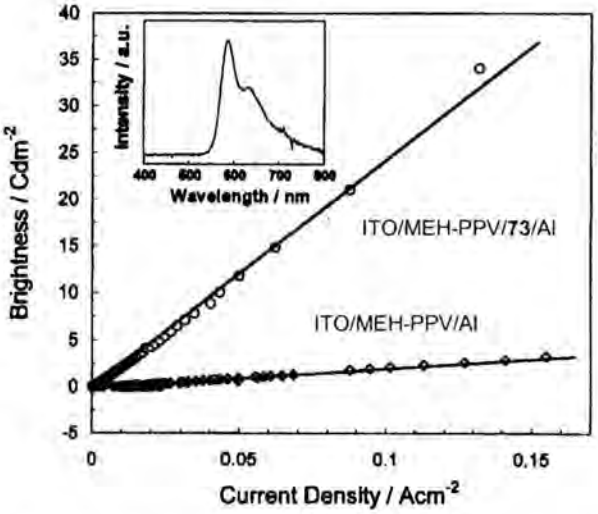

Figure 8: Light output of LEDs as a function of current density flowing through them for pyridine polymer 73 bilayer and single layer devices fabricated by Wang *et al.*[61] The inset shows the EL spectrum of the bilayer device.

An alternating copolymer composed of fluorenedivinylene as the light-emitting unit and pyridine **76** was synthesised by Kim and co-workers.[62] Polymer **76** has a *Tg* of 100 °C; the copolymer has an onset decomposition temperature of 380 °C. Blue PL emission of **76** film cast from chlorobenzene has λ_{max} 440 nm; however peak emission is significantly red-shifted to the green region with λ_{max} of 540 nm when spun from formic acid. PFPV was used as an electron transport layer in an OLED fabricated with a blend of PVK and the fluorene–based copolymer P-3, where ITO and Al were used as the anode and cathode, respectively. Blue EL emission with λ_{max} 475 nm was observed with an EQE of 0.1%.

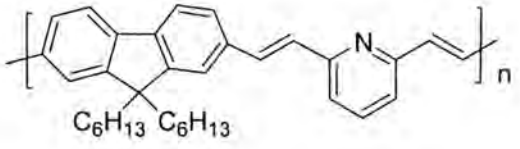

76

Scheme 31: Structure of alternating copolymer 76 synthesised by Wittig reaction by Kim et al.[62]

1.7.3 Protonation as a Method of Tuning Luminescence in Pyridine Conjugated Polymers

Following the success of pyridine conjugated polymers prepared by Wang *et al*[61], workers in our laboratory investigated protonation and subsequent intramolecular hydrogen bonding as a method to control chain structure and tune luminescence in these systems,[63] specifically focusing on the structural and spectroscopic properties of 1,4-dimethoxy-2,5-bis(2-pyridyl)benzene **77** and the related AB copolymer poly{2,5-pyridylene-co-1,4-[2,5-bis(2-ethylhexyloxy)]phenylene} **80**.

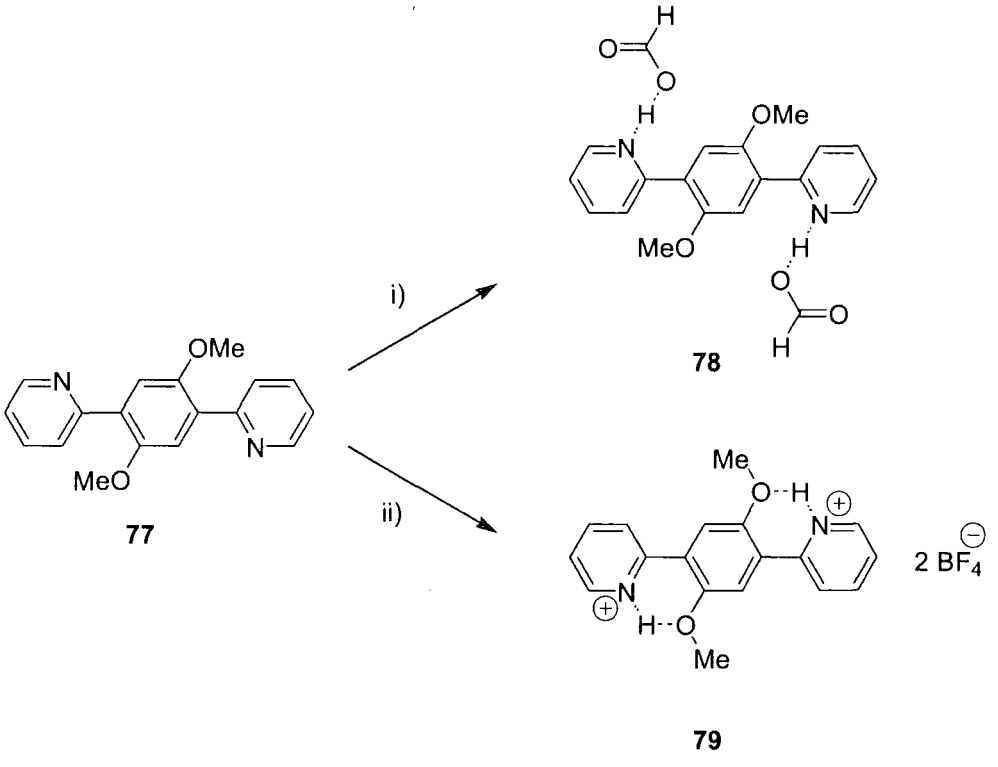

Scheme 32: Structure and subsequent protonation of 1,4-dimethoxy-2,5-bis(2-pyridyl)benzene 77: i) HCO_2H, EtOAc. ii) HBF_4, MeOH. Synthesis by Suzuki Coupling reaction of 2-bromopyridine with 2,5-dimethoxy-1,4-benzenediboronic acid.[63]

X-ray crystallographic analysis demonstrated that reaction of **77** with formic acid does not form an ionic pyridinium salt in the solid state, rather the product 1,4-dimethoxy-2,5-bis(2-pyridyl)benzene bis(formic acid) **78** is a molecular complex with strong hydrogen bonds between each nitrogen atom and the hydroxyl hydrogen in formic acid.

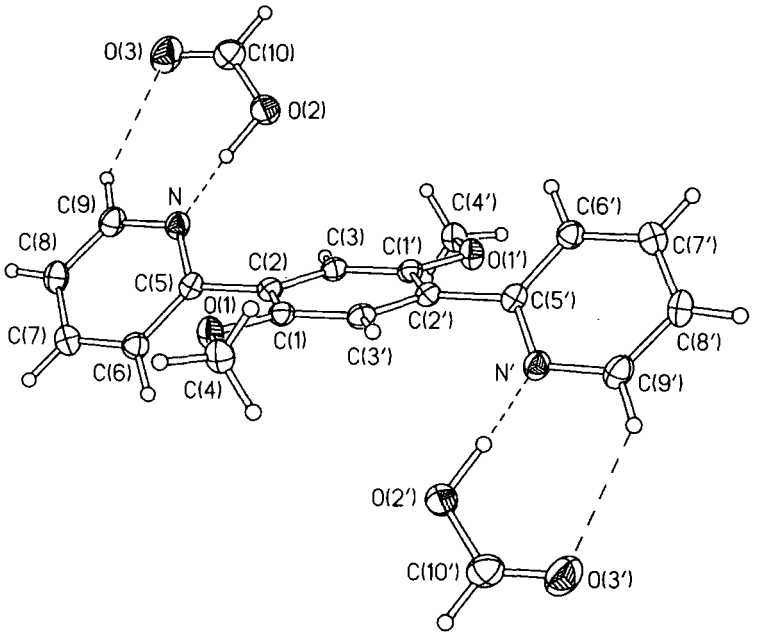

Figure 9: X-ray molecular structure of 1,4-dimethoxy-2,5-bis(2-pyridyl)benzene bis(formic acid) 78. Interaction with formic acid results in a structural twist about the horizontal axis. Pyridyl ring is now in an inverted position compared to the neutral structure.[63]

In contrast, reaction of **77** with tetrafluoroboric acid leads to the dication salt 1,4-dimethoxy-2,5-bis(2-pyridinium)benzene bis(tetrafluoroborate salt) **79** with significant intramolecular hydrogen bonding (N-H···O-Me) causing planarisation of the molecule. Optical absorption and emission spectra of **79** were significantly red-shifted in comparison to **77** and **78**.

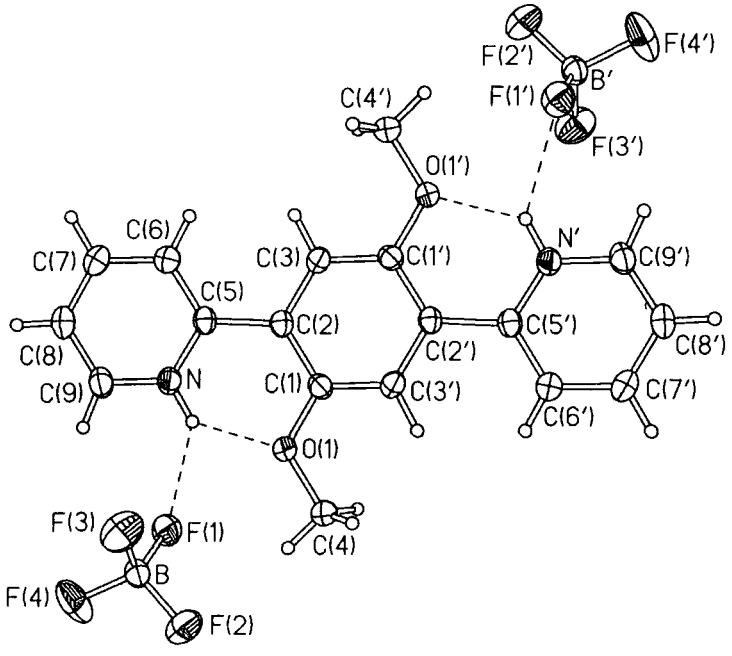

Figure 10: X-ray molecular structure of 2,5-bis(2-pyridinium)benzene bis(tetrafluoroborate salt) 79.[63]

Polymer **80** also showed similar red-shifted absorption and PL spectra when treated with strong acids in neutral solution. For instance when protonated with camphorsulfonic acid (CSA) the PL band shifted from 2.55 eV to ca. 2.2.eV. This trend was also observed for thin films of **80** doped with strong acids. Excitation profiles showed that emission arises from both protonated and nonprotonated sites in the polymer backbone. Typically EL for the device structure ITO/PEDOT/**80**/Ca/Al mirrored PL spectra upon protonation, with the EL peak being red-shifted from 2.4 to 2.15 eV. An EQE of 0.02% was measured for this device.

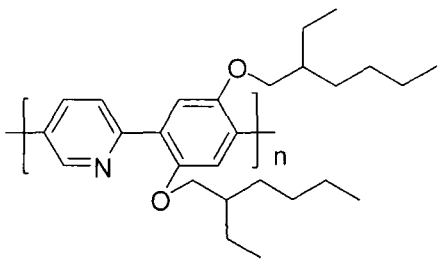

80

Scheme 33: Structure of AB copolymer poly{2,5-pyridylene-co-1,4-[2,5-bis(2-ethylhexyloxy)]phenylene} 80. Synthesised by Suzuki Coupling reaction of 2,5-dibromopyridine with 2,5-bis(2-ethylhexyloxy)benzene-1,4-diboronic acid.[63]

The protonation of the pyridine rings in polymer **80** accompanied by intramolcular hydrogen bonding to the oxygen of the adjacent solubilising alkoxy substituent (as shown in the X-ray molecular structure of **78** and **79**), provides a novel mechanism for driving the polymer into a near–planar configuration, thereby extending the π-conjugation, and tuning the emission profiles.

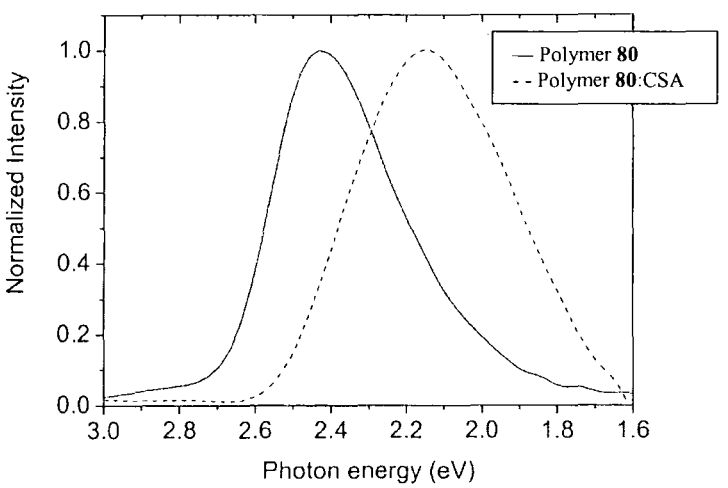

Figure 11: Electroluminescence spectra of protonated (CSA) and neutral polymer 80.[63]

Upon protonation of the red neutral *poly*[2,5-bis(3,4-ethylenedioxy-2-thienyl)pyridine] **81** Irvin *et al*[64] observed a 70 nm red shift in the absorption spectra of thin films accompanied by

a colour change to blue-indigo for the protonated species **82**. The protonated and neutral state can be reversibly switched by exposure to 1 M HCl followed by rinsing with deionised water.

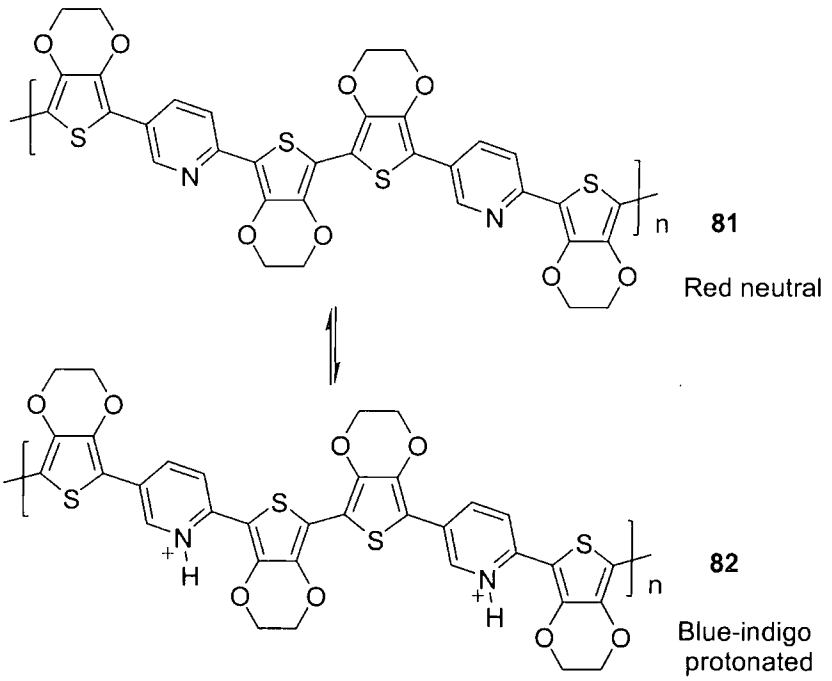

Scheme 34: Protonation and subsequent colour change of 81.[64]

Bouachrine *et al*[65] investigated protonation of the 2,2'-bipyridyl units in the main chain of the chelating conjugated copolymer **83**. In chloroform solution **83** has λ_{max} (abs) 425 nm. Thin films on glass formed by evaporation of a chloroform solution gave λ_{max} 438 nm. The absorption spectrum of **83** changed on addition of acetic acid from λ_{max} 425 nm to 492 nm. This is due to the more planar protonated bipyridyl unit leading to an increase in the conjugation length and the resulting red shift.

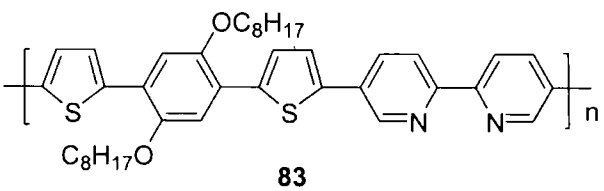

Scheme 35: Structure of chelating conjugated copolymer 83. Synthesis based on Stille coupling reaction between a dihalogeno aromatic substrate and bis(tributylstannyl) aromatic species in the presence of Pd(0) as the catalyst.[65]

1.8 PYRIMIDINES

Pyrimidine has been less exploited than pyridine although it has a number of attractive features: i) it is more electron-deficient than pyridine and ii) due to the lack of *ortho-ortho*

interactions of C-H hydrogens, 2-arylpyrimidine derivatives are more planar possessing increased π-conjugation in comparison with 2-arylpyridine or biphenyl analogues.

1.8.1 Low Molecular Weight Pyrimidines

Wong *et al*[66] reported conjugated oligomers with an alternating phenylene-pyrimidine structure. Oligomers **84a-c** exhibit high thermal stability; TG data revealed no weight loss below 380 °C. Oligomers **84a** and **84c** exhibited relatively low *Tg's* of 27.7 and 31.5 °C, respectively. The low *Tg's* are presumably due to the octyloxyl side chain on the central phenylene ring acting as a solubilising group.

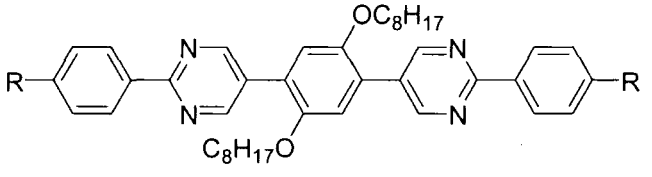

84 a R = H

84 b R = OC_4H_9

84 c R = *t*-Bu

Scheme 36: Structures of phenylene-pyrimidine alternating oligomers 84a-c, synthesised by successive Suzuki coupling reactions starting from 2-iodo-5-bromopyrimidine.[66]

Oligomers **84a-c** exhibit strong blue fluorescence with emission centred at λ_{max} 419 nm irrespective of the terminal substituents. PLQY values were determined as 37, 54 and 37% for **84a-c**, respectively. EL devices of the general configuration ITO/PEDT-PSS/NCB/**84b** or **84c**/Mg:Al (10:1)/Ag were fabricated. Oligomers **84b** and **84c** function as efficient blue emitters displaying EL spectra similar to their PL emission with EQEs of 1.3-1.8% and brightness over 2000 cd m^{-2}.

Researchers from the same group reported the pyrimidine-containing spirobifluorene-cored oligoaryl, **85**, as an emitter or a host for blue OLEDs.[67] Thermal analysis of **85** revealed its high thermal stability with a decomposition temperature of 420 °C. DSC demonstrated a high *Tg* of 195 °C, as a consequence homogeneous and amorphous films could be formed by thermal evaporation allowing fabrication of LEDs.

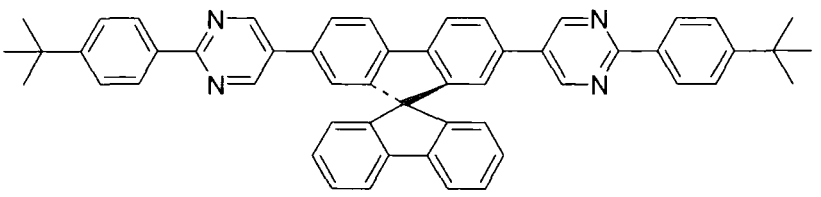

85

Scheme 37: Structure of 85. 85 was synthesised by Suzuki coupling reaction of the 2,7-diboronic ester of 9,9'-spirobifluorene and 5-bromo-2-(4-*tert*-butylphenyl)pyrimidine in the presence of $Pd(PPh_3)_4$ and P^tBu_3 catalysts.[67]

Compound **85** is a blue emitter with a PL λ_{max} 430 nm with exceptionally high PLQY in both solution and thin films with values Φ_{sol} (in chloroform) and Φ_{film} of 100 and 80%, respectively. When **85** was used as a host material for perylene in a multilayer blue emitting device, a maximum brightness of ~80000 cd m^{-2} was achieved.

1.8.2 Poly(pyrimidine-2,5-diyl) (PPym)

Poly(pyrimidine-2,5-diyl) (PPym) **86** shows highly electron accepting properties which can be utilised in n-type semiconductors.[68]

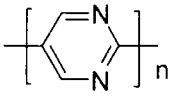

86

Scheme 38: Structure of poly(pyrimidine-2,5-diyl) (PPym) 86 prepared by dehalogenation polycondenation of 2,5-dibromopyrimidine with a zero-valent nickel complex.[68]

The cyclic voltamogram (CV) of PPym as a film showed an n-doping peak at ca. –1.75 V *vs* Ag/Ag^+ and an undoping peak at –1.65 V. The colour of PPym changes from reddish-yellow to dark purple during reduction. PPym film was electrochemically inert in the oxidative region up +1.0 V *vs* Ag/Ag^+. The polymer film electrode was stable during repeated scanning, showing essentially the same CV and colour change. This reflects the n-doping properties of PPym and confirms that the introduction of two electron-withdrawing imine nitrogens in the main chain raises the electron accepting character of the poly(arylene).

1.9 PYRAZINES

Pyrazines, like pyrimidines are highly π-electron-deficent heterocycles. In the context of materials with improved electron-transport capabilities, prior to our work in chapter 3 diarylpyrazines remain essentially unexplored although there had been several reports concerning disytrylpyrazines and the incorporation of pyrazine units into ladder polymers.

1.9.1 Distyrylpyrazines

Grimsdale and co-workers[69] demonstrated that the PL of distyrylpyrazines could be tuned from blue to red by varying the substituents. The dimethoxy compound **87** showed green emission with λ_{max} 480 nm, whereas PL for the diacetoxy derivative **88** was blue-shifted with respect to **87** by 20 nm and thus emitted in the blue region. The di-*N*-oxide **89** displayed a significant red-shifted PL emission that was red-orange with a broad λ_{max} at 540 nm.

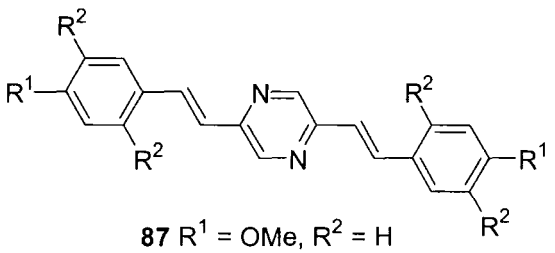

87 R^1 = OMe, R^2 = H

88 R^1 = OAc, R^2 = H

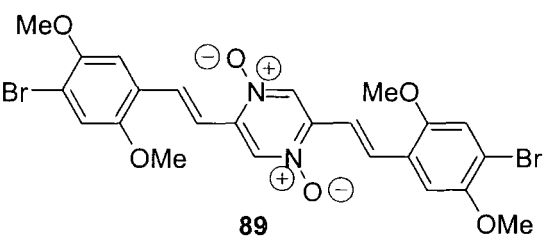

89

Scheme 39: Structures of distrylpyrazines derivatives prepared by Grimsdale *et al.*[69]

Liu *et al* [70] reported a series of blue emitting pyrazine derivatives. Compounds **90** and **91** have a PL λ_{max} of 438 and 434 nm, respectively. However PL emission peaks for **92** and **93** are red-shifted with values of λ_{max} of 476 and 473 nm, respectively. The red shift of **93** was attributed to an increase in conjugation due to the two naphthyl groups. For **92** the ethoxy-substituted phenyl groups in the backbone and the central pyrazine ring act as electron donating and withdrawing groups, respectively. The red shift for **92** is assigned to imbalanced electron distribution. For **91** the cyano-substituted phenyl groups and the pyrazine ring are both electron withdrawing so there is no charge imbalance, therefore the PL spectrum resembles that of **90**. Multilayer EL devices in conjunction with the hole-transport NPB and the host material TPBI gave bright blue emission, λ_{max} 468 nm.

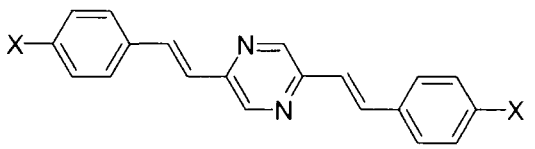

90 X = H

91 X = CN

92 X = OC_2H_5

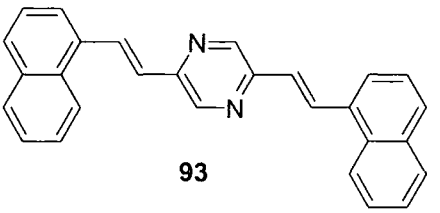

93

Scheme 40: Structures of blue emitting distyrylpyrazine derivatives prepared by Liu *et al.*[70]

1.9.2 Polymeric Pyrazines

Wu *et al*[71] fabricated EL devices consisting of fluorescent polyimides which have the 2,5-distyrylpyrazine as the active unit incorporated into the polymer backbone. Polyimide Langmuir-Blodgett (LB) films of **94** showed a UV-Vis absorption and PL λ_{max} of 396 and 564 nm, respectively. A single-layer device of the LB film of **94** using ITO as the anode and Mg:Al as the cathode emitted orange-red luminescence. Almost identical EL and PL spectra were obtained.

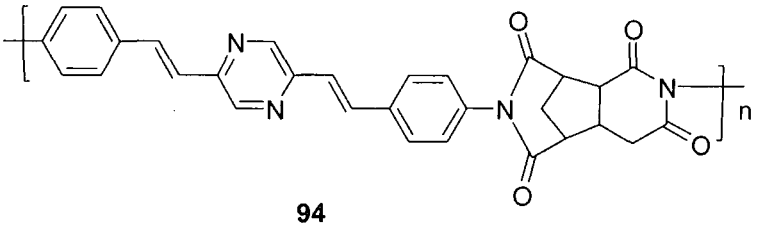

94

Scheme 41: Structure of polyimide 94, synthesised by reaction of 2,5-bis(4-aminostyryl)pyrazine with aliphatic tetracarboxylic dianhydrides.[71]

Peng and Galvin[72] reported a new pyrazine-containing PPV polymer **95**, which incorporates one pyrazine ring for every three phenyl rings. Polymer **95** is a strongly fluorescent material with a PL λ_{max} 530 nm in THF solution and 550 nm as a solid film. Orange emission was observed for a single layer device of **95** as the emissive layer using ITO and aluminium as the respective contacts. The EQE was calculated to be 0.012% at a current density of 1mA mm^{-2}. A PPV based bilayer device including **95** as an additional transport layer only showed a slightly higher EQE of 0.015%.

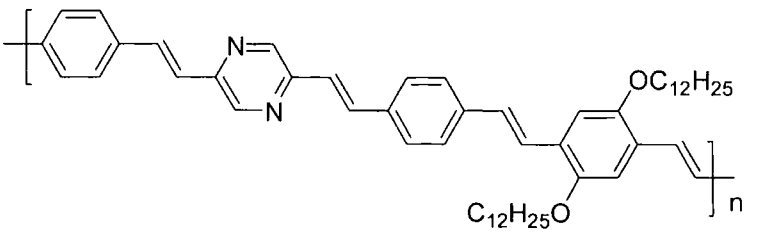

95

Scheme 42: Pyrazine-containing PPV polymer 95 prepared by Heck coupling.[72]

1.9.3 Pyrazine Ladder Polymers

Ladder polymers are uninterrupted sequences of fused rings and have been reviewed extensively within the literature.[73] Tour *et al*[74,75] reported the synthesis of highly functionalised coplanar pyrazine ladder polymers due to the presence of non-covalent linkages between adjacent aromatic rings. Hydrogen bonds are utlised to planarise the polymer backbone[63] due to the excellent hydrogen bond accepting capabilities of pyrazine. Thereby the polymeric framework can be organised into a near-planar conformation, thus extending π-conjugation and ultimately tuning the optical luminescence properties.

Delnoye *et al*[76] synthesised a range of soluble π-conjugated oligomers and co-polymers comprising of alternating pyrazine and acylated 1,4-phenylenediamine units. Self-assembled ladder like structures were obtained by the use of intramolecular hydrogen bonding.

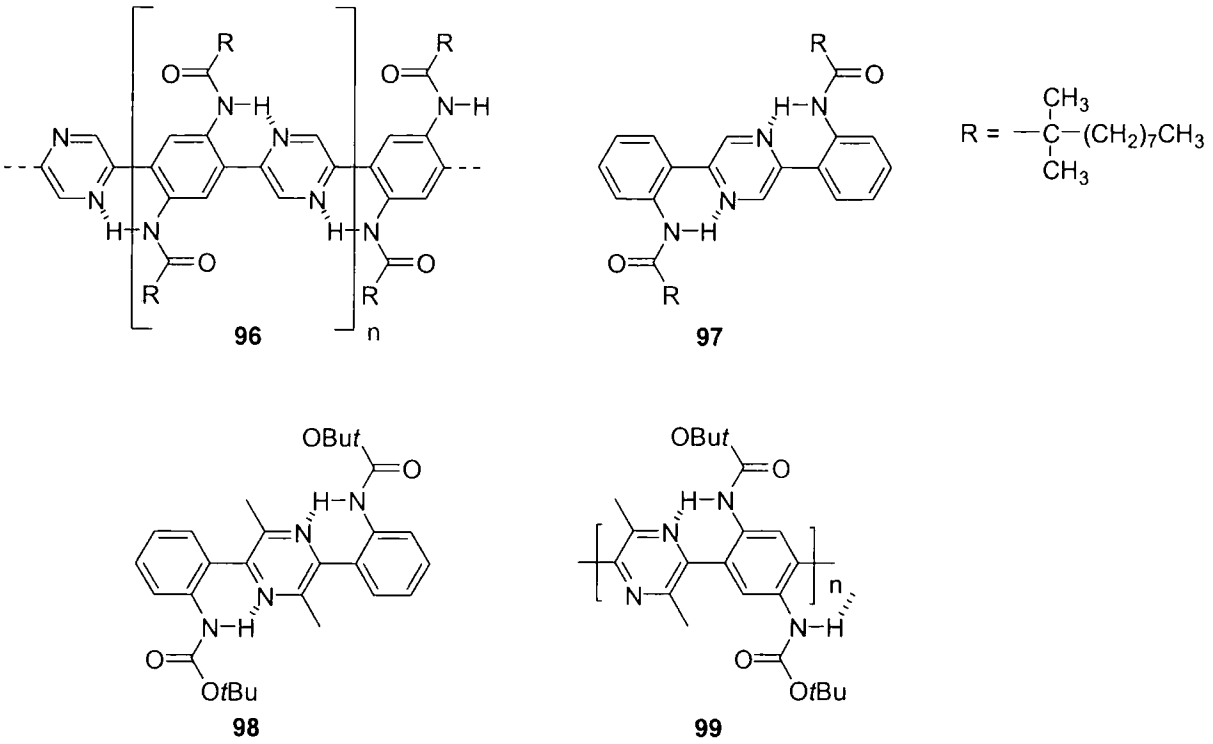

Scheme 43: Structures of self-assembled pyrazine ladder oligomers and copolymers prepared by Delnoye *et al.*[76]

Strong hydrogen bonding was evident in the ^{1}H-NMR spectra, which showed resonances for the carbamate N-H protons of **96** and **97** at δ 11.7 and 12.56 ppm, respectively. For methyl substituted pyrazines **98** and **99** higher values of δ 8.7 and 8.6 ppm were observed, indicating weaker hydrogen bonding due to severe steric hindrance. UV-Vis absorption spectra showed that in the presence of TFA, **96** is protonated and the hydrogen bonds are broken resulting in a blue-shift in the neutral compound λ_{max} from 446 to 369 nm. Pieterse and co-workers[77] demonstrated that the hydrogen bond strength, as well as the electron affinity of such pyrazine oligomers, can be increased by placing more electron withdrawing substituents on *ortho* amine bonding groups on the 1,4-phenylenediamine unit. However, no device studies utilising this concept were reported.

1.10 1,3,5-TRIAZINES

1,3,5-Triazines have high thermal stability. They are prepared by three synthetic methods; firstly symmetrically substituted 2,4,6-triaryl-1,3,5-triazines **101** are formed by cyclisation of aryl nitriles **100**; secondly, unsymmetrical diaryl triazines **104** can be obtained by ring formation of N-cyanoamidines **102** and chloromethyleniminium salt **103**; and finally, the

synthesis of unsymmetrical triaryltriazines **108** involves reaction of benzamides **107** with benzoic acid anhydride **105** or Schiff bases **106**.

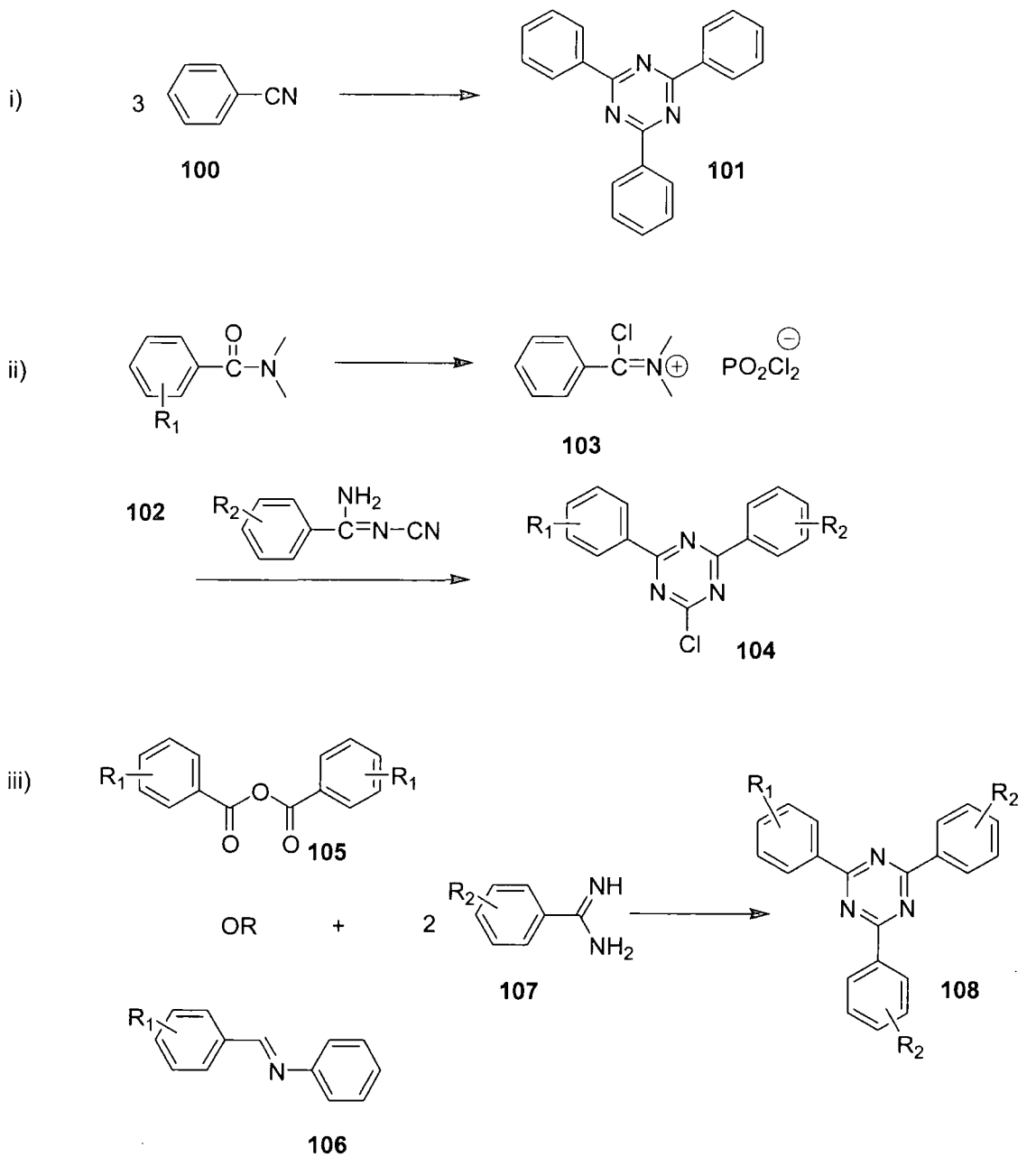

Scheme 44: i) Synthesis of symmetrically substitiuted 2,4,6-triaryl-1,3,5-triazines 101 by cyclisation of aryl nitriles 100 in the presence of PCl_5; ii) Unsymmetrical 2,5-diaryl-1,3,5-triazines 104; iii) Unsymmetrical triaryl-1,3,5-traizines 108.

1.10.1 Low Molecular Weight Triazines

Pang *et al* [78] reported the synthesis and electroluminescence of new blue luminescent star-shaped compounds based on di-2-pyridylamino derivatives of 1,3,5-triazines. 2,4,6-Tris(di-

pyridylamino)-1,3,5-triazine **109** and 2,4,6-tris[*p*-(di-pyridylamino)phenyl]-1,3,5-triazine **110** were prepared by classic Ullmann condensation reactions.

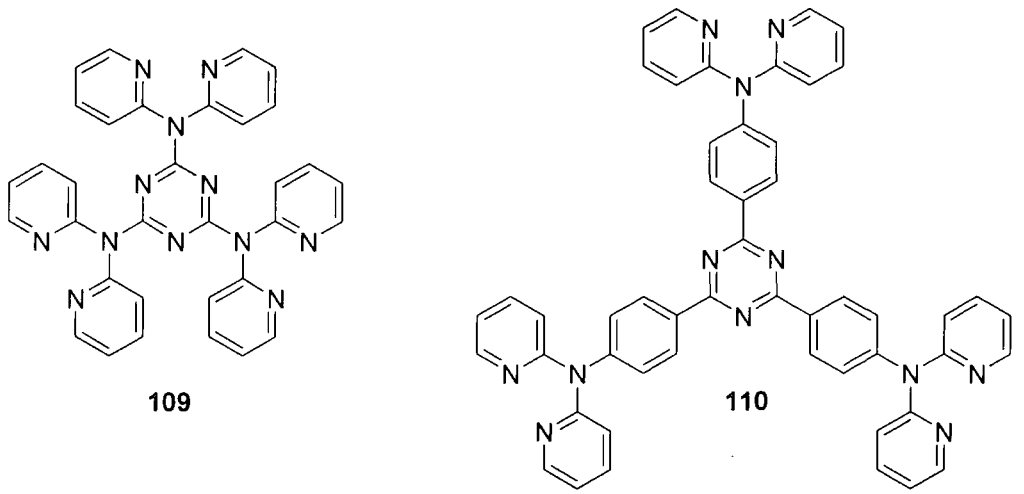

Scheme 45: Star-shaped di-2-pyridylamino-1,3,5-triazine derivatives 109 and 110 prepared by Pang *et al.*[78]

Compound **109** does not show glass formation, whereas its larger counterpart **110** has a *Tg* of 121 °C. The two di-2-pyridylamino derivatives emit blue light when irradiated in the solid state and in solution. In the solid state, PL λ_{max} values of 393 and 440 nm were recorded for **109** and **110** respectively, whilst in solution, PL λ_{max} for **109** was significantly red-shifted to 433 nm, whereas the value for larger **110** is the same value as in the solid state 440 nm. The fluorescence efficiencies recorded in solution were 0.43 and 0.78, respectively, indicating that these molecules are fairly efficient blue emitters which have potential in OLEDs.

Electrochemical investigations of **109** and **110** showed that their HOMO energy levels were similar to, or slightly below that of, ITO (-5.1 eV). In contrast, LUMO levels were found to be above that of the Al cathode (-4.2 eV), therefore the electron-transporting material PBD was incorporated into the device between the cathode and the emissive material. In addition, on the anode copper phthalocyanine (CuPc) was used to facilitate hole injection while LiF was added to the cathode to increase electron injection. EL devices were fabricated using the same device architecture, namely ITO/CuPc/compound **109-110**/PDB/LiF/Al. Both devices displayed blue emission with EL λ_{max} of 396 and 444 nm for **109** and **110** respectively, which approximately match PL solid-state values. Both devices have a high turn-on voltage of 15 V. Inclusion of the hole-transporting material TPD between CuPc and the emitting layer resulted in a lower turn-on voltage of 6 V. However, a second peak at λ_{max} 532 nm corresponding to green emission was observed. Since compound **110** shows no green emission this must arise from an exciplex state formed between the TPD and **110** layers. The

corresponding device using **109** was not stable and produced very weak blue emission at an intensity of 14.7 cd m^{-2}. Devices with Alq_3 were also constructed: instead of blue emission, green light was observed which indicated that Alq_3 was not a suitable electron transport material for triazine based systems.

Lupton *et al*[79] reported EL from a distyrylbenzene based triazine dendrimer **111**. The distyrylbenzene core moiety is a known blue light-emitting material. Within this molecule the triazine ring system has two roles; first to act as the branch point of the dendrimer; and second to behave as an electron transport component. PL and EL properties of this **111** were subsequently investigated.

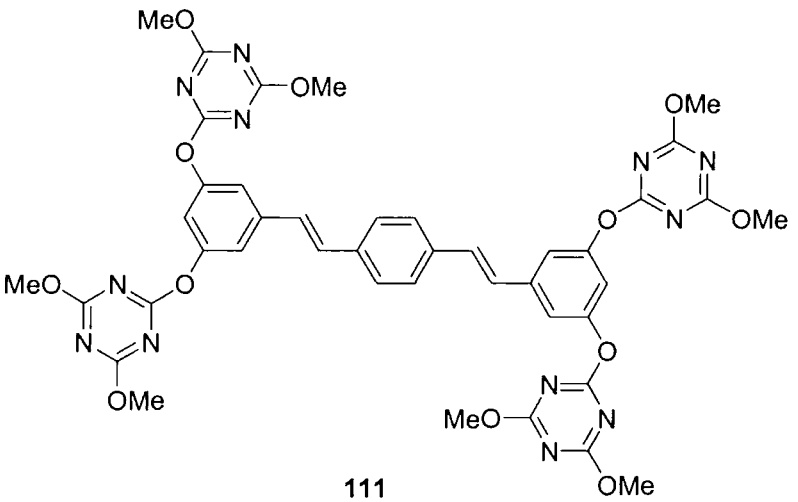

111

Scheme 46: Structure of distyrylbenzene based triazine dendrimer 111 synthesised by Lupton *et al.*[79]

The film absorption spectra of **111** with λ_{max} of 365 nm, is slightly red-shifted with respect to that of solution spectra λ_{max} 360 nm. This is in contrast to PL spectra, which showed a significant red shift in the film, λ_{max} 462 nm, with respect to the solution, λ_{max} 395, 417 and 440 nm (shoulder). The PLQY of a thin film of **111** was 31%. The dendrimer was incorporated into a single-layer OLED of configuration ITO/**111**/Ca and was found to emit blue light with an EQE of 0.003%. Comparison of EL and PL λ_{max} values showed that EL peak emission λ_{max} 506 nm was red-shifted by 44 nm with respect to that of the PL. EL intensity was weak and the emitted light changed irreversibly from blue-white to blue. The poor stability of this material during device operation suggests that the phenoxy linkage to the distyrylbenzene core was a poor choice.

Fink and co-authors[80] reported a series of 1,3,5-triazine ethers with high *Tg* and demonstrated their potential application as ECHB layers in OLEDs. Ethers **112a-b** are crystalline materials

with high melting points; they exhibit glass transition at 106 and 115 °C, respectively. Compounds **112c-e** are amorphous and exhibit *Tg* at 139, 133 and 144 °C, respectively. Compound **112b** was applied as a ECHB layer in two different types of devices; i) a polymer blend bilayer layer device, ITO/blend of PVK + TDAPB + Alq_3 (4:1:1)/**112b**/Mg:Ag (10:1) and ii) a multilayer device, ITO/TDAPB/Alq_3/**112b**/ Mg:Ag (10:1). Both device types exhibited green emission similar to the PL of Alq_3. The onset of EL was increased by the use of the triazine layer and the EQE of the bilayer layer device was twice that of its single layer counterpart. The influence of **112b** in the multilayer device was evident by a threefold increase in the EQE accompanied by an increase in EL intensity. No EQE values were reported.

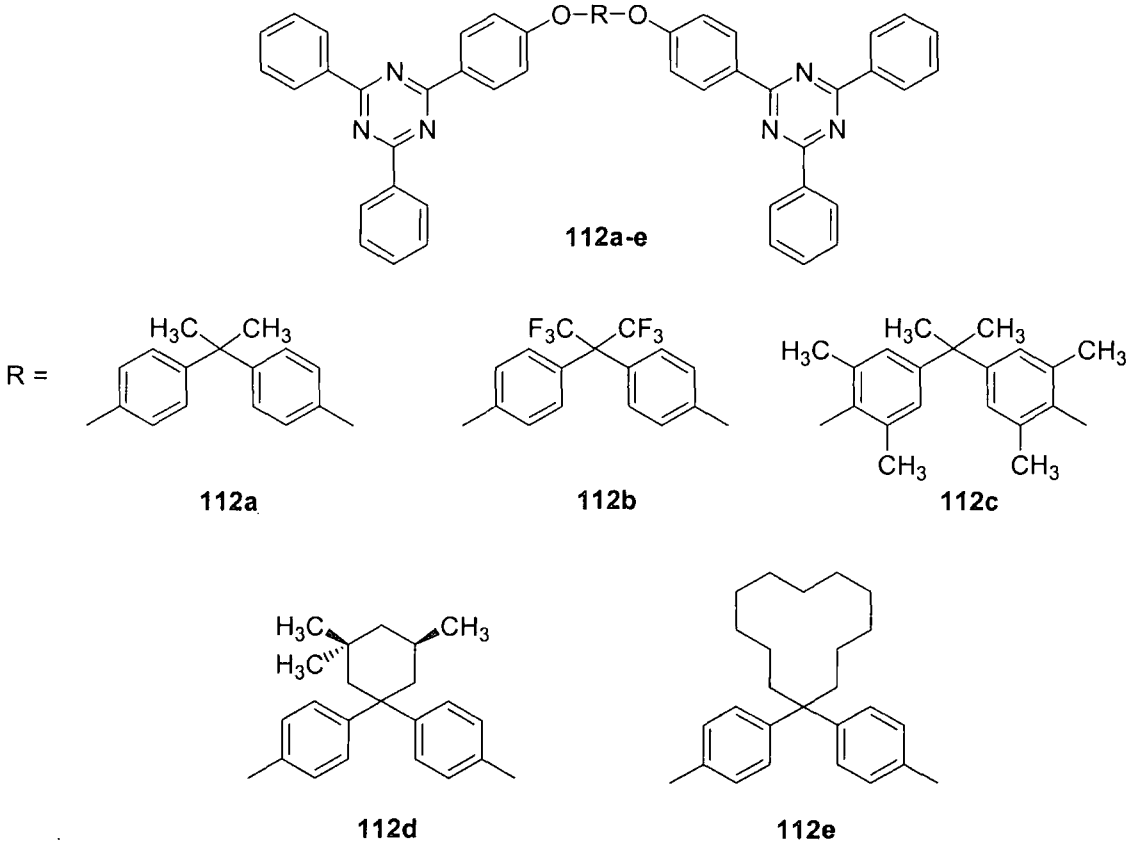

Scheme 47: Structures of 1,3,5-triazine ethers 112a-e synthesised by Fink *et al.*[80]

1.10.2 Polymeric Triazines

Poly(triazine ether)s are prepared via nucleophilic aromatic substitution reactions between triaryltriazine difluorides and various bisphenols in an aprotic solvent in the presence of base. Strukelj, however, reported a second synthetic approach involving the preparation of poly(aryl

ether benzil)s and then reacting them with (2-pyridyl)hydrazine to form poly(aryl ether pyridyltriazine)s.[81]

Pösch and co-workers[40] reported the synthesis of *p*-TRZ **113** which was utilised as an ECHB material in PPV based OLEDs.

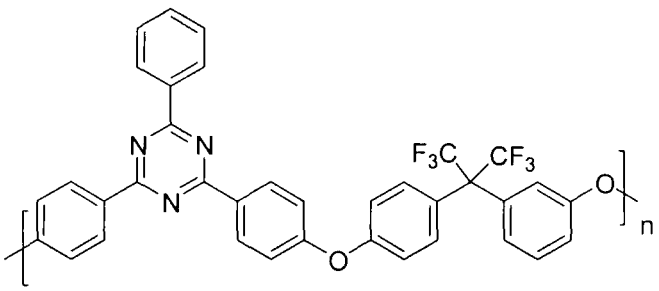

113

Scheme 48: Structure of *p*-TRZ 113 synthesised from the corresponding difluoroheterocyclic monomers with hexafluorobisphenol via a nucleophilic displacement reaction of fluorine atoms by intermediate phenolate anion.[40]

DSC measurements showed that **113** has a high *Tg* of 241 °C, in addition TGA analysis confirmed that **113** is thermally stable with a decomposition temperature of 466 °C. Optical data showed a UV-Vis absorbance at λ_{max} 293 nm, whereas the fluorescence λ_{max} was recorded as not detectable. The authors also reported that it was difficult to obtain excellent quality films by spin coating from cyclohexanone solution. **113** was used in the following device configuration ITO/PPV/**113**/Al and compared against the corresponding single layer reference device ITO/PPV/Al. The bilayer device ITO/PPV/**113**/Al gave a maximum brightness of 15 cd m^{-2} at a current density of 43 mA cm^{-2} in comparison to the reference diode which had a maximum brightness of 2 cd m^{-2} at a current density of 436 mA cm^{-2}. Whilst the bilayer device structure is more efficient than its single layer counterpart, the higher onset voltage of 8.5 V compared to 6.0 V for the reference demonstrates that **113** facilitates efficient hole blocking at the PPV/ECHB interface rather than electron injection.

1.11 QUINOLINES

As stated earlier (Alq_3) **2** was first used in by Tang and VanSlyke[5] and is probably the most widely used quinoline based electron-transport material. The quinoline moieties in the ligands of this metal complex are π-electron deficient systems, which contribute towards the electron injection/transport property of this green light-emitting complex. In addition to its

use in low molecular weight vapour-deposited OLEDs Alq_3 has been extensively used as an electron-transport material in polymer OLED systems with considerable improvements in EQEs reported.

Polyquinolines are characterised by high thermal and oxidative stability, outstanding mechanical properties, and optically clear film-forming properties. As for quinolines, polyquinolines **116** are prepared by acid catalysed Friedländer condensation reaction between bis(*o*-aminoketone)s **114** and diacetylaryl compounds **115**.

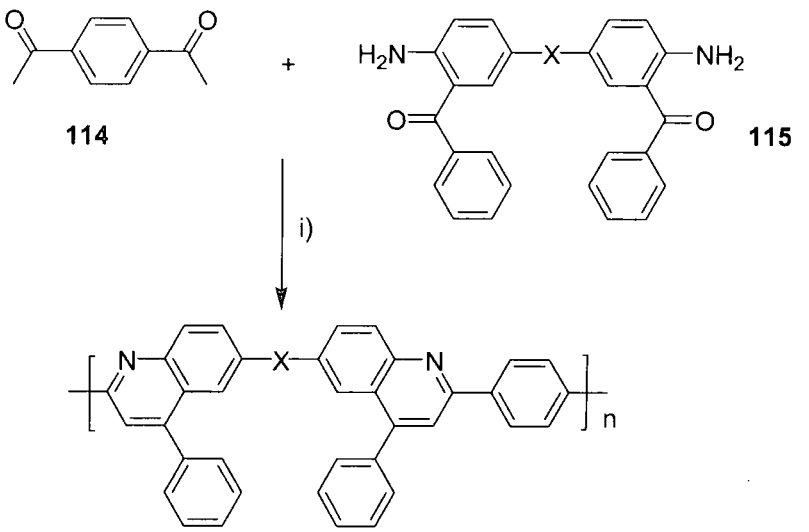

Scheme 49: Friedländer synthesis of polyquinolines 116: i) *m*-cresol, Δ.

1.11.1 Polymeric Quinolines

Kim *et al*[82] produced a series of polyquinolines containing the 9,9-di-*n*-hexylfluorene units in the main chain. Their optical absorption and luminescence properties vary with chain rigidity and conjugation length.

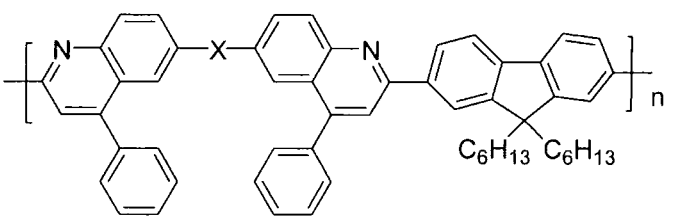

117 a X= O
117 b X= S
117 c X= nil
117d X= C=C

Scheme 50: Series of polyquinoline copolymers prepared by Kim *et al.*[82]

As the chain rigidity increases *Tg* values for this series of copolymers increase, ranging from 195 to 243 °C. Thermal stability is clearly enhanced by the quinoline ring as the *Tg* values are much higher compared to those of polyfluorene ~55 °C or MEH-PPV ~65 °C. These polyquinolines showed high thermal stabilities with initial decomposition temperatures of >388 °C.

Optical properties show longer wavelength blue emission with increasing chain rigidity and conjugation length, the PL emission in solution increases from 404 nm for **117a** to 446 nm for **117b**, and the PL emission of thin films shows the same tendency but is red-shifted, i.e. 414 nm (**117a**) to 494 nm (**117d**) with respect to solution emission. To investigate the electron-transporting/hole-blocking properties of this series of polyquinolines **117a**, and **117c** were fabricated into OLEDs using the emissive statistical copolymer **118**.

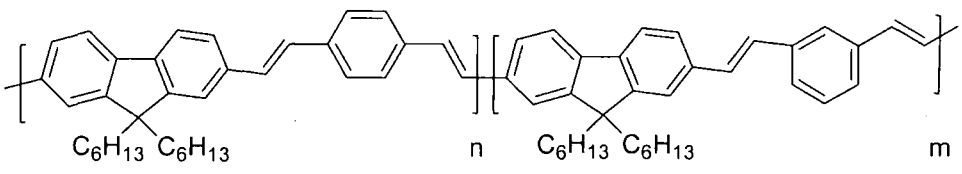

118

Scheme 51: Structure of statistical copolymer 118 with fluorene as one unit and a mixture of *p*- and *m*-divinylbenzene (n:m= 3:7).

Bi- and tri-layer devices were constructed of the form ITO/P-3:PVK blend/**117a**/Al and ITO/PVK/**118**/**117c**/Al. For the bilayer device configurations both **117a** and **117c** showed improved charge transport with increased EQE values of 0.041 and 0.052% respectively, compared to the reference value (no polyquinoline layer) of 0.0045%. Whilst bilayer layer devices operated at the same turn-on voltage of 14 V, luminance output for **117a** was slightly lower than the reference at 6.0 μW whereas a 2.7 fold increase was recorded for **117c** at 16 μW. EL spectra for OLEDs with and without **117c** demonstrated that both devices show blue emission, λ_{max} 480 nm, which is very close to the peak emission of the reference λ_{max} at 476 nm, indicating that the **118**:PVK blend acts as the emitting layer in the bi-layer device, and no exciplex formation occurs. In the case of tri-layer devices, both the light intensity (3.4 and 8.2 times increased) and EQE (17.5 and 15.6 times increased) equivalent to values of 0.014 and 0.012% respectively, were obtained compared to the control device, comprising ITO/PVK/**118**/Al.

Liu and co-workers[83] successfully synthesised two EL copolymers containing biquinolines and 2,2-diphenylhexafluoropropane **119** or pyridine moieties **120**. Both **119** and **120** possess excellent thermal stability with decomposition temperatures greater than 500 °C, a *Tg* of 286 °C for **120** was also recorded.

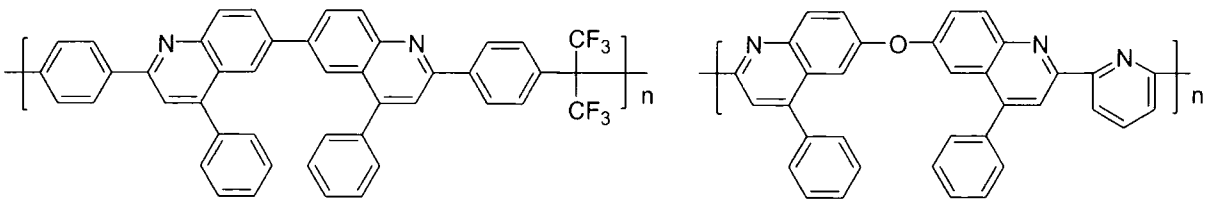

119 **120**

Scheme 52: Structures of biquinoline copolymers 119 and 120 prepared by Liu *et al.*[83]

UV-Vis absorption spectra of thin film and solution samples exhibit similar profiles with two peaks in solution (λ_{max} 283, 340 nm for **119**; λ_{max} 267, 347 nm for **120**) and as thin films (λ_{max} 283, 363 nm for **119**; λ_{max} 263, 340 nm for **120**). PL of **119** in chloroform solution showed a maximum at 408 nm with a well-defined vibronic feature at 424 nm and a weak shoulder at ca 495 nm, while the thin film has a maximum 528 nm with a well-defined vibronic feature at 450 nm. In both cases excitation was at 366 nm. The fluorescence quantum yield for **119** was calculated to be 38%. For **120** in chloroform the emission was at λ_{max} 398 nm. The thin film showed a very broad emission profile with peaks at 440, 500, and 536 nm. The weaker broad emission at 500 and 536 nm was assigned as excimer emission. Large differences between PL in solution and thin films indicate the presence of aggregates or excimer formation within the film.

Yellow-green light with λ_{max} 523 nm with a weak shoulder at around 440 nm was observed for the device configuration ITO/CuPc/**119**/Al. A significant observation for the single-layer device ITO/**120**/Al was that the turn-on voltages both for current and light were almost the same at 5.9 V, indicating balanced injection and transport of charge carriers, while for the bi-layer device ITO/CuPc/**120**/Al the turn-on voltages for current and light were 9.7 and 8.1 V respectively, when CuPc was used as a hole transport/injection layer. This high electron affinity of **120** suggests that its single layer device has balanced charge injection and the hole-transporting CuPc was unnecessary. An EQE of 0.002% was recorded for the device ITO/**120**/Al which is compatible with single layer MEH-PPV devices. The inclusion of CuPc only slightly increased the EQE to 0.003%.

Liu *et al*[84] reported a copolymer of alternating biquinoline and dialkoxyphenylene vinylene units in the polymer main chain. **121** has excellent thermal stability with a decomposition temperature above 400 °C and a *Tg* of 147 °C and is readily soluble in organic solvents.

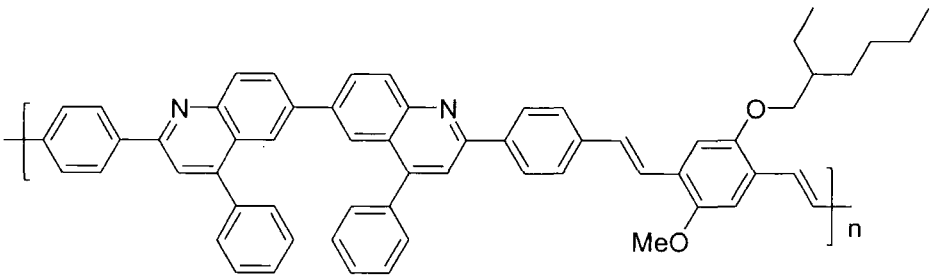

121

Scheme 53: Structure of copolymer 121 prepared by Horner-Wadsworth-Emmons olefination.[84]

UV-Vis absorption spectra in chloroform solution and thin films showed almost identical profiles with λ_{max} 406 nm. It is evident from the spectra that substituent chains prevent aggregation. PL spectra of **121** thin films and EL spectra for the device configuration ITO/**121**/Al were almost identical. Green-yellow emission was centred at λ_{max} 550 nm, slightly red-shifted in comparison with solution PL. MEH-PPV emits orange light, therefore, light emission from **121** emanates from the entire polymer chain and not just from the MEH-PPV segment. An EQE of 0.06% at a turn-on voltage of 18 V was achieved for ITO/**121**/Al.

1.12 QUINOXALINES

Polyquinoxalines are a family of polymers with quinoxaline units in the main chain. In general they possess good chemical and thermal stability and excellent solubility. Simple quinoxalines are prepared by cyclocondensation of an aromatic *o*-diamine and 1,2-dicarbonyl compounds. The synthesis of polyquinoxalines **124** and poly(phenylquinoxalines) **127** is carried out in a similar manner involving cyclocondensation reaction between bis(*o*-diamine)s **122** and **125** and aromatic bis(α-dicarbonyl) compounds, bisglyoxals **123** and bis(phenyl-α-diketones) respectively **126**.

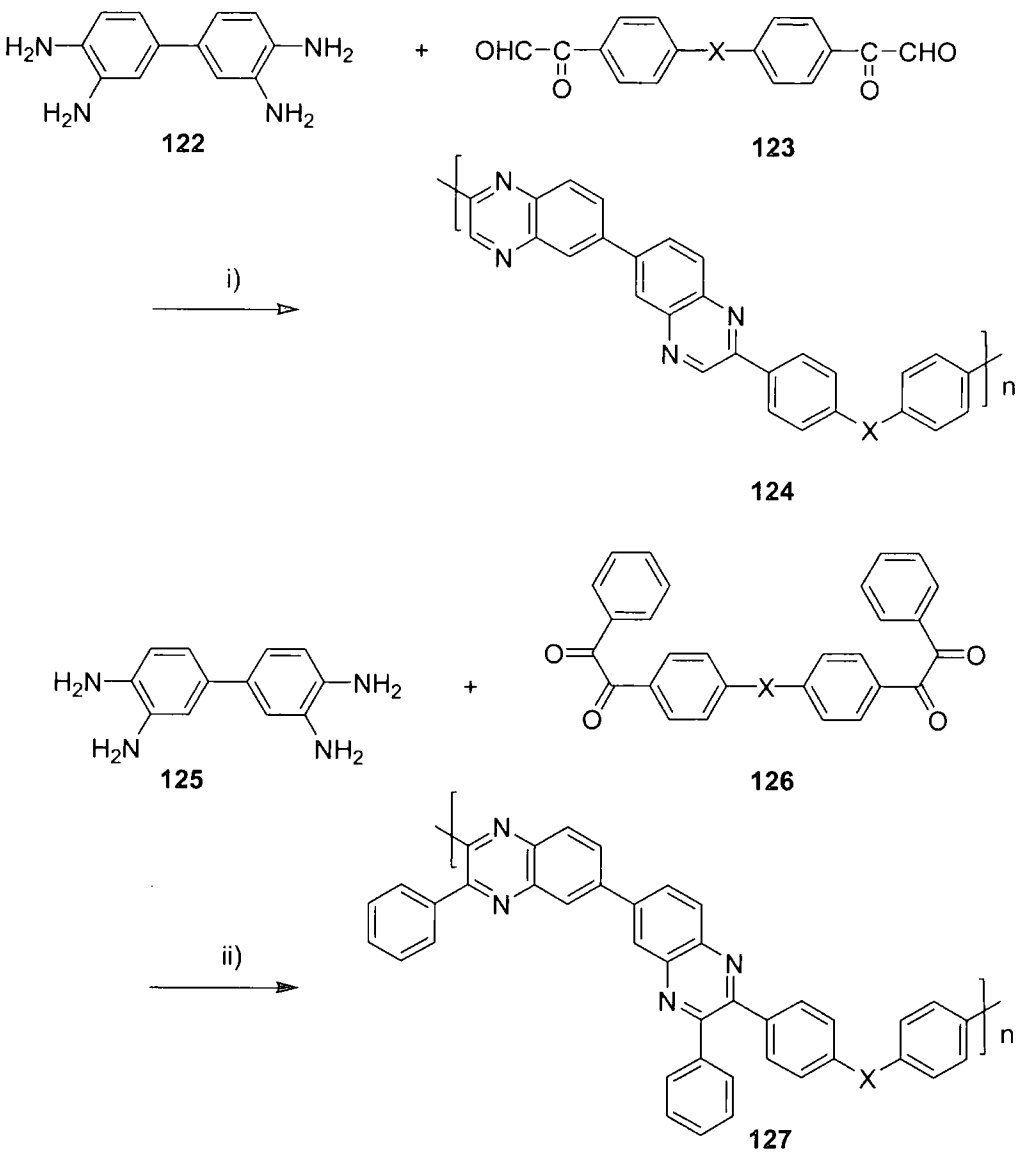

Scheme 54: Synthesis of polyquinoxalines 124 and poly(phenylquinoxalines) 127: i) *m*-cresol, 80 °C; ii) *m*-cresol, 40 °C.[50]

Poly(phenylquinoxalines) **130** can also be prepared by an activated poly(arylether) synthesis from bis(fluorophenylquinoxalines) **128** and various bisphenols **129** in the presence of base.[50]

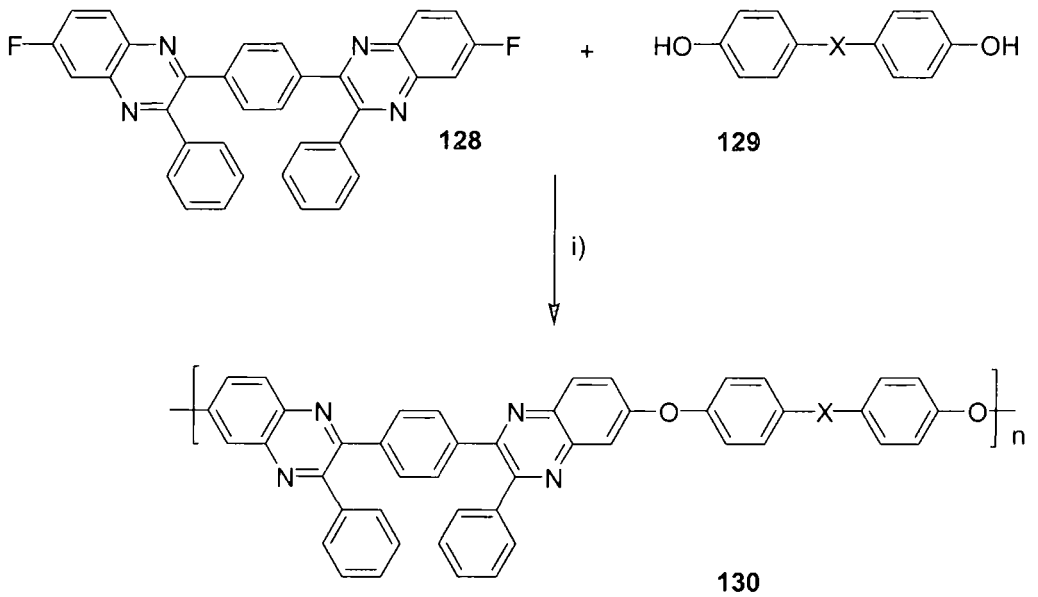

Scheme 55: Synthesis of poly(aryl ether phenylquinoxaline)s 130: i) NMP/Toluene, K_2CO_3.[50]

1.12.1 Low Molecular Weight Quinoxalines

Wang and co-workers[85] reported high EL from bilayer OLEDs composed of triphenyldiamine and quinoxaline dimer derivatives. Emission from the subsequent devices originated from exciplex formation at the interface between the two organic layers. Bilayer devices consisting of the hole-transporting materials (HT) TPD or PVK and quinoxaline derivatives (QX) **131** or **132** were fabricated in the general structure ITO/HT/QX/Mg;Ag.

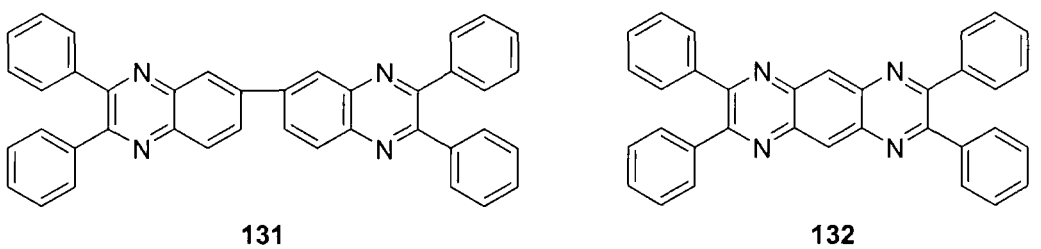

Scheme 56: Structures of quinoxaline derivatives 131 and 132 prepared by Wang *et al.*[85]

PL measurements for **131** and **132** show blue emission with λ_{max} values of 450 nm and 500 nm, respectively. Yellow-orange emission centred at λ_{max} 575 nm was observed for device A consisting of TPB/**131** and red light was witnessed for B TPB/**132** at λ_{max} 685 nm. The maximum luminances of the two devices were 600 cd m^{-2} and 70 cd m^{-2}, and the EQEs were 0.65% and 0.045%, respectively. In contrast peak emissions of bilayer devices incorporating PVK as the hole-transporting layer were blue-shifted with respect to their TPB counterparts. Blue light at λ_{max} 505 nm was emitted for device C PVK/**131** and red light for device D

PVK/**132** at λ_{max} 600 nm. Device C had a reduced brightness of 200 cd m^{-2} and EQE 0.4% when compared to its counterpart A. Device D, however, showed considerable performance improvement compared to device B, with a maximum brightness of 140 cd m^{-2} and EQE of 0.2%.

Thomas *et al*[86,87] have prepared dipolar compounds containing both quinoxaline/pyridopyrazine acceptors and arylamine/carbazole donors. It was demonstrated that the emission colour of these dipolar compounds could be tuned by modifying the donor and quinoxaline units.

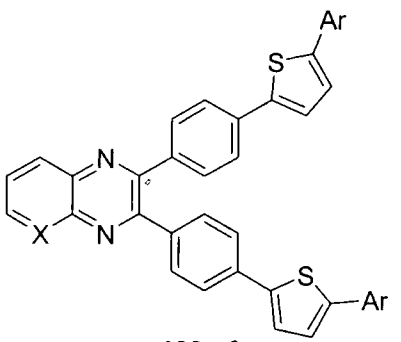

133a-f

133a: X= C, Ar =

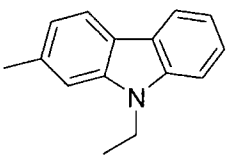

133b: X= C, Ar =

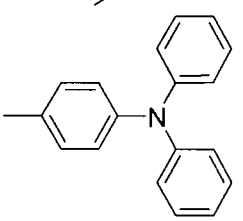

133c: X= C, Ar =

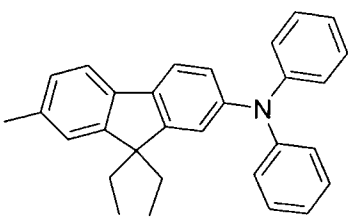

133d: X= N, Ar =

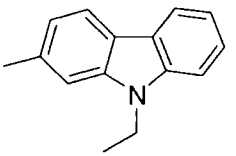

133e: X= N, Ar =

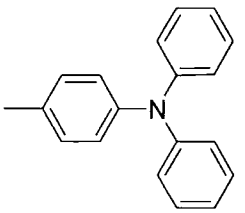

133f: X= N, Ar =

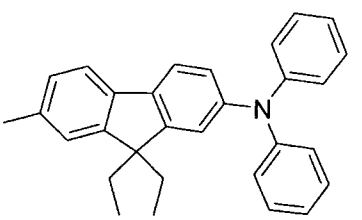

Scheme 57: Structures of dipolar quinoxaline/pyridopyrazine compounds synthesised by Thomas et al.[87]

High *Tg's* were realised for compounds **133a-f** over a range of 134-162°C. Glasses formed easily on heating with no crystallisation process observed even if the material was heated above the *Tg*. The pyridopyrazine derivatives **133d-f** possess slightly higher *Tg* (162, 148, 154 °C, respectively), than their quinoxaline counterparts **133a-c** (146, 134, 150 °C, respectively).

UV-Vis absorption spectra showed that compounds **133a-f** are green emitters in toluene solutions; however, in dichloromethane the emission is red-shifted with a reduction in quantum yield. Bright green/yellow emission was realised for the single layer device ITO/**133a**/Mg:Ag with λ_{max} 548 nm, operating at a maximum brightness of 10437 cd m^{-2} and maximum luminance efficiency 0.6 lm W^{-1}. Whilst single layer device performance was reasonable, this was enhanced by the inclusion of the electron-transport material Alq_3. The bilayer device ITO/**133a**/ Alq_3/Mg:Ag again emitted green/yellow light with λ_{max} 544 nm and the maximum brightness and luminance efficiency were increased to 42942 cd m^{-2} and 2.5 lm W^{-1} respectively. Bilayer devices were fabricated for **133b-e**. Due to its low volatility no device using **133f** could be constructed. The maximum brightness for the four devices was 4144, 41167, 6853 and 22366 cd m^{-2}, and the maximum luminance efficiencies were 0.2, 2.4, 0.3 and 0.8 lm W^{-1}, respectively. As for the previous bilayer device of **133a** all four devices showed green/yellow emission. The reduced performance of the more electron-deficient pyridopyrazine derivatives **133b** and **133d**, compared to **133a-c** is reminiscent of the work in our group by Wang *et al.*[30,42] however, this work clearly demonstrates the efficient electron-transporting qualities of quinoxaline based materials.

Wang *et al*[88] have studied the novel dihydroquinazolinone derivative **134**. PL spectra of **134** as a thin film showed green emission with λ_{max} 525 nm. A single layer device was fabricated with **134** as the emissive layer in the following configuration ITO/**134**/Al and greenish-yellow light was emitted with an EQE of 0.07%. A three-layered device with the structure ITO/TPD/**134**/Alq_3/Al was constructed. The Alq_3 layer included was to lower the energy barrier for electron injection and to improve electron transport, and conversely TPD was added to increase hole production within the organic material and enhance exciton formation. The EL maximum λ_{max} of 538 nm was consistent with the single-layered counterpart, which indicated that the emission originates from the radiative recombination of singlet excitons within **134**. The EQE increased by a factor of ten to 0.07% for the triple-layered device.

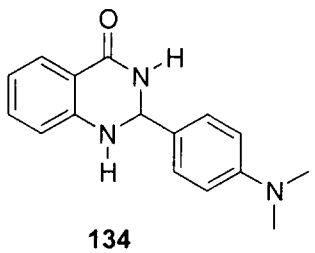

134

Scheme 58: Structure of dihydroquinazolinone derivative MAPQ 134.[88]

1.12.2 Polymeric Quinoxalines

A blue light emitting conjugated copolymer based on fluorene with a quinoxaline moiety in the main chain was reported as a potential candidate for OLEDs.[89] **135** has glass-forming character with a *Tg* of 208 °C. The absorption spectrum of **135** as a film and in chloroform solution have λ_{max} 402 nm and 404 nm, respectively. PL emission is in the blue region; in solution λ_{max} 448 nm, as a film emission is red-shifted by 7 nm to λ_{max} 455 nm. This small shift indicates that aggregation and excimer fluorescence is suppressed.

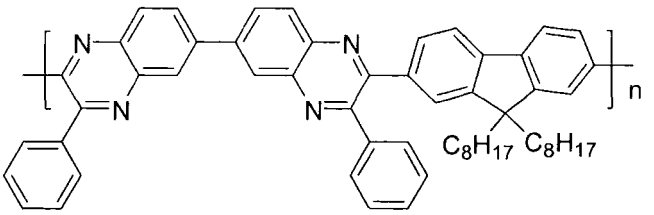

135

Scheme 59: Structure of 135 prepared by polycondensation of 2,7-bis(phenyloxoacetyl)-9,9-bis(2-ethylhexyl)fluorene and 3,3-diaminobenzidine in *m*-cresol.[92]

Polyether **136** functions as an ECHB material by lowering the current flow and increasing the EQE of PPV multilayer devices. Prepared by Pösch *et al*[40] **136** is highly soluble and thermally stable with a *Tg* and thermal decomposition of 269 °C and 484 °C, respectively. Optical data showed a UV-Vis absorbance at λ_{max} 269 nm and a fluorescence λ_{max} 431 nm.

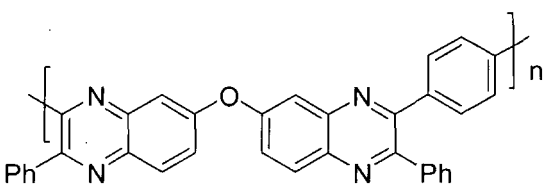

136

Scheme 60: Structure of ECHB material 136.[40]

The bilayer device ITO/PPV/**136**/Al gave a maximum brightness of 65 cd m^{-2} at a current density of 243 mA cm^{-2} in comparison to the reference diode that had a maximum brightness of 2 cd m^{-2} at a current density of 436 mA cm^{-2}. A lower onset voltage of 4.5 V was achieved compared to 6.0 V for the single layer PPV reference. EL spectra of bilayer OLEDs were identical to those of PPV devices, confirming that PPV acts as hole-transporting and emissive layer. Device performance clearly demonstrated increased injection of electrons from **136** facilitating charge recombination and photon generation in the emissive PPV material.

Dailey *et al*[90] reported a quinoxaline substituted vinylic polymer **137**, used as a homopolymer or as a copolymer with the hole-transporting material poly(4-vinyltriphenylamine) PVTPA. **137** is a charge-transport material with negligible emission properties, therefore, to evaluate its performance in emissive devices it was doped at a concentration of 0.5% (by weight) with the pyromethane laser dye PM580.

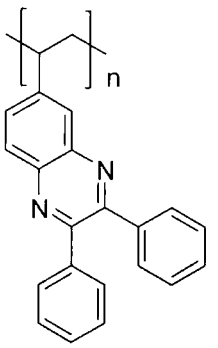

137

Scheme 61: Structure of 137 polymerised under free radical conditions using 2% AIBN under nitrogen in benzene at 70 °C.[90]

OLEDs were made using PVTPA:**137** random copolymer and a 1:1 blend of the corresponding homopolymers; both devices produced green-yellow emission from the PM580 dopant centred at λ_{max} 560 nm. For single-layer devices relatively high brightness was realised. Maximum brightness of 2290 cd m^{-2} for the blend and 1557 cd m^{-2} for the random copolymer at the same current were achieved. Overall EQEs of 0.114 and 0.073% were recorded for the blend and copolymer, respectively.

1.13 PYRAZOLO[3,4-B]QUINOLINES

Pyrazolo[3,4-b]quinoline derivatives **140** and **143** have been used as efficient blue emitters in multilayer OLEDs. They are prepared by two synthetic methods; firstly by reaction of *o*-aminobenzaldehyde **138** and 1-methyl-3-phenylpyrazol-5-one **139**; secondly substituted PAQ can be obtained by reaction of appropriately substituted aniline **141** with 5-chloro-4-formyl-1-methyl-3-phenylpyrazol **142**.[91]

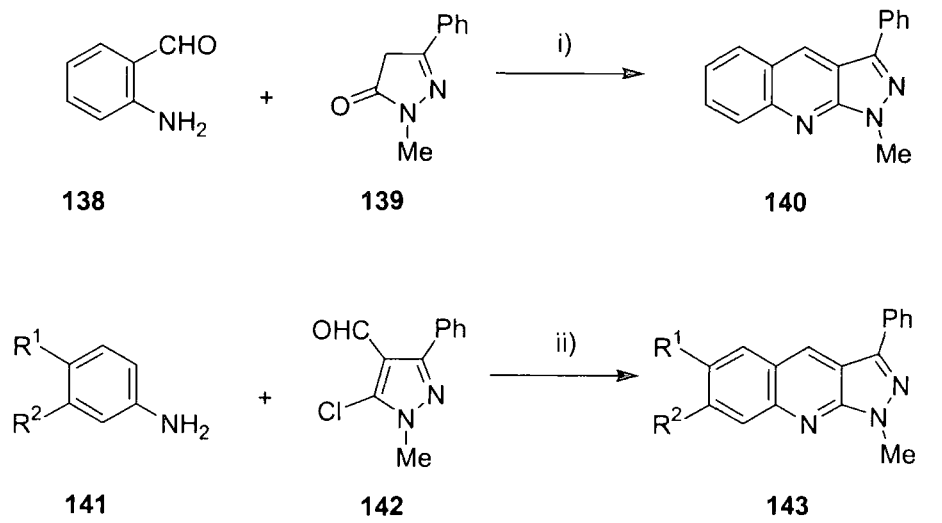

Scheme 62: Synthesis of pyrazoloquinolines: i) $POCl_3$, 100 °C, 2 h, sulfolane, 220 °C, 3 h; ii) Δ, 150-210 °C.[91]

1.13.1 Low Molecular Weight Pyrazolo[3,4-b]quinolines

Tao *et al*[92] synthesized a series of 1-methyl-3-phenyl-1*H*-pyrazolo[3,4-b]quinolines carrying various substituents at the 6- or 7-position which were studied as emitting materials in OLEDs.

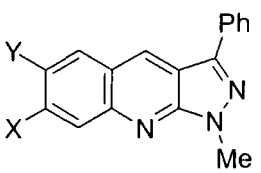

144 X = H; Y = OMe

145 X = H; Y = *t*-Bu

146 X = H; Y = H

147X = H; Y = F

148 X = CF_3; Y = H

149 X = H; Y = CN

150 X = H; Y = NEt_2

Scheme 63: Series of substituted pyrazoloquinolines prepared by Tao *et al.*[92]

The parent PAQ derivative **146** exhibits a *Tg* of 31.9 °C. With a substituent at the 6- or 7-position, the *Tg* further decreased or was undetected. UV-Vis absorption in ethyl acetate solution showed a similar absorption pattern between 300 and 450 nm for the variously substituted derivatives with the exception of **144** and **150**. A small but definite substituent effect was observed for derivatives with electron-withdrawing groups **147**, **148** and **149** are redshifted λ_{max} 398, 399 and 398 nm, respectively in comparison with the electron-donating

tert-butyl derivative **145** λ_{max} 388 nm. In contrast **144** was redshifted and splitting of λ_{max} 412 nm was observed. **150** was substantially redshifted λ_{max} 451 nm. PL in ethyl acetate solution showed that PAQ materials **144-149** are intensely blue emitters with the exception of **150** which emits in the green region λ_{max} 521 nm. The same substituent effect was observed for PL spectra. PAQ derivatives with electron-withdrawing groups **147**, **148** and **149** being redshifted λ_{max} 446, 462 and 468 nm, respectively in comparison with the electron-donating *tert*-butyl derivative **145** λ_{max} 434 nm. The parent derivative **146** and **144** were also redshifted with respect to **145** λ_{max} 438 and 442 nm, respectively. All PAQ derivatives have quantum yield greater than 0.5 with the exception of **150**, which has a quantum, yield of 0.19.

Multilayer OLED of the structure ITO/NPB/CBP/TPBI:PAQ-**144-150**/TPBI/Mg:Ag were fabricated. The TPBI was chosen as the host material for PAQ devices because it has a wide band gap material and emits strongly at λ_{max} 376 nm where most of the PAQ derivatives have strong absorption. Two-layers of hole-transporting material NPB and CBP were used because CBP serves as to provide an intermediate HOMO level by which holes can pass into the TPBI layer.[93] EL spectra of OLEDs with 2% (w/w) PAQ doped into TPBI are blue except for **150** which is green. The EQE for devices with electron-donating substituents **144** and **145** were 2.93 and 3.00%, respectively, which were higher than 2.46% recorded for the parent derivative **146**. Devices with electron-withdrawing substituents **147**, **148** and **149** have lower EQE than their electron-donating counterparts with values of 2.03, 0.49 and 1.53%, respectively. The green emitting **150** based device has a EQE of 2.12%. It is worth noting that the maximum brightness of this device was 1169 cd m^{-2} which is double the maximum brightness of 584 cd m^{-2} achieved for the highest blue emitting **144** based device.

Tao and co-workers continued this research by synthesizing a second series of 6-substituted-3-methyl-1-phenyl-4-(4-methoxyphenyl)-1*H*-pyrazolo[3,4-b]quinolines MeOPAQ.[94]

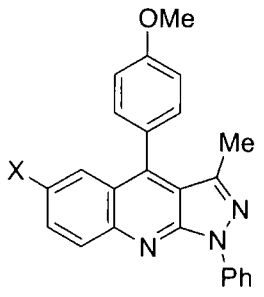

151 X = *t*-Bu **154** X = F

152 X = OMe **155** X = Cl

153 X = H **156** X = Br

Scheme 64: Series of 6-substituted-3-methyl-1-phenyl-4-(4-methoxyphenyl)-1*H*-pyrazolo[3,4-b]quinolines MeOPAQ-X prepared by Tao *et al.* [94]

Tgs were recorded for derivatives **151-153**, which were 62.6, 53.6 and 38.1 °C, respectively; no *Tg* data was recorded for the other three derivatives. All MeOPAQ derivatives have similar UV-Vis absorption profiles with a major absorption peak being around 390-400 nm. PL spectra show that all derivatives are blue emitting λ_{max} for **151-153** 448, 452, 450 nm, respectively; halogen derivatives **154-156** are redshifted in comparison λ_{max} 460, 459 and 460 nm, respectively.

Four MeOPAQ derivatives **151-154** were selected for OLED fabrication of general configuration ITO/NPB/CBP/TPBI:2%-**151-154**/TPBI/Mg:Ag. Bright blue EL λ_{max} 442, 454, 454 and 458 nm, respectively, was observed for all four dopants tested with emission originating from the MeOPAQ derivatives. The luminance reaches as high as 13,500 cd m^{-2} in the case of **153** with an EQE of 3.4%. Other substituents also have similar performance but are less bright than **153**.

Tao *et al* have also reported very bright blue OLEDs using highly fluorescent dipyrazolopyridine derivatives 4-(4-substituted-phenyl)-1,7-diphenyl-3,5-dimethyl-1,7-dihydrodipyrazolo[3,4-b,4′,3′-e]pyridine (PAP), as emitter by doping the dye in a electron-transport host (TPBI).[93,95]

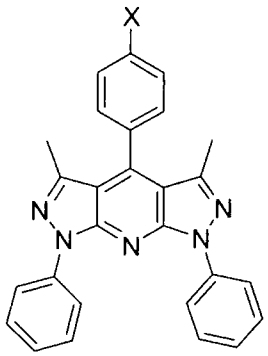

157 X = OMe

158 X = Ph

159 X = CN

Scheme 65: Dipyrazolopyridine derivatives prepared by Tao and co-workers.[95]

PL in ethyl acetate solution showed blue emission for **157-159** with λ_{max} 426, 440 and 463 nm, respectively. Thin film emission was slightly redshifted with respect to solution λ_{max} 438, 443 and 466 nm, respectively. The electron-withdrawing cyano derivative **159** has the lowest relative quantum yield of 0.50 in comparison to 0.76 for **157** and 0.89 for **158**.

OLEDs with a general configuration ITO/NPB/CBP/TPBI:2%-PAP-**157-159**/Mg:Ag showed blue emission. As the substituent changes from electron-donating to electron-withdrawing EL emission is redshifted λ_{max} 440, 448 and 462 nm, respectively. The **159** based device is exceptionally good, with a brightness of 11,200 cd m^{-2} at 14.2 V and EQE of 3.2%.

1.14 CONCLUSIONS

In conclusion, since the initial discovery that organic conjugated polymers such as PPV could be used as emissive materials in OLEDs[7] there has been a plethora of publications describing new light-emitting polymers. An important aspect of this work has been the emergence of π-electron deficient heterocyclics carrying imine nitrogen atoms being used to improve electron injection/transport and hole-blocking properties. This chapter has reviewed and updated the literature regarding the use of low molecular weight, oligomeric and polymeric π-electron deficient heterocycles, as emissive and ECHB layers in OLEDs.

2 New Pyrimidine- and Fluorene-containing Oligo(arylene)s

2.1 Introduction

It is surprising that pyrimidine units have been only very rarely incorporated into conjugated oligomer or polymer structures. For example, poly(pyrimidine-2,5-diyl) **86** is an electron accepting material which can be doped with sodium to obtain an n-type semiconductor,[68] a 1,3,4-oxadiazole–pyrimidine hybrid oligo(arylene) **37h** has been shown to function as an electron conducting/hole blocking (ECHB) layer in bilayer LEDs using poly[2-methoxy-5-(2-ethylhexyloxy)-1,4-phenylene-vinylene] (MEH-PPV) as the emissive material.[30] In addition, the linear phenylene-pyrimidine penta-arylene systems **84a-c** and the spirobifluorene–pyrimidine hybrid **85** are blue emitters.[66,67]

Pyrimidine was attractive to us for two main reasons: (i) it has a higher electron affinity than pyridine;[96] and (ii) due to the lack of *ortho–ortho* interactions of C–H hydrogens, 2-arylpyrimidine derivatives should be more planar (i.e. possess increased π–conjugation) compared with 2-arylpyridine (or biphenyl) analogues. Our initial aim, therefore, was to develop efficient syntheses of new and versatile functionalised pyrimidines, especially pyrimidine-containing oligo(arylene) systems. This chapter reports the synthesis of such compounds, namely **166** and **172–175**, along with the X-ray crystal structures of **165**, **166** and **174**, *ab initio* calculations, optical absorption and photoluminescence spectra, and OLED studies using compound **175** as the emissive layer. The fluorenyl core of **172–175** was chosen because of its known high stability and luminescence efficiency, with the alkyl chains at C(9) imparting good solubility in organic solvents.[97,98]

2.2 Results and Discussion

2.2.1 Synthesis

Suzuki cross-coupling methodology is a very versatile route to oligo(arylene)s[99] and for this purpose we required 2,5-dibromopyrimidine **163** as a starting material. Compound **163** was

readily obtained in 29% yield from commercial 2-hydroxypyrimidine hydrochloride **160** using a procedure that proved to be considerably more convenient than the literature routes.[100] Goodby *et al.*[101] reported the syntheis of **163** direct from the starting material **160** using Br_2, water then reflux in $POBr_3$. However, no detailed experimental procedure of percentage yield was reported therefore this method was not pursued.

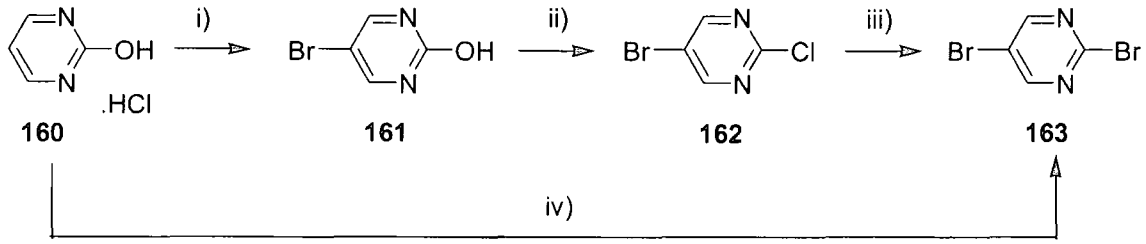

Scheme 66: Synthesis of 2,5-dibromopyrimidine 163: i) Na_2CO_3 (aq), Br_2; ii) $POCl_3$; iii) 48% HBr; iv) Br_2, H_20. Then $POBr_3$.[101]

There are very few examples of Suzuki reactions on halopyrimidines,[66,102] so as a test reaction, **163** was treated with benzeneboronic acid **164** (3.0 equivalents) in the presence of catalytic $Pd(PPh_3)_4$ in refluxing tetrahydrofuran (THF). Two products were obtained which were easily separated and identified as 2-phenyl-5-bromopyrimidine **165** (43% yield) and 2,5-diphenylpyrimidine **166** (32% yield), both of which had been obtained previously by different routes.[103] This reaction is of fundamental interest in that it established that the bromine atom at C(2) of compound **166** is more labile under standard Suzuki conditions. Compound **166** was obtained in higher yield (62%) using benzeneboronic acid **164** (2.0 equivalents) and $Pd_2(dba)_3$ catalyst[104] at 20 °C.

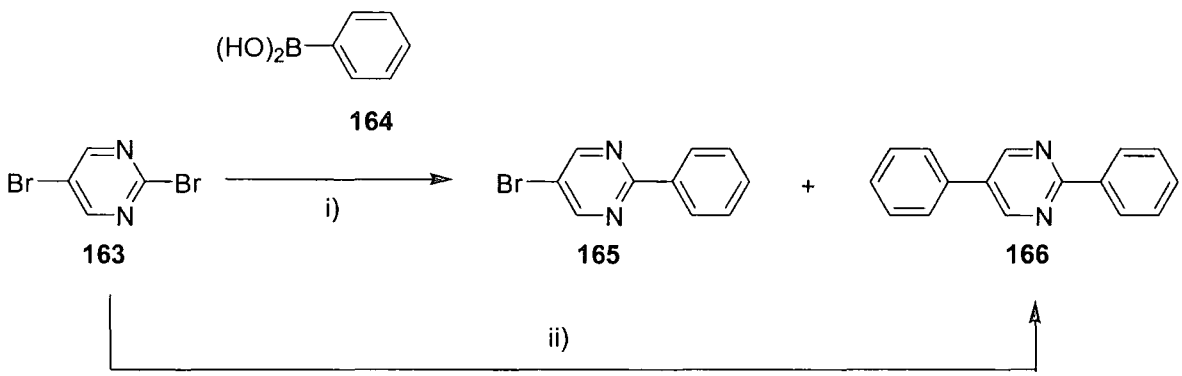

Scheme 67: Synthesis of 165 and 166: i) benzeneboronic acid 164, $Pd(PPh_3)_4$, THF, Na_2CO_3, Δ; ii) benzeneboronic acid 164, $Pd_2(dba)_3$, THF, 20 °C.

2,7-Dibromo-9,9-dihexylfluorene **168** was obtained in 85% yield from commercial dibromofluorene **167** by deprotonation with potassium *t*-butoxide followed by alkylation with bromohexane.[105] This procedure seems more convenient than the two-step route from

fluorene (alkylation, then bromination) reported by several other groups.[97b,98] 9,9-Dihexylfluorene-2,7-diboronic acid **169**, which is a key reagent for many fluorene-based luminophores, was obtained in 86% yield from **168** by reaction with *n*-butyllithium and triisopropylborate, followed by aqueous workup.[106] All the data obtained for **168** and **169** confirm no detectable contamination with unwanted fluorenone by-products. Compound **169** is a shelf-stable solid, and its reaction with two equivalents of 2-bromopyrimidine **170**, 5-bromopyrimidine **171** and 2,5-dibromopyrimidine **163**, as above, gave **172**, **173** and **174** in 34, 32 and 23% yields, respectively. A further two-fold Suzuki reaction of benzeneboronic acid with compound **174** afforded the hexa(arylene) system **175** (35% yield) bearing terminal phenyl groups. The low yield of pure product from this capping reaction was primarily due to difficulties in the purification of **174**.

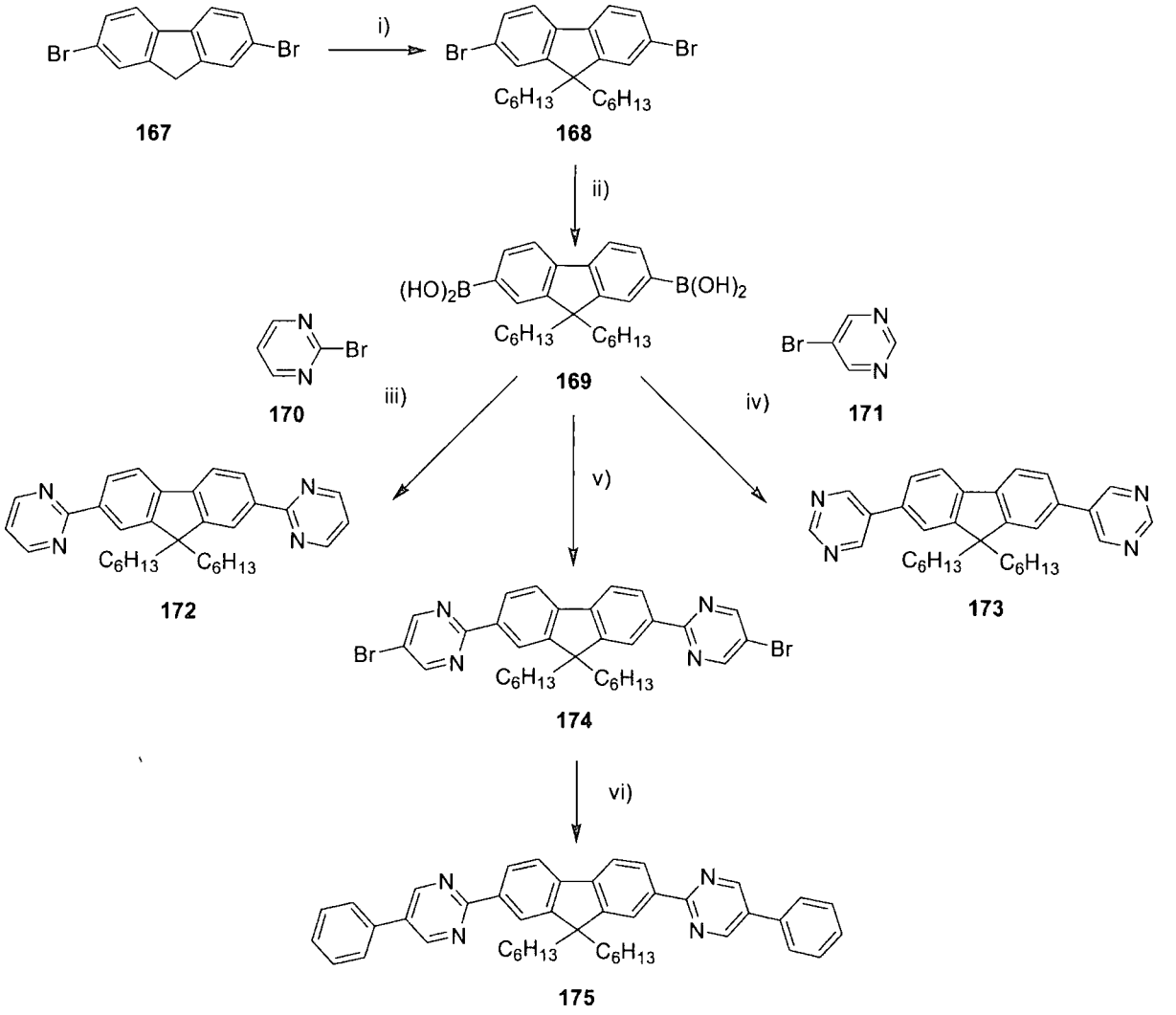

Scheme 68: Synthesis of compounds 168-175: i) 1-bromohexane, *t*-BuOK, THF, 0 °C → 20 °C ; ii) *n*-BuLi, THF, –78 °C, triisopropylborate. –78 °C → 20 °C, then H_2O; iii) 2-bromopyrimidine 170, THF, $Pd(PPh_3)_4$, Na_2CO_3, Δ; iv) 5-bromopyrimidine 171, THF, $Pd(PPh_3)_4$, Na_2CO_3, Δ; v) 2,5-dibromopyrimidine 163, THF,

$Pd(PPh_3)_4$, Na_2CO_3, Δ; (vi) benzeneboronic acid 164, THF, $Pd(PPh_3)_4$, Na_2CO_3, Δ.

2.2.2 X-Ray Crystal Structures of Compounds 165, 166 and 174

Crystal structures were solved by Dr A. Batsanov. Molecule **165** (Figure 12) is twisted around the C(2)–C(11) bond by 18.3° which is smaller than that observed in biphenyl (see discussion below), thus confirming that nitrogen atoms facilitate planarisation of the system.

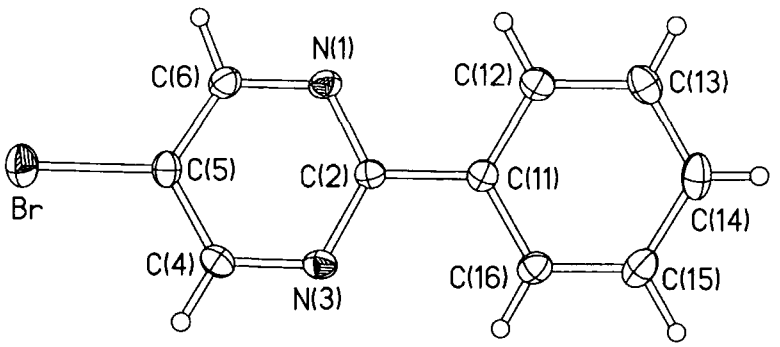

Figure 12: X-ray molecular structure of 165 (henceforth thermal ellipsoid are drawn at 50% probability level).

Molecule **166** (Figure 13) is located on a crystallographic twofold axis, normal to the long axis of the molecule. The central pyrimidine ring is disordered between two orientations, related via this axis and forming an interplanar angle of 14.8°. In each case, the pyrimidine ring is inclined by 19.8° and 34.6° to the phenyl groups in positions 2 and 5, respectively that reflects the same tendency of planarisation of the system via substitution of C–H by nitrogen atoms in oligophenylenes.

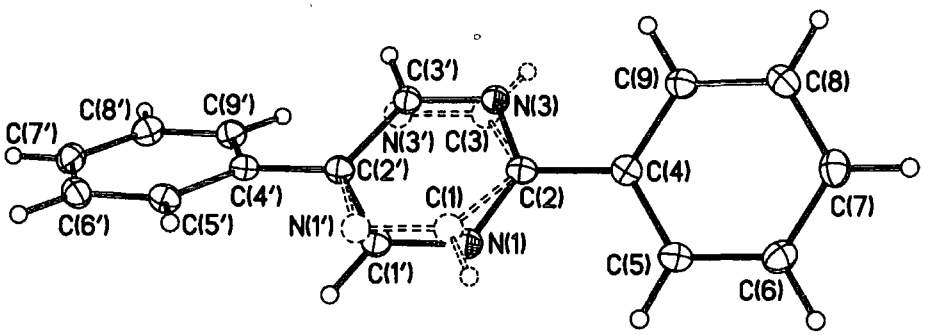

Figure 13: X-ray molecular structure of 166, showing the disorder of the pyrimidine ring. Atoms, symmetrically dependant via the twofold axis, are primed.

In molecule **174** the fluorene moiety is planar, while the pyrimidine rings bonded to C(4) and C(10) are inclined to its plane by 5.1° and 5.6°, respectively (Figure 14). These angles are much smaller that those observed for **165** and **166**, which could be a result of better

conjugation of the pyrimidine rings with the central planar fluorene core in this extended π–system. One *n*-hexyl chain entirely and the other one nearly [with the exception of the terminal C(33) atom], adopt an all-*trans* conformation and lie in one plane, perpendicular to the fluorene plane.

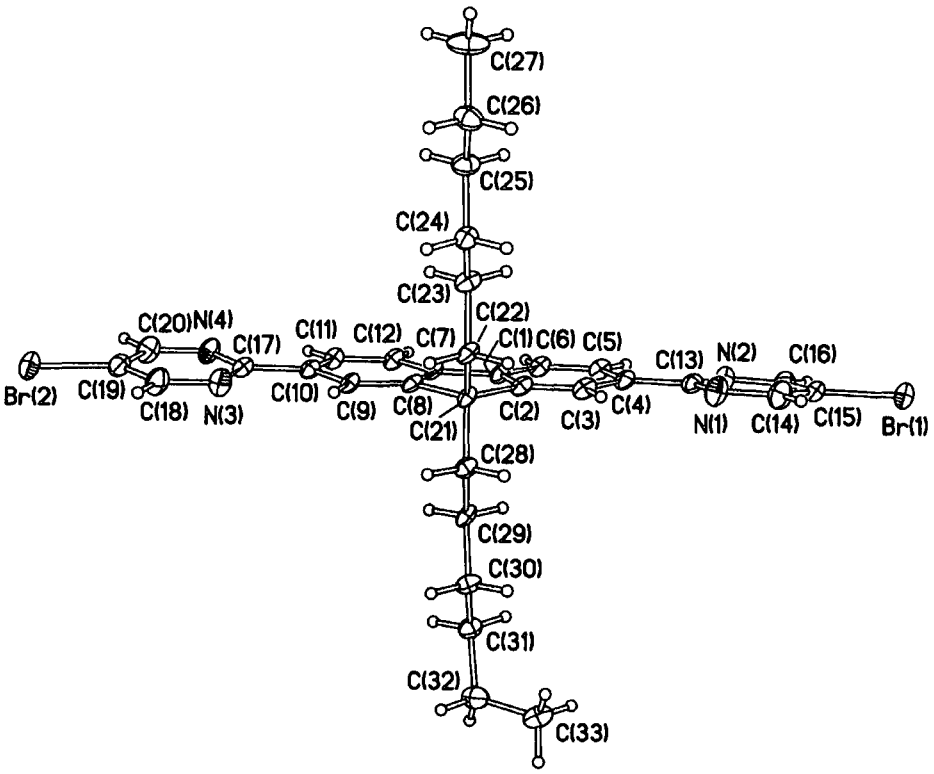

Figure 14: X-ray molecular structure of 174.

In an isolated molecule, the twist angle (ω) between two bonded aromatic rings depends on the balance between π conjugation (which favours planarity) and steric repulsion between H atoms (or substituents) in *peri*-positions. For the latter, heteroatoms and substituents in *meta*- and *para*-positions are largely irrelevant. Hence a 5-phenylpyrimidine (or 5,5′-bispyrimidine) moiety (type A link) can be expected to behave in the same way as the biphenyl molecule, which has potential barriers (albeit low, 2 to 2.5 kcal mol^{-1}) at both $\omega = 0$ and $\omega = 90°$,[107] and the stable conformation with an intermediate twist, as observed in the gas phase by electron diffraction ($\omega = 45°$),[108] Raman ($\omega = 25°$)[109] or electron spectroscopy ($\omega = 40°$),[107d] as well as in solutions and melts ($\omega = 32 \pm 2°$).[110] Although in the solid state the molecule lies at a crystallographic inversion centre (which implies planarity) there are indications of disorder, so that the actual conformation is probably a slightly twisted one,[111] as in fact is observed in the non-centrosymmetric low-temperature phase.[107a] In any case, a 2-phenylpyrimidine moiety (type B link) lacks the main driving force for twisting, the pyrimidine having no peri-H atoms. Indeed, in eight previously studied structures with sterically unhindered 2-

phenylpyrimidine moiety,[96,112] the dihedral angle between the phenyl and pyrimidine rings varies from 0 to 14.5°. Four of these contain simultaneously type A and B links, and present two different conformations. In 2-(4-*n*-propoxyphenyl)- and 2-(4-*n*-butoxyphenyl)-5-phenylpyrimidines[112b] and 1,4-bis(5-phenyl-2-pyrimidinyl)-phenylene[96] the B-link is twisted much more (35 – 39°) than the A-link (3 – 9°); while in 2-phenyl-5-(4-*n*-pentoxyphenyl)pyrimidine[112d] *both* A and B-twists are small (6–9°) and the molecule is approximately planar.

2.2.3 Optical Absorption and Photoluminescence Properties

Solution UV-Vis absorption and photoluminescence (PL) spectra for **172–175** were recorded in DCM. There is a progressive red shift in the value of λ_{max} of the low energy band in the sequence **173** (328 nm), **172** (352.5 nm), **174** (365 nm) and **175** (371.5 nm) (Figure 15, Table 1). Estimated from the low-energy absorption edge, HOMO–LUMO energy gaps (E_g) are 3.39, 3.47, 3.28 and 3.13 eV, for compounds **173**, **172**, **174** and **175**, respectively. This order of E_g evolution is expected: twisting between pyrimidine and fluorene rings in compound **173** as compared to its planar isomer **172** (see calculation section below) hinders electron delocalisation and therefore results in an increase of E_g, whereas π–extension of the system by attaching additional phenyl rings to **172** to give **175** leads to E_g contraction. This trend in HOMO–LUMO gap changes is well reproduced by *ab initio* calculations (see **Appendix 1**).

Compound	UV-Vis Absorption, λ_{max}/nm	PL, λ_{max}/nm
172	317.0, 337.5, 352.5	366, 384
173	328.0	361, 378
174	348.0, 365.0	377, 396
175	365.5, 371.5	391, 412

Table 1: UV-Vis absorption and emission λ_{max} values for compounds 172-175 in dichloromethane, 20°C.

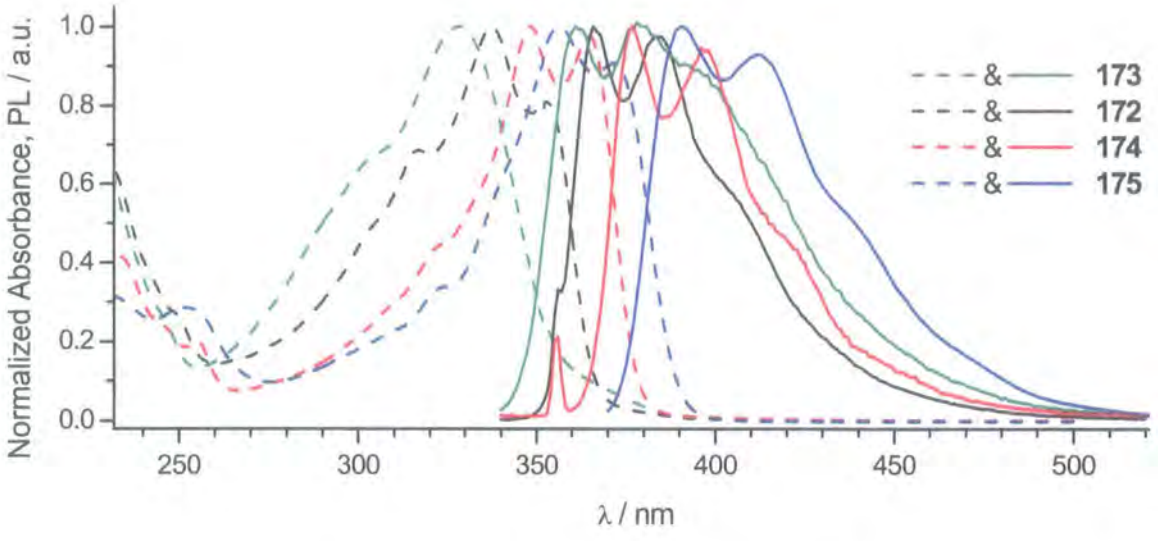

Figure 15: Normalised UV–Vis absorption (dashed lines) and PL (solid lines) (excitation at 355 nm) spectra for compounds 172-175 in DCM, 20 °C.

The λ_{max} values for the emission spectra obtained by excitation at 355 nm are also red shifted in the same sequence as the absorption spectra (Figure 15, Table 1). Absorption of light by the conjugated organic molecules **172-175** gives rise to an n-π^* or π-π^* transition and promotes an electron to the LUMO. The energy levels are broadened by vibration and rapid vibronic relaxation to the bottom of the LUMO, followed by radiative decay to the ground state. Hence, the UV-Vis absorption and PL emission spectra (Figure 15) are broad bands, with the latter red-shifted to longer wavelengths.[3] The photoluminescence quantum yield (PLQY) for **174** and **175** in DCM solution were 25% and 85%, respectively. The high PLQY value obtained for **175** is consistent with that observed in other fluorene-containing oligomers,[97,113] and, importantly, confirms that the presence of the pyrimidine units is not detrimental to the high luminescence efficiency of the fluorene moiety. It has been reported that when some heterocyclic segments, e.g. 2,1,3-benzothiadiazoles, are incorporated into poly(fluorene) chains the fluorene photoluminescence is completely quenched due to exciton confinement.[114] The considerably lower PLQY value for **174** can be explained by quenching of the emission by the bromine substituents.

The PL spectra of solution and thin film of **175** (Figure 16) show well-structured emission bands with λ_{max} = 414 nm (toluene solution) and 418, 440 nm (film). We calculate a solid state PLQY of 21%, similar to that of many polyfluorenes.[97]

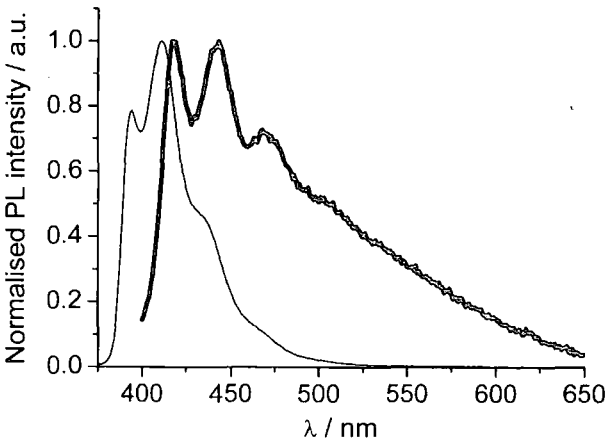

Figure 16: Photoluminescence spectra of 175 in toluene solution (thin line) and solid state (thick line). Excitation was at 350 nm.

2.2.4 Light-Emitting Device Studies

The light-emitting diodes comprising a thin film (300 nm) of compound **175**, sandwiched between poly(ethylenedioxy-thiophene) (PEDOT)-coated ITO glass and Ca electrodes, ITO/PEDOT/**175**/Ca/Al, were fabricated by B. P. Lyons in collaboration with Prof A. Monkman's group in the Department of Physics, University of Durham. These devices had turn-on voltages of 40 – 50 V, such that an electric field of ~1.5 MV/cm (typical for this class of material)[115] was required to achieve electroluminescence (EL). This luminescence was blue-green (λ_{max} 500 nm) and of low intensity < 10 cd m^{-2} (Figure 17). This low-energy emission is absent from the PL spectra of the solution, suggesting that it arises from aggregates in the film.[116] To support this point, Figure 13 also shows the difference between the PL in solid state and in solution. This represents emission from dimeric states in the film that are not present in the solution. As the film absorption spectrum (not shown) shows no evidence of a corresponding ground state absorption to the red side of the π-π^* absorption band, these states are most likely to be excimers, which are formed by strong coupling between excited and ground state molecules, and usually have very low quantum yields. Small molecules like **175** (as opposed to polymers) are renowned for excimer formation.[117] We can discount the presence of defect sites (e.g. ketones which can be formed during the operation of polyfluorene-based LEDs[118]) as the source of low EL intensity as related fluorene-based compounds synthesized in our laboratory have been shown not to possess these defects.[119] There is a reasonable match between this excimer emission and the EL spectra, supporting our claim that EL emanates from these excimer states. The high turn-on

voltage and low intensity of the emission will preclude practical device applications, so we have not explored **175** further in this context.

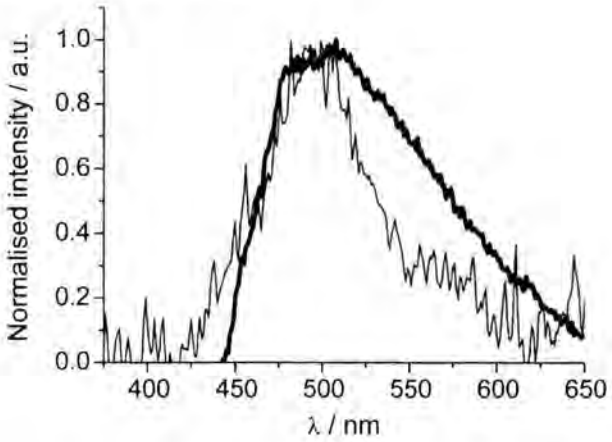

Figure 17: Electroluminescence spectra (thin line) and excimer emission (thick line) from 175. The excimer emission was calculated by first red-shifting the solution photoluminescence by 31 nm, such that the emission modes coincided with those in the solid state. The spectra were then normalised and the solution emission was subtracted from that of the thin film.

2.2.5 Electrochemical Properties

The electrochemical behaviour of compounds **172**, **173,** and **175** was studied by cyclic voltammetry (CV) in DCM solution at room temperature using Bu_4NPF_6 (0.2 M) as supporting electrolyte.

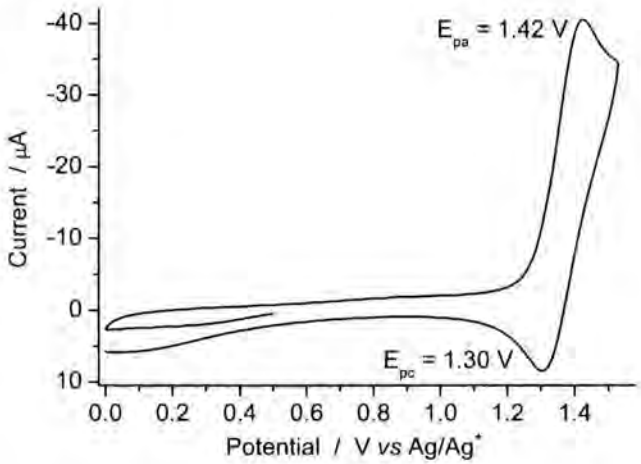

Figure 18: Cyclic voltammogram of compound 175 in 0.2 M Bu_4NPF_6 / DCM, scan rate 100 mVs^{-1}, 20 °C.

The CV of compound **175** (Figure 18) shows a quasi-reversible (ΔE_{pa-pc} = 120 mV) oxidation peak at $E_{1/2}^{0}$ = +1.36 V (vs. Ag/Ag^{+}). Compared to compound **175**, compound **172** is a poorer donor with an oxidation observed at higher potentials. Moreover, the oxidation process

becomes irreversible showing only an anodic peak at E_{pa} = +1.50 V (at 100 mV s^{-1}) [in addition, the adsorption of the material on the electrode surface occurs during the CV experiment, so the current on subsequent scans is decreased]. The observed difference in E_{pa} values between **172** and **175** (1.50 – 1.42 = 0.08 V) is in good agreement with the difference in the energies of their HOMO orbitals calculated at both Hartree-Fock(HF) and density functional theory (DFT) levels of theory (0.11 – 0.12 eV). For compound **173** we were not able to measure an E_{ox} potential which should lie at much more positive potentials. Thus, the calculated energy of the HOMO orbital (Table A **Appendix 1**) for **173** is 0.41–0.45 eV lower than that of **175**, so its E_{pa} value is estimated to be around +(1.91 – 1.96 V) which is out of the range of the electrochemical transparency of DCM.

The estimated HOMO–LUMO gaps for all compounds **172–175** from their optical spectra are higher than 3 eV, therefore, reduction is predicted to occur at potentials around –2 V, which is out of the window of electrochemical transparency of DCM, so it is not possible to experimentally determine the electrochemical band gap for these compounds (although E_{red} values for some oligo/poly-fluorenes were measured in THF or acetonitrile.[120]

2.2.6 Quantum Chemical Calculations

Ab initio calculations were performed by Dr I. F Perepichka in our group. The geometries and electronic structures at the Hartree-Fock (HF) and density functional theory (DFT) levels of theory were determined for compounds **172**, **173** and **175** (with ethyl substituents replacing hexyl) and for their dipyrazinyl and bistetrazenyl analogues, **176**, **177**, **179** and **180**. The heterocyclic nitrogen atoms of **172** and **175** facilitate planarisation of the system, compared to **173**, which is in agreement with X-ray structural data obtained for 5-bromo-2-phenylpyrimidine **166**, 2,5-diphenylpyrimidine **167** and compound **174**. Bistetrazenyl derivative **180** is calculated to be a fully planar system. (For a more detailed discussion of Quantum Chemical Calculations see **Appendix 1**).

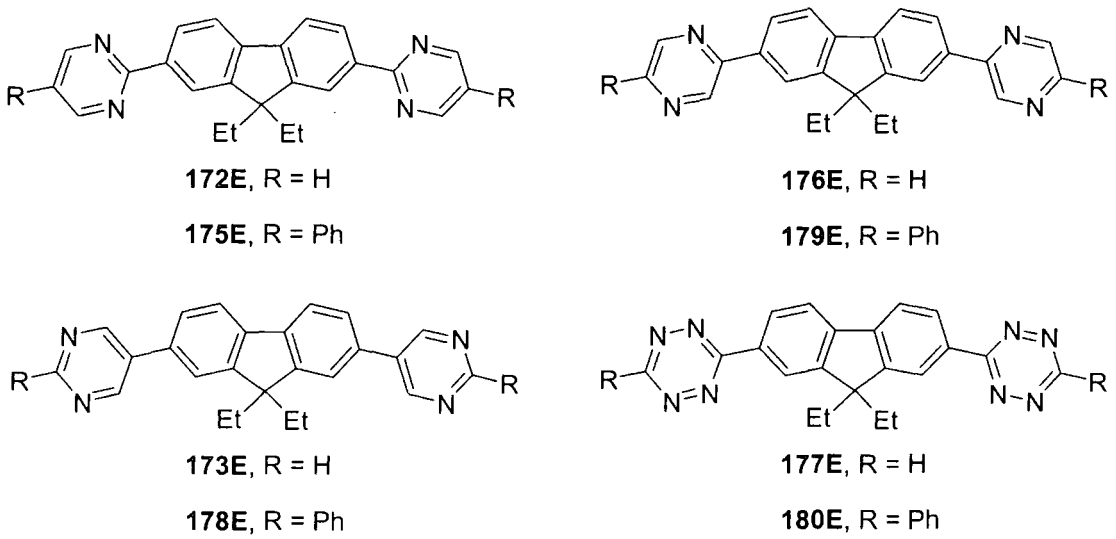

172E, R = H

175E, R = Ph

176E, R = H

179E, R = Ph

173E, R = H

178E, R = Ph

177E, R = H

180E, R = Ph

Scheme 69: Structures of compounds 17E, 173E, 175E-180E studied by *ab inito* calculations.

2.3 CONCLUSIONS

A series of new pyrimidine-containing oligo(arylenes) has been synthesised by Suzuki cross-coupling methodology and shown to possess interesting X-ray structural intramolecular twisting torsion angles, photophysical and electronic properties. Theoretical calculations for pyrimidine, pyrazine and tetrazine derivatives establish that the nitrogen atoms decrease steric repulsion, which exists in biphenyl derivatives, resulting in planarisation of the system as could be predicted from molecular models additional trends in HOMO and LUMO levels have been determined. X-ray crystal structures of **166**, **167** and **174** together with *ab inito* calculations demonstrate that the nitrogen atoms of the pyrimidine ring facilitate planarisation allowing efficient electron transport through this class of material. Compound **175** has been used as the emissive layer in an OLED: at a high turn-on voltage blue-green light (λ_{max} 500 nm) is emitted, which most likely emanates primarily from excimer states. Our synthetic methodology is versatile and further chemical modifications within this class of oligomers are underway to provide new materials with tunable optoelectronic and photophysical properties.[121]

3 NEW PYRAZINE CO-OLIGOMERS

3.1 INTRODUCTION

In the search for materials with improved electron transport and tailored luminescence properties, the incorporation of electron deficient-heterocycles, e.g. 1,3,4-oxadiazole, pyridine, pyrimidine, quinoline, quinoxaline and 1,3,5-triazine into conjugated backbones is being vigorously pursued, as discussed in Chapter 1. In this context the symmetry of 2,5-disubstituted pyrazines has obvious attractions, and although distyrylpyrazines have been reported by several groups, *diarylpyrazines and related oligomers remain essentially unexplored.* Hasegawa *et al.*[122] reported that substituted distyrylpyrazines show green electroluminescence, and Grimsdale *et al.*[69] demonstrated that the photoluminescence of these materials [including a pyrazine-di(*N*-oxide) derivative] can be tuned from blue to red by changing the substituents. In conjunction with a substituted 1,1'-biphenyl-4,4'-diamine derivative as a hole transport layer, blue emission has been observed from distyrylpyrazines.[70] Peng and Galvin reported orange electroluminescence from a single-layer LED using a pyrazine-containing PPV derivative as the emissive layer.[72] Katimoto *et al.* reported orange-red luminescence from thin films of polyimides containing distyrylpyrazine units in the backbone.[71] A bilayer device using 2,3-dicyano-5-phenyl-6-[2-(4-formylphenyl)ethenyl]pyrazine gave low intensity electroluminescence (λ_{max} not reported).[123] In a different context, intramolecular hydrogen bonding in 2,5-bis(2-aminophenyl)pyrazine derivatives has recently been exploited in the construction of ladder-like oligomers,[76] and condensation polymerisations of functionalised pyrazine monomers have been reported.[74]

For heteroatomic systems with a basic nitrogen atom, protonation can provide a means of tuning the optoelectronic properties. For example, upon protonation of poly[2,5-bis(3,4-ethylenedioxy-2-thienyl)pyridine] Reynolds *et al.* observed a 70 nm red shift in the absorption spectra,[64] and work in our group in collaboration with Monkman *et al.* established a similar shift in the absorption and emission spectra of poly{2,5-pyridylene-*co*-1,4-[2,5-bis(2-ethylhexyloxy)]phenylene}.[63] We recognised, therefore, that it would be of interest to explore the protonation of pyrazine systems, for which, unlike the aforementioned pyridine systems, diprotonation of the heterocycle might be achieved.

3.2 Results and Discussion

3.2.1 Synthesis

3.2.1.1 Attempted Preparation of 2,5-Dibromopyrazine 191

Our initial target molecule was 2,5-dibromopyrazine **191** with the intention of utilising the hydrogen bonding capacity of the pyrazine ring in driving the resulting oligomers into a planar configuration, thus extending the π-conjugation and tuning the optoelectronic properties. A review of the literature showed that **191** would require a lengthy and time-consuming synthesis. The published synthesis of 2,5-dibromopyrazine **191** by Ellingson and Henry[124] started from 2-aminopyrazinecarboxylic acid methyl ester **186**, which at the time of this work was not commercially available. Compound **186** was subsequently prepared as described by Chen *et al* (Scheme 70).[125]

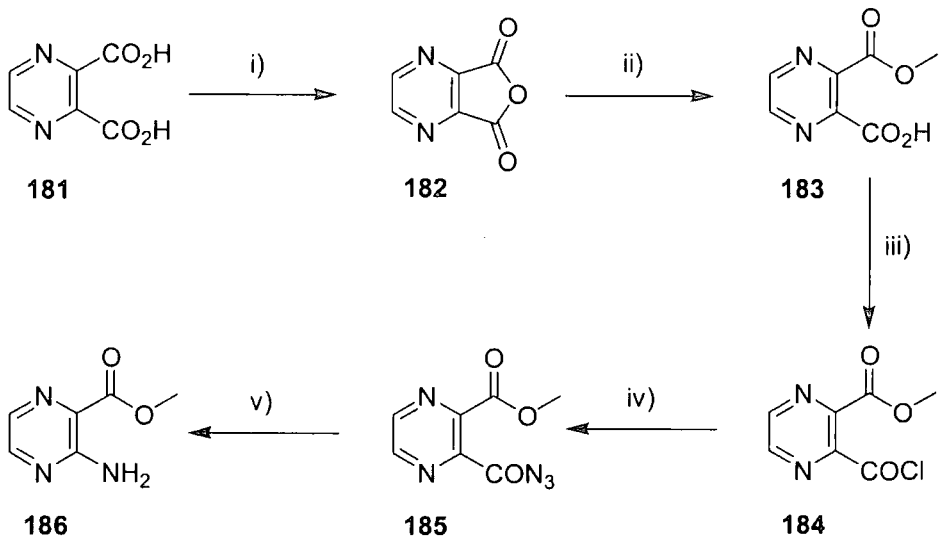

Scheme 70: Synthesis of 3-aminopyrazinecarboxylic acid, methyl ester 186 by Chen *et al.*[125]: i) Ac_2O, Δ; ii) CH_3OH, 20 °C; iii) $SOCl_2$, Δ; iv) NaN_3, acetone, H_20, 0 °C; v) PhH, Δ.

Reaction of commercially available 2,3-pyrazinedicarboxylic **181** with acetic anhydride gave **182** in 92% yield; the reaction with methanol gave the methyl ester **183** in 89% yield. Treatment of **183** with thionyl chloride gave the acid chloride **184**, which was not isolated, and reaction of **184** with sodium azide gave the acyl azide **185**, which without isolation smoothly underwent a Curtis rearrangement to give **186** in 33% yield: 10 g batches of **186** were conveniently prepared by this procedure.

Due to the presence of the *para* directing amine substituent, bromination of **186** occurs at C-5 of the pyrazine ring yielding **187** in 36%. Following the literature precedent[126] we initially brominated using Br_2 in glacial acetic acid 36% yield. However, we found it far more convenient using *N*-bromosuccinimide (NBS), which gave **187** in a significantly higher 86% yield. Hydrolysis of **187** with NaOH gave 2-amino-5-bromopyrazinoic acid **188** in 78% yield. Decarboxylation of **188** readily occurred in tetralin yielding 2-amino-5-bromopyrazine **189** in 67% yield (Scheme 71).

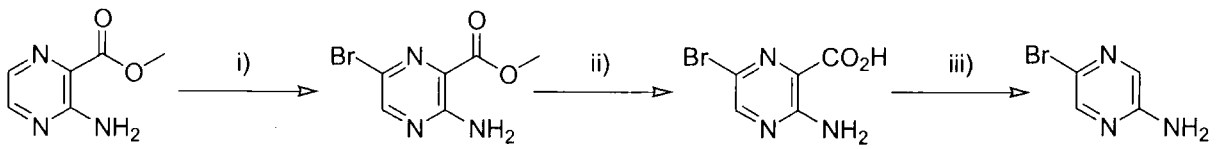

Scheme 71: Synthesis of 2-amino-5-bromopyrazine 189: i) AcOH, Br_2 or alternatively, NBS, DMF; ii) 5% NaOH (aq), Δ, 48% HBr; iii) Tetralin, Δ.

Whilst this route could prepare sufficient quantities of **189**, the overall synthesis was time-consuming. We, therefore, attempted the direct bromination of commercially available aminopyrazine **190** with NBS that had previously been successful in preparing **187**. This reaction was successful which allowed us to prepare **189** in a one step synthesis in 36% yield in 5 g batches (Scheme 72).

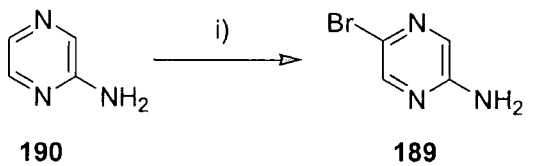

Scheme 72: One step synthesis of 2-amino-5-bromopyrazine 189: i) NBS, DMF.

2,5-Dibromopyrazine **191** has been prepared from its amino precursor **189** by means of the Sandmeyer reaction involving diazotisation in the presence of 48% hydrobromic acid.[126,127] Our initial test reaction was successful in low yield (Scheme 73). However, subsequent attempts were unsuccessful and intractable mixtures were obtained even though the temperature was regulated carefully (-10 °C to 0 °C) and reaction time varied. Under these conditions, according to literature, 2-amino-5-bromopyridine cleanly afforded 2,5-dibromopyridine (30% not optimised).[128]

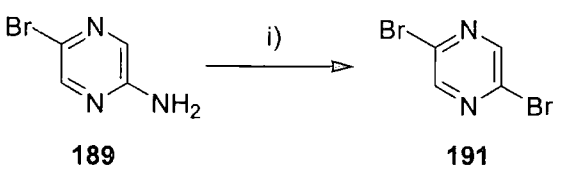

Scheme 73: Synthesis of 2,5-dibromopyrazine[124] 191 via the Sandmeyer reaction: i) 48% HBr, Br_2, $NaNO_2$

(aq).

Since the conventional synthesis of 2,5-dibromopyrazine **191** had been unsuccessful we adopted a different strategy and attempted to prepare 2,5-dichloropyrazine **197** on which we could perform a halogen exchange reaction. A search of the literature revealed two possible synthetic routes to **197** (Schemes 74 and 75).

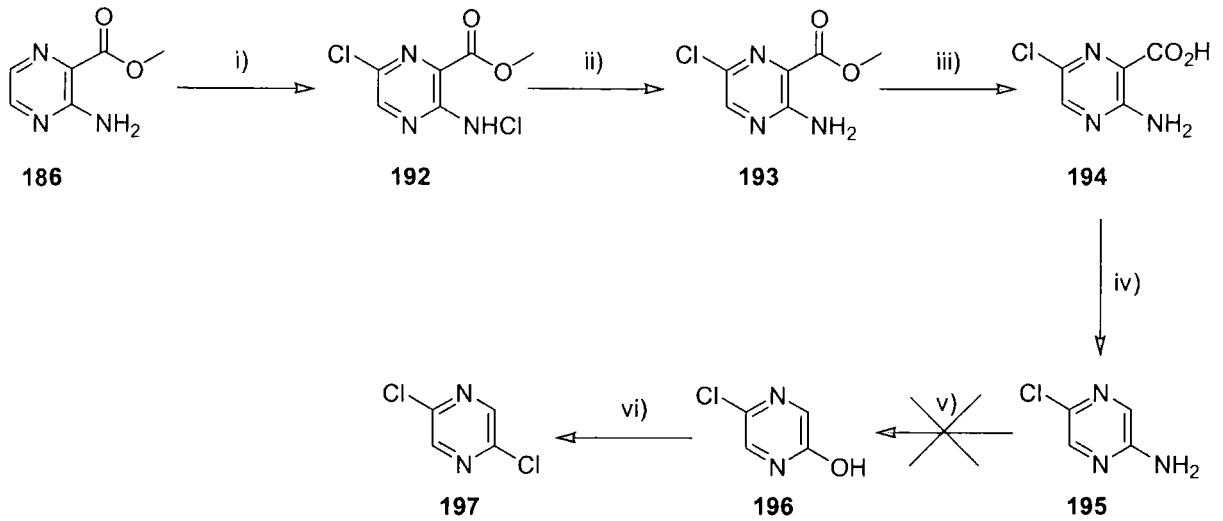

Scheme 74: Proposed synthesis of 2,5-dichloropyrazine 197: i) AcOH, H_2O, 41 °C → 0 °C, Cl_2 (g); ii) Sodium bisulfite, H_2O, 20 °C; iii) 5% NaOH (aq), Δ, conc HCl; iv) Tetralin, Δ; v) $NaNO_2$ (aq); vi) $POCl_3$.

Chlorination[129] of 2-aminopyrazinecarboxylic acid methyl ester **186** via the chloramine **192** gave 2-amino-5-chloropyrazine carboxylic acid methyl ester **193** in 56% yield. Hydrolysis of **193** gave 2-amino-5-chloropyrazinoic acid **194** in 84% yield. Decarboxylation of **194** in refluxing tetralin afforded 2-amino-5-chloropyrazine **195** in 74% yield.[130] However, despite numerous efforts we were again thwarted in our attempt to convert **195** in to 2-hydroxy-5-chloropyrazine **196** by the Sandmeyer reaction. No product was isolated and starting material could not be recovered.

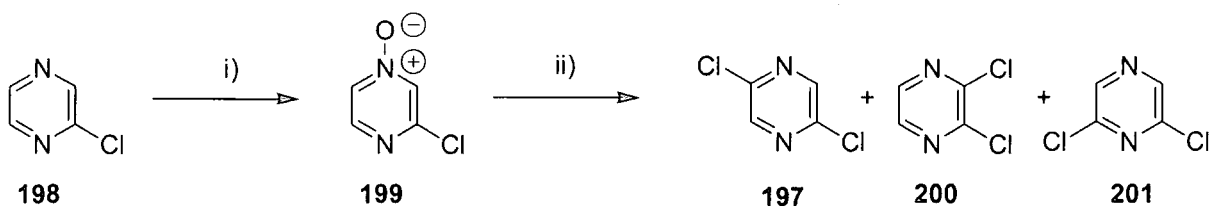

Scheme 75: Synthesis of 2,5-dichloropyrazine 197: i) AcOH, H_2O_2, 65-75 °C; ii) $POCl_3$, 80 °C.

3-Chloropyrazine-1-oxide **199** was prepared from commercially available chloropyrazine **198** in 50% yield in accordance with the literature method.[131] As described in the literature we anticipated isolating **197** directly from the *N*-oxide intermediate. However, ^{1}H-NMR spectroscopy and GCMS showed that a complex mixture of dichloropyrazine isomers had

been obtained, presumably the 2,5- **197**, 2,3- **200** and 2,6-isomer **201**, which could not be separated. We, therefore, abandoned 2,5-dichloropyrazine as a target compound.

3.2.1.2 Suzuki Cross-coupling Reactions of 2-Amino-5-bromopyrazine

Although our efforts in synthesising 2,5-dibromopyrazine **191** had been unsuccessful we recognised that novel chemistry could be developed using 2-amino-5-bromopyrazine **189** in palladium-catalysed Suzuki cross-coupling reactions. The resulting heteroaromatics bearing a primary amine group would also be potential candidates for Sandmeyer reactions.

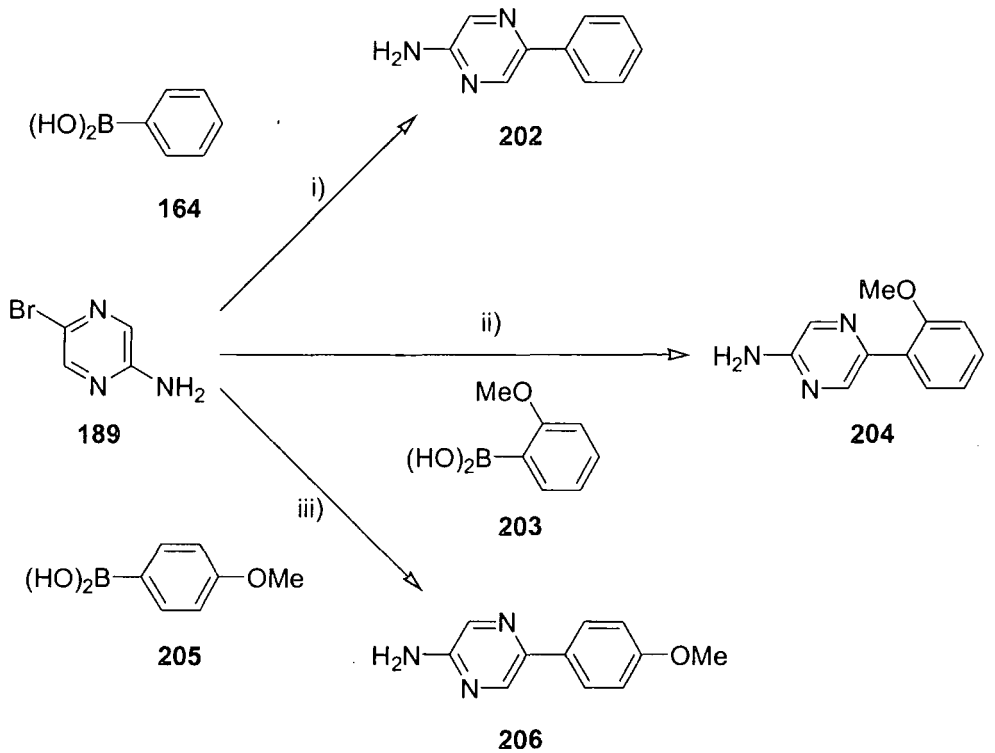

Scheme 76: Suzuki cross-coupling of 2-amino-5-bromopyrazine 189: i) benzeneboronic acid 164, THF, $Pd(PPh_3)_4$, Na_2CO_3, Δ; ii) 2-methoxy-benzeneboronic acid 203, THF, $Pd(PPh_3)_4$, Na_2CO_3, Δ; iii) 4-methoxy-benzeneboronic acid 205, THF, $Pd(PPh_3)_4$, Na_2CO_3, Δ.

Reaction of **189** with benzeneboronic acid **164** (3.0 equivalents) in the presence of catalytic $Pd(PPh_3)_4$ in refluxing THF gave 2-amino-5-phenylpyrazine **202** (59% yield) (Scheme 76). This was a key result as it demonstrated that the primary amine group could survive palladium-catalysed Suzuki cross-coupling conditions in spite of literature claims that the amine group usually needs to be protected for successful Suzuki reactions.[132,133] Our second objective of performing the Sandmeyer reaction on **202** was, however, unsuccessful. The reasoning behind the synthesis of **204** and **206** (35 and 23% yields, respectively) was to modify the electronic structure of the pyrazine ring in the diarylamine system in the hope that

Sandmeyer reactions would be successful. However yet again our efforts were in vain. Two-fold reactions of **189** with the diboronic acids 2,5-dimethoxy-1,4-diboronic acid[61] **207** and 9,9-dihexylfluorene-2,7-diboronic acid **169**, respectively yielded products **208** and **209** (56 and 51% yields) (Scheme 77). The oligo(arylene) systems **208** and **209** were not considered as suitable candidates for electron-transporting molecules in optoelectronic devices. This was due to the enormous potential for hydrogen bonding between the terminal amine group of adjacent molecules, which would cause crystallisation and ultimately degrade the device thin film. In addition the physical properties of **208** high melting point (> 300 °C) and unprocessability severely limit this compound as an electron-transport material.

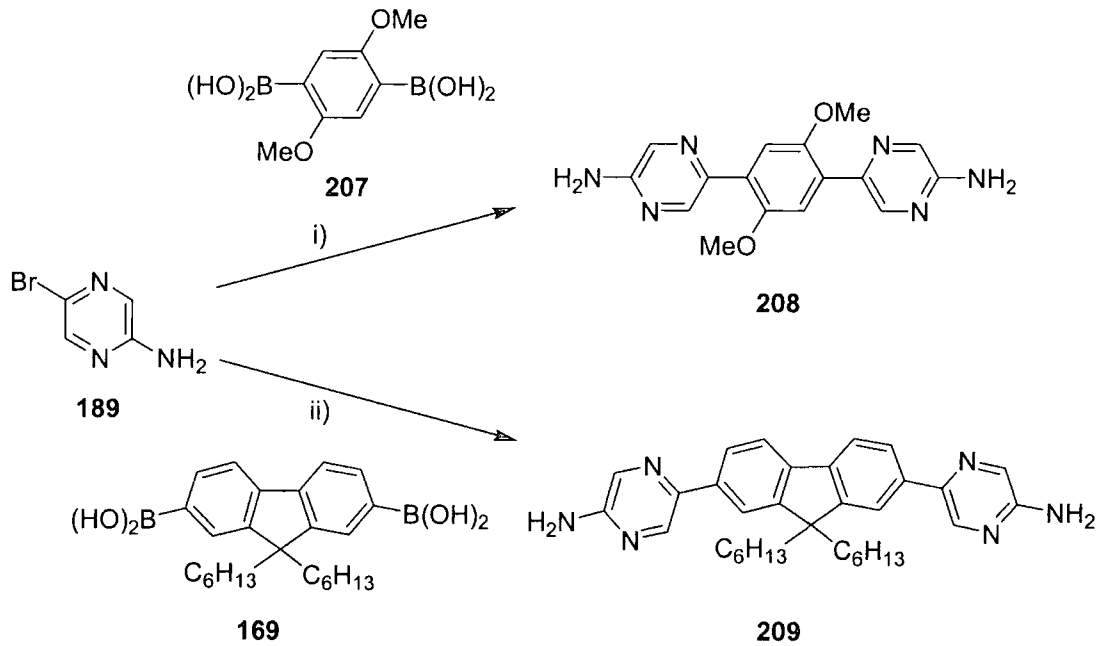

Scheme 77: Two-fold Suzuki cross-coupling of 2-amino-5-bromopyrazine 189: i) 2,5-dimethoxy-1,4-di boronic acid 207, THF, $Pd(PPh_3)_4$, Na_2CO_3, Δ; ii) 9,9-dihexylfluorene-2,7-diboronic acid 169, THF, $Pd(PPh_3)_4$, Na_2CO_3, Δ.

In summary, this work establishes that heteroaromatics bearing a primary amine group are suitable substrates for Suzuki cross-coupling reactions under standard conditions, without the need for protection/deprotection steps that are traditionally considered to be necessary for these reactions to proceed cleanly. The presence of the primary amine group offers attractive prospects for further synthetic transformations as well as supramolecular and coordination chemistry.[134]

3.2.1.3 Additional Heteroaromatic Oligomers

The versatility of the Suzuki cross-coupling reaction was further demonstrated by the synthesis of a series of heteroaromatic oligomers, the structures of which are shown below (Scheme 78). The same cross-coupling conditions were used starting from the aryl halide (bromo or iodo precursor) and the diboronic acids **169** and **207**. Compounds **210-214** were prepared in moderate yields with **212** and **213** having terminal bromines being the most significant as they have the capacity to undergo further cross-coupling reactions. The high melting points of compounds **210** (235 °C), **211** (232 °C), **212** (192 °C) and **213** (153 °C) demonstrate that such compounds are not feasible for use in OLEDs. It is generally considered that low-molar-mass-materials and oligomers that are oils preclude practical device applications, so we have not explored **214** further in this context.[135]

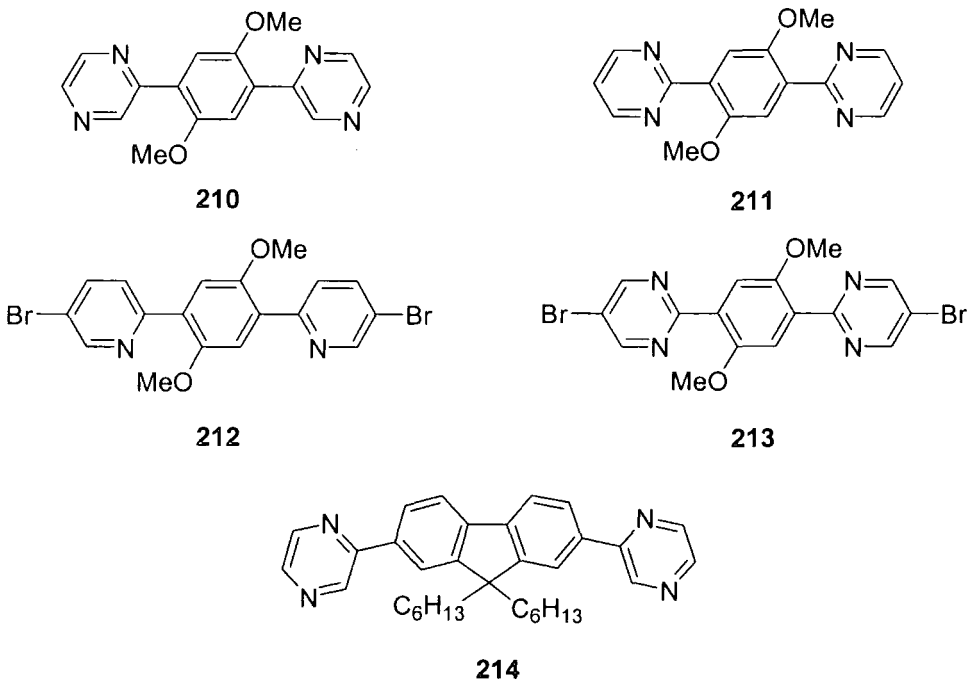

Scheme 78: Structures of additional heteroaromatic oligomers 210-214.

3.2.1.4 Phenylene-2,5-dimethylpyrazine *co*-Oligomers

We chose 2,5-dibromo-3,6-dimethylpyrazine **219** as our starting material with the expectation that steric effects of the methyl substituents would restrict backbone planarity in the derived 2,5-diaryl-3,6-dimethylpyrazine systems, thereby achieving a wider energy band gap and hence shifting emission into the blue region of the spectrum. New blue emitters are much sought after not only because blue is a primary colour and emission in this region of the

spectrum is crucial for full-colour displays,[136] but also as energy transfer donors in conjunction with lower bandgap fluorophores.[137]

Our initial synthesis of 2,5-dibromo-3,6-dimethylpyrazine **219** began from commercially available 2,5-dimethylpyrazine **215** and its oxidation with hydrogen peroxide in aqueous acetic acid gave the di-*N*-oxide **216** (50% yield) (Scheme 79). Compound **216** was subsequently refluxed in $POCl_3$ to give 2,5-dichloro-3,6-dimethylpyrazine **217** in accordance with the literature.[138] After initial difficulties in forming the di-*N*-oxide **216** we experienced extremely low yields for the conversion to the dichloro derivative **217** whilst mostly isolating the monochloro product. We therefore sought an alternative synthesis of 2,5-dichloro-3,6-dimethylpyrazine **217**.

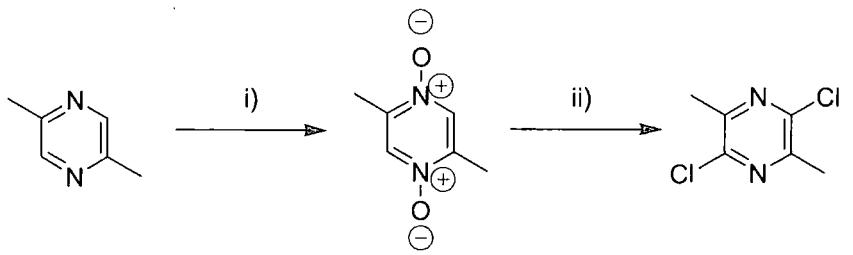

215 **216** **217**

Scheme 79: Synthesis of 2,5-dichloro-3,6-dimethylpyrazine 217 according to Newbold and Spring[138] : i) H_2O_2, AcOH (aq); ii) $POCl_3$.

Alanine anhydride **218** can be dehydrated in refluxing $POCl_3$ to gave 2,5-dichloro-3,6-dimethylpyrazine **217**.[139] Although this reaction step was low yielding (17%) we were able to perform this reaction on a 20 g scale which produced sufficient **217** for the synthesis of 2,5-dibromo-3,6-dimethylpyrazine **219** by halogen exchange (69% yield) (Scheme 80).[140]

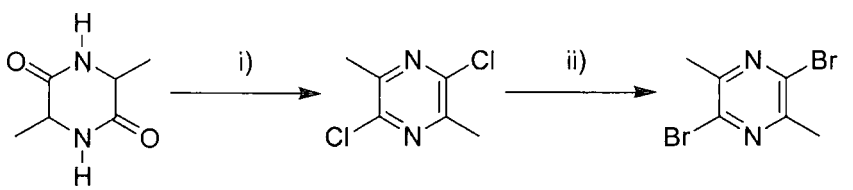

218 **217** **219**

Scheme 80: Synthesis of 2,5-dibromo-3,6-dimethylpyrazine 219 : i) $POCl_3$;[139] ii) PBr_3.[140]

Following the unsuitability of compounds **208-214** in device applications we progressed to side-group substituted oligomers. Incorportion of *tert*-butyl side chains enhances oligomer solubility, increases the viscosity of the thin film and promotes a glassy state thus inhibiting thin film crystallisation.[135] Suzuki cross-coupling methodology is known to be a versatile route to oligo(arylenes)[99] and reaction of **219** with benzeneboronic acid **164**, 2-

methoxybenzeneboronic acid **203** and 4-*tert*-butylbenzeneboronic acid **220** gave products **221** (73% yield), **222** (73% yield) and **224** (39% yield) respectively (Scheme 81). Further reaction of **224** with 2,5-dimethoxy-1,4-benzeneboronic acid **207** gave the linear penta-arylene system **225** (16% yield). A second reaction of **219** with 2-methoxybenzeneboronic acid **203** (0.5 equivalents) gave compound **226** (52% yield). However a subsequent reaction **226** with 2,5-dimethoxy-1,4-benzeneboronic acid **207** failed to give the second linear penta-arylene system **227** in sufficient purity. Analogous reaction of **219** with 2-methoxy-5-pyridylboronic acid **228**[141] gave the 2,5-dipyridylpyrazine derivative **229** (73% yield). This last reaction establishes that Suzuki reactions of **219** should enable a range of heteroaryl moieties to be incorporated into the oligomer chain: also the methoxy substituents in **229** should be amenable to further useful synthetic transformations. Reaction of **222** with tetrafluoroboric acid afforded the crystalline diprotonated bis(tetrafluoroborate) salt **223**.

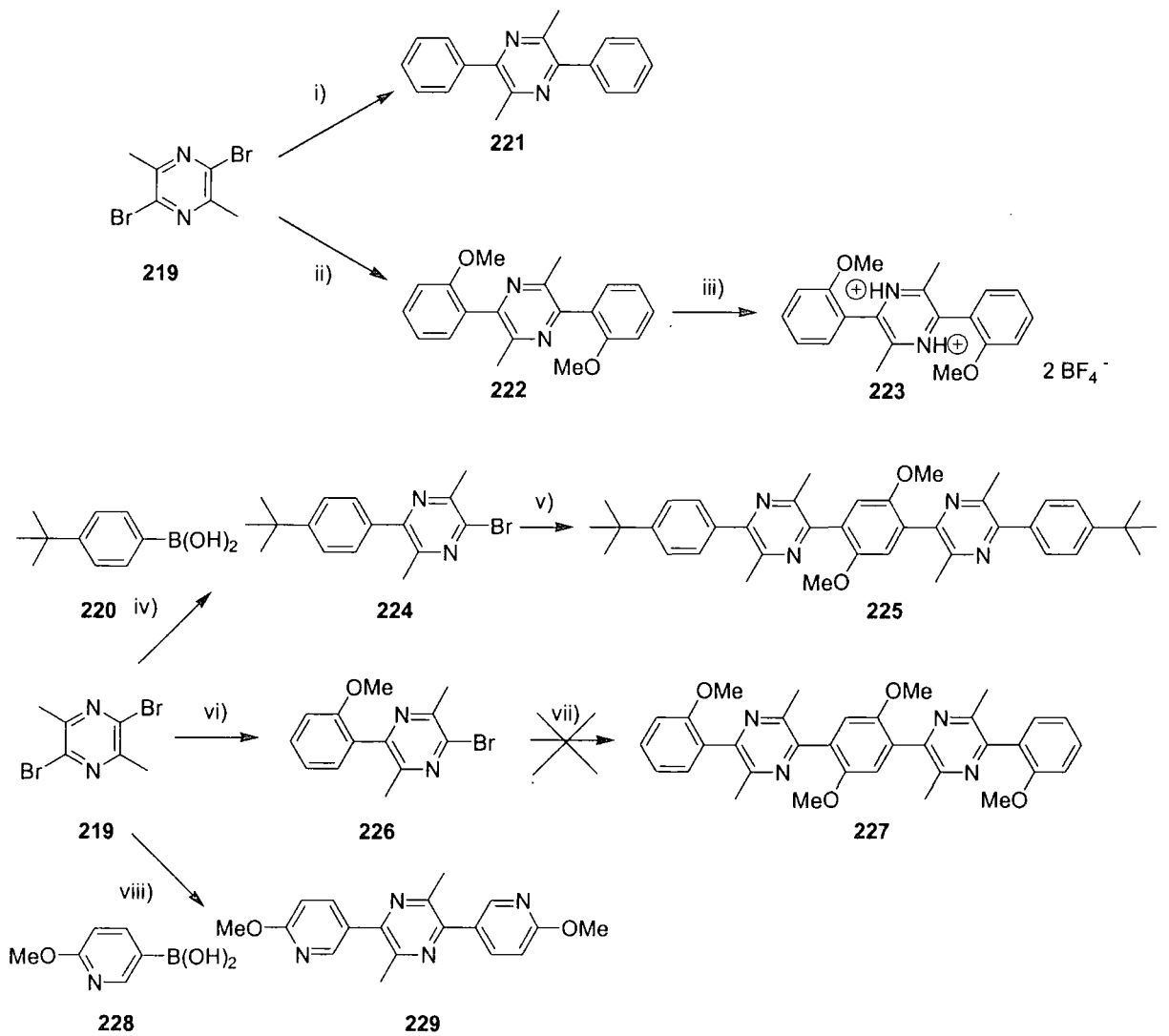

Scheme 81: Reagents and conditions: i) benzeneboronic acid 164, THF, $Pd(PPh_3)_4$, Na_2CO_3, Δ; ii) 2-methoxybenzeneboronic acid 203, THF, $Pd(PPh_3)_4$, Na_2CO_3, Δ; iii) HBF_4, MeCN; iv) 4-*tert*-

butylbenzeneboronic acid 220, THF, $Pd(PPh_3)_4$, Na_2CO_3, Δ; v) 2,5-dimethoxy-1,4-diboronic acid 207, THF, $Pd(PPh_3)_4$, Na_2CO_3, Δ; vi) 2-methoxybenzeneboronic acid 203, THF, $Pd(PPh_3)_4$, Na_2CO_3, Δ; vii) 2,5-dimethoxy-1,4-diboronic acid 207, THF, $Pd(PPh_3)_4$, Na_2CO_3, Δ; vii) 2-methoxy-5-pyridylboronic acid 228, THF, $Pd(PPh_3)_4$, Na_2CO_3, Δ.

3.2.2 X-ray Crystal Structures of Compounds 208, 222, 223 and 229.

Crystal structures were solved by Dr A. Batsanov. Compound **208** crystallized from DMF/ethanol as a **208**·DMF solvate. The structure contains two crystallographically non-equivalent molecules of **208**, both located at inversion centres, but adopting different conformations (Figure 19). The dihedral angle between the central benzene and the pyrazine ring is 25.6° in molecule A and nil in molecule B. In both cases, the methoxy group lies in a *syn*-position to the CH, rather than N, probably due to attractive electrostatic H...O interactions. The methoxy groups deviate from the ideal in-plane conformations by the rotations of 3.0° and 8.0° around the C(2)–O(1) and C(10)–O(2) bonds, respectively.

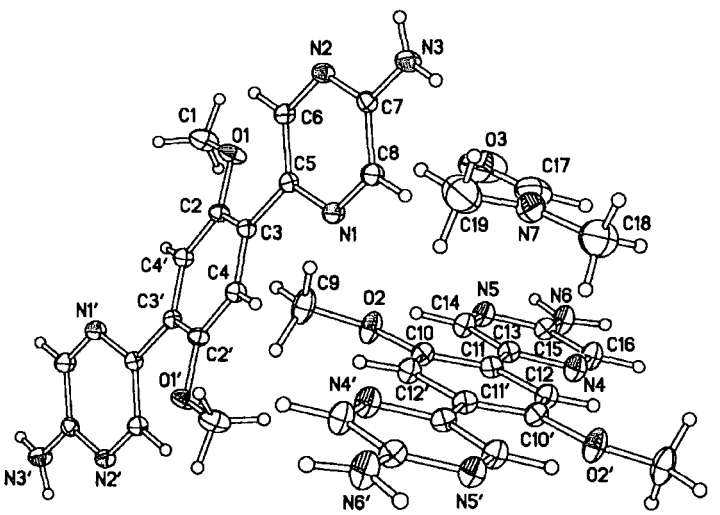

Figure 19: Independent molecules of 208 and DMF in the structure of 208 DMF (showing 50% thermal ellipsoids).

Molecules **222** and **229** and the dication in **223** have crystallographic C_i symmetry and adopt twisted conformations: dihedral angles between the phenyl and pyrazine rings are 74.0° (**222**), 56.4° (**223**) and 44.6° (**229**) (Figure 20).

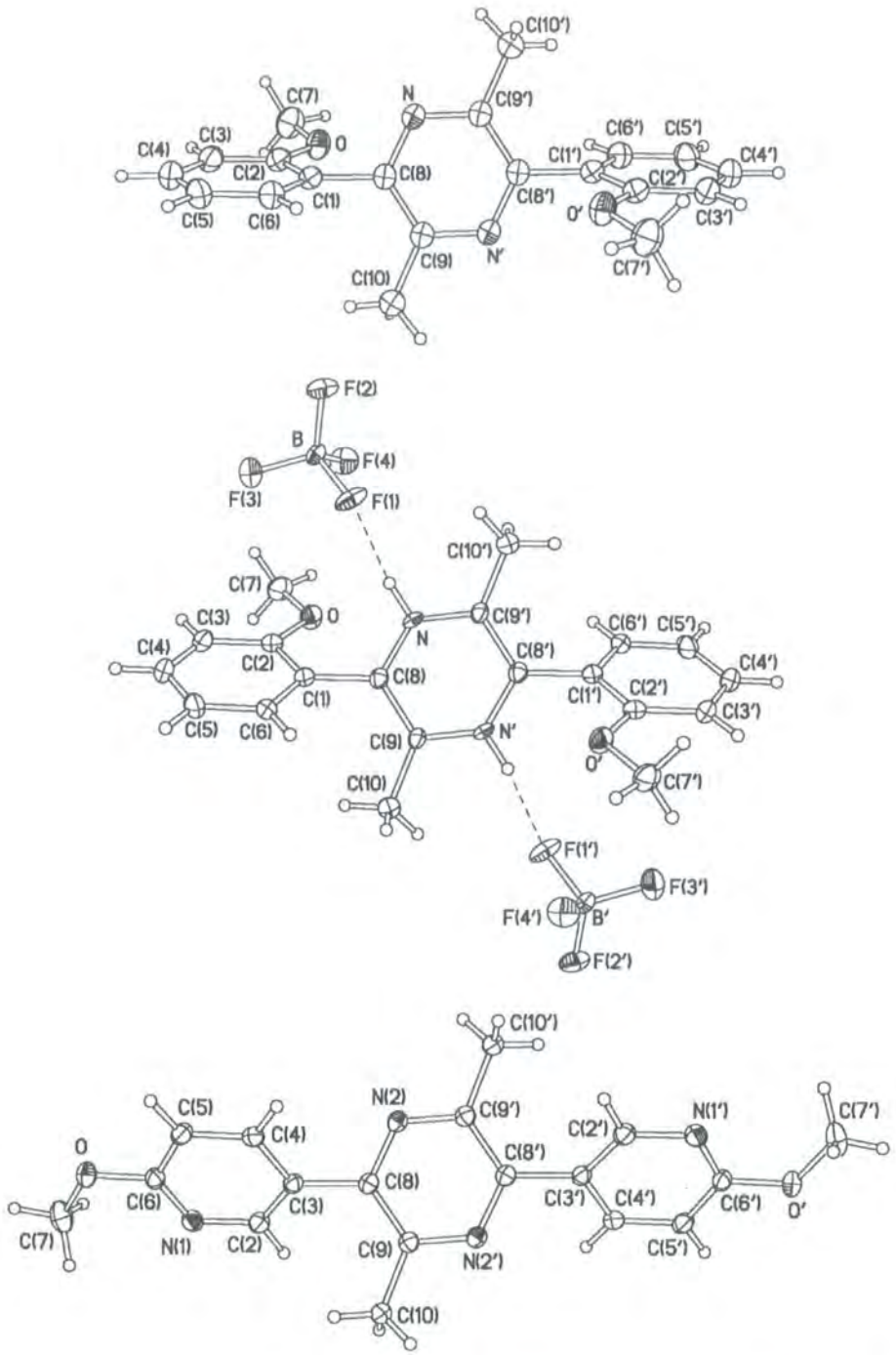

Figure 20: X-ray molecular structure of 222, 223 and 229 (50% displacement ellipsoids). Primed atoms generated and by inversion centres.

Dication **223** is the first reported diprotonated pyrazine derivative in which the hydrogen atoms were actually located (cf. the four tetramethylpyrazinium salts reported previously).[142] There are relatively strong N–H...F hydrogen bonds with the tetrafluoroborate anions [N–H 0.88(3), N...F 2.701(2), H...F 1.83(3) Å, N-H-F angle 172(3)°] but no *intra*molecular hydrogen bonds. Protonation widens the C-N-C angle from 118.1(1)° (**222**) to 126.2(2)° (**223**),

while the C–N bond lengths are unaffected, viz. N–C(8) 1.339(2) and N–C(9') of 1.344(2) Å in **222** against 1.341(3) and 1.339(3) Å, respectively, in **223**.

3.2.3 Optical Absorption and Photoluminescence

The absorption spectra in ethanol solution show the lowest energy bands at wavelengths characteristic of twisted oligoaryl structures: viz. compound **221** λ_{max} 300 nm; **222** λ_{max} 330 nm; **225** λ_{max} 315 nm; **229** λ_{max} 322 nm (Table 2). Upon addition of H_2SO_4 to these solutions, there is a red shift of this band to λ_{max} 340, 360 and 342 nm for compounds **221**, **222** and **225**, respectively, but essentially no change was seen for compound **229**. This shift is consistent with protonation of the pyrazine unit of **221**, **222** and **225**, leading to a reduction in the HOMO–LUMO gap. Evidence in favour of diprotonation (not monoprotonation) in these studies is provided by the identical spectra of the isolated salt **223** and that obtained *in situ* from **222** and H_2SO_4.

Compound	Neutral UV-Vis Absorption, λ_{max}/nm	Protonated UV-Vis Absorption, λ_{max}/nm	PL, λ_{max}/nm
221	300	340	Not Recorded
222	330	360	372
225	315	342	418
229	322	322	387

Table 2: UV-Vis absorption and emission λ_{max} values for compounds 221, 222, 225 and 229 in ethanol, 20°C.

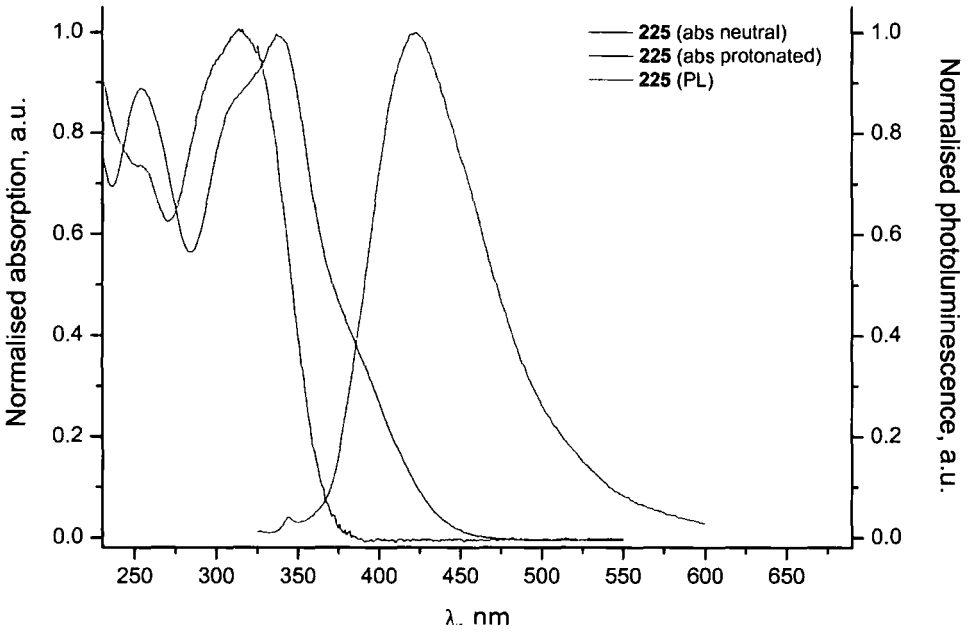

Figure 21: UV-Vis absorption of spectra of 225 in EtOH before and after the addition of H_2SO_4; PL spectra of 225 in EtOH, λ_{ex} 312 nm.

For compound **229** we suggest that protonation occurs at both of the terminal pyridyl nitrogens, rather than at the central pyrazinyl sites. This would be consistent with literature pK_a values in aqueous solution: viz. 2-methoxypyridine 3.28; pyrazine 0.51 and –6.6, for mono- and di-protonation, respectively.[143] The experimental evidence for this is that upon addition of tetrafluoroboric acid to **229** the ^{1}H NMR spectrum showed protonation of the pyridyl nitrogen atom at δ_H 7.18 ppm accompanied by a small downfield shift of all protons (and the OMe protons) on the pyridyl ring (Figure 22).

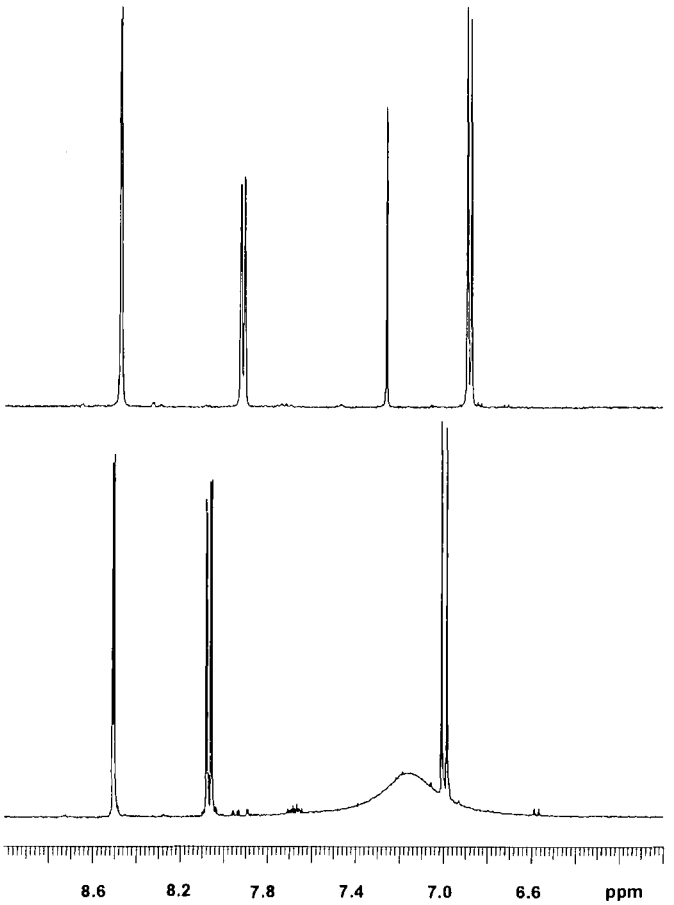

Figure 22: Stacked ^{1}H NMR spectrum of 229 showing aromatic region of neutral (upper: 500 MHz, $CDCl_3$) and protonated (lower: 400 MHz, D_6-DMSO) states.

Photoluminescence (PL) spectra in ethanol, with excitation at 312 and 346 nm, show violet-blue emission: **222** λ_{max} 372 nm; **225** λ_{max} 418 nm (Figure 21); **229** λ_{max} 387 nm. The wavelength of PL emission was unaffected by the addition of H_2SO_4 to the solutions, although the intensity was reduced. This is probably due to the presence of a mixture of emissive neutral species and non-emissive protonated species. When isolated salt **223** was dissolved in ethanol the PL spectrum of the solution was identical to that of neutral precursor **222**, although of significantly lower intensity, suggesting that partial deprotonation had occurred to give some neutral **222** in the solution. This is in contrast to the stability of related protonated diarylpyridine systems under these conditions.[63] Protonation of some nitrogen heterocycles is known to reduce drastically their fluorescence quantum yield.[136h]

3.2.4 Electroluminescence

Initial studies by Dr T. Sato show that OLEDs can be fabricated using **225** as the emissive layer. A single-layer device was obtained by spin-coating **225** (50-60 nm thick layer) from $CHCl_3$ solution onto an ITO substrate followed by evaporation of a Ca cathode. The EL emission peak (blue colour; λ_{max} 444 nm) was slightly red shifted from the solid state PL (λ_{max} 430 nm; Φ_{em} 0.36).[144] No long-wavelength π–aggregates/exciton emission was observed, probably due to the non-planar structure of **225**. A common problem with blue emitting materials is the difficulty of charge injection leading to low device efficiency. One strategy is to modify the anode with a thin layer of poly(3,4-ethylenedioxythiophene) (PEDOT).[145] For the device structure ITO/PEDOT/**225**/Ca blue light emission was observed with an onset of 6.5 V, brightness 110 cd m^{-2} at a current density of 40 mA cm^{-2}; a maximum EL quantum efficiency of 0.09% was attained.

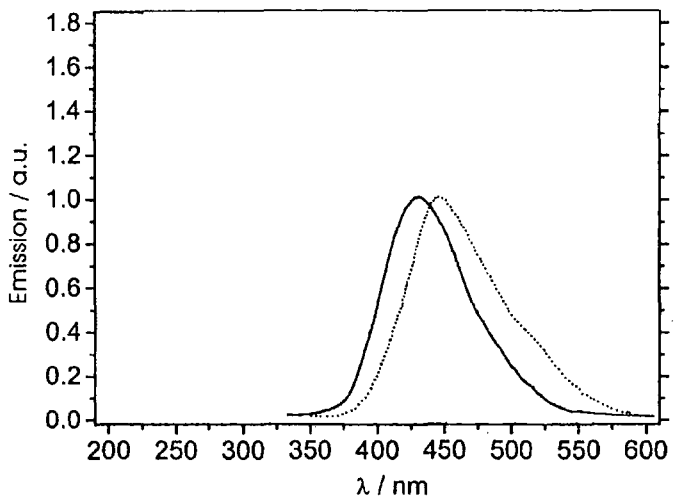

Figure 23: Thin film PL λ_{ex} 350 nm (thin line) and EL spectra (dashed line) of compound 225 in the device configuration ITO/PEDOT/225/Ca.

3.3 Conclusions

We have successfully demonstrated that pyrazine heteroaromatics bearing a primary amine group are suitable substrates for Suzuki cross-coupling reactions under standard conditions, without the need for protection/deprotection steps as verified by X-ray crystallography for compound **208**. The first well-defined pyrazine-containing tertaryl and penta-aryl oligomers have been synthesised by Suzuki methodology, and their structures confirmed by X-ray crystallography for compounds **222**, **223** and **229**. Blue luminescence has been observed in PL and EL experiments, with no long wavelength emission arising from π–aggregates or

excitons. The applicability of compound **225** as an emissive layer in OLEDs has been established.[146]

4 NEW 2,5-DIPHENYL-1,3,4-OXADIAZOLES AND 2-PHENYL-5-(2-THIENYL)-1,3,4-OXADIAZOLES

4.1 INTRODUCTION

2,5-Diphenyl-1,3,4-oxadiazole derivatives have been widely studied in diverse areas of chemistry. In particular, due to the electron-deficient properties of the oxadiazole ring, their luminescence properties and their good thermal and chemical stabilities,[147] a range of derivatives (e.g. low molecular weight monomers,[30,148] star-shaped oligomers[34] and polymers[37-46]) have been used as emissive materials and/or electron-transporting/hole-blocking compounds in organic light emitting devices (OLEDs).[11,21] Furthermore, many 1,3,4-oxadiazole derivatives are biologically-active and continue to find applications in medicinal chemistry.[149] This combination of properties ensures that new functionalised derivatives are of considerable interest.

Very recently, the first 2,5-diphenyl-1,3,4-oxadiazole derivative possessing an alkyne substituent, **230**, was reported independently by Cha *et al*[34] and by workers in our group.[150] From a synthetic viewpoint, the ethynyl substituent offers unprecedented scope for functionalisation reactions, which will extend the π–conjugation at the periphery of the framework. Compound **230** is, therefore, a very attractive building block in the light of the current interest in conjugation of aryl/heteroaryl rings through *sp* hybridised carbon linkages,[151] and the study of ethynyl derivatives of arenes and heteroarenes as "molecular wires".[152] In this chapter we report the synthesis of the novel thienyl analogue **238** and describe organometallic cross-coupling reactions at the terminal alkyne positions of **230** and **238** to obtain heteroaryl-functionalised derivatives possessing extended π–electron conjugation. We also demonstrate that 2-iodo-5-bromo-pyrimidine **241** is a useful synthetic intermediate in selective palladium catalysed cross-coupling reactions. The optical absorption and photoluminescence properties of these products are reported, along with X-ray crystal structures for compounds **232d**, **232g** and **239d**. In addition EL from a OLED fabricated using a 50% blend of MEH-PPV and a new 2,5-diaryl-1,3,4-oxadiazole-fluorene hybrid compound **248c** is also reported.

4.2 Results and Discussion

4.2.1 Synthesis

Our initial reaction of **230** with 2-bromopyrimidine **170** under standard Sonogashira conditions[153] [$Pd(PPh_3)_2Cl_2$, triethylamine, CuI, THF] yielded only the self-coupling product **231** which indicated that heteroaryl bromides were not sufficiently reactive for this type of organometallic cross-coupling reaction (Scheme 82). Compound **230** was therefore reacted with a series of heteroaryl iodides under the same standard conditions to afford products **232a-g**[1] in 40-79% yields. Electron-deficient heterocycles (pyridyl, pyrazyl and pyrimidyl: **a-e**) and electron-rich thienyl derivatives (**f,g**) reacted similarly.

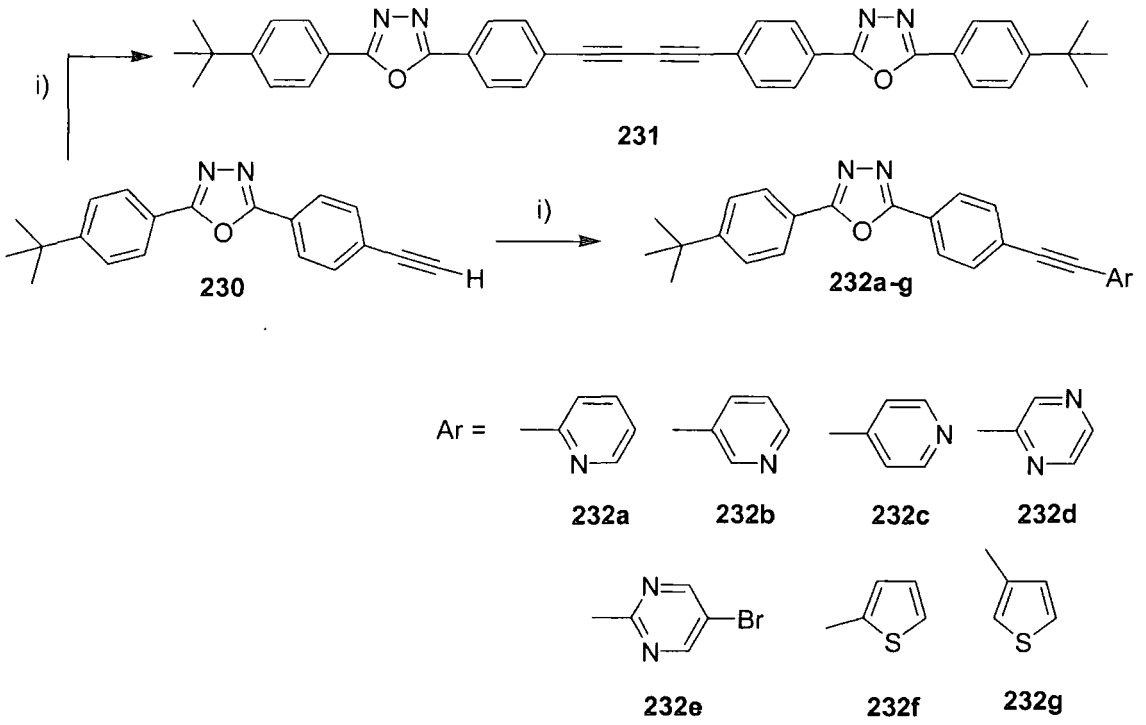

Scheme 82: Sonogashira cross-coupling reactions of 230: i) $Pd(PPh_3)_2Cl_2$, CuI, NEt_3/THF.

To explore the effect of replacing the alkynylphenyl moiety of compound **230** with an alkynylthienyl moiety, a series of novel 2-phenyl-5-(2-thienyl)-1,3,4-oxadiazole derivatives was synthesised as shown in Scheme 83.[154] The readily available thiophene derivative **233**[155] was converted into the hydrazide derivative **234**. Reaction of **234** with *tert*-butylbenzoyl chloride gave the intermediate diacylhydrazine compound **235** which was not purified. The crude product **235** was cyclodehydrated under standard conditions for the formation of 1,3,4-

[1] Compound **232f** was prepared by Dr. D. Kreher in our laboratory.

oxadiazoles[156] using phosphorus oxychloride, to give the 2-phenyl-5-(2-thienyl)-1,3,4-oxadiazole system **236**. Sonogashira reaction of **236** with 2-methyl-3-butyn-2-ol gave **237** from which the target alkyne **238** was obtained (16% overall yield from compound **233**). Cross-coupling reactions analogous to those shown in Scheme 82, using the corresponding iodo-heterocycle gave the terminal heteroaryl derivatives **239a-g** in 33-65% yields. Two-fold reaction of **239** with 2,5-diiodothiophene gave the π–extended bis(ethynylthienyl)thiophene derivative **240** in 30% yield. The self-coupling compound of **238** was not isolated.

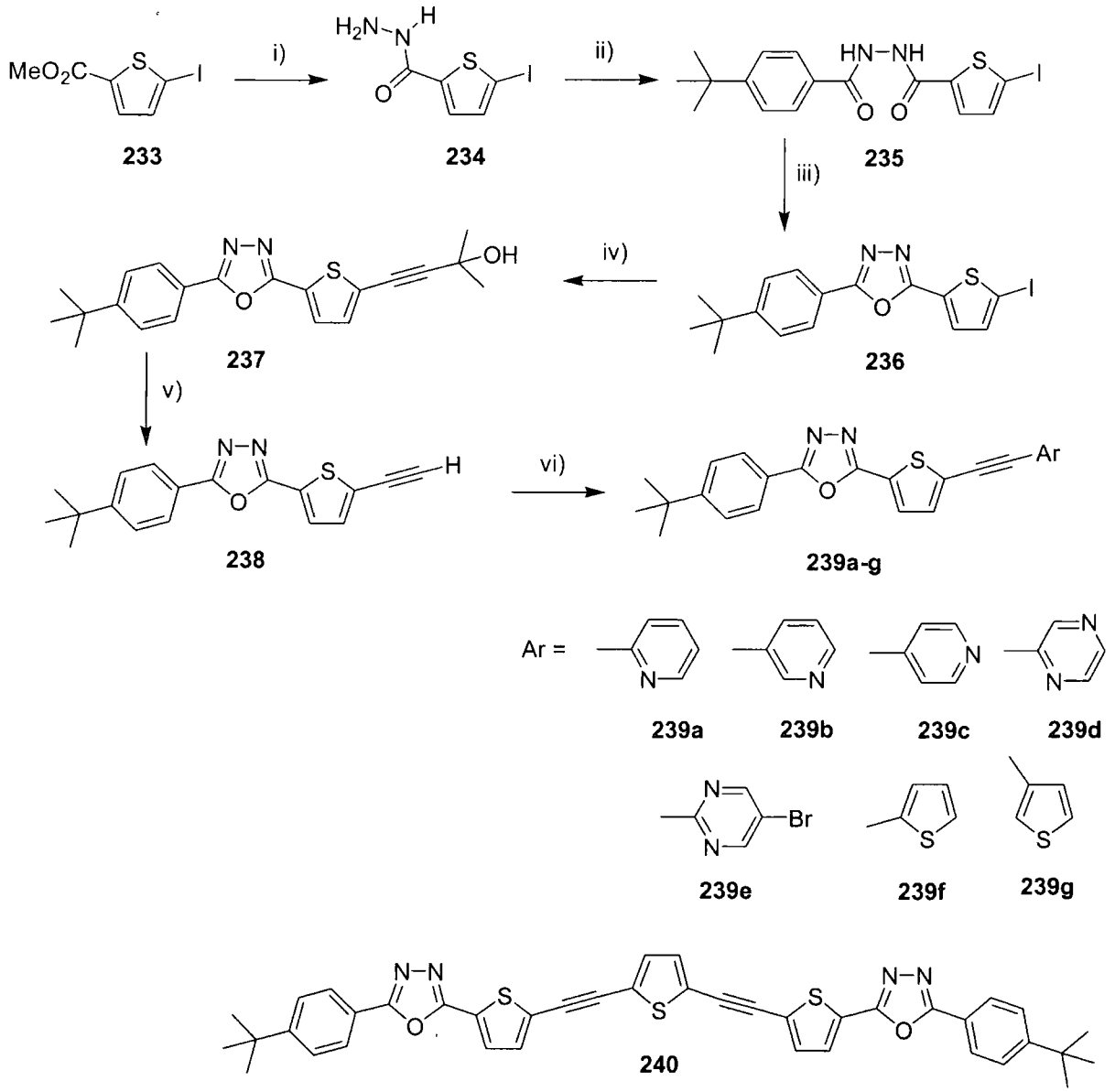

Scheme 83: Synthesis of novel 2-phenyl-5-(2-thienyl)-1,3,4-oxadiazole derivatives: i) NH_2NH_2. H_2O CH_3OH; ii) 4-*tert*-benzoyl chloride, pyridine, 20 °C 1 h, Δ 1h; iii) $POCl_3$; iv) 2-methyl-3-butyn-2-ol, $Pd(PPh_3)_2Cl_2$, CuI, NEt_3/THF; v) NaOH, Toluene; vi) $Pd(PPh_3)_2Cl_2$, CuI, NEt_3/THF.

We recognised the potential for products **232e** and **239e** to undergo a further Suzuki cross-coupling reactions at the 5-position of the pyrimidine ring. Goodby *et al.*[101] had previously reported both Sonogashira and Suzuki cross-coupling reactions of 2-iodo-5-bromopyrimidine **241**. An initial reaction of 2-iodo-5-bromopyrimidine **241** with phenylacetylene **242** afforded **243** in 53% yield. Subsequent Suzuki reaction of **243** with benzeneboronic acid gave **244** 39%. Compound **232e** has poor solubility in organic solvents, we therefore reacted the ethylhexoxy analogue[157] of compound **230** with 2-iodo-5-bromopyrimidine **241**, which afforded **245** in 71% yield. The ethylhexoxy side chain imparts good solubility allowing us to perform a further Suzuki cross-coupling reaction with benzeneboronic acid to yield **246** in a disappointing 10% yield. Due to this last result we did not pursue any further Suzuki cross-coupling reactions with thienyl analogues of **245**.

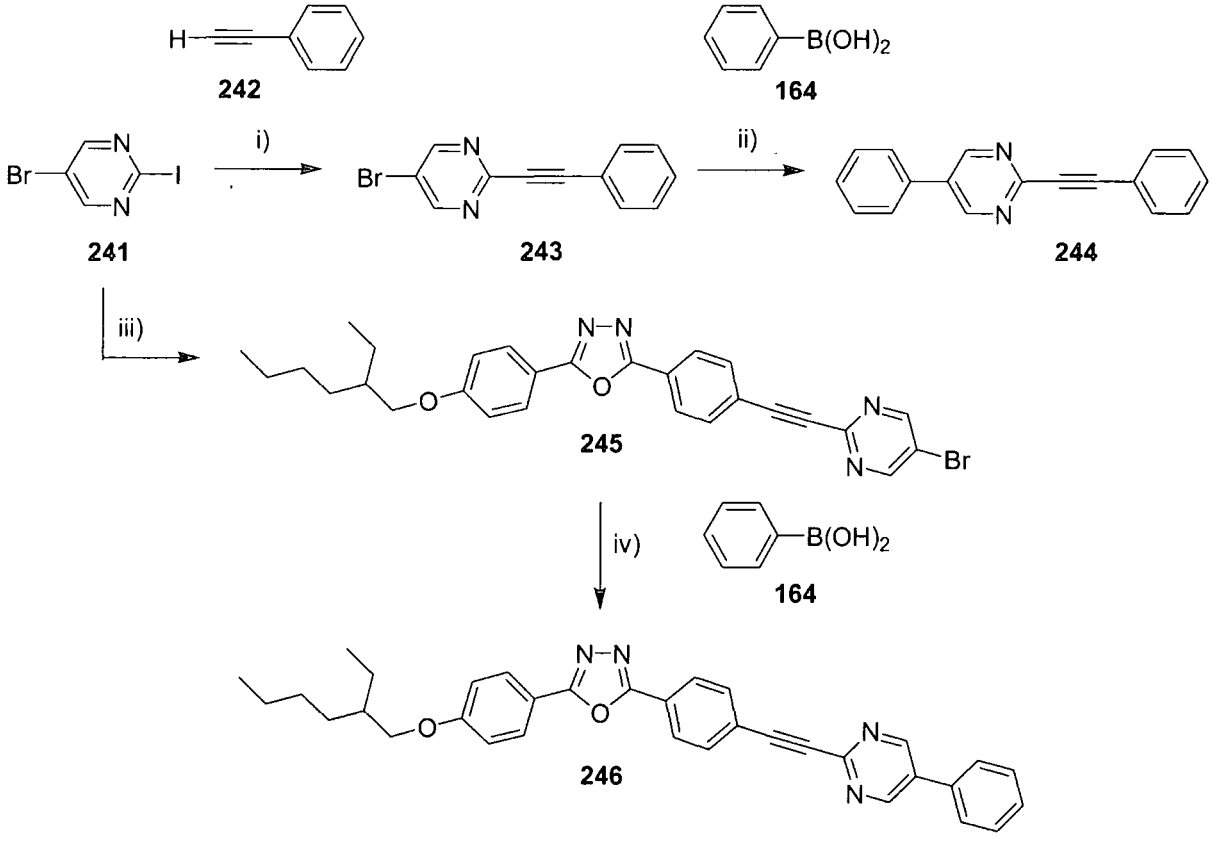

Scheme 84: Sonogashira and Suzuki cross-coupling reactions of 2-iodo-5-bromopyrimidine: i) phenylacetylene $Pd(PPh_3)_2Cl_2$, CuI, NEt_3/THF; ii) benzeneboronic acid , $Pd(PPh_3)_4$, THF, Na_2CO_3, Δ; iii) 2-[4-(2-ethylhexyloxy)phenyl]-5-(4-ethynylphenyl)-1,3,4-oxadiazole, $Pd(PPh_3)_2Cl_2$, CuI, NEt_3/THF; iv) benzeneboronic acid , $Pd(PPh_3)_4$, THF, Na_2CO_3, Δ.

Suzuki cross-coupling of 2-(4-iodophenyl)-5-(4-*tert*-butylphenyl)-1,3,4-oxadiazole[158] **247** with three different diboronic acids afforded new 2,5-diaryl-1,3,4-oxadiazole hybrid compounds **248a-c** in moderate yields (Scheme 85).

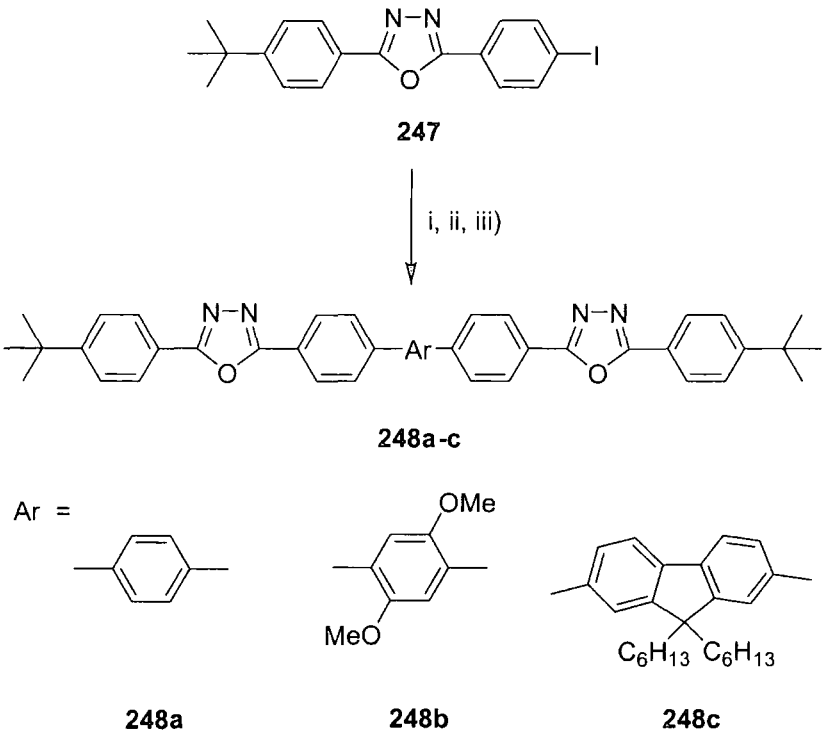

Scheme 85: Synthesis of new 2,5-diaryl-1,3,4-oxadiazole hybrids 248a-c: i) 1,4-benzenediboronic acid, $Pd(PPh_3)_4$, THF, Na_2CO_3, Δ; ii) 2,5-dimethoxy-1,4-benzenediboronic acid, $Pd(PPh_3)_4$, THF, Na_2CO_3, Δ; iii) 9,9-dihexylfluorene-2,7-diboronic acid, $Pd(PPh_3)_4$, THF, Na_2CO_3, Δ.

4.2.2 X-ray Crystal Structures of 232d, 232g and 239d.

The molecular structures of **232d**, **232g**, and **239d**, solved by Dr A. S. Batsanov and shown in (Figure 24), can be described as approximately planar. The deviations of all non-hydrogen atoms (except the methyl carbons) from their mean plane average 0.22 (**232d**), 0.21 (**232g**), and 0.15 Å (**239d**), compared to the total lengths of the molecules, ca. 22.5 (**232d**, **232g**), and 23.2 Å (**239d**). Largely, this planarity is due to the molecule having few degrees of conformational freedom, comprising as it does a number of planar rings on a rigid 'rod'. However, the rings can rotate, and there are substantial differences in the conformations. The asymmetric unit of structure **232d** comprises two molecules. In each of them, both benzene rings are nearly coplanar (within 1.5 to 4.8°) to the oxadiazole ring, while the angle between benzene ring B and the pyrazine ring is 42.5 or 39.3°. In molecule **232g** the oxadiazole ring is inclined by 24.7 and 18.1° (in opposite sense) to the benzene rings A and B, while the latter is inclined to the thiophene ring by 3.5°. Compound **239d** crystallises as a monosolvate, with the asymmetric unit comprising one molecule of **239d** and one of $CHCl_3$, linked by a weak hydrogen bond Cl_3C–H...N(2) (H...N 2.48 Å for the idealised C–H distance of 1.08 Å). The

dihedral angles between benzene and oxadiazole rings 13.6°, oxadiazole and thiophene 6.1°, thiophene and pyrazine 18.5°.

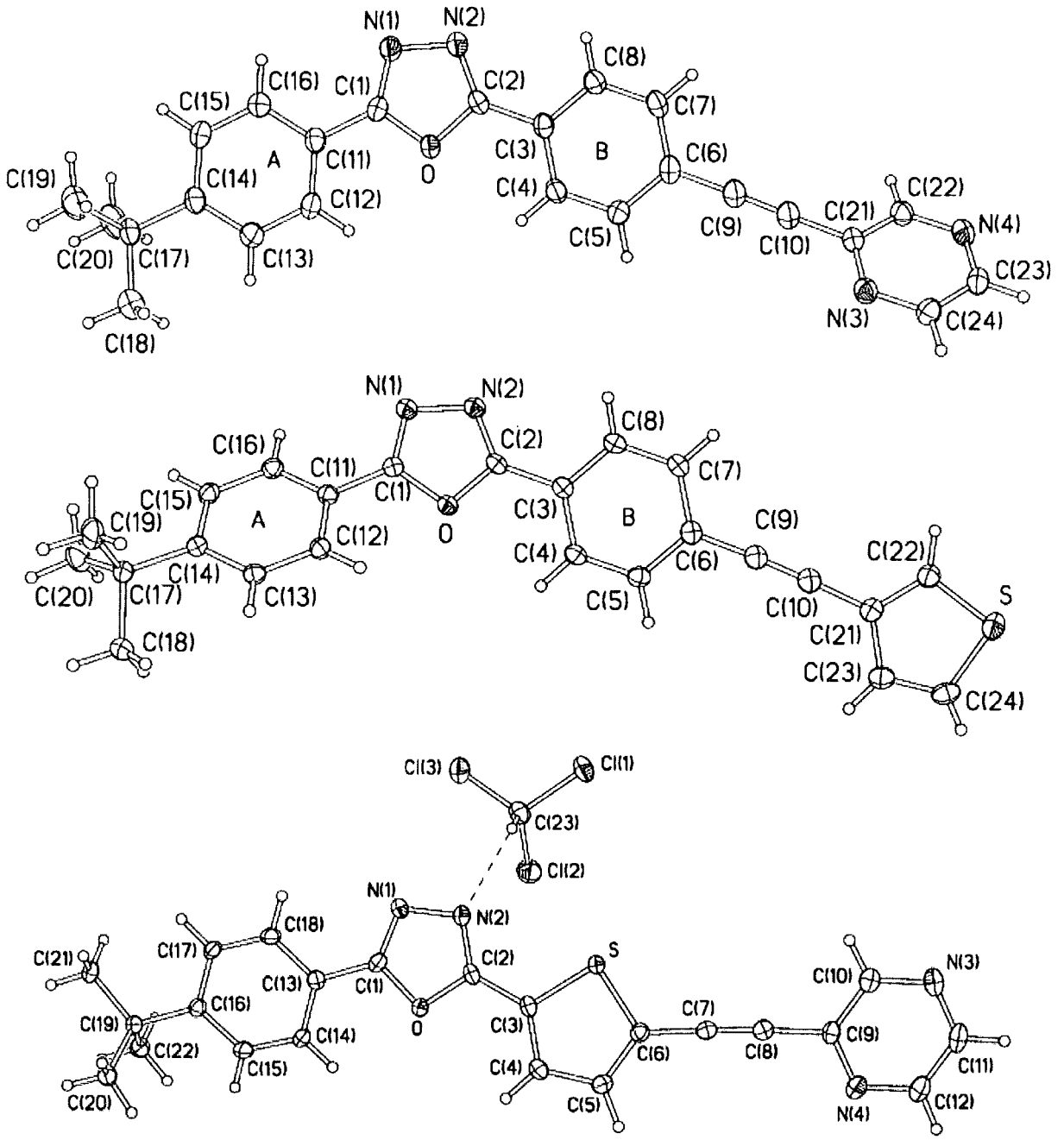

Figure 24: X-ray molecular structures of 232d, 232g and 239d.

4.2.3 Optical Absorption and Emission Properties

The solution UV-Vis absorption and photoluminescence properties for the two series of compounds **232a-g** and **239a-g** are collated in Table 3. The Stokes shift in λ_{max} values for all the compounds is in the range 50-80 nm, which agrees with known diphenyl-1,3,4-oxadiazole

derivatives[159] and diaryl(heteroaryl)ethynes where there is a relatively small conformational change upon photoexcitation.[151a]

Compound	UV-Vis Absorption λ_{max} / nm	PL (PLQY) λ_{max} / nm
232a	322	354, 374
232b	319	354, 373
232c	320	375
232d	323	380 (24%)
232e	325	384
232f	335	389 (10%)
232g	325	361, 376 (28%)
239a	352	386, 408
239b	348	385, 408
239c	351	388, 409
239d	353	396, 415 (22%)
239e	361	420
239f	355	407, 425
239g	347	395, 413
240	400	452, 480

Table 3: UV-Vis absorption and PL (λ_{ex} 350 nm) λ_{max} values for compounds 232a-g, 239a-g and 240 in DCM, 20 °C. PLQY values for 232d, 232f, 232g and 239d shown in brackets. The standards for PLQY measurements were quinine sulfate (Φ = 0.577 in 0.5 M H_2SO_4) and β-carbolene (Φ = 0.60 in 0.5 M H_2SO_4).

An interesting trend is that replacement of a phenyl ring (compounds **232a-g**) by the thienyl ring (compounds **232a-g**) leads to a red shift in the lowest energy band in both the absorption and emission spectra. This can be explained by a "push–pull effect" of the conjugated electron-donating thiophene ring and the electron-accepting oxadiazole ring lowering the HOMO–LUMO gap.[160] In the absorption spectra, this shift is largest for the terminal 5-bromo-2-pyrimidyl derivatives **232e/239e** (36 nm). For all other derivatives in Table 3 the shift is within the range 21-31 nm. In the PL spectra the red shift which occurs on replacing phenyl with thienyl is remarkably similar for all the analogues [$\Delta\lambda_{max}$ (em) 34-37 nm].

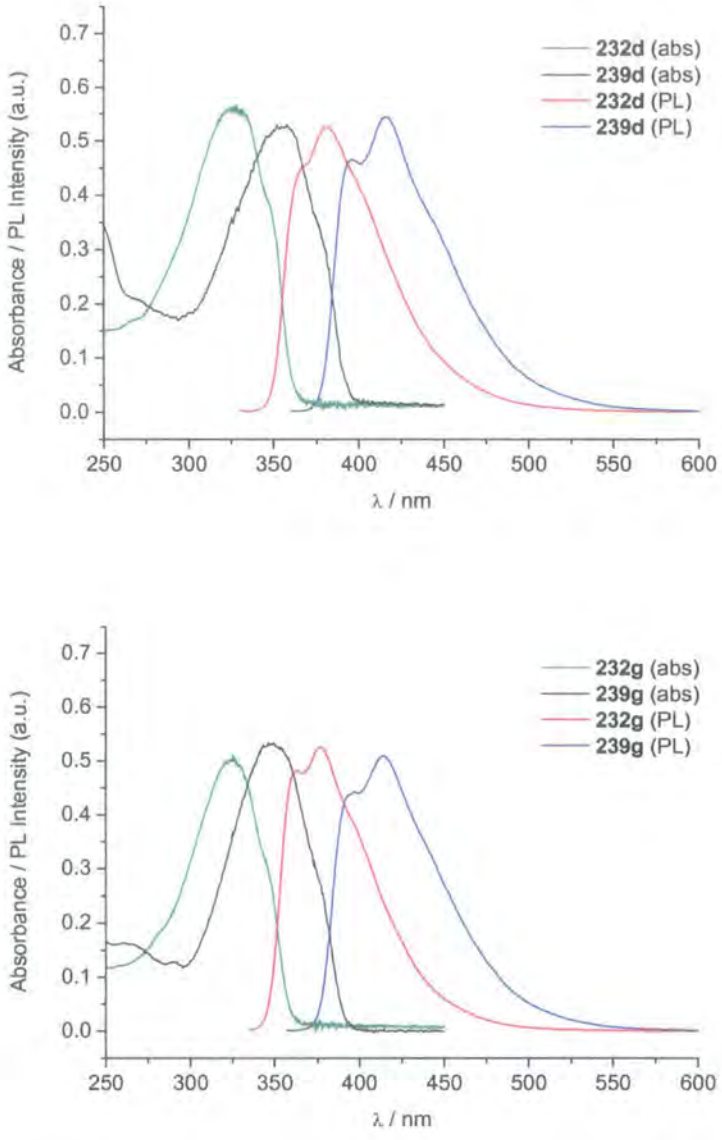

Figure 25: UV-Vis absorption and PL spectra for compounds 232d, 239d, 232g and 239g in DCM, 20 °C.

An additional feature of the data in Table 3 is a further red shift in the absorption and emission peaks of **240** compared to **239f** [$\Delta\lambda_{max}$ (abs) 45 nm; $\Delta\lambda_{max}$ (em) 55 nm] which is consistent with extended π–conjugation through the central bis(ethynylthiophene) unit of **240**.[161] PLQY values were obtained for compounds **232d**, **232f**, **232g** and **239d** and fall within the range 10-28% (Table 3). These values are considerably lower than those reported for model compounds which lack the ethynyl bond, viz. 2,5-diphenyl-1,3,4-oxadiazole (89%) and 2-(4-biphenyl)-5-phenyl-1,3,4-oxadiazole (83%) in non-polar solvents,[162] and are consistent with the data obtained for a series of simpler di(aryl/heteroaryl)ethynl derivatives.[163]

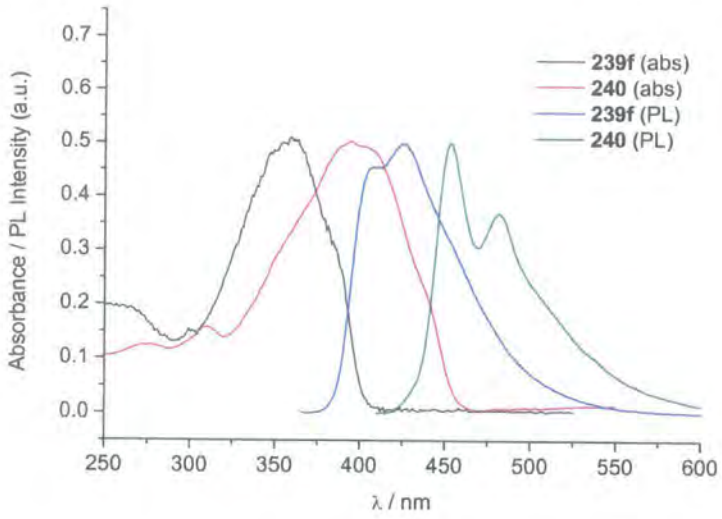

Figure 26: UV-Vis absorption and PL spectra for compounds 239f and 240 in DCM, 20 °C.

4.2.4 Electroluminescence from Blended MEH-PPV Devices

Compound **248c** is blue-emitting PL λ_{max} 421 nm in solution and has been successfully blended with 50% MEH-PPV into the following device ITO/MEH-PPV:**248c** (50:50)/Al. Light emission originates from the MEH-PPV, as EL λ_{max} ~580 nm was identical to the pure MEH-PPV device. However, for compound **249**[164] under the same conditions used for **248c** emission is red-shifted to λ_{max} 600 nm.

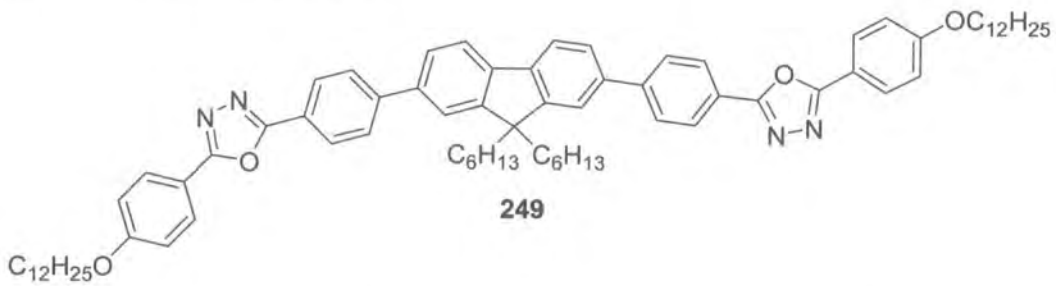

249

Scheme 86: 2,5-Diaryl-1,3,4-oxadiazole-fluorene hybrid 249 prepared by Oyston and co-workers.[164]

We propose that it is the dodecyloxy side chains of **249** that are responsible for the red shift in EL emission which would be in agreement with Baigent *et al* who also observed a significant Stokes' shift for cyano-derivatives of PPV with increasing side chain length.[165] A detailed discussion of MEH-PPV blended devices, using **248c** and **249** is underway in the laboratories of our collaborators.[164]

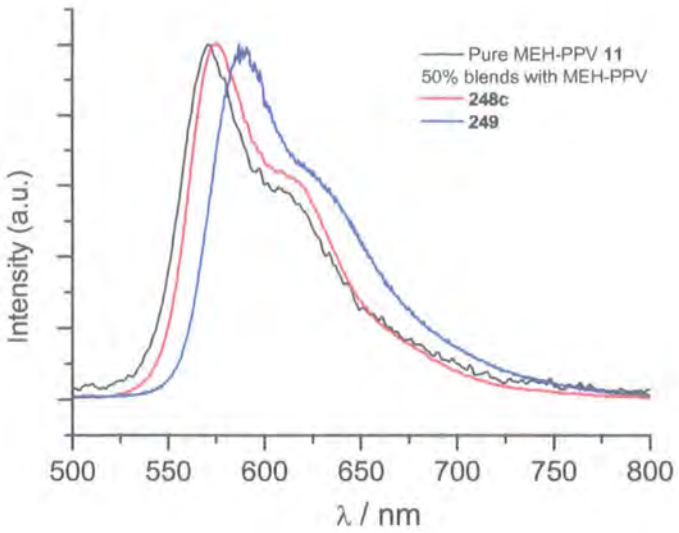

Figure 27: Emission of pure MEH-PPV and 50% blends of MEH-PPV with 248c and 249.[164]

4.3 CONCLUSIONS

We have achieved efficient functionalisation of the terminal ethynyl carbon of compound **230** by cross-coupling reactions with a series of heteroaryl iodides using Sonogashira methodology. The first derivatives of 2-phenyl-5-(2-thienyl)-1,3,4-oxadiazole are reported: a five-step sequence from the readily-available 2-iodo-5-methoxycarbonylthiophene gives 2-(4-*tert*-butylphenyl)-5-(4-ethynylthienyl)-1,3,4-oxadiazole **238** in 13% overall yield. Subsequent functionalisation of **238** proceeds smoothly by analogy with **230**. Spectroscopic studies in solution establish that replacement of the phenyl ring (i.e. the 2,5-diphenyl-1,3,4-oxadiazole series **232a-g**) by a thienyl ring (i.e. the 2-phenyl-5-thienyl-1,3,4-oxadiazole series **239a-g**) leads to a significant red shift in the lowest energy band in both the absorption spectra (21-56 nm shift) and emission spectra (34-37 nm shift). Conjugation is extended further in the bis(ethynylthienyl)thiophene derivative **240**. X-Ray crystal structure analyses reveal that the π–systems of compounds **232d, 232g** and **239d** adopt predominantly planar conformations. This work clearly establishes that the alkynes **230** and **238** are synthetically viable and versatile building-blocks for the construction of extended functional π–electron systems with interesting optoelectronic and structural properties.[166] We have also successfully fabricated MEH-PPV blend devices with new 2,5-diaryl-1,3,4-oxadiazole-fluorene hybrid compounds **248c** and **249** and demonstrated that EL is red shifted with varying side chain length.

5 EXPERIMENTAL PROCEDURES

This chapter details the experimental procedures and analytical data for each of the novel compounds presented in this thesis. This chapter also includes the experimental procedures for some compounds, which were already known in the literature that were used in the course of this work.

5.1 GENERAL METHODS

All reactions that required inert or dry atmospheres were carried out under a blanket of argon, which was dried by passage through a column of phosphorus pentoxide. All reagents employed were of standard reagent grade and purchased from Aldrich, Lancaster, Avocado, Fluka or Merck and used as supplied unless otherwise stated. The following solvents were dried and distilled immediately prior to use: acetone, over Drierite ($CaSO_4$), acetonitrile and dichloromethane over calcium hydride, diethyl ether and toluene over sodium metal, tetrahydrofuran over potassium metal. *N,N*-Dimethylformamide was dried by standing over 4 Å molecular sieves for at least 48 h and was not distilled prior to use. Ethanol and methanol were dried and distilled over magnesium turnings and stored under dry argon over 3 Å molecular sieves. Pyridine was dried by standing over potassium hydroxide overnight followed by vacuum distillation and stored under dry argon over 3 Å molecular sieves. Chlorobenzene, cyclohexane, ethyl acetate, hexane, and petroleum ether were used without prior purification.

Column chromatography was carried out using Prolabo silica (70-230 mesh). Solvents used for chromatography were distilled prior to use, with the exception of dichloromethane, chloroform and petroleum ether, which were used as supplied. Analytical Thin Layer Chromatography (tlc) was performed on Merck DC-Alufolien Silica gel, 60 F_{254} 0.2 mm thickness or Merck DC-Alufolien oxide neutral (Type E), 60 F_{254} 0.2 mm thickness precoated tlc plates.

Cyclic voltammetry experiments were performed on a BAS CV50W electrochemical analyser with *i*R compensation. Platinum wire, platinum disk (Ø 1.6 mm) and Ag/Ag^+ were used as counter, working, and reference electrodes, respectively. CV experiments were performed in

dry dichloromethane with 0.2 M $Bu_4N^+PF_6^-$ as supporting electrolyte; concentrations of compounds were *ca.* 10^{-3} M^{-1}. The scan rate was varied from 50 to 500 mV s^{-1}. The potentials were referenced to Fc/Fc^+ couple as the internal reference, which showed a potential of +0.17 V vs. Ag/Ag^+ in our conditions.

UV-vis spectra were recorded using a Varian Cary 5 spectrophotometer at ambient temperatures. Photoluminescence spectra were recorded using a Jobin-Yvon Horiba Flurolog 3-22 Tau-3 spectrofluorimeter with a 0.5-2 nm bandpass using a Xenon lamp. Spectra were recorded using conventional 90 °C geometry with an excitation at 355 nm. PLQY of thin films were measured using a Jobin-Yvon Fluromax spectrofluorimeter equipped with integrating sphere.[167] The standards for PLQY were quinine sulfate (Φ = 0.577 in 0.5 M H_2SO_4) and β-carbolene (Φ = 0.60 in 0.5 M H_2SO_4).

For fabrication of light-emitting devices using **175** a hole-conducting poly(ethylenedioxythiophene) (PEDOT) layer (30 nm thick) was spun onto an etched ITO glass substrate (20 Ω/□), and then baked overnight in a vacuum oven at 50 °C to remove residual water. A dilute solution of compound **175** in toluene (*ca.* 0.5 mg/ cm^3) was then drop-cast onto the PEDOT to form an active layer (ca. 300 nm thick, as confirmed by AlphaStep measurements). On top of this layer, a cathode of 50 nm thick calcium capped with 50 nm thick aluminium was deposited by evaporation under high vacuum (ca 10^{-6} mbar). A single-layer device using **225** was constructed as follows: a layer of **225** (50-60 nm thickness) was assembled by spin-coating a solution of **225** in chloroform onto a ITO substrate, followed by evaporation of a calcium cathode under high vacum. Blended-layer devices using **248c** and **249** were fabricated as follows: a mixture of MEH-PPV and **248c** or **249** dissolved in chloroform was spin-coated onto a ITO anode followed by evaporation of the aluminium top electrode (thickness ca 150 nm).

Electron Impact (EI) mass spectra were recorded on a Micromass Autospec spectrometer operating at 70 eV with the ionisation mode as indicated. Electrospray (ES) mass spectra were recorded on a Micromass LCT spectrometer. Gas Chromatography Mass Spectra (GCMS) were recorded on a Finnigan Trace MS spectrometer using a HP5MS column (30 L, ID 0.25 mm, Film 0.25 μm).

^{1}H NMR spectra were recorded on a Varian Unity 300 at 300 MHz, a Varian VXR 400s at 400 MHz or a Varian Inova 500 at 500MHz using deuteriated solvent as lock. Chemical shifts are quoted in ppm, relative to tetramethylsilane (TMS), using TMS or the residual solvent as internal reference. ^{13}C NMR were recorded using broad band decoupling, using Varian VXR 400s or Varian Inova 500 spectrometer at 100 MHz and 125 MHz, respectively. The following abbreviations are used in listing NMR spectra: s = singlet, d = doublet, dd = doublet of doublets, dt = doublet of triplets, t = triplet, m = multiplet, br = broad.

Elemental analyses were obtained on an Exeter Analytical Inc. CE-440 elemental analyser. Melting points were recorded on a Stuart Scientific SMP3 melting points apparatus.

5.2 Experimental Procedures of Chapter 2

5.2.1 Suzuki Cross-Coupling: General Method

The boronic acid, the halide, and the catalyst (5 mol% relative to the boronic acid) were added sequentially to distilled organic solvent (30 cm^3) in the absence of light. The reaction mixture was stirred at 20 °C for 30 min. Degassed aqueous base was added and the reaction mixture was heated at reflux under a blanket of argon until tlc monitoring showed that the reaction was complete, typically 36 h. Solvent was evaporated and water (50 cm^3) was added to the residue, which was extracted into DCM (3 x 50 cm^3). The organic layer was dried ($MgSO_4$) then concentrated under reduced pressure and purified by chromatography on a silica column.

2-Chloro-5-bromopyrimidine 162

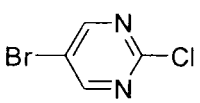

2-Hydroxypyrimidine hydrochloride **160** (12.5 g, 93.4 mmol) was dissolved in a Na_2CO_3 solution (5.0 g, 47.2 mmol) in water (275 cm^3). Bromine (5.0 cm^3, 97.6 mmol) was added slowly and the reaction stirred at 20 °C for 30 min. The water was removed *in vacuo* to leave a yellow solid. Toluene (225 cm^3) was added and the solution refluxed via an azeotropic distillation (24 h). Toluene was removed by distillation and the resultant solid, dried under vacuum (24 h). Phosphorus oxychloride (45.0 cm^3) and *N,N*-dimethylaniline (4.5 cm^3) were added and the reaction heated under reflux (8 h). Excess phosphorus oxychloride was removed under reduced pressure with any residual hydrolysed with external cooling. The product was extracted into diethyl ether (150 cm^3) and washed with saturated Na_2CO_3 solution and dried over $MgSO_4$. The solution was concentrated and purified by silica column chromatography (eluent DCM-hexane, 1:1 v/v) and then recrystallised from hexane to yield **162** as colourless crystals (8.26 g, 45%) m.p 78-78.6 °C (lit. 79 °C).[100a] m/z (EI) 196 (M^+, 18%, ^{81}Br, ^{37}Cl), 194 (M^+, 100%, ^{81}Br, ^{35}Cl, or ^{79}Br, ^{37}Cl), 192 (M^+, 57%, ^{79}Br, ^{37}Cl). δ_H ($CDCl_3$) 8.68 (s, 2H). δ_C ($CDCl_3$) 118.82, 159.90, 160.04.

2,5-Dibromopyrimidine 163

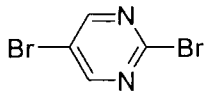

2-Chloro-5-bromopyrimidine **162** (8.00 g, 41.4 mmol) dissolved in dichloromethane (25 cm^3) was added to stirred 48% hydrobromic acid (25 cm^3), along with a few drops of Aliquat 336. The two-phase system was strirred at 20 °C for 72 h. A white solid was visible after 24 h. The solvent was removed *in vacuo* and extracted into diethyl ether (150 cm^3), neutralised with saturated Na_2CO_3 (aq), and dried over $MgSO_4$. Diethyl ether was removed *in vacuo* to leave a white solid, which was recrystallised from hexane to yield **163** as white crystalline needles (6.33 g, 64%). m.p 84 °C (lit. 81-83 °C).[100b] m/z (EI) 240 (M^+, 40%, ^{81}Br, ^{81}Br), 238 (M^+, 84%, ^{81}Br, ^{79}Br), 236 (M^+, 44%, ^{79}Br, ^{79}Br). δ_H ($CDCl_3$) 8.63 (s, 2H). δ_C ($CDCl_3$) 119.70, 150.84, 159.90.

5-Bromo-2-phenylpyrimidine 165 and 2,5-Diphenylpyrimidine 166

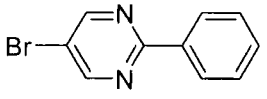

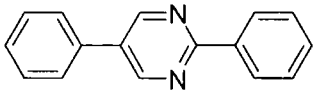

In accordance with the general method for Suzuki cross-coupling reactions; 2,5-dibromopyrimidine **163** (190 mg, 0.80 mmol), benzeneboronic acid **164** (293 mg, 2.4 mmol), THF (15 cm^3), $Pd(PPh_3)_4$ (40 mg) and Na_2CO_3 (1M, degassed, 2.0 cm^3). After cooling to 20 °C, THF was evaporated and the resulting aqueous suspension of compounds **165** and **166** was suction filtered to obtain a white solid which was washed with water then hexane. Chromatography (eluent DCM-hexane 1:1 v/v) gave a colourless solid which was recrystallised from toluene to yield 2,5-diphenylpyrimidine **166** as colourless crystals (60 mg, 32%), m.p 185.0-185.5 °C (lit[103a], 180-181 °C). m/z (EI) 232 (M^+, 100%). δ_H (500 MHz, $CDCl_3$) 7.45 (t, 2H, J = 8.0 Hz), 7.52 (m, 4H), 7.64 (d, 2H, J = 8.0 Hz), 8.50 (dd, 2H, J = 2.0, 7.58 Hz), 9.03 (s, 2H). δ_C (500 MHz, $CDCl_3$) 127.07, 128.11, 128.76, 129.55, 130.70, 155.41, 155.91.

The combined mother toluene liquor and DCM-hexane eluent (apart from the DCM-hexane solution of product **166**) was evaporated and the residue was chromatographed (eluent DCM-hexane 1:1 v/v) gave to yield **165** as a white solid which was recrystallised from ethanol to yield **165** as a white crystalline solid (80 mg, 43%), m.p 104.0-104.6 °C, (lit[103b], 104-105 °C). *m/z* (EI) 234 (M^+ [^{79}Br], 100%), 236 (M^+ [^{79}Br], 93%). δ_H (500 MHz, $CDCl_3$) 7.50 (m, 3H),

8.40 (m, 2H), 8.84 (s, 2H). δ_C (500 MHz, $CDCl_3$) 118.29, 128.13, 128.69, 131.12, 136.45, 157.82, 162.84.

2,7-Dibromo-9,9-dihexylfluorene 168

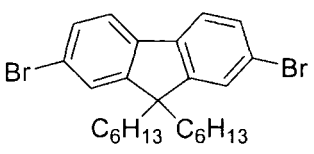

2,7-Dibromofluorene **167** (3.24 g, 10 mmol) and bromohexane (7.0 cm^3, 50 mmol) were added to freshly distilled THF (80 cm^3), which was subsequently cooled to 0 °C. Potassium *tert*-butoxide (1M 10 cm^3) was added slowly with stirring (30 min) resulting in a pink suspension. After stirring at 0 °C for 1 h an additional portion of potassium tert-butoxide (1M, 10.5 cm^3) was added and the solution was stirred at 20 °C overnight. THF was removed *in vacuo*, dry DCM (100 cm^3) was added and the inorganic salts were removed by filtration. The organic solution was concentrated and purified by chromatography (eluent hexane) to give a light yellow oil, which was recyrstallised from ethanol to yield white plates of compound **168** (4.1 g, 83%), mp 72-73 °C (lit 67.5-68.5 °C).[97b] Anal. calcd. for $C_{25}H_{32}Br_2$ C, 60.99, H, 6.60. Found: C, 60.89, H, 6.60%. *m/z* (EI) 490 (M^+, ^{79}Br, ^{79}Br, 13%), 492 (M^+, ^{79}Br, ^{81}Br, 100%,), 494 (M^+, ^{81}Br, ^{81}Br, 13%). δ_H (500 MHz, $CDCl_3$) 0.59 (m, 4H), 0.79 (m, 6H), 1.10 (m, 12H), 1.93 (m, 4H, $\underline{CH_2}$-C(Ar)$_2$-CH_2), 7.46 (m, 4H), 7.53 (m, 2H). δ_C (500 MHz, $CDCl_3$) 13.98, 22.56, 23.61, 29.56, 31.44, 40.17, 55.65, 121.09, 121.43, 126.12, 130.10, 139.01, 152.50.

9,9-Dihexylfluorene-2,7-diboronic acid 169

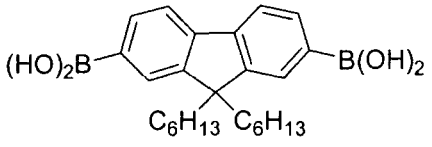

To a solution of **168** (2.46 g, 5.00 mmol) in dry THF (10 cm^3) was added *n*-butyllithium solution in hexane (1.6M, 6.8 cm^3, 11.04 mmol) dropwise at –78 °C. The mixture was stirred at –78 °C under argon for an additional 6 h to give a white suspension. Triisopropyl borate (5.0 cm^3) was syringed in quickly at –78 °C and the mixture was stirred overnight with a cooling bath allowing the temperature to rise gradually to 20 °C. Water (30 cm^3) was added to the white suspension and the mixture was stirred at 20 °C for a further 4 h. THF was removed *in vacuo*. Water (100 cm^3) was added and the product extracted into diethyl ether (3x 50 cm^3) and dried ($MgSO_4$). Diethyl ether was removed *in vacuo* giving a white solid, which was recyrstallised from acetonitrile to yield a white crystalline solid **169** (1.68 g, 80%), mp 297-298 °C (lit 294-295 °C).[106c] Anal. calcd. for $C_{25}H_{32}B_2O_4$ C, 71.12, H,

8.60. Found C, 71.62, 8.70%. δ_H (400 MHz, DMSO-d_6) 0.45 (s, 4H), 0.68 (m, 6H, J = 6.6 Hz), 0.98 (m, 12H), 1.93 (m, 4H, $\underline{CH_2}$-C(Ar)$_2$-CH_2), 7.73 (m, 4H, J = 1.8 Hz) 7.81 (s, 2H) 8.00 (s, 4H). δ_C (400 MHz, DMSO-d_6) 13.78, 21.95, 23.43, 29.00, 30.93, 54.17, 119.01, 128.37, 132.88, 142.31, 149.36.

2,7-Bis(2-pyrimidyl)-9,9-dihexylfluorene 172

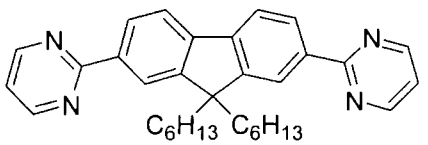

In accordance with the general method for Suzuki cross-coupling reactions: 2-bromopyrimidine **170** (0.28 g, 1.78 mmol), 9,9-dihexylfluroene-2,7-diboronic acid **169** (0.25 g, 0.60 mmol), THF (30 cm^3), $Pd(PPh_3)_4$ (69.35 mg) and Na_2CO_3 (1 M, degassed, 2.5 cm^3). Followed by column chromatography (eluent DCM: ethyl acetate 9:1 v/v) to yield compound **172** as a yellow solid (100 mg, 34%), mp 155.1-156.9 °C. *m/z* (EI) 490 (M^+, 100%). HRMS (EI) (M^+) 490.3094 (calcd. for $C_{33}H_{38}N_4$: 490.3096). δ_H (400 MHz, $CDCl_3$) 0.66 (m, 10H), 0.93 (m, 12H), 2.07 (m, 4H, $\underline{CH_2}$-C(Ar)$_2$-CH_2), 7.16 (t, 2H, J = 4.8 Hz), 7.81 (d, 2H, J = 8.0 Hz), 8.39 (s, 2H), 8.45 (d, 2H,d J = 8.0 Hz), 8.78 (d, 4H, J = 4.9 Hz). δ_C (400 MHz, $CDCl_3$) 13.95, 22.56, 23.71, 29.69, 31.48, 40.36, 55.55, 118.84, 120.35, 122.44, 127.40, 136.75, 143.28, 152.07, 157.23, 164.97. UV-Vis λ_{max} 317.0, 337.5, 352.5 nm, PL λ_{max} 366, 384 nm.

2,7-Bis(5-pyrimidyl)-9,9-dihexylfluorene 173

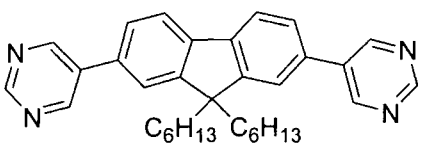

By analogy with the synthesis of **172**. 5-bromopyrimidine **171** (0.28 g, 1.78 mmol), 9,9-dihexylfluorene-2,7-diboronic acid **169** (0.25 g, 0.60 mmol), THF (30 cm^3), $Pd(PPh_3)_4$ (69.35 mg) and Na_2CO_3 (1 M, degassed, 2.5 cm^3). Followed by column chromatography (eluent DCM: ethyl acetate 9:1 v/v) to yield compound **173** as a yellow solid (93 mg, 32%), mp 157-157.8 °C. *m/z* (EI) 490 (M^+, 100%). HRMS (EI) (M^+) 490.3101 (calcd. for $C_{33}H_{38}N_4$: 490.3096). δ_H (400 MHz, $CDCl_3$) 0.65 (m, 10H), 1.00 (m, 12H), 2.01 (m, 4H, $\underline{CH_2}$-C(Ar)$_2$-CH_2), 7.50 (s, 2H), 7.53 (d, 2H, J = 8.0 Hz), 7.81 (d, 2H, J = 7.6 Hz), 8.97 (s, 4H), 9.17 (s, 2H). δ_C (400 MHz, $CDCl_3$) 14.20, 22.75, 24.05, 29.79, 31.65, 40.50, 55.93, 121.46, 126.40, 128.82, 132.52, 133.74, 134.88, 141.32, 152.65, 155.14, 157.49. UV-Vis λ_{max} 328.0 nm, PL λ_{max} 361, 378 nm.

2,7-Bis(5-bromo-2-pyrimidyl)-9,9-dihexylfluorene 174

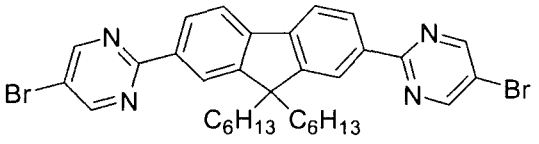

By analogy with the synthesis of **172**. 2,5-dibromopyrimidine **163** (0.28 g, 1.78 mmol), 9,9-dihexylfluorene-2,7-diboronic acid **169** (0.25 g, 0.60 mmol), THF (30 cm^3) $Pd(PPh_3)_4$ (69.0 mg) and Na_2CO_3 (1 M, degassed, 2.5 cm^3). Followed by column chromatography (eluent DCM: petroleum ether, 9:1 v/v) giving a white solid, which was recrystallised form hexane to yield compound **174** as white needles (87 mg, 23%). m.p 179.3-179.8°C. *m/z* (EI) 646 (M^+, ^{79}Br, ^{79}Br, 46%), 648 (M^+, ^{79}Br, ^{81}Br, 100%), 648 (M^+, ^{81}Br, ^{81}Br, 13%). HRMS (EI) (M^+) 646.1304 (calcd. for $C_{33}H_{36}Br_2N_4$: 646.1306). δ_H (500 MHz, $CDCl_3$) 0.71 (m, 10H), 1.07 (m, 12H), 2.12 (m, 4H, $\underline{CH_2}$-C(Ar)$_2$-CH_2), 7.85 (d, 2H, J = 8.5 Hz), 8.41 (s, 2H), 8.47 (d, 2H, J = 8.2 Hz), 8.86 (s, 4H). δ_C (500 MHz, $CDCl_3$) 13.96, 22.55, 23.81, 29.66, 31.48, 40.28, 55.55, 117.95, 120.48, 122.51, 127.48, 135.86, 143.45, 152.18, 157.78, 163.08. UV-Vis λ_{max} 348.0, 365.0 nm, PL λ_{max} 377, 396 nm.

2,7-Bis(5-phenyl-2-pyrimidyl)-9,9-dihexylfluorene 175

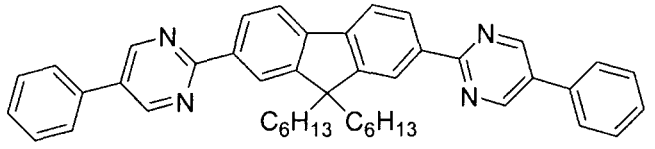

A solution of 2,7-bis(5-bromo-2-pyrimidyl)-9,9-dihexylfluorene **174** (100 mg, 0.154 mmol), benzeneboronic acid **164** (60 mg, 0.46 mmol), THF (30 cm^3), $Pd(PPh_3)_4$ (53.5 mg) and Na_2CO_3 (1 M, degassed, 2.0 cm^3). Followed by column chromatography (eluent DCM: petroleum ether 4:1 v/v) yielded compound **175** as a white/yellow solid (35 mg, 35%), mp 185.5-186.5°C. *m/z* (EI) 642 (M^+, 100%). HRMS (EI) (M^+) 642.3719 (calcd. for $C_{45}H_{46}N_4$: 642.3722). δ_H (400 MHz, $CDCl_3$) 0.71 (m, 10H), 1.07 (m, 12H), 2.19 (m, 4H, $\underline{CH_2}$-C(Ar)$_2$-CH_2), 7.47 (m, 2H), 7.54 (t, 4H, J = 7.0 Hz), 7.65 (d, 4H, J = 11.50 Hz), 7.91 (d, 2H, J = 8.0 Hz), 8.53 (s, 2H), 8.58 (d, 2H, J = 8.0 Hz), 9.07 (s, 4H). δ_C (400 MHz, $CDCl_3$) 13.96, 22.57, 23.85, 29.72, 31.53, 40.41, 55.58, 120.41, 122.38, 126.70, 127.40, 128.70, 129.40, 131.38, 134.59, 136.54, 143.28, 152.12, 155.17, 163.69. UV-Vis λ_{max} 365.5, 371.5 nm, PL λ_{max} 391, 412 nm.

5.3 EXPERIMENTAL PROCEDURES OF CHAPTER 3

Pyrazine-2,3-dicarboxylic acid anhydride 182

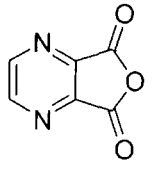

Pyrazine-2,3-dicarboxylic acid **181** (49.8 g, 0.30 mole) was added to acetic anhydride (128 cm^3) and heated under reflux for 2 h. Once the solution was a dark brown colour refluxing was continued for an additional 10 min. The mixture was then cooled in an ice bath. The product was separated by filtration and washed with diethyl ether (3 x 50 cm^3) to yield **182** as white needles (40.8 g, 92%), mp 218-219 °C (lit[125] 221-222 °C). *m/z* (EI) 150 (M^+, 100%). δ_H (250 MHz DMSO-d_6) 9.19 (s, 2H). δ_C (250 MHz DMSO-d_6) 146.09, 151.56, 166.84.

Pyrazine-2-carboxylic acid-3-methyl ester 183

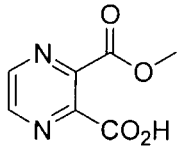

Pyrazine-2,3-dicarboxylic acid anhydride **182** (38.8 g, 0.26 moles) was added to methanol (125 cm^3). The resultant yellow solution was stirred at 20 °C overnight. Methanol was evaporated revealing a white solid, which was dissolved in ethyl acetate and purified by chromatography (eluent ethyl acetate). The organic solvent was removed *in vacuo* and the resulting white solid recrystallised from toluene to yield **183** as a white crystalline solid (41.7 g, 89%), mp 115.9-117.8 °C (lit[125] 115-116 °C). *m/z* (EI) 182 (M^+, 100%). δ_H (250 MHz DMSO-d_6) 3.95 (s, 3H), 9.01 (d, 2H, J = 12.3 Hz). δ_C (250 MHz DMSO-d_6) 53.02, 144.51, 144.72, 145.93, 146.10, 164.99, 165.57.

Methyl-3-aminopyrazine carboxylate 186

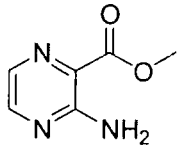

Pyrazine-2-carboxylic acid-3-methyl ester **183** (38.52 g, 0.21 moles) was added to $SOCl_2$ (43 cm^3), and the mixture heated under reflux for 2 h followed by a second addition of $SOCl_2$ (2.6 cm^3) and reflux for an additional 1 h. The excess $SOCl_2$ was removed by distillation with toluene (3 x 25 cm^3) leaving a brown oil. Acetone (analytical grade, 100 cm^3) was added followed by NaN_3 (33.5 g, 0.48 moles) dissolved in H_2O (110 cm^3), which was added in portions over 1 h. Water (90 cm^3) was

added and the mixture was stirred at 0 °C for 18 h. The organic portion was extracted into benzene (4 x 50 cm^3) and the combined extracts heated under reflux for 24 h. Benzene was removed *in vacuo* and the resulting, yellow solid was dissolved in methanol and filtered via a celite bed whilst hot. Upon filtration, the product crystallized. The product was therefore directly recrystallised from the mother liquor and separated by filtration to yield **186** as golden yellow needles (10.83 g 33%), mp 170.3-171.1 °C (lit[125] 172-173 °C). *m/z* (EI) 95 (M^+, 100%) 153 (M^+, 64%). δ_H (250 MHz DMSO-d_6) 3.96 (s, 3H), 7.43 (s, 2H), 7.93 (d, 1H, J = 2.2 Hz), 8.26 (d, 1H, J = 2.0 Hz). δ_C (250 MHz DMSO-d_6) 52.06, 123.13, 132.43, 147.77, 155.84, 166.43.

2-Amino-5-bromopyrazine-3-carboxylic acid methyl ester 187

Method 1

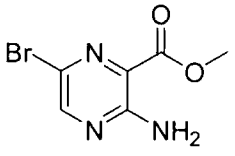

3-Aminopyrazine carboxylic acid methyl ester **186** (3.00 g, 1.95 mmol) was added to warm glacial acetic acid (16.5 cm^3). Bromine (1.05 cm^3, 2.00 mmol) was added dropwise during 15 min and the reaction mixture was allowed to stand at 20 °C for 30 min. The reaction mixture was washed with K_2CO_3 (aq), then extracted into ethyl acetate and dried ($MgSO_4$). Purification by chromatography (eluent DCM-ethyl acetate 3:1 v/v) gave a yellow solid, which was recrystallised from ethanol. An insoluble impurity was removed by hot filtration. The product, which precipitated from the filtrate, was recrystallised from the ethanol mother liquor to yield long yellow needles of **187** (1.63 g, 36%), mp 172-173.5 °C (lit[126] 175.3-175.9 °C). Spectroscopic data were identical to those obtained by method 2.

Method 2

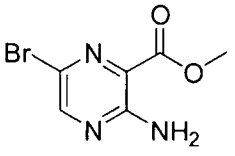

3-Aminopyrazine carboxylic acid methyl ester **186** (10.0 g, 65.3 mmol) was dissolved in DMF (79 cm^3), to which a solution of NBS (11.6 g, 65.3 mmol) in DMF (77 cm^3) was added and the mixture was stirred overnight at 20 °C. Sodium metabisulfite (2.9 g) dissolved in H_2O (73 cm^3) was added, a precipitate formed immediately. Water (60 cm^3) was added and the crude product was extracted into DCM (250 cm^3) and dried over $MgSO_4$. Purification by column chromatography (eluent

DCM-diethyl ether 1:1 v/v). Solvent was removed *in vacuo* leaving pale a yellow solid, which was recrystallised from ethanol to yield **187** as long yellow needles (12.4 g, 82%), mp 175.4-176.7 °C (lit[126] 175.3-175.9 °C). *m/z* (EI) 231 (M^+, ^{79}Br, 78%), 233 (M^+, ^{81}Br, 76%). δ_H (250 MHz DMSO-d_6) 3.96 (s, 3H), 7.54 (s, 2H), 8.46 (s, 1H). δ_C (250 MHz DMSO-d_6) 52.27, 122.34, 122.59, 150.05, 154.88, 165.30.

2-Amino-5-bromopyrazinoic acid 188

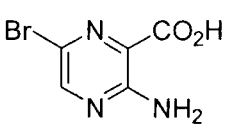

2-Amino-5-bromopyrazine carboxylic acid methyl ester **187** (10.0 g, 43 mmol) was added to NaOH (5% aq) (200 cm^3) and heated under reflux for 2 h. The mixture was acidified with HBr (48% aq, 28 cm^3). The product **188** that precipitated was recrystallised from the aqueous mother liquor and isolated as green needles (7.30 g, 78%), mp 182.1-182.3 °C (lit[126] 184-186 °C). *m/z* (EI) 217 (M^+, ^{79}Br, 65%), 219 (M^+, ^{81}Br, 65%). δ_H (250 MHz DMSO-d_6) 7.60 (s, 2H), 8.41 (s, 1H). δ_C (250 MHz DMSO-d_6) 122.45, 123.30, 149.61, 155.16, 166.90.

2-Amino-5-bromopyrazine 189

Method 1

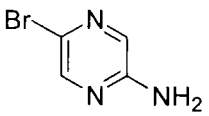

2-Amino-5-bromopyrazinoic acid **188** (4.55 g, 20 mmol) was added to tetralin (35 cm^3) and heated under reflux for 2.5 h. Petroleum ether (bp 100-120 °C) (20 cm^3) was added causing product precipitation, which was separated by filtration, then dissolved in diethyl ether and purified by chromatography (eluent diethyl ether) to give a yellow solid, which was recrystallised from toluene / petroleum ether to yield **189** as yellow crystals (2.45 g, 67%), mp 113.7-115.0 °C (lit[126] 113 °C). Data were identical to that obtained by method 2.

Method 2

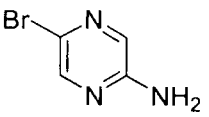

Aminopyrazine **190** (5.00 g, 52.5 mmol) was added to DCM (150 cm^3), which had previously been cooled to 0 °C. NBS (9.40 g, 52.5 mmol) was added and the reaction mixture was stirred at 0 °C for 20 h. Saturated Na_2CO_3 (aq) was added followed by water (50 cm^3). The organic component was then

washed with water, dried ($MgSO_4$), then concentrated under reduced pressure and purified by column chromatography (eluent DCM-ethyl acetate, 1:1 v/v) to give a yellow solid which was recrystallised from toluene / petroleum ether (bp 100-120 °C) to yield **189** as golden needles (3.25 g, 36%), mp 114.3-115.9 °C (Lit[126] 113 °C). *m/z* (GCMS)172.9 (^{79}Br), 174.9 (^{81}Br). δ_H (400 MHz $CDCl_3$) 4.68 (s, 2H), 7.76 (d, 1H, J = 1.6 Hz), 8.07 (d, 1H, J = 1.6 Hz). δ_C (400 MHz $CDCl_3$) 127.06, 131.76, 144.12, 153.37.

2,5-Dibromopyrazine 191

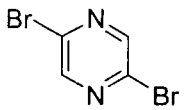

HBr solution (48% aq 5 cm^3) was cooled to 0 °C. 2-Amino-5-bromopyrazine **189** (0.5 g, 2.87 mmol) was added in small portions with stirring until a clear solution was obtained. Bromine (0.2 cm^3, 3.90 mmol) was added dropwise over a 20 min period. The reaction was stirred at 0 °C for 30 min. $NaNO_2$ (0.91 g, 13.2 mmol) dissolved in water (1.5 cm^3) was added dropwise ensuring that the internal reaction flask temperature did not rise above 0 °C. After stirring for 30 min, Na_2SO_3 (0.63 g, 5.00 mmol) dissolved in water (6.5 cm^3) was added again whilst maintaining a reaction temperature below 0 °C. The solution was made alkaline (pH 9) with the addition of 10% Na_2CO_3 (aq) and extracted into diethyl ether (3 x 25 cm^3). The combined organic extracts were dried ($MgSO_4$) and the solvent removed *in vacuo* to yield **191** as a yellow solid (100 mg, 15%), mp 40-42 °C (lit[126] 38-44 °C). δ_H (200 MHz $CDCl_3$) 8.47 (s, 2H). δ_C (200 MHz $CDCl_3$) 139.25, 147.46. This reaction proved to be capricious, and on some occasions no pure product could be isolated.

2-Amino-5-chloropyrazine carboxylic acid methyl ester 193

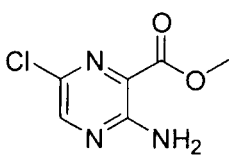

3-Aminopyrazine carboxylic acid methyl ester **186** (10.0 g, 53.3 mmol) was added to a mixture of glacial acetic acid (69 cm^3) and H_2O (292 cm^3). The reaction mixture was heated to give a clear yellow solution. With external cooling Cl_2 (g) was bubbled into the solution for 10 min forming a white solid. The resulting chloroamine **192** was isolated by filtration and added to a solution of sodium bisulfite (10.73 g) in H_2O (65 cm^3). The white suspension was stirred at 20 °C for 1.5 h. A light yellow solid was isolated by filtration and washed with water and isopropyl alcohol and identified as **193** (5.40 g, 56%), mp 158-159 °C (lit[129] 159-161 °C). *m/z* (GCMS) 186.9 (^{35}Cl),

188.8 (^{37}Cl). δ_H (500 MHz DMSO-d_6) 3.83 (s, 3H), 7.54 (s, 2H), 8.37 (s, 1H). δ_C (500 MHz DMSO-d_6) 52.35, 120.97, 132.74, 147.65, 154.79, 165.40.

2-Amino-5-chloropyrazinoic acid 194

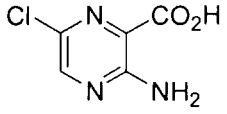

2-Amino-5-chloropyrazine carboxylic acid methyl ester **193** (5.21 g, 30 mmol) was added to NaOH (10% aq) solution (50 cm^3) and heated under reflux for 1.5 h. The sodium salt was removed by filtration and dissolved in water (30 cm^3), boiled then acidified with conc HCl precipitating **194** as yellow needles (4.03 g, 84%), mp 179-180 °C (lit[130] 177-180 °C). *m/z* (GCMS) 172.9 (^{35}Cl), 174.8 (^{37}Cl). δ_H (300 MHz DMSO-d_6) 7.54 (s, 2H), 8.34 (s, 1H). δ_C (500 MHz DMSO-d_6) 121.94, 132.58, 147.24, 155.07, 167.01.

2-Amino-5-chloropyrazine 195

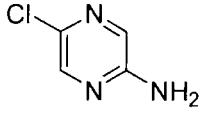

2-Amino-5-chloropyrazinoic acid **194** (3.18 g, 18.32 mmol) was added to tetralin (48 cm^3) and heated under reflux for 2.5 h. The solution was cooled in an ice bath for 1 h. **195** was isolated as a yellow solid (1.75 g, 74%), mp 130-131 °C (lit[130] 129-130 °C). *m/z* (GCMS) 128.9 (^{35}Cl), 130.8 (^{37}Cl). δ_H (500 MHz $CDCl_3$) 4.61 (s, 2H), 7.76 (d, 1H, J = 0.5 Hz), 8.01 (d, 1H, J = 0.5 Hz). δ_C (500 MHz $CDCl_3$) 130.72, 137.52, 141.36, 153.09.

3-Chloropyrazine-1-Oxide 199

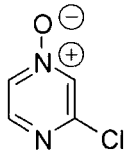

Chloropyrazine **198** (5.50 cm^3, 61.2 mmol) was added to a solution of glacial acetic acid (18.5 cm^3) and hydrogen peroxide (aq 35%) (10.5 cm^3) and refluxed for 17 h. The reaction volume was reduced by 50% and diluted with an equal volume of water. The product was extracted into chloroform (3 x 25 cm^3) and dried ($MgSO_4$). Solvent was evaporated *in vacuo* to give a white solid, which was recrystallised from ethanol to yield **199** as white needles (3.97 g, 50%), mp 97-99 °C (lit[131] 95-96 °C). *m/z* (EI) 130 (M^+ ^{35}Cl, 100%), 132 (M^+ ^{35}Cl, 47%). δ_H (400 MHz $CDCl_3$) 8.02 (dd, 1H, J = 4.0, 1.0 Hz), 8.15 (d, 1H, J = 0.5 Hz), 8.25 (d, 1H, J = 4.0 Hz). δ_C (400 MHz $CDCl_3$) 133.18, 133.51, 145.97, 151.77.

2,5-Dichloropyrazine 197

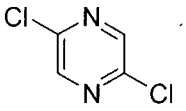

3-Chloropyrazine-1-oxide **197** (2.00 g, 15.32 mmol) was added to $POCl_3$ (5.0 cm^3) and refluxed for 1 h. The solution was cooled to 20 °C and poured cautiously onto crushed ice with good stirring. The product was extracted with DCM (3 x 25 cm^3) washed with water (50 cm^3) and 5% $NaHCO_3$ (50 cm^3), dried ($MgSO_4$). Solvent was removed under reduced pressure and the product was purified by chromatography (eluent DCM) to give a colourless oil (0.23 g). *m/z* (GCMS) 147.9 (^{35}Cl, ^{35}Cl), 149.8 (^{35}Cl, ^{37}Cl), 151.7 (^{37}Cl, ^{37}Cl). δ_H (400 MHz $CDCl_3$) 8.32 (s, 2H), 8.39 (s, 2H), 8.52 (s, 2H). δ_C (400 MHz $CDCl_3$) 141.76, 142.43, 143.79, 147.83, 148.03. These NMR data showed that the product was a mixture of isomers **197**, **200** and **201** see page 74.

2-Amino-5-phenylpyrazine 202

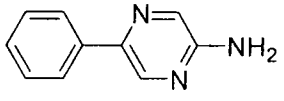

In accordance with the general method for Suzuki cross-coupling reactions. 2-amino-5-bromopyrazine **189** (1.00 g, 5.75 mmol), benzeneboronic acid **164** (0.84 g, 6.29 mmol), THF (30 cm^3), $Pd(PPh_3)_4$ (398 mg) and Na_2CO_3 (1 M, degassed, 5 cm^3). Followed by column chromatography (eluent DCM-diethyl ether, 1:2 v/v) gave a pale yellow solid which was recrystallised from toluene to yield compound **202** as off-white needles (0.58 g, 59%), mpt 147-149 °C. Anal. calcd. for $C_{10}H_9N_3$: C, 70.16; H, 5.30, N, 24.54. Found: C, 70.35; H, 5.32; N, 24.41%. *m/z* (EI) 171 (M^+, 100%). δ_H (400 MHz $CDCl_3$) 7.36 (m, 1H), 7.45 (t, 2H, J = 7.2 Hz), 7.87 (d, 2H, J = 7.2 Hz), 8.07 (d, 2H, J = 1.6 Hz), 8.45 (d, 2H, J = 1.6 Hz). δ_C (400 MHz $CDCl_3$) 125.63, 128.17, 128.82, 131.60, 136.93, 139.01, 142.96, 153.02.

2-Amino-5-(2-methoxyphenyl)pyrazine 204

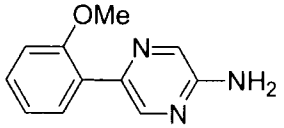

By analogy with the synthesis of **202**, 2-amino-5-bromopyrazine **189** (0.27 g, 1.44 mmol), 2-methoxybenzeneboronic acid **203** (0.26 g, 1.72 mmol), THF (30 cm^3), $Pd(PPh_3)_4$ (99.4 mg) and Na_2CO_3 (1 M, degassed, 4.5 cm^3). Followed by column chromatography (eluent DCM-diethyl ether, 1:2 v/v) gave a yellow oil which crystallised under vacuum. This product was recrystallised from toluene / hexane mixture to yield **204** as yellow crystals (0.12 g, 35%), mp 100-102 °C. Anal.

calcd. for $C_{11}H_{11}N_3O$: C, 65.66; H, 5.51, N, 20.88. Found: C, 65.55; H, 5.52; N, 20.88%. *m/z* (GCMS) 201.1. δ_H (400 MHz $CDCl_3$) 3.85 (s, 3H), 4.69 (s, 2H), 6.98 (d, 1H, J = 7.9 Hz), 7.06 (td, 1H, J = 7.6, 1.2 Hz), 7.33 (ddd, 1H, J = 8.8, 8.0, 7.2 Hz), 7.73 (dd, 1H, J = 7.6, 1.6 Hz), 8.07 (d, 1H, J = 1.6 Hz), 8.58 (d, 1H, J = 1.6 Hz). δ_C (400 MHz $CDCl_3$) 55.48, 111.20, 121.02, 126.24, 129.36, 130.15, 131.39, 141.13, 143.15, 152.51, 156.60.

2-Amino-5-(4-methoxyphenyl)pyrazine 206

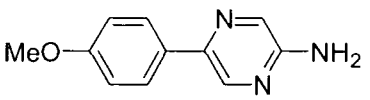

By analogy with the synthesis of **202**, 2-amino-5-bromopyrazine **189** (1.00 g, 5.74 mmol), 4-methoxybenzeneboronic acid **205** (1.05 g, 6.89 mmol), THF (30 cm^3), $Pd(PPh_3)_4$ (398 mg) and Na_2CO_3 (1M, degassed, 21.0 cm^3). Followed by column chromatography (eluent DCM-diethyl ether, 1:1 v/v) gave a yellow solid which was recrystallised from toluene / petroleum ether (bp 100-120 °C) mixture to yield compound **206** as pale yellow crystals (0.27 g, 23%), mp 98-100 °C. Anal. calcd. for $C_{11}H_{11}N_3O$: C, 65.66; H, 5.51, N, 20.88. Found: C, 65.64; H, 5.50; N, 21.02%. *m/z* (GCMS) 201.0. δ_H (400 MHz $CDCl_3$) 3.85 (s, 3H), 6.98 (d, 2H, J = 8.8 Hz), 7.80 (d, 2H, J = 8.8 Hz), 8.03 (d, 1H, J = 1.6 Hz), 8.39 (d, 1H, J = 1.6 Hz). δ_C (400 MHz $CDCl_3$) 55.32, 114.21, 126.88, 129.66, 131.39, 138.41, 142.94, 152.60, 159.78.

2,5-Dimethoxy-1,4-benzenediboronic acid 207

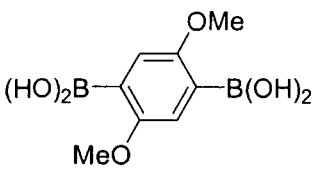

To a solution of 1,4-dibromo-2,5-dimethoxybenzene (4.34 g, 14.8 mmol) in dry THF (150 cm^3) was added *n*BuLi solution in hexane (1.6 M, 20.2 cm^3, 32.32 mmol) dropwise at –78 °C under argon. The mixture was stirred and allowed to warm to 20 °C over 9 h to give a clear light yellow solution. Triisopropylborate (14.8 cm^3) was syringed in quickly at –78 °C and the mixture was stirred for 12 h with a cooling bath allowing the temperature to rise gradually to 20 °C. HCl solution (5%) (30 cm^3) was syringed in and the reaction stirred at 20 °C for 0.5 h. THF was evaporated and the white solid was isolated and washed with a large volume of water. The solid was recrystallised from acetonitrile / water mixture to yield **207** as white needles (84 mg, 25%), mp 268 °C (Lit.[61] > 250 °C). δ_H (300 MHz DMSO-d_6) 3.72 (s, 6H), 7.10 (s, 2H), 7.75 (s, 4H). δ_C (300 MHz DMSO-d_6) 55.84, 116.86, 124.56, 157.47.

1,4-Dimethoxy-2,5-bis[2-(5-aminopyrazyl)]benzene 208

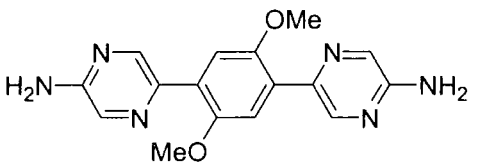

By analogy with the synthesis of **202**, 2-amino-5-bromopyrazine **189** (0.42 g, 2.44 mmol), 2,5-dimethoxy-1,4-benzenediboronic acid **207** (0.25 g, 1.11 mmol), THF (30 cm^3), $Pd(PPh_3)_4$ (128 mg) and Na_2CO_3 (1 M, degassed, 7.0 cm^3). The crude reaction residue was recrystallised from DMF / ethanol to yield **208** as brown crystals (0.20 g, 56%), mp >300 °C. *m/z* (EI) 324 (M^+, 100%). HRMS (EI) (M^+) 324.1338 (calcd, for $C_{16}H_{16}N_6O_2$ 324.1334). δ_H (400 MHz DMSO-d_6) 3.81 (s, 6H), 6.51 (s, 4H), 7.49 (s, 2H), 7.98 (d, 2H, J = 1.6 Hz), 8.54 (d, 2H, J = 1.6 Hz). δ_C (400 MHz DMSO-d_6) 56.71, 113.20, 126.42, 132.11, 137.81, 143.47, 151.13, 154.99.

2,7-Bis[2-(5-aminopyrazyl)]-9,9-dihexylfluorene 209

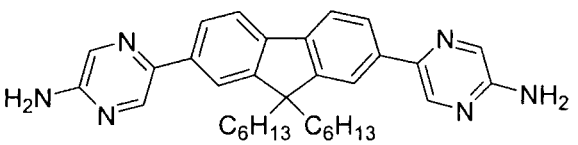

By analogy with the synthesis of **202**, 2-amino-5-bromopyrazine **189** (0.50 g, 2.88 mmol), THF (30 cm^3), $Pd(PPh_3)_4$ (55.5 mg), 9,9-dihexylfluorene-2,7-diboronic acid **169** (0.50 g, 0.50 mmol) and Na_2CO_3 (1 M, aqueous, degassed, 5.0 cm^3). Followed by column chromatography [eluent ethyl acetate-petroleum ether (bp 40-60 °C) 1:1 v/v] gave a golden solid which was recrystallised from toluene / hexane mixture to yield compound **209** as pale golden crystals (0.32 g, 51%), mp 161.5-163.5 °C. *m/z* (ES+) 521.3, 543.3 (M^+, Na). HRMS (ES+) (M^+) 521.3387 (calcd. for $C_{33}H_{41}N_6$ 521.3393). δ_H (400 MHz $CDCl_3$) 0.71 (m, 10H), 1.04 (m, 12H), 2.06 (m, 4H, $\underline{CH_2}$-C(Ar)$_2$-CH_2), 4.68 (s, 4H), 7.80 (d, 2H, J = 8.8 Hz), 7.87 (m, 4H), 8.10 (d, 2H, J = 1.6 Hz), 8.53 (d, 2H, J = 1.2 Hz). δ_C (400 MHz $CDCl_3$) 13.95, 22.55, 23.77, 29.67, 31.46, 40.40, 55.41, 119.90, 120.15, 124.46, 131.43, 135.87, 139.22, 140.84, 143.37, 151.86, 152.91.

1,4-Dimethoxy-2,5-bis(2-pyrazyl)benzene 210

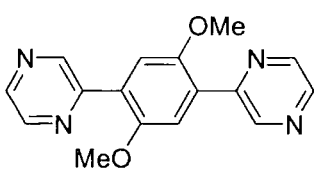

By analogy with the synthesis of **202**, iodopyrazine (0.62 g, 3.00 mmol), 2,5-dimethoxy-1,4-benzenediboronic acid **207** (0.23 g, 1.00 mmol), THF (30 cm^3), $Pd(PPh_3)_4$ (116 mg) and Na_2CO_3 (1 M, degassed, 6.0 cm^3). The product was isolated as white needles by filtration of the reaction

mother liquor and washed with a large amount of water to yield **210** (0.35 g, 84%), mp 235-237 °C. *m/z* (EI) 294 (M^+, 74%), 277 (M^+, 100%). HRMS (EI) (M^+) 294.1110 (calcd, for $C_{16}H_{14}N_4O_2$ 294.1116). δ_H (400 MHz DMSO-d_6) 3.88 (s, 6H), 7.61 (s, 2H), 8.59 (d, 2H, J = 2.4 Hz), 8.77 (dd, 2H, J = 2.4, 1.6 Hz), 9.18 (d, 2H, J = 2.4 Hz). δ_C (400 MHz DMSO-d_6) 56.27, 114.43, 127.06, 142.59, 143.95, 145.26, 149.94, 151.08.

1,4-Dimethoxy-2,5-bis(2-pyrimidyl)benzene 211

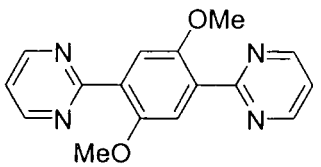

By analogy with the synthesis of **202**, 2-bromopyrimidine **170** (0.48 g, 3.00 mmol), 2,5-dimethoxy-1,4-benzenediboronic acid **207** (0.23 g, 1.00 mmol), THF (30 cm^3), $Pd(PPh_3)_4$ (116 mg) and Na_2CO_3 (1M, degassed, 6.0 cm^3) and preparative tlc (eluent ethyl acetate-acetonitrile 1:1 v/v) gave **211** as a pale green solid (56 mg, 19 %), mp 232-234 °C. *m/z* (EI) 294 (M^+, 100%). HRMS (EI) (M^+) 294.1117 (calcd. for $C_{16}H_{14}N_4O_2$ 294.1116). δ_H (400 MHz DMSO-d_6) 3.73 (s, 6H), 7.33 (s, 2H), 7.46 (t, 2H, J = 4.8 Hz), 8.90 (d, 4H, J = 4.8 Hz). δ_C (400 MHz DMSO-d_6) 57.10, 116.21, 120.30, 130.73, 151.66, 157.97, 165.18.

1,4-Dimethoxy-2,5-bis[2-(5-bromopyridyl)]benzene 212

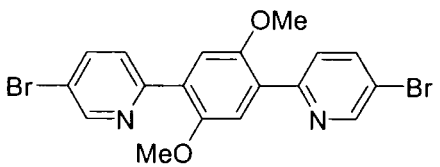

By analogy with the synthesis of **202**, 2,5-dibromopyridine (0.94 g, 3.98 mmol), 2,5-dimethoxy-1,4-benzenediboronic acid **207** (0.30 g, 1.33 mmol), THF (30 cm^3), $Pd(PPh_3)_4$ (154 mg), Na_2CO_3 (1 M, degassed, 8.0 cm^3). Followed by column chromatography (eluent DCM-hexane 1:1 v/v) gave a yellow solid which was recrystallised from a toluene / hexane mixture to yield **212** as a yellow solid (0.13 g, 22%), mp 192-194 °C. *m/z* (EI) 448 (M^+, 50%, ^{79}Br, ^{79}Br), 450 (M^+, 100%, ^{79}Br, ^{81}Br), 452 (M^+, 49%, ^{81}Br, ^{81}Br). HRMS (EI) (M^+) 447.9421 (calcd. for $C_{16}H_{14}Br_2N_4O_2$ 447.9422). δ_H (400 MHz $CDCl_3$) 3.91 (s, 6H), 7.57 (s, 2H), 7.83 (dd, 2H, J = 8.4, 2.4 Hz), 7.92 (dd, 2H, J = 8.4, 0.8 Hz), 8.75 (dd, 2H, J = 2.4, 0.8 Hz). δ_C (500 MHz $CDCl_3$) 56.24, 114.21, 119.11, 126.47, 128.78, 138.37, 150.35, 151.36, 153.54.

1,4-Dimethoxy-2,5-bis[2-(5-bromopyrimidyl)]benzene 213

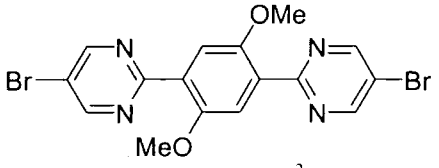

By analogy with the synthesis of **202**, 2,5-dibromopyrimidine **163** (0.47 g, 2.00 mmol), 2,5-dimethoxy-1,4-benzenediboronic acid **207** (0.15 g, 0.70 mmol), THF (30 cm^3), $Pd(PPh_3)_4$ (70 mg) and Na_2CO_3 (1 M, degassed, 4.0 cm^3)and chromatography [eluent DCM-Petroleum ether (bp 40-60) 9:1 v/v] gave **213** as a white solid (75 mg, 25%), mp 153-154 °C. *m/z* (EI) 450 (M^+, 44%, ^{79}Br, ^{79}Br), 452 (M^+, 84%, ^{79}Br, ^{81}Br), 454 (M^+, 40%, ^{81}Br, ^{81}Br). HRMS (EI) (M^+) 449.9333 (calcd. for $C_{16}H_{12}Br_2N_4O_2$ 449.9326). δ_H (500 MHz $CDCl_3$) 3.92 (s, 6H), 7.53 (s, 2H), 8.92 (s, 4H). δ_C (500 MHz $CDCl_3$) 57.26, 116.62, 118.63, 129.65, 152.26, 157.90, 163.34.

2,7-Bis(2-pyrazyl)-9,9-dihexylfluorene 214

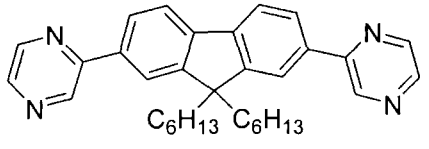

By analogy with the synthesis of **202**, iodopyrazine (0.37 g, 0.60 mmol), 9,9-dihexylfluorene-2,7-diboronic acid **169** (0.25g, 0.60 mmol), THF (30 cm^3), $Pd(PPh_3)_4$ (68 mg) and Na_2CO_3 (1 M, degassed, 3.0 cm^3). Followed by column chromatography (eluent DCM-ethyl acetate, 9:1 v/v) gave **214** as a yellow oil (0.35 g, 40%). *m/z* (EI) 490 (M^+, 79%), 405 (M^+, 100%). HRMS (EI) (M^+) 490.3076 (cald, for $C_{33}H_{38}N_4$ 490.3096). δ_H (500 MHz $CDCl_3$) 0.71 (m, 10H), 1.05 (m, 12H), 2.04 (m, 4H, $\underline{CH_2}$-C(Ar)$_2$-CH_2), 7.88 (d, 2H, J = 7.5 Hz), 8.05 (m, 4H), 8.52 (d, 2H, J = 2.5 Hz), 8.68 (dd, 2H, J = 2.5, 1.5 Hz), 9.12 (d, 2H, J = 1.5 Hz). δ_C (500 MHz $CDCl_3$) 14.21, 22.80, 24.08, 29.90, 31.73, 40.60, 55.94, 121.00, 121.59, 126.28, 135.86, 142.46, 142.53, 142.86, 144.44, 152.56, 153.34.

2,5-Dimethylpyrazine-*N,N*-Dioxide 216

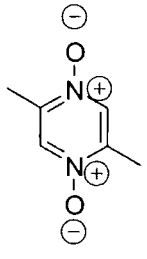

2,5-Dimethylpyrazine **215** (2.65 g, 24.5 mmol) was dissolved in acetic acid (15 cm^3). Hydrogen peroxide (35%) (25 cm^3) was added and the solution heated at 80 °C for 24 h. Solvent was removed *in vacuo* to give a white solid. Methanol (25 cm^3) was added and the residue was heated vigorously for 2 h, then cooled to 20 °C and the white solids were isolated by suction filtration and washed with a large volume of methanol. The white solids were then recrystallised from an acetic acid /

methanol mixture to yield **216** as white crystals (1.72 g, 50%), mp 283-284 °C (lit.[138] 280 °C). *m/z* (EI) 140 (M^+, 100%). δ_H (500 MHz, D_2O) 2.40 (s, 6H), 8.46 (s, 2H). δ_C (500 MHz, D_2O) 14.06, 136.42, 146.29.

2,5-Dichloro-3,6-dimethylpyrazine 217

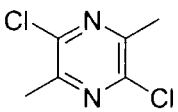

Alanine anhydride **218** (20.0 g, 0.14 moles) was added to $POCl_3$ (60 cm^3) and the mixture was heated under reflux for 24 h. The excess $POCl_3$ was removed by vacuum distillation. With external cooling, water (75 cm^3) was added slowly to the white residue, which was extracted into DCM (3 x 50 cm^3). The organic layer was dried ($MgSO_4$) then concentrated under reduced pressure and purified by chromatography (eluent DCM) to give **217** as a white solid (4.12 g, 17%), mp 72-73 °C (lit.[138] 70-72 °C). *m/z* (GCMS) (EI) 175.9 (M^+ ^{35}Cl), 177.8 (M^+ ^{35}Cl, ^{37}Cl), 179.9 (M^+ ^{37}Cl). δ_H (400 MHz, $CDCl_3$) 2.58 (s, 6H). δ_C (400 MHz, $CDCl_3$) 21.32, 145.59, 149.84.

2,5-Dibromo-3,6-dimethylpyrazine 219

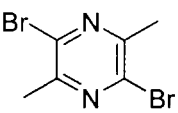

2,5-Dichloro-3,6-dimethylpyrazine **217** (4.60 g, 25.80 mmol) was added to PBr_3 (23 cm^3) and the mixture was heated under reflux for 4 days. The excess PBr_3 was removed by vacuum distillation. With external cooling, water (75 cm^3) was added slowly to the white / yellow residue, which was extracted into DCM (3 x 50 cm^3). The organic layer was dried ($MgSO_4$) then concentrated under reduced pressure and purified by chromatography (eluent diethyl ether) to give **219** as a yellow solid (3.22 g, 47%), mp 79-81 °C (lit.[140] 80-81 °C). *m/z* (GCMS) (EI) 263.8 (M^+ ^{79}Br), 265.8 (M^+ ^{79}Br, ^{81}Br), 267.7 (M^+ ^{79}Br, ^{81}Br), 268.9 (M^+ ^{81}Br). δ_H (400 MHz, $CDCl_3$) 2.62 (s, 6H). δ_C (400 MHz, $CDCl_3$) 22.96, 138.77, 152.41.

2,5-Diphenyl-3,6-dimethylpyrazine 221

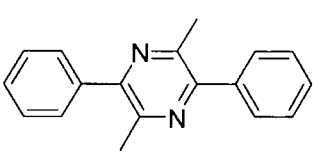

By analogy with the synthesis of **202**, 2,5-dibromo-3,6-dimethylpyrazine **219** (0.10 g, 0.38 mmol), benzeneboronic acid **164** (0.18 g, 1.50 mmol), THF (30 cm^3), $Pd(PPh_3)_4$ (173 mg) and Na_2CO_3 (1 M, degassed, 7.5 cm^3). Followed by column chromatography (eluent DCM) gave

221 as a white solid (69 mg, 70%), mp 178-180 °C. *m/z* (EI) 260 (M^+ 100%). δ_H (400 MHz, $CDCl_3$) 2.65 (s, 6H), 7.48 (m, 6H), 7.63 (m, 4H). δ_C (400 MHz, $CDCl_3$) 22.62, 128.44, 128.56, 129.02, 138.66, 147.82, 151.04.

2,5-Bis(2-methoxyphenyl)-3,6-dimethylpyrazine 222

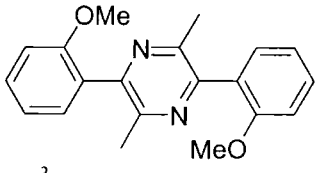

By analogy with the synthesis of **202**, 2,5-dibromo-3,6-dimethylpyrazine **219** (0.10 g, 0.38 mmol), 2-methoxybenzeneboronic acid **203** (0.14 g, 0.94 mmol), THF (30 cm^3), $Pd(PPh_3)_4$ (109 mg) and Na_2CO_3 (1 M, degassed, 6.0 cm^3) and chromatography (eluent DCM) gave **222** as a yellow solid (92 mg, 76%), mp 232-236 °C . *m/z* (EI) 320 (M^+, 100%). HRMS (EI) (M^+) 320.1524 (calcd. $C_{20}H_{20}N_2O_2$ 320.1524). δ_H (500 MHz, $CDCl_3$) 2.42 (s, 6H), 3.83 (s, 6H), 7.00 (d, 2H, J = 8.5 Hz), 7.10 (t, 2H, J = 7.0 Hz), 7.38 (d, 2H, J = 7.0 Hz), 7.42 (t, 2H, J = 7.0 Hz). δ_C (500 MHz, $CDCl_3$) 21.51, 55.32, 110.76, 120.95, 128.22, 130.00, 130.89, 149.43, 149.48, 156.67.

2,5-Bis(2-methoxyphenyl)-3,6-dimethylpyrazinium bis(tetrafluoroborate) salt 223

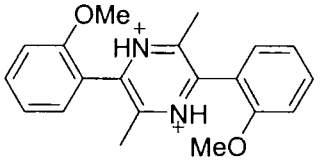

$2\ BF_4^-$

To a solution of 2,5-bis(2-methoxyphenyl)-3,6-dimethylpyrazine **222** (10 mg) in chloroform (10 cm^3) was added a few drops of tetrafluoroboric acid. After 1 h at 20 °C the solvent was evaporated and the residue was recrystallised from acetonitrile. After a few days crystals of salt **223** were collected. Anal. cald. for $C_{20}H_{22}B_2F_8N_2O_2$: C, 48.43; H, 4.47; N, 5.65. Found C, 48.30; H, 4.22; N, 5.85%.

2-Bromo-5-(*tert*-butylphenyl)-3,6-dimethylpyrazine 224

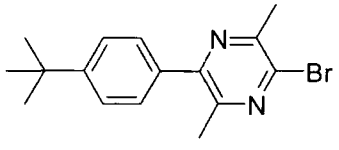

By analogy with the synthesis of **202**, 2,5-dibromo-3,6-dimethylpyrazine **219** (0.90 g, 3.37 mmol), 4-*tert*-butylbenzeneboronic acid **220** (0.50 g, 2.81 mmol), THF (30 cm^3), $Pd(PPh_3)_4$ (325 mg) and Na_2CO_3 (1 M, degassed, 8.5 cm^3) and chromatography (eluent DCM hexane, 1:1 v/v) gave compound **224** as a white solid (0.35 g, 39%), mp 69 °C. *m/z* (EI) 319 (M^+, ^{81}Br 44%), 317 (M^+, ^{79}Br 44%). HRMS (EI) (M^+) 318.0726 (calcd.

$C_{16}H_{19}BrN_2$ 318.0731). δ_H (500 MHz, $CDCl_3$) 1.35 (s, 9H), 2.59 (s, 3H), 2.68 (s, 3H), 7.49 (s, 4H). δ_C (500 MHz, $CDCl_3$) 22.70, 23.38, 31.24, 34.72, 125.50, 128.58, 134.59, 138.40, 149.22, 150.94, 151.54, 152.03.

1,4-Dimethoxy-2,5-bis{2(5-*tert*-butylphenyl-3,6-dimethylpyrazinyl)benzene} 225

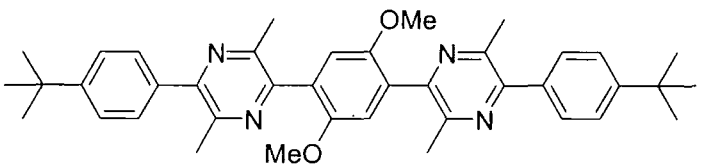

By analogy with the synthesis of **202**, 2-bromo-5-(*tert*-butylphenyl)-3,6-dimethylpyrazine **224** (0.57 g, 1.78 mmol), 2,5-dimethoxy-1,4-benzenediboronic acid **207** (0.17 g, 0.75 mmol), THF (30 cm^3), $Pd(PPh_3)_4$ (77 mg) and Na_2CO_3 (1 M, degassed, 4.5 cm^3) and chromatography (eluent DCM-ethyl acetate, 9.5 : 0.5 v/v) gave compound **225** as a white solid (0.18 g, 16%), mp 348-350 °C. Anal. calcd. for $C_{40}H_{46}N_4O_2$: C, 78.14; H, 7.54, N, 9.11. Found: C, 77.98; H, 7.48; N, 9.01%. *m/z* (EI) 614 (M^+, 100%). δ_H (500 MHz, $CDCl_3$) 1.37 (s, 18H), 2.49 (s, 6H), 2.69 (s, 6H), 3.83 (s, 6H), 7.04 (s, 2H), 7.58 (d, 4H J = 8.5 Hz), 7.59 (d, 4H J = 8.0 Hz). δ_C (500 MHz, $CDCl_3$) 21.70, 22.68, 31.31, 34.71, 55.94, 113.82, 125.41,128.74, 129.07, 135.92, 147.50, 148.61, 150.07, 150.86, 151.48, 151.55.

2-Bromo-5-(2-methoxyphenyl)-3,6-dimethylpyrazine 226

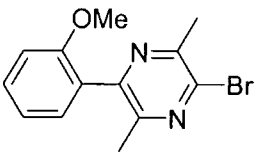

By analogy with the synthesis of **202**, 2,5-dibromo-3,6-dimethylpyrazine **219** (1.05 g, 4.00 mmol), 2-methoxybenzeneboronic acid **203** (0.5 g, 3.30 mmol), THF (30 cm^3), $Pd(PPh_3)_4$ (190 mg) and Na_2CO_3 (1 M, degassed, 10.0 cm^3) and chromatography (eluent DCM-petroleum ether (bp 60-80 °C) 9.0 : 1.0 v/v) gave compound **226** as a yellow solid (0.6 g, 52 %), mp 134-135 °C. Anal. calcd. for $C_{13}H_{13}BrN_2O$: C, 53.26; H, 4.47, N, 9.56. Found: C, 53.80; H, 4.48; N, 9.32%. *m/z* (EI) 292 (M^+, ^{79}Br 67%), 294 (M^+, ^{81}Br 63%). δ_H (400 MHz, $CDCl_3$) 2.28 (s, 3H), 2.60 (s, 3H), 3.72 (s, 3H), 6.90 (d, 1H, J = 8.0 Hz), 7.00 (t, 1H, J = 8.0 Hz), 7.21 (d, 1H, J = 8.0 Hz), 7.35 (t, 1H, J = 8.0 Hz). δ_C (400 MHz, $CDCl_3$) 21.12, 23.39, 55.34, 110.89, 121.02, 126.83, 130.47, 130.54, 139.02, 149.93, 150.64, 151.35, 156.47.

2,5-Bis(6-methoxypyridin-3-yl)-3,6-dimethylpyrazine 229

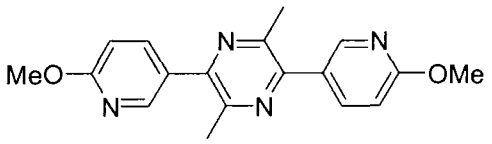

By analogy with the synthesis of **202**, 2,5-dibromo-3,6-dimethylpyrazine **219** (0.10 g, 0.38 mmol), 2-methoxy-5-pyridylboronic acid[141] **228** (0.14 g, 0.90 mmol), THF (30 cm^3), $Pd(PPh_3)_4$ (103 mg) and Na_2CO_3 (1M, degassed, 5.50 cm^3) and chromatography (eluent initially DCM followed by DCM-ethyl acetate 9.0 : 1.0 v/v) gave compound **229** off-white needles (88 mg, 73%), mp 179-181 °C. *m/z* (EI) 321 (M^+, 100%). HRMS (EI) (M^+) 322.1429 (calcd. for $C_{18}H_{18}N_4O_2$ 322.1429). δ_H (500 MHz $CDCl_3$) 2.66 (s, 6H), 4.01 (s, 6H), 6.88 (d, 2H, J = 9.0 Hz), 7.91 (dd, 2H, J = 2.5, 8.5 Hz), 8.47 (d, 2H, J = 2.0 Hz). δ_C (500 MHz $CDCl_3$) 22.72, 53.74, 110.80, 127.60, 139.40, 147.26, 148.05, 148.17, 164.15.

Protonation of compound 229. To a solution of compound **229** in methanol was added tetrafluoroboric acid (50% aqueous) dissolved in ether dropwise at 20 °C. The white precipitate which formed was collected and dissolved in DMSO-d_6. δ_H (400 MHz DMSO-d_6) 2.59 (s, 6H), 3.93 (s, 6H), 6.99 (d, 2H, J = 8.4 Hz), 7.18 (s, br, 2H), 8.07 (dd, 2H, J = 2.8, 2.4 Hz), 8.50 (d, 2H, J = 2.6 Hz). δ_C (400 MHz DMSO-d_6) 22.40, 53.75, 110.31, 127.45, 140.26, 146.99, 147.49, 147.86, 163.51.

5.4 Experimental Procedures of Chapter 4

5.4.1 Sonogashira Cross-Coupling: General Method

The alkyne, the halide, the catalyst and CuI (10 mol% relative to the alkyne) were added sequentially to a degassed solution of THF/Et_3N [50 cm^3 (3:2 v/v)] and the mixture was stirred at 20 °C overnight under a blanket of argon until tlc monitoring showed that the reaction was complete. Solvent was evaporated and the residue was dissolved in chloroform. The organic layer was purified by chromatography on a silica column.

Attempted Synthesis of 2-(4-*tert*-Butylphenyl)-5-{4-[2-(2-pyrimidyl)ethynyl]phenyl}-1,3,4-oxadiazole

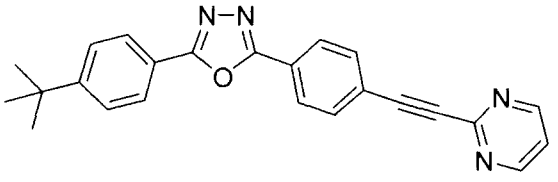

Synthesis in accordance with the general Sonogashira cross-coupling method. 2-Bromopyrimidine **170** (0.32 g, 1.98 mmol), **230** (0.20 g, 0.66 mmol), $Pd(PPh_3)_2Cl_2$ (46 mg), CuI (12 mg) and chromatography (eluent DCM-diethyl ether, 9.5:0.5 v/v) gave a white solid (0.15 g) which was identified as the self coupling product **231**.

Bis-{4-[2-(4-*tert*-butylphenyl)-1,3,4-oxadiazol-5-yl]-phenyl}-butadiyne 231

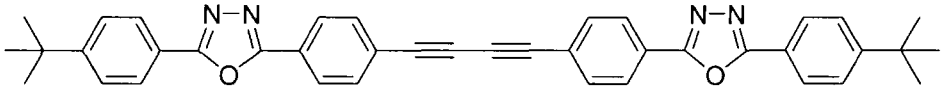

231 (0.15 g, 37%) mp 307-309 °C, (lit[168] 308-309 °C). *m/z* (EI) 602 (M^+ 100%). δ_H (300 MHz $CDCl_3$) 1.37 (s, 9H), 7.54 (d, 4H, J = 8.7 Hz), 7.67 (d, 4H, J = 8.7 Hz), 8.04 (d, 4H, J = 8.7 Hz), 8.11 (d, 4H, J = 8.4 Hz). δ_C (300 MHz $CDCl_3$) 31.10, 35.12, 74.69, 81.91, 120.80, 124.42, 124.74, 126.09, 126.79, 126.81, 133.11, 155.58, 163.61, 164.94.

2-(4-*tert*-Butylphenyl)-5-{4-[2-(2-pyridyl)ethynyl]phenyl}-1,3,4-oxadiazole 232a

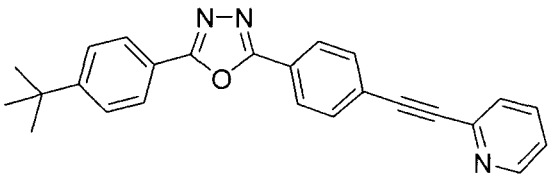

2-Iodopyridine (0.22 g, 1.05 mmol), **230** (0.32 g, 1.05 mmol), $Pd(PPh_3)_2Cl_2$ (74 mg), CuI (20 mg) and chromatography (eluent DCM-diethyl ether, 9.5:0.5 v/v) gave a yellow solid which was recrystallized from petroleum ether (bp 100-120 °C) yielding **232a** as a yellow solid (0.30 g, 73%), mp 180-181 °C. *m/z* (ES+) 380.3. HRMS (ES+) (M^+) 380.1790 (calcd. for $C_{25}H_{21}N_3O$ 380.1763). δ_H (400 MHz acetone-d_6) 1.38 (s, 9H), 7.42 (ddd, 1H, J = 7.6, 4.8, 1.2 Hz), 7.69 (m, 3H), 7.86 (m, 3H), 8.12 (d, 2H, J = 8.8 Hz), 8.23 (d, 2H, J = 8.4 Hz), 8.65 (ddd, 1H, J = 4.8, 2.4, 1.6 Hz). δ_C (400 MHz acetone-d_6) 31.29, 35.64, 87.92, 92.23, 122.09, 124.37, 125.25, 126.34, 127.08, 127.53, 127.72, 128.34, 133.42, 137.29, 143.65, 151.15, 156.24, 164.51, 165.55.

2-(4-*tert*-Butylphenyl)-5-{4-[2-(3-pyridyl)ethynyl]phenyl}-1,3,4-oxadiazole 232b

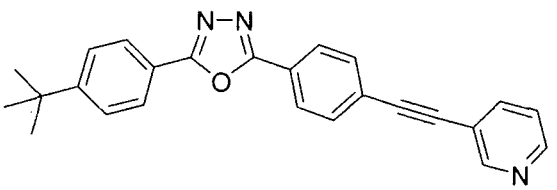

3-Iodopyridine (0.22 g, 1.05 mmol), **230** (0.32 g, 1.05 mmol), $Pd(PPh_3)_2Cl_2$ (74 mg), CuI (20 mg) and chromatography (eluent DCM-Diethyl ether, 9.5:0.5 v/v) gave a yellow solid which was recrystallized from petroleum ether (bp 100-120 °C) yielding **232b** as a yellow solid (0.23 g, 56%), mp 182-183 °C. Anal. calcd. for $C_{25}H_{21}N_3O$: C, 79.13; H; 5.58; N, 11.07. Found: C, 78.60; H; 5.56; N, 10.83%. *m/z* (EI) 379 (M^+ 100%). δ_H (500 MHz acetone-d_6) 1.38 (s, 9H) 7.46 (dd, 1H, J = 7.5, 4.5 Hz), 7.68 (d, 2H, J = 8.5 Hz), 7.82 (d, 2H, J = 8.5 Hz), 7.99 (dt, 1H, J = 8.0, 2.0 Hz), 8.11 (d, 2H, J = 8.5 Hz), 8.22 (d, 2H, J = 8.5 Hz), 8.61 (d, 1H, J = 3.5 Hz), 8.79 (s, 1H). δ_C (500 MHz acetone-d_6) 31.30, 35.64, 89.39, 92.07, 120.46, 122.10, 124.27, 125.10, 126.54, 127.08, 127.52, 127.71, 133.21, 139.26, 150.19, 152.89, 156.24, 164.51, 165.54.

2-(4-*tert*-Butylphenyl)-5-{4-[2-(4-pyridyl)ethynyl]phenyl}-1,3,4-oxadiazole 232c

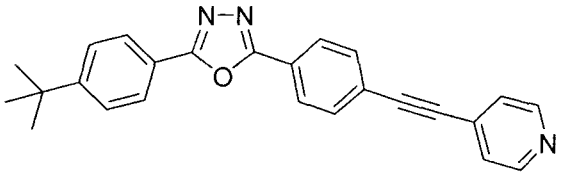

4-Iodopyridine (0.22 g, 1.05 mmol), **230** (0.32 g, 1.05 mmol), $Pd(PPh_3)_2Cl_2$ (74 mg), CuI (20 mg) and chromatography (eluent DCM-diethyl ether, 9.5:0.5 v/v) gave a yellow solid which was recystallized from petroleum ether (bp 100-120 °C) yielding **232c** as a yellow solid (0.16 g, 40%), mp 196-198 °C. Anal. calcd. for $C_{25}H_{21}N_3O$: C, 79.13; H, 5.58; N, 11.07. Found: C, 78.60; H, 5.56; N, 10.83%. *m/z* (EI) 379 (M^+ 100%). δ_H (500 MHz acetone-d_6) 1.38 (s, 9H), 7.53 (d, 2H, J = 5.0 Hz), 7.68 (d, 2H, J = 8.5 Hz), 7.84 (d, 2H, J = 8.5 Hz), 8.12 (d, 2H, J = 8.0 Hz), 8.24 (d, 2H, J = 8.5 Hz), 8.66 (s, br, 2H). δ_C (500 MHz acetone-d_6) 31.30, 35.64, 89.76, 93.03, 122.08, 125.49, 126.02, 126.22, 127.09, 127.54, 127.75, 131.11, 133.44, 150.98, 156.28, 164.47, 165.59.

2-(4-*tert*-Butylphenyl)-5-{4-[2-(2-pyrazyl)ethynyl]phenyl}-1,3,4-oxadiazole 232d

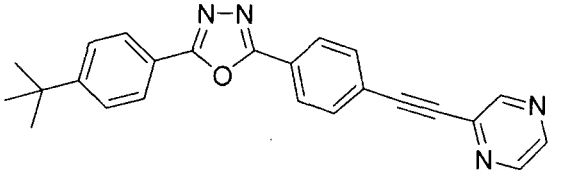

Iodopyrazine (0.22 g, 1.05 mmol), **230** (0.32 g, 1.05 mmol), $Pd(PPh_3)_2Cl_2$ (74 mg), CuI (20 mg) and chromatography (eluent DCM-diethyl ether, 9.5:0.5 v/v) gave a yellow solid which was recystallized from Petroleum Ether (100—120 °C) yielding **232d** as thin yellow needles (0.28 g, 69%), mp 190-192 °C. Anal. calcd. for $C_{24}H_{20}N_4O$: C, 75.77; H, 5.30; N, 14.73. Found: C, 75.65; H, 5.34; N, 14.60%. *m/z* (ES+) 381.3. δ_H (500 MHz $CDCl_3$) 1.37 (s, 9H), 7.55 (d, 2H, J = 8.5 Hz), 7.77 (d, 2H, J = 8.5 Hz), 8.06 (d, 2H, J = 8.5 Hz), 8.17 (d, 2H, J = 8.5 Hz), 8.53 (d, 1H, J = 3.0 Hz), 8.16 (dd, 1H, J = 2.5, 1.5 Hz), 8.80 (d, 1H, J = 1.5 Hz). δ_C (500 MHz $CDCl_3$) 31.09, 35.11, 88.15, 92.05, 120.82, 124.65, 124.69, 126.11, 126.83, 126.87, 132.74, 139.88, 143.24, 144.59, 147.85, 155.59, 163.66, 164.98.

2-(4-*tert*-Butylphenyl)-5-{4-[2-(5-bromo-2-pyrimidine)ethynyl]phenyl}-1,3,4-oxadiazole 232e

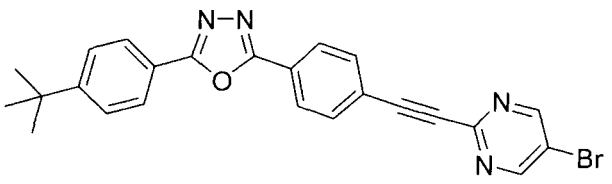

2-Iodo-5-bromopyrimidine (0.32 g, 1.05 mmol), **230** (0.32 g, 1.05 mmol), $Pd(PPh_3)_2Cl_2$ (74 mg), CuI (20 mg) and chromatography (eluent DCM-diethyl ether, 9.5:0.5 v/v) gave a pale yellow solid which was recystallized from chlorobenzene to yield **232e** as a white solid (0.35 g, 72%), mp 268-270 °C. *m/z* (EI) 458 (M^+ ^{79}Br, 43%), 459 (M^+ 100%), 460 (M^+ ^{81}Br, 42%). HRMS (EI) (M^+) 458.0730 (calcd. for $C_{24}H_{19}BrN_4O$ 458.0742). δ_H (400 MHz $CDCl_3$) 1.37 (s, 9H), 7.55 (d, 2H, J = 8.4 Hz), 7.81 (d, 2H, J = 8.4 Hz), 8.06 (d, 2H, J = 8.8 Hz), 8.16 (d, 2H, J = 8.8 Hz), 8.83 (s, 2H). δ_C (400 MHz $CDCl_3$) 31.10, 35.12, 87.96, 89.36, 109.75, 119.48, 120.82, 124.25, 124.96, 126.13, 126.86, 133.18, 150.73, 155.18, 164.64, 165.01.

2-(4-*tert*-Butylphenyl)-5-{4-[2-(3-thienyl)ethynyl]phenyl}-1,3,4-oxadiazole 232g

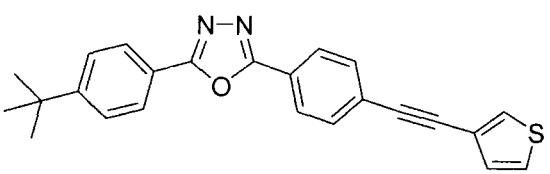

3-Iodothiophene (0.22 g, 1.05 mmol), **230** (0.32 g, 1.05 mmol), $Pd(PPh_3)_2Cl_2$ (74 mg), CuI (20 mg) and chromatography (eluent DCM-diethyl ether, 9.8:0.2 v/v) gave a yellow solid which was recystallized from ethanol yielding **232g** as off white plates (0.16 g, 40%), mp 169-170 °C. *m/z* (EI) 384 (M^+ 100%). HRMS (EI) (M^+) 384.1299 (calcd. for $C_{24}H_{20}N_2OS$ 384.1296). δ_H (500 MHz acetone-d_6) 1.39 (s, 9H), 7.30 (dd, 1H, J = 5.0, 1.0 Hz), 7.60 (dd, 1H, J = 5.0, 3.0 Hz), 7.68 (d, 2H, J = 8.5 Hz), 7.76 (d, 2H, J = 8.5 Hz), 7.84 (dd, 1H, J = 3.0, 1.0 Hz), 8.12 (d, 2H, J = 8.5 Hz), 8.20 (d, 2H, J = 8.5 Hz). δ_C (500 MHz acetone-d_6) 31.29, 35.62, 88.15, 88.60, 122.11, 122.42, 124.52, 127.06, 127.24, 127.28, 127.49, 127.64, 130.51, 130.78, 132.90, 156.18,164.57, 165.44.

5-Iodothiophene-2-carboxylic acid methyl ester 233

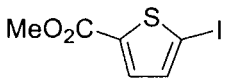

To a solution of methyl thiophene-2-carboxylate (10.0 g, 70.3 mmol) and CCl_4 (89.0 cm^3) was added I_2 (8.93 g, 35.2 mmol) and bis-(trifluoroacetoxy)iodobenzene (16.4 g, 38.2 mmol) and the mixture was stirred at 20°C overnight to give a deep purple solution. The reaction was then refluxed at 70 °C for 3 h and allowed to cool to 20 °C. Solvent was evaporated and the residue dissolved in DCM (150 cm^3), washed with saturated KI (100 cm^3) and sodium thiosulfate (100 cm^3) and dried ($MgSO_4$). The organic layer was concentrated under reduced pressure and purified by chromatography on a silica column (eluent DCM-hexane, 1:1 v/v) to give a white solid which was recrystallised from cyclohexane to yield **233** as white crystalline solid (11.0 g, 58%), mp 84-85 °C, (lit[155] mp 89 °C). *m/z* (EI) 268 (M^+ 92%), 237 (M^+ 100%). δ_H (500 MHz acetone-d_6) 3.84 (s, 3H), 7.43 (d, 1H, J = 4.0 Hz), 7.46 (d, 1H, J = 4.0 Hz). δ_C (500 MHz acetone-d_6) 52.46, 83.81, 135.38, 139.05, 139.91, 161.39.

5-Iodothiophene-2-carboxylic acid hydrazide 234

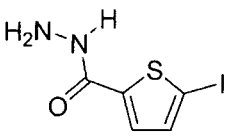

233 (10.0 g, 37.3 mmol) was dissolved in methanol (70 cm^3). $NH_2NH_2 \cdot H_2O$ (7.23 cm^3, 149.2 mmol) was added. The reaction was heated under reflux overnight. Solvent was evaporated to ca 50% of the original volume and the yellow solid was isolated by suction filtration and air-dried. The dried solid was recrystallised from methanol to yield **234** as yellow crystals (4.60 g, 46%), mp 146-147 °C. Anal. calcd. for $C_5H_5IN_2OS$: C, 22.40; H, 1.88; N, 10.45. Found: C, 22.35; H, 1.87; N, 10.49%. *m/z* (EI) 268 (M^+ 100%). δ_H (500 MHz DMSO-d_6) 4.44 (s, 2H), 7.34 (d, 1H, J = 4.0 Hz), 7.37 (d, 1H, J = 4.0 Hz), 9.77 (s, 1H). δ_C (500 MHz DMSO-d_6) 82.43, 129.09, 137.72, 144.08, 160.02.

2-(4-*tert*-Butylphenyl)-5-(5-iodothienyl)-1,3,4-oxadiazole 236

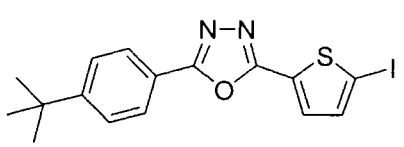

234 (7.50 g, 27.9 mmol) was dissolved in pyridine (20 cm^3) and 4-*tert*-butylbenzoyl chloride (5.50 g, 27.9 mmol) was added. The mixture was stirred at 20 °C under Ar for 1 h then refluxed for 1 h. Pyridine was removed *in vacuo*, to leave a white residue. Methanol

(100 cm^3) was added to the suspension and boiled for 2 min. The white solid **235** was separated by suction filtration and dried under vacuum overnight. This intermediate product was mixed with phosphorus oxychloride (75 cm^3) and the mixture gently refluxed for 3 h. The excess $POCl_3$ was removed by vacuum distillation. The viscous residue was crystallised from a chloroform-ethanol mixture, yielding **236** as light yellow plates (6.04 g, 53%), mp 170-172 °C. Anal. calcd. for $C_{16}H_{15}IN_2OS$: C, 46.84; H, 3.69; N, 6.83. Found: C, 46.58; H; 3.62; N, 6.73%. *m/z* (EI) 410 (M^+ 100%). δ_H (400 MHz $CDCl_3$) 1.37 (s, 9H), 7.33 (d, 1H, J = 4.0 Hz), 7.46 (d, 1H, J = 4.0 Hz), 7.52 (d, 2H, J = 8.4 Hz), 8.00 (d, 2H, J = 8.4 Hz). δ_C (400 MHz $CDCl_3$) 31.08, 35.09, 79.61, 120.60, 126.08, 126.79, 130.67, 1311.10, 137.99, 155.55, 159.44, 164.16.

2-(4-*tert*-Butylphenyl)-5-[5-(3-hydroxy-3-methylbutynyl)thienyl]-1,3,4-oxadiazole 237

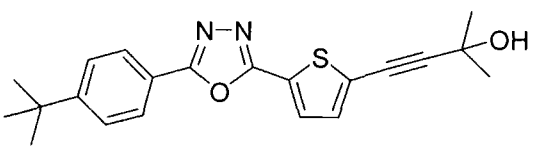

236 (5.0 g, 12.2 mmol), 2-methyl-3-butyn-2-ol (2.6 cm^3, 26.7 mmol), $Pd(PPh_3)_2Cl_2$ (0.86 g), CuI (0.23 mg) were added to a THF/Et_3N (100 cm^3, 1:1 v/v) mixture, stirred at 20 °C overnight then refluxed for 3 h, followed by chromatography (eluent DCM-diethyl ether, 9.5:0.5 v/v) to give a yellow solid which was recystallized from ethanol-H_2O mixture yielding **237** as golden needles (3.2 g, 72%), mp 161-163 °C. Anal. calcd. for $C_{21}H_{22}N_2O_2S$: C, 68.82; H, 6.05; N, 7.64. Found: C, 68.61; H; 6.00, N, 7.54%. *m/z* (EI) 366 (M^+ 100%). δ_H (500 MHz $CDCl_3$) 1.41 (s, 9H), 1.69 (s, 6H), 2.30 (s, 1H), 7.20 (d, 1H, J = 3.5 Hz), 7.53 (d, 2H, J = 8.0 Hz), 7.66 (d, 1H, J = 4.0 Hz), 8.01 (d, 2H, J = 8.0 Hz). δ_C (500 MHz $CDCl_3$) 31.08, 31.16, 65.74, 74.59, 100.59, 120.62, 125.70, 126.08, 126.80, 127.32, 129.20, 132.64, 155.55, 159.87, 164.26.

2-(4-*tert*-Butylphenyl)-5-(5-ethynylthiophene)-1,3,4-oxadiazole 238

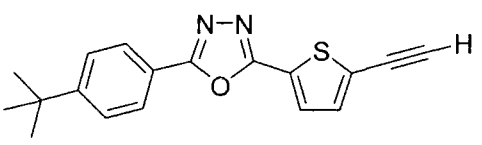

237 (2.62 g, 7.15 mmol) was dissolved in dry toluene (40 cm^3). Sodium hydroxide powder (freshly ground from pellets) (0.34 g) was added and the mixture was stirred in an oil bath at 130 °C, under Ar, for 40 min, until the reaction was complete (tlc monitoring). Toluene was removed *in vacuo* and the residue dissolved in DCM (15 cm^3), followed by chromatography (eluent DCM-diethyl ether, 9.8:0.2 v/v) to give a pale yellow

solid, which was recystallized from ethanol-H_2O mixture yielding **238** as golden needles (1.54 g, 72%), mp 165-166 °C. Anal. calcd. for $C_{18}H_{16}N_2OS$: C, 70.10; H, 5.23; N, 9.08. Found: C, 69.93; H, 5.22; N, 8.93%. *m/z* (EI) 308 (M^+ 100%). δ_H (500 MHz $CDCl_3$) 1.36 (s, 9H), 3.51 (s, 1H), 7.31 (d, 1H, J = 3.5 Hz), 7.53 (d, 2H, J = 8.0 Hz), 7.67 (d, 1H, J = 3.5 Hz), 8.01 (d, 2H, J = 9.0 Hz). δ_C (500 MHz $CDCl_3$) 31.08, 35.10, 75.85, 84.30, 120.59, 126.09, 126.28, 126.41, 126.83, 129.05, 133.71, 155.60, 159.76, 164.35.

2-(4-*tert*-Butylphenyl)-5-{5-[2-(2-pyridyl)ethynyl]thienyl}-1,3,4-oxadiazole 239a

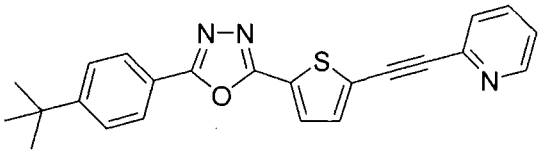

2-Iodopyridine (0.10 g, 0.50 mmol), **238** (0.15 g, 0.50 mmol), $Pd(PPh_3)_2Cl_2$ (34 mg), CuI (10 mg) and chromatography (eluent DCM-diethyl ether, 9.8:0.2 v/v) gave a orange solid which was recrystallised from a ethanol-H_2O mixture yielding **239a** as copper coloured needles (86.3 mg, 46%), mp 158-160 °C. *m/z* (EI) 385 (M^+ 100%). HRMS (EI) (M^+) 385.1247 (calcd. for $C_{23}H_{19}N_3OS$ 385.1248). δ_H (500 MHz $CDCl_3$) 1.37 (s, 9H), 7.28 (dd, 1H, J = 7.0, 5.5 Hz), 7.41 (d, 1H, J = 4.0 Hz), 7.54-7.57 (m, 3H), 7.71-7.74 (m, 2H), 8.03 (d, 2H, J = 8.5 Hz), 8.56 (s, br 1H). δ_C (500 MHz $CDCl_3$) 31.09, 35.12, 81.37, 95.20, 120.60, 123.36, 126.11, 126.65, 126.86, 127.27, 129.36, 133.91, 136.32, 142.53, 150.28, 155.61, 159.84, 164.39. δ_C (500 MHz CD_2Cl_2) 31.15, 35.36, 81.12, 95.37, 121.02, 123.76, 126.53, 126.82, 127.02, 127.29, 127.67, 129.74, 134.32, 136.60, 142.77, 150.65, 156.06, 160.18, 164.76.

2-(4-*tert*-Butylphenyl)-5-{5-[2-(3-pyridyl)ethynyl]thienyl}-1,3,4-oxadiazole 239b

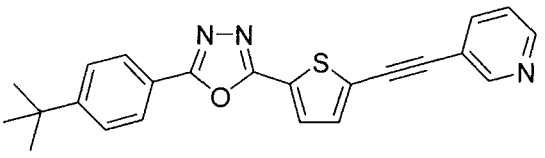

3-Iodopyridine (0.10 g, 0.50 mmol), **238** (0.15 g, 0.50 mmol), $Pd(PPh_3)_2Cl_2$ (34 mg), CuI (10 mg) and chromatography (eluent DCM-diethyl ether, 9.8:0.2 v/v) gave a orange solid **239b** (61.6 mg, 33%), mp 164-166 °C. Anal. calcd. for $C_{23}H_{19}N_3OS$: C, 71.66; H, 4.97; N, 10.90. Found: C; 71.29, H; 5.24, N, 10.31%. *m/z* (EI) 385 (M^+ 100%). δ_H (500 MHz acetone-d_6) 1.38 (s, 9H), 7.46 (dd, 1H, J = 8.0, 5.0 Hz), 7.56 (d, 1H, J = 4.0 Hz), 7.68 (d, 2H, J = 8.0 Hz), 7.90 (d, 1H, J = 4.0 Hz), 8.00 (dt, 1H, J = 8.0, 2.5 Hz), 8.07 (d, 2H, J = 8.5 Hz), 8.62 (d, 1H, J = 3.5 Hz), 8.79 (s, br 1H). δ_C (500 MHz

acetone-d_6) 31.28, 35.65, 84.93, 93.29, 119.93, 121.80, 124.31, 127.08, 1127.12, 127.53, 127.55, 130.81, 134.75, 139.18, 150.46, 152.69, 156.38, 160.50, 165.10.

2-(4-*tert*-Butylphenyl)-5-{5-[2-(4-pyridyl)ethynyl]thienyl}-1,3,4-oxadiazole 239c

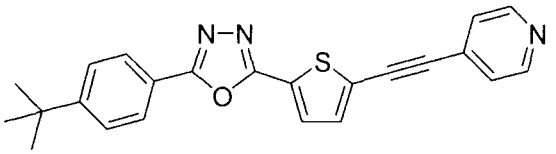

4-Iodopyridine (0.10 g, 0.50 mmol), **238** (0.15 g, 0.50 mmol), $Pd(PPh_3)_2Cl_2$ (34 mg), CuI (10 mg) and chromatography (eluent DCM-diethyl ether, 9.8:0.2 v/v) gave **239c** as an orange solid (61.8 mg, 33%), mp 198-199 °C. Anal. calcd. for $C_{23}H_{19}N_3OS$: C, 71.66; H, 4.97; N, 10.90. Found: C; 71.74, H; 4.89, N, 10.34%. *m/z* (EI) 385 (M^+ 100%). δ_H (500 MHz acetone-d_6) 1.38 (s, 9H), 7.52 (d, 2H, J = 6.0 Hz), 7.60 (d, 1H, J = 4.0 Hz), 7.67 (d, 2H, J = 8.8 Hz), 7.91 (d, 1H, J = 4.0 Hz), 8.06 (d, 2H, J = 8.8 Hz), 8.66 (d, 2H, J = 6.0 Hz). δ_H (500 MHz acetone-d_6) 31.27, 35.65, 85.93, 93.64, 121.74, 125.87, 126.42, 127.11, 127.53, 128.19, 130.49, 130.83, 135.44, 152.00, 156.39, 160.43, 165.14.

2-(4-*tert*-Butylphenyl)-5-{5-[2-(2-pyrazyl)ethynyl]thienyl}-1,3,4-oxadiazole 239d

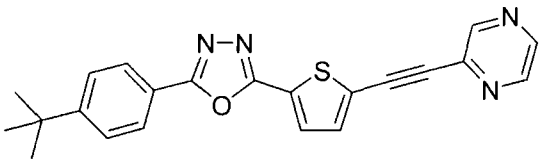

Iodopyrazine (0.10 g, 0.50 mmol), **238** (0.15 g, 0.50 mmol), $Pd(PPh_3)_2Cl_2$ (34 mg), CuI (10 mg) and chromatography (eluent DCM-diethyl ether, 9.8:0.2 v/v) gave a yellow solid which was recrystallised from ethanol to yield **239d** as fine yellow needles (0.10 g, 54%), mp 197-198 °C. Anal. calcd. for $C_{22}H_{18}N_4OS$: C, 68.37; H, 4.69; N, 14.50. Found: C; 67.90; H; 4.68; N, 14.34%. *m/z* (EI) 386 (M^+ 100%). δ_H (500 MHz $CDCl_3$) 1.37 (s, 9H), 7.47 (d, 1H, J = 4.0 Hz), 7.54 (d, 2H, J = 8.5 Hz), 7.75 (d, 1H, J = 4.0 Hz), 8.03 (d, 2H, J = 9.0 Hz), 8.54 (d, 1H, J = 2.5 Hz), 8.61 (dd, 1H, J = 2.5, 1.5 Hz), 8.79 (d, 1H, J = 1.0 Hz). δ_C (500 MHz $CDCl_3$) 31.09, 35.13, 85.31, 92.06, 120.58, 125.63, 126.14, 126.90, 127.78, 129.35, 134.58, 139.57, 143.35, 144.64, 147.69, 155.74, 159.70, 164.53.

2-(4-*tert*-Butylphenyl)-5-{5-{2-(5-bromo-2-pyrimidine)ethynyl]thienyl}-1,3,4-oxadiazole 239e

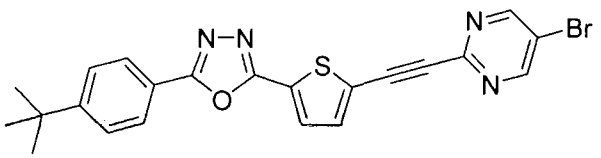

2-Iodo-5-bromopyrimidine (0.14 g, 0.50 mmol), **238** (0.15 g, 0.50 mmol), $Pd(PPh_3)_2Cl_2$ (34 mg), CuI (10 mg) and

chromatography (eluent DCM-diethyl ether, 9.8:0.2 v/v) gave a yellow solid which was recrystallised from ethanol to yield **239e** as a yellow crystalline solid (0.14 g, 65%), mp 200 °C (dec). *m/z* (EI) 464 (M^+ ^{79}Br, 49%), 465 (M^+ 100%), 466 (M^+ ^{81}Br, 49%). HRMS (EI) (M^+) 464.0317 (calcd. for $C_{22}H_{17}BrN_4OS$ 464.0306). δ_H (500 MHz $CDCl_3$) 1.37 (s, 9H), 7.41 (d, 1H, J = 4.0 Hz), 7.54 (d, 2H, J = 8.5 Hz), 7.52 (d, 1H, J = 4.0 Hz), 8.02 (d, 2H, J = 9.9 Hz), 8.83 (s, 2H). δ_C (500 MHz $CDCl_3$) 31.09, 35.13, 81.36, 93.37, 120.55, 125.75, 126.14, 126.90, 127.69, 129.27, 129.34, 135.55, 150.52, 155.75, 158.19, 159.67, 164.56.

2-(4-*tert*-Butylphenyl)-5-{5-[2-(2-thienyl)ethynyl]thienyl}-1,3,4-oxadiazole 239f

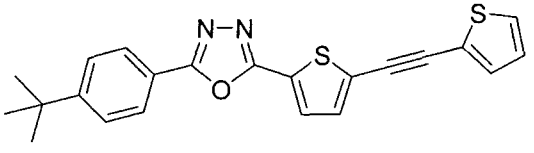

2-Iodothiophene (0.10 g, 0.50 mmol), **238** (0.15 g, 0.50 mmol), $Pd(PPh_3)_2Cl_2$ (34 mg), CuI (10 mg) and chromatography (eluent DCM-diethyl ether, 9.9:0.1 v/v) gave a pale yellow solid which was recrystallised from ethanol to yield **239f** as yellow plates (72 mg, 38%), mp 168-169 °C. Anal. calcd. for $C_{22}H_{18}N_2OS$: C, 67.66; H, 4.65; N, 7.17. Found: C; 67.62; H; 4.61; N, 7.19%. *m/z* (EI) 390 (M^+ 100%). δ_H (500 MHz acetone-d_6) 1.38 (s, 9H), 7.16, (dd, 1H, J = 5.0, 4.0 Hz), 7.46 (dd, 1H, J = 3.5, 0.5 Hz), 7.50 (d, 1H, J = 4.0 Hz), 7.67 (m, 3H), 7.87 (d, 1H, J = 4.0 Hz), 8.06 (d, 2H, J = 8.5 Hz). δ_C (500 MHz acetone-d_6) 31.28, 35.65, 85.49, 89.79, 121.81, 122.24, 127.11, 127.21, 127.38, 127.51, 128.61, 130.31, 130.83, 134.24, 134.29, 156.34, 160.51, 165.05.

2-(4-*tert*-Butylphenyl)-5-{5-[2-(3-thienyl)ethynyl]thienyl}-1,3,4-oxadiazole 239g

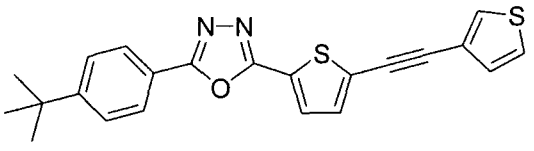

3-Iodothiophene (0.10 g, 0.50 mmol), **238** (0.15 g, 0.50 mmol), $Pd(PPh_3)_2Cl_2$ (34 mg), CuI (10 mg) and chromatography (eluent DCM-diethyl ether, 9.9:0.1 v/v) gave a pale yellow solid which was recrystallised from ethanol to yield **239g** as yellow plates (70 mg, 36%), mp 161-162 °C. Anal. calcd. For $C_{22}H_{18}N_2OS$: C, 67.66; H, 4.65; N, 7.17. Found: C; 67.54; H; 4.61; N, 7.22%. *m/z* (EI) 390 (M^+ 100%). δ_H (500 MHz acetone-d_6) 1.38 (s, 9H), 7.29 (dd, 1H, J = 5.0, 1.5 Hz), 7.46 (d, 1H, J = 4.0 Hz), 7.61 (dd, 1H, J = 5.0, 3.0 Hz), 7.67 (d, 2H, J = 8.5 Hz), 7.86 (d, 1H, J = 4.0 Hz), 7.88 (dd, 1H, J = 3.0, 1.0 Hz), 8.06 (d, 2H, J = 8.5 Hz). δ_C (500 MHz acetone-d_6) 31.28, 35.64, 81.43, 92.09,

121.75, 121.83, 126.74, 127.11, 127.49, 127.50, 127.98, 130.33, 130.79, 131.36, 133.91, 156.32, 160.55, 165.00.

2,5-Bis-{5-[4-*tert*-butylphenyl)-1,3,4-oxadiazol-5-yl]thien-2yl}-thiophene 240

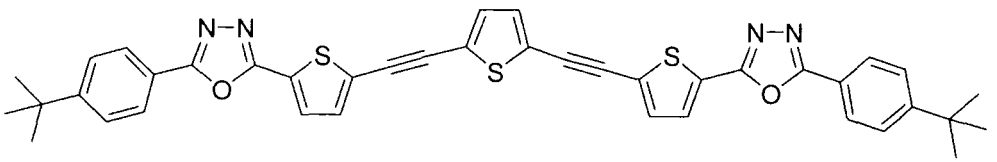

2,5-iodothiophene (0.30 g, 0.50 mmol), **238** (0.16 g, 1.00 mmol), $Pd(PPh_3)_2Cl_2$ (68 mg), CuI (18.52 mg) and chromatography (eluent DCM-diethyl ether, 9.8:0.2 v/v) gave a yellow solid which was recrystallised from toluene to yield **240** as a yellow crystalline solid (70 mg, 30%), mp decomposed at 288 °C. *m/z* (EI) 696 (M^+ 100%). HRMS (EI) (M^+) 696.1697 (calcd. for $C_{40}H_{32}N_4O_2S_3$ 696.1687). δ_H (400 MHz $CDCl_3$) 1.37 (s, 18H), 7.25 (s, 2H), 7.34 (d, 2H, J = 4.0 Hz), 7.54 (d, 4H, J = 8.8 Hz), 7.73 (d, 2H, J = 4.0 Hz), 8.02 (d, 4H, J = 8.4 Hz). δ_C (400 MHz $CDCl_3$) 31.09, 35.13, 86.95, 88.74, 120.60, 124.47, 126.12, 126.58, 126.84, 126.88, 129.43, 132.84, 133.12, 155.63, 159.82, 164.39.

2-Iodo-5-bromopyrimidine 241

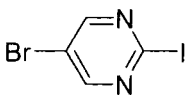

To a solution of 2-chloro-5-bromopyrimidine **162** (1.40 g, 0.72 mmol) in DCM (10 cm^3) cold hydroiodic acid (57% aq 0.6 cm^3, 4.60 mmol) was added. The solution was stirred at 0 °C for 24 h then neutralised with solid sodium carbonate. The organic layer was separated and the aqueous layer washed with DCM (3 x 50 cm^3). The combined organic washings were dried ($MgSO_4$) and the solvent evaporated. The residue was recrystallised from hexane yielding **241** as off-white flakes (0.12 g, 58%), mp 99-100 °C (lit[101] 101-102 °C). *m/z* (EI) 284 (M^+,^{79}Br, 44%), 286 (M^+,^{81}Br, 46%). δ_H (400 MHz $CDCl_3$) 8.52 (s, 2H). δ_C (400 MHz $CDCl_3$) 120.99, 125.87, 159.20.

5-Bromo-2-(phenylethynyl)-pyrimidine 243

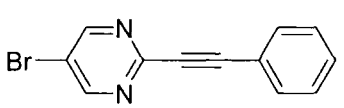

2-Iodo-5-bromopyrimidine **241** (0.2 g, 0.70 mmol), phenylacetylene **242** (0.16 g, 1.54 mmol), $Pd(PPh_3)_2Cl_2$ (49 mg), CuI (14 mg) and chromatography (eluent DCM-hexane, 8:2 v/v) gave **243** as a golden solid

(96 mg, 53%), mp 143-145 °C. Anal. calcd. for $C_{12}H_7BrN_2$: C, 55.63; H; 2.72; N, 10.81. Found: C, 55.20; H, 2.73; N, 10.30%. *m/z* (GCMS) 257.8 (M^+ ^{79}Br), 261.0 (M^+ ^{81}Br). δ_H (400 MHz acetone-d_6) 7.49-7.52 (m, 3H), 7.66-7.69 (m, 2H), 8.95 (s, 2H). δ_C (400 MHz acetone-d_6) 88.46, 120.07, 121.95, 129.70, 130.91, 133.08, 151.75, 159.06. δ_C (400 MHz C_6D_6) 88.84, 88.96, 119.10, 121.79, 128.58, 129.67, 132.75, 151.72, 157.77.

5-Phenyl-2-phenylethynyl-pyrimidine 244

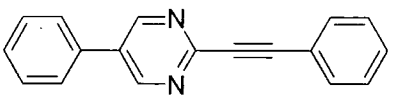

243 (0.1 g, 0.39 mmol) benzeneboronic acid **164** (0.11 g, 0.87 mmol), THF (30 cm^3), $Pd(PPh_3)_4$ (50.3 mg) and Na_2CO_3 (1 M degassed 4 cm^3) and chromatography (eluent DCM) gave **244** as a yellow solid (38 mg, 39%), mp 132-134 °C. *m/z* (GCMS) 256.1. HRMS (EI) (M^+) 256.1001 (calcd. for $C_{18}H_{12}N_2$ 256.1000). δ_H (500 MHz acetone-d_6) 7.49-7.52 (m, 4H), 7.57 (t, 2H, J = 8.0 Hz), 7.69 (dd, 2H, J = 7.5, 1.5 Hz), 7.83 (d, 2H, J= 7.0 Hz), 9.11 (s, 2H). δ_C (500 MHz acetone-d_6) 87.31, 89.27, 122.34, 127.70, 129.53, 129.80, 130.11, 130.51, 132.92, 132.96, 134.69, 152.31, 155.84.

2-[4-(2-Ethylhexyloxy)phenyl]-5-{4-[2-(5-bromo-2-pyrimidine)ethynyl]phenyl}-1,3,4-oxadiazole 245

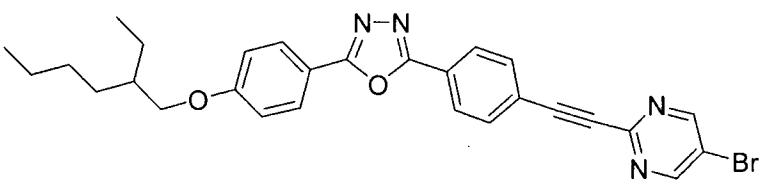

2-Iodo-5-bromopyrimidine **241** (0.30 g, 1.05 mmol), 2-[4-(2-ethylhexyloxy)phenyl]-5-(4-ethynylphenyl)-1,3,4-oxadiazole (0.39 g, 1.05 mmol), $Pd(PPh_3)_2Cl_2$ (74 mg), CuI (20 mg) and chromatography (eluent DCM-diethyl ether, 9.5:0.5 v/v) gave a white solid which was recystallized from cyclohexane yielding **245** as a white crystalline solid (0.40 g, 71%), mp 180-182 °C. *m/z* 530 (M^+ ^{79}Br, 13%), 531 (M^+ 41%), 532 (M^+ ^{81}Br, 13%). HRMS (EI) (M^+) 530.1313 (calcd. for $C_{28}H_{27}BrN_4O_2$ 530.1317). δ_H (400 MHz $CDCl_3$) 0.95 (m, 6H), 1.31-1.58 (m, 8H), 1.76 (m, 1H), 3.91 (d, 2H, J = 5.9 Hz), 7.01 (d, 2H, J = 8.8 Hz), 7.79 (d, 2H, J = 8.8 Hz), 8.05 (d, 2H, J = 8.8 Hz), 8.14 (d, 2H, J = 8.8 Hz), 8.83 (s, 2H). δ_C (400 MHz $CDCl_3$) 11.09, 14.08, 23.01, 23.78, 26.88, 29.04, 30.43, 39.27, 70.72, 88.02, 89.31, 115.03, 115.75, 124.09, 126.75, 128.73, 133.11, 133.15, 150.73, 158.16, 162.36, 163.34, 164.95.

2-[4-(2-Ethylhexyloxy)phenyl]-5-{4-[2-(5-phenyl-2-pyrimidine)ethynyl]phenyl}-1,3,4-oxadiazole 246

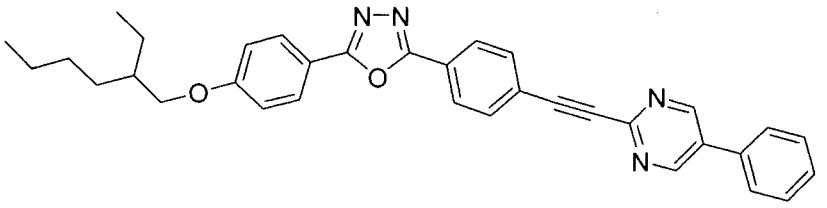

245 (0.20 g, 0.38 mmol), benzene boronic acid **164** (0.14 g, 1.12 mmol), THF (30 cm^3) $Pd(PPh_3)_4$ (50.3 mg) and Na_2CO_3 (1M degassed 4 cm^3) and chromatography (eluent DCM-diethyl ether, 9.5:0.5 v/v) gave an off white solid which was recystallized from toluene yielding **246** as a white solid (20 mg, 10%), mp 233-235 °C. *m/z* 528 (M^+ 28%). HRMS (EI) (M^+) 528.2549 (calcd. for $C_{34}H_{32}N_4O_2$ 528.2525). δ_H (500 MHz $CDCl_3$) 0.95 (m, 6H), 1.35-1.58 (m, 8H), 1.76 (m, 1H), 3.95 (d, 2H, J = 5.9 Hz), 7.01 (d, 2H, J = 8.9 Hz), 7.50 (d, 1H, J = 6.9 Hz), 7.55 (t, 2H, J = 7.9 Hz), 7.62 (d, 2H, J = 6.9 Hz), 7.83 (d, 2H, J = 7.9 Hz), 8.06 (d, 2H, J = 8.5 Hz), 8.16 (d, 2H, J = 7.9 Hz), 9.00 (s, 2H). δ_C (500 MHz $CDCl_3$) 11.10, 14.08, 23.02, 223.80, 29.05, 30.46, 39.29, 70.74, 87.10, 90.17, 115.05, 115.82, 124.52, 124.80, 126.75, 126.94, 128.74, 129.36, 129.55, 132.70, 133.16, 133.66, 151.39, 155.27, 162.36, 163.43, 164.93.

1,4-Bis-[2-phenyl-5-(4-tert-butylphenyl)-1,3,4-oxadiazole]-benzene 248a

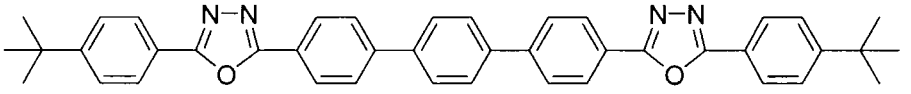

1,4-Benzenediboronic acid (80 mg, 0.48 mmol), 2-(4-iodophenyl)-5-(4-*tert*-butylphenyl)-1,3,4-oxadiazole **247** (0.3 g, 0.74 mmol), THF (30 cm^3) $Pd(PPh_3)_4$ (50.3 mg) and Na_2CO_3 (1 M degassed 4 cm^3). A white highly insoluble precipitate of **248a** was isolated from the reaction flask (68 mg, 15%), mp >300 °C. *m/z* (EI) 630 (M^+ 8%), 41 (M^+ 100%). HRMS (EI) (M^+) 630.2997 (calcd. for $C_{42}H_{38}N_4O_2$ 630.2994). δ_H (500 MHz TCE-d_2) 1.30 (s, 18H), 7.49 (d, 4H, J = 8.0 Hz), 7.73 (s, 4H), 7.77 (d, 4H, J = 8.0 Hz), 7.99 (d, 4H, J = 8.0 Hz), 8.14 (d, 4H, J = 7.5 Hz). δ_C (500 MHz TCE-d_2) 31.32, 35.22, 121.65, 123.70, 126.24, 127.15, 127.69, 127.82, 127.91, 139.96, 143.87, 155.88, 164.45, 165.03.

1,4-Bis-[2-phenyl-5-(4-tert-butylphenyl)-1,3,4-oxadiazole]-2,5-dimethoxybenzene 248b

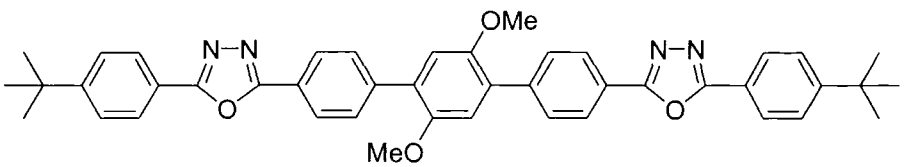

2,5-Dimethoxy-1,4-benzenediboronic acid **207** (100 mg, 0.48 mmol), 2-(4-iodophenyl)-5-(4-*tert*-butylphenyl)-1,3,4-oxadiazole **247** (0.3 g, 0.74 mmol), THF (30 cm^3) $Pd(PPh_3)_4$ (50.5 mg) and Na_2CO_3 (1 M degassed 4 cm^3) and chromatography (eluent initially DCM-ethyl-acetate, 9.9:0.1 v/v, then DCM-ethyl-acetate, 1:1 v/v) gave **248b** as a yellow solid (80 mg, 24%), mp 224-226 °C. *m/z* (EI) 690 (M^+ 100%). HRMS (EI) (M^+) 690.3227 (calcd. for $C_{44}H_{32}N_4O_4$ 690.3206). δ_H (500 MHz $CDCl_3$) 1.37 (s, 18H), 3.86, (s, 6H), 7.05 (s,2H), 7.56 (d, 4H, J = 8.5 Hz), 7.77 (d, 4H, J = 8.5 Hz), 8.08 (d, 4H, J = 8.5 Hz), 8.21 (d, 4H, J = 8.5 Hz). δ_C (500 MHz $CDCl_3$) 31.11, 35.09, 56.47, 114.46, 121.10, 122.67, 126.06, 126.67, 126.77, 129.84, 130.11, 141.50, 150.77, 155.34, 164.32, 164.67.

1,4-Bis-[2-phenyl-5-(4-tert-butylphenyl)-1,3,4-oxadiazole]-9,9-dihexylfluorene 248c

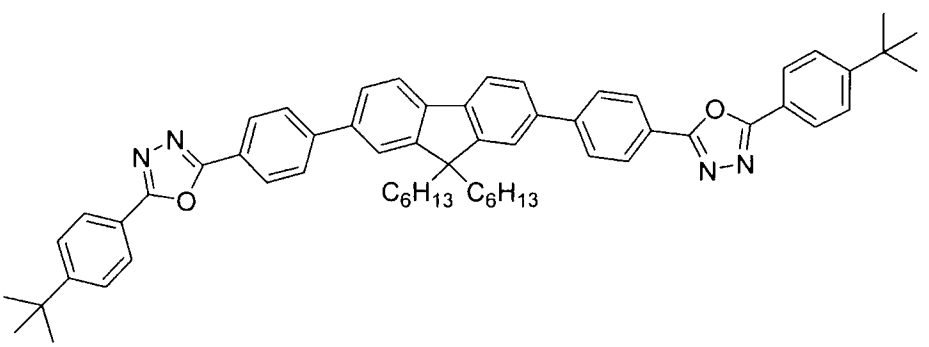

9,9-Dihexylfluorene-2,7-diboronic acid **169** (0.20 g, 0.48 mmol), 2-(4-iodophenyl)-5-(4-*tert*-butylphenyl)-1,3,4-oxadiazole **247** (0.3 g, 0.74 mmol), THF (30 cm^3) $Pd(PPh_3)_4$ (55.48 mg) and Na_2CO_3 (1M degassed 4 cm^3) and (eluent initially DCM-ethylacetate, 9.9:0.1 v/v, then DCM-ethylacetate, 1:1 v/v) gave a yellow oil; crystallisation from cyclohexane/hexane mixture precipitated a yellow solid impurity which was removed by suction filtration. The filtrate was removed *in vacuo* to yield **248c** as a white solid (70 mg, 11%), mp 187-189 °C. *m/z* (ES+) 887.7. HRMS (ES+) (M^+) 886.5184 (calcd. for $C_{61}H_{66}N_4O_2$ 886.5186). δ_H (500 MHz $CDCl_3$) 0.75 (m, 10H), 1.06 (m, 12H), 1.39 (s, 18H), 2.08 (m, 4H, J = 8.0 Hz), 7.57 (d, 4H, J = 8.0 Hz), 7.65-7.68 (m, 4H), 7.83-7.86 (m, 6H), 8.09 (d, 4H, J = 8.5 Hz), 8.24 (d, 4H, J = 8.5 Hz). δ_C (500 MHz $CDCl_3$) 13.98, 22.54, 23.79, 29.64, 31.11, 31.43, 35.09, 40.36, 55.45,

120.40, 121.11, 121.46, 122.63, 126.06, 126.25, 126.78, 127.35, 127.70, 138.92, 140.68, 144.70, 151.98, 155.34, 164.31, 164.68.

6 REFERENCES

[1] Haskal, E. I.; Buchel, M.; Duinevald, P. C.; Sempel, A.; van der Weijer, P. *MRS Bulletin* **Nov 2002**, 864-869.

[2] Pope, M.; Kallmann, H.; Magnante, P. *J. Chem. Phys.* **1963**, *38*, 2042-2043.

[3] For a monograph on organic materials for display technology (liquid crystal displays and OLEDs) see: Kelly, S. M. *Flat Planel Displays*, ed. Connor, J. A. Royal Society of Chemistry, Cambridge, **2000**.

[4] Vincett, P. S.; Barlow, W. A.; Hann, R. A.; Roberts, G. G. *Thin Solid Films* **1982**, *94*, 171-183.

[5] Tang, C. W.; VanSlyke, S. A. *Appl. Phys. Lett.* **1987**, *51*, 913-915.

[6] Forrest, S. R.; Burrows, P. E.; Thompson, M. E. *Chem. & Ind.* **1998**, 1023-1026.

[7] Burroughs, J. H.; Bradley, D. D. C.; Brown, A. R.; Marks, R. N.; Mackay, K.; Friend, R. H.; Burn, P. L.; Holmes, A. B. *Nature* **1990**, *347*, 539-541.

[8] Braun, D.; Heeger, A. J. *Appl. Phys. Lett.* **1991**, *58*, 1982-1985.

[9] Stevenson, R. *Chem. & Ind.* **2003**, 33-37.

[10] Müllen, K.; Wegner, G. *Electronic Materials: The Oligomer Approach*, Wiley-VCH, New York, **1998**, pg. 1.

[11] Kraft, A.; Grimsdale, A. C.; Holmes, A. B. *Angew. Chem. Int. Ed.* **1998**, *37*, 402-428.

[12] Wessling, R. A.; Zimmerman, R.G. (Dow Chemical), US-B 3401 152, **1968**, [*Chem Abstr.* **1968**, *69*, 87735q].

[13] Wessling, R. A. *J. Polym. Sci. Polym. Symp.* **1985**, *72*, 55-66.

[14] Chang, W. –P.; Whang, P. –W.; Lin, P.-W. *Polymer* **1996**, *37*, 1513-1518.

[15] Miao, Y. –J.; Bazan, G. C. *J. Am. Chem. Soc.* **1994**, *116*, 9379-9380.

[16] Conticello, V. P.; Gin, D. L.; Grubbs, R. H. *J. Am. Chem. Soc.* **1992**, *114*, 9708-9710.

[17] Moratti, S. C.; Cervini, R.; Holmes, A. B.; Baigent, D, R.; Friend, R. H.; Greenham, N. C.; Gruner, J.; Hamer, P. *J. Synth. Met.* **1995**, *71*, 2117-2120.

[18] Greenham, N. C.; Moratti, S. C.; Bradley, D. D. C.; Holmes, A. B. *Nature* **1993**, *365*, 628-630.

[19] Hwang, D. H.; Kim, S. T.; Shim, H. K.; Holmes, A. B.; Moratti, S. C.; Friend, R. H. *Chem. Commun.* **1996**, 2241-2244.

[20] Hsieh, B. R.; Yu, Y.; Forysthe, E. W.; Schaaf, G. M.; Feld, W. A. *J. Am. Chem. Soc.* **1998**, *120*, 231-232.

[21] Mitschke, U.; Bäuerle, P. *J. Mater. Chem.* **2000**, *10*, 1472-1507.

[22] Chen, J.; Pan, J.; Gao, Z. *Gaodeng Xuexiao Huaxue Xuebao* **1987**, *8*, 325-328.

[23] Sauer, J.; Huisgen, R.; Sturm, H. J. *Tetrahedron* **1960**, *11*, 241-251.

[24] Brown, A. R.; Bradley, D. D. C.; Burroughs, J. H.; Friend, R. H.; Greenham, N. C.; Burn, P. L.; Kraft, A. *Appl. Phys. Lett.* **1992**, *61*, 2793-2795.

[25] Zhang, C.; Höger, S.; Pakbaz, K.; Wudl, F.; Heeger, A. J. *J. Electron. Mater.* **1994**, *23*, 453-458.

[26] Vaeth, K. M.; Tang, C. *J. Appl. Phys.* **2002**, *92*, 3447-3453.

[27] Chien, Y.; Wong, K.; Chou, P.; Cheng, Y. *Chem. Commun.* **2002**, 2874-2875.

[28] Guan, M.; Bian, Z. Q.; Zhou, Y. F.; Li, F. Y.; Li, Z. J.; Huang, C. H. *Chem. Commun.* **2003**, 2708-2709.

[29] Wang, C.; Jung, G. –Y.; Hua, Y.; Pearson, C.; Bryce, M. R.; Petty, M. C.; Batsanov, A. S.; Goeta, A. E.; Howard, J. A. K. *Chem. Mater.* **2001**, *13*, 1167-1173.

[30] Wang, C.; Jung, G. –Y.; Batsanov, A. S.; Bryce, M. R.; Petty, M. C. *J. Mater. Chem.* **2002**, *12*, 173-180.

[31] OXD-7 has been used in OLEDs with different emissive materials by Tsutsui and co-workers: O'Brien, D.; Bleyer, A.; Lidzey, D. G.; Bradley, D. D. C.; Tsutsui, T. *J. Appl. Phys.* **1997**, *82*, 2662-2670.

[32] Jung, G. –Y. *Ph.D. Thesis*, University of Durham, **2001**.

[33] Kraft, A. *Liebigs Ann./Recueil* **1997**, 1463-1471.

[34] Cha, S. W.; Choi, S. –H.; Kim, K.; Jin, J. –Il. *J. Mater. Chem.* **2003**, *13*, 1900-1904.

[35] Yeh, H. –C.; Lee, R. –H.; Chan, L. –H.; Lin, T. –Y. J.; Chen, C. –T.; Balasubramaniam, E.; Tao, Y. –T. *Chem. Mater.* **2001**, *13*, 2788-2796.

[36] Liang, F.; Chen, J.; Wang, L., Ma, D.; Jing, X.; Wang, F. *J. Mater. Chem.* **2003**, *13*, 2922-2926.

[37] Zheng, M.; Ding, L.; Gürel, E. E.; Lahti, P. M.; Karasz, F. E. *Macromolecules* **2001**, *34*, 4124-4129.

[38] Zhang, Z.; Hu, Y.; Li, H.; Wang, L.; Jing, X.; Wang, F.; Ma, D. *J. Mater. Chem.* **2003**, *13*, 773-777.

[39] Meng, H.; Chen, Z. –K.; Liu, X. –L.; Lai, Y. –H.; Chua, S. –J.; Huang, W. *Phys. Chem. Chem. Phys.* **1999**, *1*, 3123-3127.

[40] Pösch, P.; Fink, R.; Thelakkat, M.; Schmidt, H. –W. *Acta Polym.* **1998**, *49*, 487-494.

[41] Peng, Z.; Boa, Z.; Galvin, M. E. *Chem. Mater.* **1998**, *10*, 2086-2090.

[42] Wang, C.; Kilitziraki, M.; Pålsson, L.-O.; Bryce, M. R.; Monkman, A. P.; Samuel, I. D. W. *Adv. Funct. Mater.* **2001**, *11*, 47-50.

[43] Chen, Z. –K.; Meng, H.; Lai, Y. –H.; Huang, W. *Macromolecules* **1999**, *32*, 4351-4358.

[44] Lee, D. W.; Kwon, K. –Y.; Jin, J. –I.; Park, Y.; Kim, Y. –R.; Hwang, I. –W. *Chem. Mater.* **2001**, *13*, 565-574.

[45] Wudl, F.; Allemand, P. M.; Srdanov. G.; Ni, Z.; Mcbranch, D. *ACS Symp. Ser.* **1991**, *455*, 683-686.

[46] Peng, Z.; Zhang, J. *Synth. Metals* **1999**, *105*, 73-78.

[47] Davies, D. T. *Aromatic Heterocyclic Chemistry*, ed. Davies, S. G.; Compton, R. G.; Evans, J.; Gladden, L. F., Oxford University Press, **2002**, p. 22.

[48] Jordan, R. H.; Dodabalapur, A.; Strukelj, M.; Miller, T. M. *Appl. Phys. Lett.* **1996**, *68*, 1192-1194.

[49] Strukelj, M.; Jordan, R. H.; Dodabalapur, A. *J. Am. Chem. Soc.* **1996**, *118*, 1213-1214.

[50] Thelakkat, M.; Schmidt, H. W. *Polym. Adv. Technol.* **1998**, *9*, 429-442.

[51] Kido, J.; Hongawa, K.; Okuyama, K.; Nagai, K. *Appl. Phys. Lett.* **1993**, *63*, 2627-2629.

[52] Kido, J.; Hongawa, K.; Okuyama, K.; Nagai, K. *Appl. Phys. Lett.* **1994**, *64*, 815-817.

[53] Jiang, X.; Zhang, Z.; Zhao, W.; Zhu, W.; Zhang, B.; Xu, S. *J. Phys. D: Appl. Phys.* **2000**, *33*, 473-476.

[54] Ma, Y.; Che, C. –M.; Chao, H. –Y.; Zhou, X.; Chan, W. –H.; Shen, J. *Adv. Mater.* **1999**, *11*, 852-857.

[55] Grice, A. W.; Tajbakhsh, A.; Burn, P. L.; Bradley, D. D. C. *Adv. Mater.* **1997**, *9*, 1174-1178.

[56] Burn, P. L.; Grice, A. W.; Tajbakhsh, A.; Bradley, D. D. C.; Thomas, A. C. *Adv. Mater.* **1997**, *9*, 1171-1174.

[57] Halim, M.; Samuel, I. D. W.; Pillow, J. N. G.; Monkman, A. P.; Burn, P. L. *Synth. Metals* **1999**, *102*, 1571-1574.

[58] Hwang, M. –Y.; Hua, M. –Y.; Chen, S. –A. *Polymer* **1999**, *40*, 3233-3235.

[59] Dailey, S.; Halim, M.; Rebourt, E.; Horsburgh, L. E.; Samuel, I. D. W.; Monkman, A. P. *J. Phys.: Condens. Mater.* **1998**, *10*, 5171-5178.

[60] Ng, S. –C.; Lu, H. –F.; Chan, H. S. O.; Fujil, A.; Laga, T.; Yoshino, K. *Adv. Mater.* **2000**, *12*, 1122-1125.

[61] Wang, C.; Kilitziraki, M.; Macbride, J. A. H.; Bryce, M. R.; Horsburgh, L. E.; Sheridan, A. K.; Monkman, A. P.; Samuel, I. D. W. *Adv. Mater.* **2000**, *12*, 217-222.

[62] Kim, J. K.; Yu, J. W.; Hong, J. M.; Cho, H. N.; Kim, D. Y.; Kim, C. Y. *J. Mater. Chem.* **1999**, *9*, 2171-2176.

[63] Monkman, A. P.; Pålsson, L. –O.; Higgins, R. W. T.; Wang, C.; Bryce, M. R.; Batsanov, A. S.; Howard, J. A. K. *J. Am. Chem. Soc.* **2002**, *124*, 6049-6055.

[64] Irvin, D. J.; Dubois, C. J.; Reynolds, J. R. *Chem. Commun.* **1999**, 2121-2122.

[65] Bouachrine, M.; Lére-Porte, J. –P.; Moreau, J. J. E.; Serein-Spirau, F.; Torreilles, C. *J. Mater. Chem.* **2000**, *10*, 263-268.

[66] Wong, K. –T.; Hung, T. S.; Lin, Y.; Wu, C. –C.; Lee, G. –H.; Peng, S. –M.; Chou, C. H.; Su, Y. O. *Org. Lett.* **2002**, *4*, 513-516.

[67] Wu, C. –C.; Lin, Y.; Chiang, H. H.; Cho, T. Y.; Chen, C. W.; Wong, K. –T.; Liao, Y. L.; Lee, G. –H.; Peng, S. –M. *Appl. Phys. Lett.* **2002**, *81*, 577-579.

[68] Kanbara, T.; Kushida, T.; Saito, N.; Kuwajima, I.; Kubota, K.; Yamamoto, T. *Chem. Lett.* **1992**, 583-586.

[69] Grimsdale, A. C.; Cervini, R.; Friend, R. H.; Holmes, A. B.; Kim, S. T.; Moratti, S. C. *Synth. Met.* **1997**, *85*, 1257-1258.

[70] Liu, M. W.; Zhang, X. H.; Lai, W. Y.; Lin, X. Q.; Wong, F. L.; Gao, Z. Q.; Lee, C. S.; Hung, L. S.; Lee, S. T.; Kwong, H. L. *Phys. Stat. Sol. A-Appl. Res.* **2001**, *185*, 203-211.

[71] Wu, A.; Akagi, T.; Jikei, M.; Kakimoto, M.; Imai, Y.; Ukishima, S.; Takahashi, Y. *Thin Solid Films* **1996**, *273*, 214-217.

[72] Peng, Z.; Galvin, M. E. *Chem. Mater.* **1998**, *10*, 1785-1788.

[73] Scherf, U.; Müllen, K. *Adv. Polym. Sci.* **1995**, *123*, 1-40.

[74] Zhang, Y.; Zhang, Q.; Lamba, J. J. S.; Tour, J. M.; *Polm. Prep. Cam (Am. Chem. Soc., Div. Polym. Chem.),* **1994**, *35*, 691-692.

[75] Zhang, C. Y.; Tour, J. M. *J. Am. Chem. Soc.* **1999**, *121*, 8783-8790.

[76] Delnoye, D. A. P.; Sijbesma, R. P.; Vekemans, J. A. J. M.; Meijer, E. W. *J. Am. Chem. Soc.* **1994**, *118*, 8717-8718.

[77] Pieterse, K.; Vekemans, J. A. J. M.; Kooijman, H.; Spek, A. L.; Meijer, E. W. *Chem. Eur. J.* **2000**, *6*, 4597-4603.

[78] Pang, J.; Freiberg, S.; Yang, X. –P.; D'Iorio, M.; Wang, S. *J. Mater. Chem.* **2002**, *12*, 206-212.

[79] Lupton, J. M.; Hemingway, L. R.; Samuel, I. D. W.; Burn, P. L. *J. Mater. Chem.* **2000**, *10*, 867-871.

[80] Fink, R.; Heischkel, Y.; Thelakkat, M.; Schmidt, H. –W. *Chem. Mater.* **1998**, *10*, 3620-

3625.

[81] Strukelj, M.; Hedrick, J. C. *Macromolecules* **1994**, *27*, 7511-7521.

[82] Kim, J. L.; Kim, J. K., Cho, H. N.; Kim, D. Y., Kim, C. Y.; Hong, S. I. *Macromolecules* **2000**, *33*, 5880-5885.

[83] Liu, Y.; Ma, H.; Jen, A. K. –Y. *J. Mater. Chem.* **2001**, *11*, 1800-1804.

[84] Liu, M. S.; Liu, Y.; Urian, C.; Ma, H.; Jen, A. K. –Y. *J. Mater. Chem.* **1999**, *9*, 2201-2204.

[85] Wang, J. –F.; Kawabe, Y.; Shaheen, S. E.; Morrell, M. M.; Jabbour, G. E.; Lee, P. A.; Anderson, J.; Armstrong, N. R.; Kippelen, B.; Mash, E. A.; Peyghambarian, N. *Adv. Mater.* **1998**, *10*, 230-233.

[86] Thomas, K. R. J.; Lin, J. T.; Tao, Y. –T.; Chuen, C. –H. *Chem. Mater.* **2002**, *14*, 2796-2802.

[87] Thomas, K. R. J.; Lin, J. T.; Tao, Y. –T.; Chuen, C. –H. *J. Mater. Chem.* **2002**, *12*, 3516-3522.

[88] Wang, S.; Lou, H.; Liu, Y.; Yu, G.; Lu, P.; Zhu, D. *J. Mater. Chem.* **2001**, *11*, 2971-2973.

[89] Zhan, X.; Liu, Y.; Wu, X.; Wang, S.; Zhu, D. *Macromolecules* **2002**, *35*, 2529-2537.

[90] Dailey, S.; Feast, W. J.; Peace, R. J.; Sage, I. C., Till, S.; Wood, E. L. *J. Mater. Chem.* **2001**, *11*, 2238-2243.

[91] Tomasik, D.; Tomasik, P. *J. Heterocyclic Chem.* **1983**, *20*, 1539-1543.

[92] Tao, Y. T.; Balasubramaniam, E.; Danel, A.; Jarosz, B.; Tomasik, P. *Chem. Mater.* **2001**, *13*, 1207-1212.

[93] Tao, Y. T.; Balasubramaniam, E.; Danel, A.; Tomasik, P. *Appl. Phys. Lett.* **2000**, *77*, 933-935.

[94] Tao, Y. T.; Balasubramaniam, E.; Danel, A.; Wisla, A.; Tomasik, P. *J. Mater. Chem.* **2001**, *11*, 768-772.

[95] Balasubramaniam, E.; Tao, Y. T.; Danel, A.; Tomasik, P. *Chem. Mater.* **2000**, *12*, 2788-2793.

[96] Gompper, R.; Mair, H.; Polborn, K. *Synthesis* **1997**, 696-718

[97] (a) Bernius, M. T.; Inbasekaran, M.; O'Brien, J.; Wu, W. *Adv. Mater.* **2000**, *12*, 1737-1750; (b) Destri, S.; Pasini, M.; Botta, C.; Porzio, W.; Bertini, F.; Marchio, L. *J. Mater. Chem.* **2002**, *12*, 924-933; (c) Review: Scherf, U.; List, E. J. W. *Adv. Mater.* **2002**, *14*, 477-487

[98] (a) Chang, S. W.; Hong, J.-M.; Hong, J. W.; Choi, H. N. *Polym. Bull.* **2001**, *47*, 231-238; (b) Beaupré, S.; Ranger, M.; Leclerc, M. *Macromol. Rapid Commun.* **2000**, *21*, 1013-1018; (c) Cho, H. N.; Kim, J. K.; Kim, D. Y.; Kim, C. Y.; Song, N. W.; Kim, D. *Macromolecules* **1999**, *32*, 1476-1481; (d) Ranger, M.; Rondeau, M.; Leclerc, M. *Macromolecules* **1997**, *30*, 7686-7691.

[99] For a review of cross-coupling methodology in oligomer/polymer synthesis see: (a) Schluter, A. D. *J. Polym. Sci. A: Polym. Chem.* **2001**, *39*, 1533-1556; (b) Hassan, J. Sévignon, M.; Gozzi, C. Schulz, E.; Lemaire, M. *Chem. Rev.* **2002**, *102*, 1359–1469.

[100] (a) Brown, D, J.; Lyall, J, M. *Aust. J. Chem.* **1964,** *17,* 794-802; (b) Arantz, B, W.; Brown, D, J. *J. Chem. Soc. C,* **1971,** 1889-1891; (c) Schlosser, H.; Wingen, R. U. S. Patent, **1994**, 5, 371, 224.

[101] Goodby, J. W.; Hird, M.; Lewis, R. A.; Toyne, K. J. *Chem. Commun.* **1996**, 2719-2720.

[102] (a) Cooke, G.; de Cremiers, A.; Rotello, V. M.; Tarbit, B.; Vanderstraeten, P. E. *Tetrahedron* **2001**, *57*, 2787-2789; (b) Schoemaker, J. M.; Delia, T. J.; *J. Org. Chem.* **2001**, *66*, 7125-7128; (c) Murphy, P. M.; Phillips, V. A.; Jennings, S. A.; Garbett, N. C.; Chaires, J. B.; Jenkins, T. C; Wheelhouse, R. T. *Chem. Commun.* **2003**, 1160-1161.

[103] (a) Compound **165**: Nasielski, J.; Kirsh-Demesmaeker, A.; Nasielski-Hinkens, R. *Tetrahedron* **1972**, *28*, 3767-3772; (b) Compound **166**: Wagner, R. M.; Jutz, C. *Chem. Ber.* **1971**, *104*, 2975-2983.

[104] Littke, A. F.; Dai, C. Fu, C. G. *J. Am. Chem. Soc.* **2000**, *122*, 4020-4028.

[105] For alternative procedures for alkylation of 2,7-dibromofluorene to yield **168** see: (a) Wong, W. -Y.; Choi, K. -H.; Lu, G. -L.; Shi, J. -X.; Lai, P. -Y.; Chan, S.-M. *Organometallics* **2001**, *20*, 5446-5454; (b) Wong, W. -Y.; Lu, G. -L.; Shi, J. -X.; Choi, K. -H.; Shi, J. -X. *Macromolecules*, **2002**, *35*, 3506-3513; (c) Lee, S. H.; Tsutsui, T. *Thin Solid Films* **2000**, *363*, 76-80; (d) Yu, W. –L.; Pei, J.; Cao, Y.; Huang, W.; Heeger, A. J. *Chem. Commun.* **1999**, 1837-1839; (e) Ranger, M.; Leclerc, M. *Chem. Commun.* **1997**, 1597-1598.

[106] For alternative procedures of obtaining compound **169** from **168** see: (a) Liu, B. Yu, W. -L. Lai, Y. -H., Huang, W. *Macromolecules* **2000**, *33*, 8945-8952; (b) Zhan, X.; Liu, Y.; Zhu, D.; Huang, W.; Gong, Q. *Chem. Mater.* **2001**, *13*, 1540-1544; (c) Yu, W.; Pei, J.; Huang, W.; Heeger, A. J. *Chem. Commun.* **1999**, 1837-1838.

[107] (a) Cailleau, H.; Baudour, J. L.; Zeyen, C. M. E. *Acta Crystallogr.* **1979**, *B35*, 426-432; (b) Häfelingen, G.; Regelmann, C. *J. Comput. Chem.* **1985**, *6*, 368-376; (c) Häfelingen,

G.; Regelmann, C. *J. Comput. Chem.* **1987**, *8*, 1057-1065; (d) Takei, Y.; Yamaguchi, T.; Osamura, Y.; Fuke, K.; Kaya, K. *J. Phys. Chem.* **1988**, *92*, 577-581.

[108] (a) Bastiansen, O. *Acta Chem. Scand.* **1950**, *4*, 926-936; (b) Bastiansen, O.; Traetenberg, M. *Tetrahedron* **1962**, *17*, 147-154.

[109] Schmid, E. D.; Brosa, B. *J. Chem. Phys.* **1972**, *56*, 6267-6268.

[110] (a) Barrett, R. M.; Steele, D.; *J. Mol. Struct.* **1972**, *11*, 105-125; (b) Eaton, V. J.; Steele, D. *J. Chem. Soc. Faraday Trans. II*, **1973**, *69*, 1601-1604.

[111] (a) Charbonneau, G. -P.; Delugeard, Y. *Acta Crystallogr.* **1976**, *B32*, 1420-1424; (b) Charbonneau, G. -P.; Delugeard, Y. *Acta Crystallogr.* **1977**, *B33*, 1586-1591.

[112] (a) Rapthel, I.; Hartung, H.; Richter, R.; Jaskolski, M. *J. Prakt. Chem. Chem. Zeit.* **1983**, *325*, 489-495; (b) Winter, G.; Hartung, H.; Jaskolski, M. *Mol. Cryst. Liq. Cryst.* **1987**, *149*, 17-27; (c) Winter, G.; Hartung, H.; Jaskolski, M. *Mol. Cryst. Liq. Cryst.* **1987**, *150*, 289-300; (d) Mandal, P.; Majumdar, B.; Paul, S.; Schenk, H.; Goubitz, K.; *Mol. Cryst. Liq. Cryst.* **1990**, *180B*, 369-378; (f) Babu, A. M.; Bellad, S. B.; Sridhar, M. A.; Indira, A.; Madhava, M. S.; Prasad, J. S. *Z. Kristallogr.* **1992**, *202*, 25-32.

[113] Anémain, R.; Mulatier, J. -C.; Andraud, C. Stéphan, O.; Vial, J. -C. *Chem. Commun.* **2002**, 1608-1619.

[114] Hou, Q.; Xu, Y.; Yang, W.; Yuan, M.; Peng, J.; Cao, Y. *J. Mater. Chem.* **2002**, *12*, 2887-2892.

[115] Woo, H. S.; Lee, J. G.; Min, H. K.; Oh, E. J.; Park, S. J.; Lee, K. W.; Lee, J. H.; Cho, S. H. Kim, T. W.; Park, C. H. *Synth. Met.* **1995**, *71*, 2173-2174.

[116] Hsu, J. H.; Fann, W. S.; Meng, H. F.; Chen, E. S.; Chang, E. C.; Chen, S. A.; To, K. W. *Chem. Phys.* **2001**, *269*, 367-379.

[117] Adamovich, V.; Brocks, J.; Tamayo, A.; Alexander, A. M.; Djurovich, P. I.; S'Andrade, B. W.; Forrest, S. R.; Thompson, M. E. *New J. Chem.* **2002**, *26*, 1171-1178.

[118] List, E. J. W.; Guentner, R.; Scanducci de Freitas, P.; Scherf, U. *Adv. Mater.* **2002**, *14*, 374-378.

[119] Pålsson, L.-O.; Wang, C.; Russel, D. L.; Monkman, A. P.; Bryce, M. R.; Rumbles, G.; Samuel, I. D. W. *Chem. Phys.* **2002**, *279*, 229-237 and references therein.

[120] (a) Wong, K. -T.; Chien, Y. -Y.; Chen, R. -T.; Wang, C. -F.; Lin, Y. -T.; Chiang, H. -H.; Hsieh, P. -Y.; Wu, C. -C.; Chou, C. H.; Su, Y. O.; Lee, G. -H.; Peng, S. -M. *J. Am. Chem. Soc.* **2002**, *124*, 11576-11577; (b) Pei, J.; Yu, W. -L.; Huang, W.; Heeger, A. J. *Chem. Commun.* **2000**, 1631-1632; (c) Kim, J. K.; Yu, J. W.; Hong, J. M.; Cho, H. N.;

Kim, D. Y.; Kim, C. Y. *J. Mater. Chem.* **1999**, 9, 2171-2176; (d) Prieto, I.; Teetsov, J.; Fox, M. A.; Vanden Bout, D. A.; Bard, A. J. *J. Phys. Chem. A*, **2001**, *105*, 520-523.

[121] Hughes, G.; Wang, C.; Batsanov, A. S.; Fern, M.; Frank, S.; Bryce; M. R.; Perepichka, I. F.; Monkman, A. P.; Lyons, B. P. *Org. Biomol. Chem.* **2003**, *1*, 3069-3077.

[122] Nohara, N.; Hasegawa, M.; Hosokawa, C.; Tokailin, H.; Kusumoto, T. *Chem. Lett.* **1990**, 189-191.

[123] Jaung, J.; Matsuoka, M.; Fukunishi, K. *Dyes and Pigments* **1996**, *36*, 395-405.

[124] Ellingson, R. C.; Henry, R. L. *J. Am. Chem. Soc.* **1949**, *71*, 1711-1713.

[125] Chen, J. J.; Hinkley, J. M.; Wise, D. S.; Townsend, L. B. *Synth. Commun.* **1996**, *26*, 617-622.

[126] Ellingson, R. C.; Henry, R. L. *J. Am. Chem. Soc.* **1949**, *71*, 2798-2800.

[127] Martin, R. E.; Wytko, J. A.; Diederich, F.; Boudon, C, Gisselbrecht, J. –P.; Gross, M. *Helv. Chim. Acta* **1999**, *82*, 1470-1485.

[128] Craig, L. C. *J. Am. Chem. Soc.* **1934**, *56*, 231-232.

[129] Bickling, J. B.; Mason, J. W.; Woltersdorf, O. W.; Jones, J. H.; Kwong, S. F.; Robb, C. M.; Cragoe, E. J. *J. Med. Chem.* **1965**, *8*, 638-642.

[130] Palamidessi, G.; Bernardi, L. *J. Org. Chem.* **1964**, *29*, 2491-2492.

[131] Klein, B.; Hetman, N. E.; O'Donnell, M. E. *J. Org. Chem.* **1963**, *28*, 1682-1686.

[132] Meier, P.; Legraverant, S.; Müller, S.; Schaul, J. *Synthesis* **2003**, 551-554.

[133] Caron, S.; Massett, S. S.; Bogle, D. E.; Castaldi, M. J.; Braisch, T. F. *Org. Proc. Res. Dev.* **2001**, *5*, 254-256.

[134] Thompson, A. E.; Hughes, G.; Batsanov, A. S.; Bryce, M. R.; Parry, P. R.; Tarbit, B. *Org. Biomol. Chem.* manuscript submitted.

[135] Kelly, S. M. personal communication.

[136] (a) Kim, D. Y.; Cho, H. N.; Kim, C. Y. *Prog. Polym. Sci.* **2000**, *25*, 1089-1139; (b) Che, C. –M.; Wan, C. -W.; Yu, W. -Y.; Zhou, Z. -Y.; Lai, W. -Y.; Lee, S. -T. *Chem. Commun.* **2001**, 721-722. (c) Tang, H. -Z.; Fujiki, M.; Zhang, Z. -B.; Torimitsu, K.; Motonaga, M. *Chem. Commun.* **2001**, 2426-2427. (d) Zheng, S.; Shi, J. *Chem. Mater.* **2001**, *13*, 4405-4407. (e) Marsitzky, D.; Scott, J. C.; Chen, J. -P.; Lee, V. Y.; Miller, R. D.; Setayesh, S. Müllen, K. *Adv. Mater.* **2001**, *13*, 1096-1099. (f) K. Okumoto, K.; Shirota, Y. *Appl. Phys. Lett.* **2001**, *79*, 1231-1233. (g) Kim, Y. -H.; Shin, D-C.; Kwon, S. –K.; Lee, J. -H. *J. Mater. Chem.* **2002**, *12*, 1280-1283. (h) Cheng, Y.; Ma, B.; Wudl, F. *J. Mater. Chem.* **1999**, *9*, 2183-2188.

[137] Virgili, T.; Lidzey, D. G.; Bradley, D. D. C. *Adv. Mater.* **2000**, *12*, 58-62.

[138] Newbold, G. T.; Spring, F. S. *J. Chem. Soc.* **1947**, 1183-1185.

[139] Blake, K. W.; Sammes, P. G. *J. Chem. Soc.* **1970**, 1070-1073.

[140] Ogura, F.; Hama, Y.; Aso, Y.; Otsubo, T. *Synth. Met.* **1988**, *27*, B295-B300.

[141] Parry, P. R.; Wang, C.; Batsanov, A. S.; Bryce, M. R.; Tarbit, B. *J. Org. Chem.* **2002**, *67*, 7541-7543.

[142] (a) Hu, S.; Chin. –Z. *J. Struct. Chem.* **2000**, *19*, 234-237. (b) Bailey, R. D.; Pennington, W. T. *Acta Crystallogr. Sect. C*, **1995**, *51*, 226-236. (c) Modec, B.; Brencic, J. V.; Zubieta, J. *J. Chem. Soc., Dalton Trans.* **2001**, 1500-1510.

[143] Gilchrist, T. L.; *Heterocyclic Chemistry*, 3rd Edition, Longman, Harlow, **1997**, pp 136 and 259.

[144] Comparative values for solid state PL efficiencies of other blue emitters: poly[2,8-(indenofluorene-*co*-anthracene)] Φ_{em} 0.35;[136e] 3,3'-5,5'-tetraethoxycarbonyl-4,4'-diphenyl-2,2'-bipyrrole Φ_{em} 1.0;[136b] poly(4,4'-biphenylylene-α-phenyvinylene) Φ_{em} 0.43;[136g] polymers containing 9,10-di(2-naphthyl)anthracene chromophores Φ_{em} 0.22–0.37.[136d]

[145] Groenendaal, L.; Jonas, F.; Freitag, D.; Pielartzik, H.; Reynolds, J. R. *Adv. Mater.* **2000**, *12*, 481-494.

[146] Türksoy, F.; Hughes, G.; Batsanov, A. S.; Bryce, M. R. *J. Mater. Chem.* **2003**, *13*, 1554-1557.

[147] Schultz, B. *Adv. Mater.* **1997**, *9*, 601-613.

[148] Chien, Y. –Y.; Wong, K. –T.; Chou, P. –T.; Cheng, Y. –M. *Chem. Commun.* **2002**, 2874-2875.

[149] Park, Y. –D.; Kim, J. –J.; Chung, H. –A.; Kweon, D. –H.; Cho, S. –D.; Lee, S. –G.; Yoon, Y. –J. *Synthesis* **2003**, 560-564.

[150] (a) Kreher, D.; Batsanov, A. S.; Wang, C.; Bryce, M. R. *Org. Biomol. Chem.* **2004**, *2*, 858-862. (b) Wang, C.; Batsanov, A. S.; Bryce, M. R. *Chem. Commun.* **2004**, 578-579.

[151] (a) Akhtaruzzmam, M.; Tomura, M.; Zaman, M. B.; Nishida, J.; Yamashita, Y. *J. Org. Chem.* **2002**, *67*, 7813-7818. (b) Screen, T. O.; Thorne, J. R. G.; Denning, R. G.; Bucknall, D. G.; Anderson, H. L. *J. Mater. Chem.* **2003**, *13*, 2796-2808.

[152] Tour, J. M. *Acc. Chem. Res.* **2000**, *33*, 791-804.

[153] (a) Songashira, K. *Comprehensive Organic Synthesis*, ed Trost, B. M.; Fleming, I. Pergamon Press, Oxford, **1991**, vol 3, pg. 521. (b) Songashira, K. *J. Organomet. Chem.*

2002, *653*, 46-49.

[154] The parent 2-phenyl-5-(2-thienyl)-1,3,4-oxadiazole system is known: Hayes, F. N.; Rogers, B. S.; Ott, D. G. *J. Amer. Chem. Soc.* **1955**, *77*, 1850-1852. During the course of our work, 2-furyl-5-phenyl-1,3,4-oxadiazole derivatives were synthesised using different methodology[149] from that shown in Scheme 82.

[155] D'Auria, M.; Mauriello, G. *Tetrahedron Lett.* **1995**, *36*, 4883-4884.

[156] Hetzheim, A.; Möchel, K. *Adv. Heterocycl. Chem.* **1966**, *7*, 186-220.

[157] Synthesis of 2-[4-(2-ethylhexyloxy)phenyl]-5-(4-ethynylphenyl)-1,3,4-oxadiazole: Wang, C.; Batsanov, A. S.; Bryce, M. R. manuscript in preparation. For other reactions of this compound see Ref 150b.

[158] Synthesis of 2-(4-iodophenyl)-5-(4-*tert*-butylphenyl)-1,3,4-oxadiazole: See Ref 157.

[159] Horrocks, D. L. *J. Chem. Phys.* **1969**, *50*, 4962-4966.

[160] (a) Roncail, J. *Chem. Rev.* **1997**, *97*, 173-206. (b) Tachibana, M.; Tanaka, S.; Yamashita, Y.; Yoshizawa, K. *J. Phys. Chem. B.* **2002**, *106*, 3549-3556.

[161] For a synthesis of oligo(2,5-thienylethylene)s see Pearson, D. L.; Tour, J. M. *J. Org. Chem.* **1997**, *62*, 1376-1387.

[162] Berlman, I. B.; *Handbook of Fluorescence Spectra of Aromatic Molecules*, Academic Press, New York, 2nd Ed, **1971**, pg 473.

[163] Beeby, A.; Findlay, K. S.; Rutter, S. personal communication.

[164] Oyston, S.; Wang, C.; Hughes, G.; Bryce, M. R.; Batsanov, A. S.; Ahn, J.; Petty, M. C. manuscript in preparation.

[165] Baigent, D. R.; Holmes, A. B.; Moratti, S. C.; Friend, R. H. *Synth. Met.* **1996**, *80*, 119-124.

[166] Hughes, G.; Kreher, D.; Batsanov, A. S.; Wang, C.; Bryce, M. R. *Org. Biomol. Chem.* to be submitted.

[167] Pålsson, L. –O.; Monkman, A. P. *Adv. Mater.* **2002**, *14*, 757-758.

[168] Compound **231** was identical with a sample obtained previously in our laboratory: Wang, C. unpublished results.

1 Appendix One: New Pyrimidine- and Fluorene-containing Oligo(arylene)s: *ab initio* Calculations

1.1 Quantum Chemical Calculations

These calculations were performed by Dr I. Perepichka. For modelling compounds **172**, **173** and **175**, geometries and electronic structures were calculated for compounds **172E**, **173E**, and **175E** which have ethyl substituents at C(9) instead of hexyl. In addition, the same calculations were performed for derivatives **176E–180E**, to study the influence of the position and the number of nitrogen atoms in the heterocycle attached to the fluorene moiety (Scheme A).

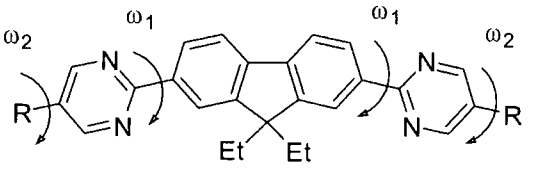

172E, R = H

175E, R = Ph

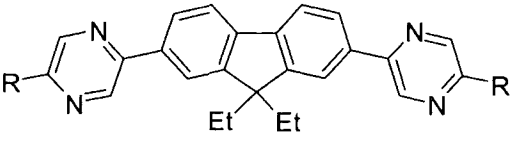

176E, R = H

179E, R = Ph

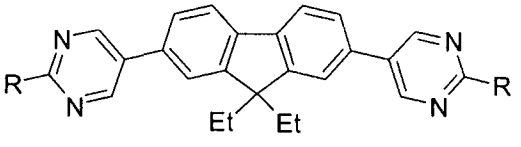

173E, R = H

178E, R = Ph

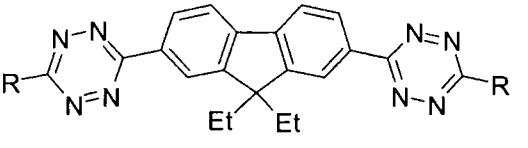

177E, R = H

180E, R = Ph

Scheme A: Structures of compounds 17E, 173E, 175E-180E studied by *ab inito* calculations.

Ab initio calculations of the geometries and electronic structures were performed at the HF and DFT levels of theory at HF/6-31G(d,p), B3LYP/6-31G(d,p) and B3PW91/6-31G(d,p). Both DFT methods (B3LYP and PW91) gave similar results for the optimised geometries and electronic structures of the compounds (Table A). Electronic structures were also calculated at the HF/6-31G(d,p)//B3LYP/6-31G(d,p) level (Figure A).

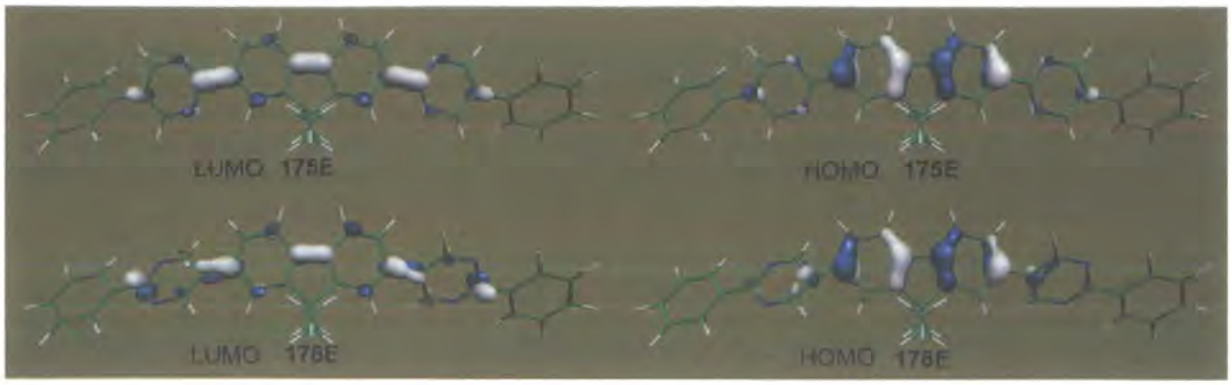

Figure A: Frontier orbitals of compounds 175E and 178E calculated by HF/6-31G(d,p)//B3LYP/6-31G(d,p) *ab initio* methods.

Both HF and DFT calculations indicate that the 2-pyrimidyl ring in the optimised geometries of **172E** and **175E** is in the plane of the fluorene moiety ($\omega_1 \approx 0°$). These results correspond well with experimental X-ray structural data for **175**, which showed only small deviations of the pyrimidine rings from the plane of the fluorene moiety [5.1° and 5.6° (Figure 14)]. These small experimental distortions could probably be a result of crystal packing (in any case, the expected energy loss for such distortions is quite low). Their isomers **173E** and **178E**, however, have a twisted structure with the dihedral angle between the 1,3-pyrimidin-5-yl ring and fluorene moiety ω_1 ca. 45° (HF) or 37° (DFT) (Table A).[i] Again, these values are in the normal range of distortions in biphenyls (see Crystal Structures section in Chapter 2). On the other hand, the ω_2 dihedral angle in **175E** between the phenyl ring and the planar pyrimidine-fluorene moiety is also pronounced ($\approx 45°$ and $\approx 37°$ by HF and DFT, respectively) whereas in **178E** the phenyl-pyrimidine moiety is completely planar ($\omega_2 = 0°$). Thus, as seen in the crystal structures (Figures 12, 13 and 14), the nitrogen atoms in the pyrimidine fragment decrease the steric repulsion which exists between adjacent benzene rings in biphenyl derivatives resulting in planarisation and hence facilitating conjugation between the aromatic rings in oligo(arylenes). This effect is clearly illustrated by the fluorene-tetrazine derivative **180E** which represents a fully planar system ($\omega_1 = \omega_2 = 0°$). Pyrazine derivatives **176E** and **179E**, which have only one nitrogen atom adjacent to the fluorene or phenyl ring, have dihedral angles ω_1 and ω_2 of 28 – 29° and 19 – 21° by HF and DFT, respectively (Table A) which are intermediate between those observed for phenyl and 2-phenylpyrimidine moieties.

Compound	E_h/ hartree	LUMO/ eV	Homo/ eV	$\Delta E_{HOMO-LUMO}$/ eV	ω_1, ° / ω_2, ° [a]
HF/6-31G(d,p)					
172E	-1177.40334	+1.74	-7.36	9.10	0.0
173E	-1177.38722	+1.86	-7.81	9.67	45.3
176E	-1177.37228	+1.70	-7.52	9.21	28.9
177E	-1241.19547	+1.04	-8.00	9.04	0.0
175E	-1636.52019	+1.64	-7.24	8.88	0.5 / 44.7
178E	-1636.51919	+1.71	-7.55	9.26	44.4 / 0.6
179E	-1636.49503	+1.59	-7.28	8.82	27.6 / 27.7
180E	-1700.32632	+0.97	-7.68	8.65	0.1 / 0.1
B3LYP/6-31G(d,p)					
172E	–1184.98926	–1.80	–5.60	3.80	0.0
173E	–1184.97407	–1.86	–6.01	4.15	37.5
176E	–1184.96753	–1.95	–5.77	3.82	20.1
177E	–1248.98090	–2.88	–6.30	3.42	0.0
175E	–1647.11847	–1.90	–5.48	3.58	0.2 / 36.7
178E	–1647.11750	–1.94	–5.74	3.80	36.2 / 0.2
179E	–1647.10330	–2.05	–5.55	3.50	18.5 / 18.9
180E	–1711.12568	–2.65	–5.97	3.32	0.0 / 0.0
B3PW91/6-31G(d,p)					
172E	–1184.54102	–1.90	–5.72	3.82	0.0
173E	–1184.52583	–1.96	–6.13	4.17	38.3
176E	–1184.51868	–2.05	–5.90	3.85	20.8
177E	–1248.50605	–2.96	–6.42	3.46	0.0
175E	–1646.49303	–2.01	–5.61	3.61	0.1 / 37.6
178E	–1646.49199	–2.05	–5.87	3.82	36.9 / 0.1
179E	–1646.47718	–2.16	–5.68	3.52	18.5 / 19.4
180E	–1710.47354	–2.74	–6.10	3.35	0.0 / 0.0

Table A: Calculated energy parameters and dihedral angles for compounds 172E, 173E, and 175E–180E.

A HOMO–LUMO energy diagram (Figure B) shows that at both HF and DFT levels of theory HOMO energies are monotonously decreased in the sequence **172E** > **176E** > **173E** > **177E** (and for phenyl-substituted derivatives **175E** > **178E** > **179E** > **180E**). In contrast, changes in LUMO energies are less pronounced for pyrimidine and pyrazine derivatives (**172E**, **173E**, **175E**, **176E**, **178E**, **179E**) but decreased for tetrazine derivatives **177E** and **180E**. At HF level, the addition of terminal phenyl substituents in all these series increased the HOMO and decreased the LUMO orbital energies, thus resulting in a contraction of the HOMO-LUMO

gap (Table A, Figure B). A similar tendency was observed in the DFT calculations, however, for tetrazine derivatives addition of terminal phenyl substituents (**177E** → **180E**) resulted in increasing LUMO energy (nevertheless HOMO-LUMO gap decreased). Although the exact physical meaning of DFT orbital energies is a controversial subject[ii] and B3LYP/6-31G(d,p) gave too high energies for the HOMO orbitals, it gives quite reliable HOMO-LUMO energy gaps, consistent with the spectroscopic data.

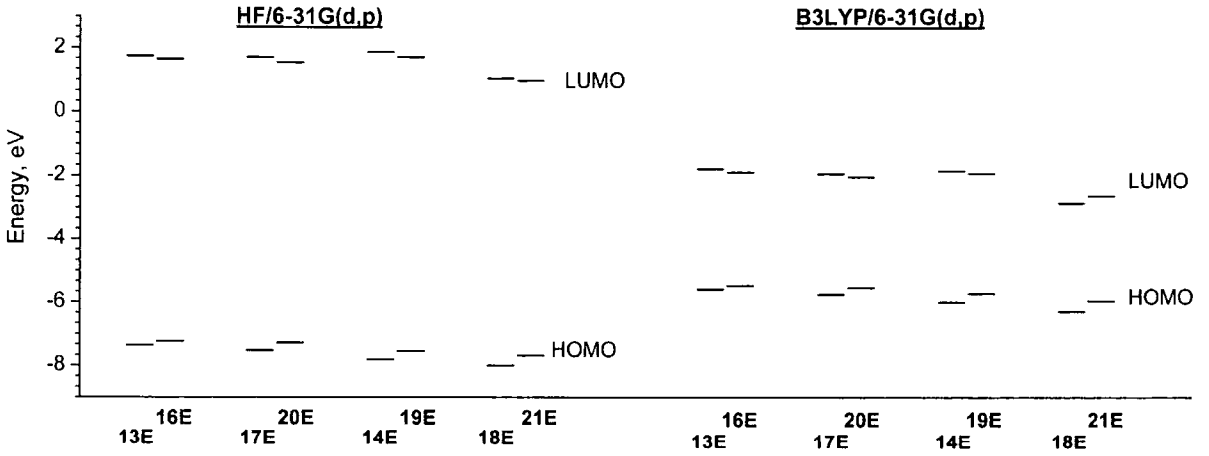

Figure B: Energy levels diagram of compounds 172E, 173E, and 175E–180E.

Analysis of the frontier orbitals reveals that for all these compounds the HOMOs, which are located at the fluorene moiety, populate on the same carbon atoms of the benzene rings whereas the LUMOs are localised at C–C bonds between the 6-membered aromatic rings. Therefore, HOMO–LUMO excitation should increase the quinoidal character of the system, especially the central fluorene moiety. As a result of planarity between the pyrimidine and fluorene rings in **172E** and **175E** the population of the LUMO on the C–C bonds between these rings is more pronounced than that for **173E** and **178E**, where the dihedral angle ω_1 is quite large (Table A).

1.2 Computational Procedure

The *ab initio* computations were carried out with the Gaussian 98[iii] package of programs at both Hartree-Fock and density-functional theory levels using Pople's 6–31G split valence basis set supplemented by *d*-polarisation functions on heavy atoms and *p*-polarisation functions on hydrogens. DFT calculations were carried out using Becke's three-parameter hybrid exchange functional[iv] with either Lee–Yang–Parr correlation functional[v] (B3LYP) or Perdew–Wang 1991 gradient-corrected correlation functional[vi] (B3PW91). Geometries were

optimised with HF/6-31G(d,p), B3LYP/6-31G(d,p) and B3PW91/6-31G(d,p) and electronic structures were calculated at the same levels. Contours of HOMO and LUMO orbitals were also calculated at HF/6-31G(d,p)//B3LYP/6-31G(d,p) level and visualisation of frontier orbital populations was performed using Mølekel v.4.2 program.[vii] No constraints of bonds/angles/dihedral angles were applied in the calculations and all the atoms were free to optimise.

REFERENCES

i HF/6-31G(d) calculated dihedral angles between the phenyl substituents and the fluorene moiety in 2,7-diphenyl-9,9-dioctylfluorene were found to be 45.5°: Belletete, M.; J.-F. Morin, J.-F.; Beaupre, S.; Leclerc. M.; Durocher, G. *Synth. Met.* **2002**, *126*, 43-51.

ii Salzner, U. *J. Phys. Chem. B*, **2002**, *106*, 9214-9220 and references cited therein.

iii Frisch, M. J., Trucks, G. W.; Schlegel, H. B.; Scuseria, G. E.; Robb, M. A.; Cheeseman, J. R.; Zakrzewski, V. G.; Montgomery, Jr., J. A.; Stratmann, R. E.; Burant, J. C.; Dapprich, S.; Millam, J. M.; Daniels, A. D.; Kudin, K. N.; Strain, M. C.; Farkas, O.; Tomasi, J.; Barone, V.; Cossi, M.; Cammi, R.; Mennucci, B.; Pomelli, C.; Adamo, C.; Clifford, S.; Ochterski, J.; Petersson, G. A.; Ayala, P. Y.; Cui, Q.; Morokuma, K.; Malick, D. K.; Rabuck, A. D.; Raghavachari, K.; Foresman, J. B.; Cioslowski, J.; J. V. Ortiz, J. V.; Baboul, A. G.; Stefanov, B. B.; Liu, G.; Liashenko, A.; Piskorz, P.; Komaromi, I.; Gomperts, R.; Martin, R. L.; Fox, D. J.; Keith, T.; Al-Laham, M. A.; Peng, C. Y.; Nanayakkara, A.; Challacombe, Gill, P. M. W.; Johnson, B.; Chen, W.; Wong, M. W.; Andres, J. L.; Gonzalez, C.; Head-Gordon, M.; Replogle E. S.; Pople, J. A. Gaussian 98, Revision A.9, Gaussian, Inc., Pittsburgh PA, 1998.

iv A. D. Becke, *Phys. Rev. A*, 1988, **38**, 3098; A. D. Becke, *J. Chem. Phys.*, 1993, **98**, 5648-5652.

v Lee, C.; Yang, W.; Parr, R. G. *Phys. Rev. B.* **1988**, *37*, 785-789.

vi (a) Perdew, J. P.; Wang, Y. *Phys. Rev. B.* 1992, 45, 13244-13249; (b) Perdew, J. P. in *Electronic Strucure of Solids '91*, ed, Ziesche, P.; Eschrig, H. Akademie Verlag, Berlin, **1991**, pg 11.

vii Flükiger, P.; Lüthi, H. P.; Portmann, S.; Weber, J. Molekel Version 4.2, Swiss Centre for Scientific Computing, Manno (Switzerland), **2000**; http://www.cscs.ch/molekel/; (b) Portmann, S.; Lüthi, H. P. *Chimia*, **2000**, *54*, 766.